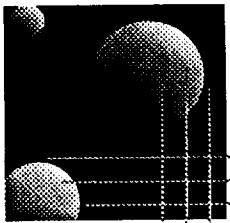


MIT
Space
Engineering
Research
Center



(NASA-CR-192993) THE 3RD ANNUAL
CONTROLLED STRUCTURES TECHNOLOGY
SYMPOSIUM (MIT) 251 P

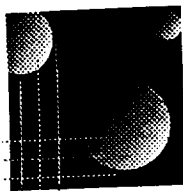
Controlled Structures Technology 3rd Annual Symposium

July 1, 1991

MIT Space Engineering Research Center

N93-28167
--THRU--
N93-28176
Unclass

G3/39 0160322



MIT
Space
Engineering
Research
Center

Controlled Structures Technology
M.I.T. Space Engineering Research Center

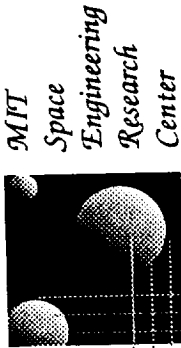
3rd Annual Symposium

July 1, 1991 - 8:00 am to 5:00 pm

Location: Building 9, Rm. 150
Massachusetts Institute of Technology
Cambridge, MA 02139

AGENDA

8:00	Registration	
8:30	Welcome and Introduction	E. Crawley
9:00	Optical Interferometer Testbed -	G. Blackwood -1
9:30	Active Impedance Matching of Complex Structural Systems	D. MacMartin -2
10:00	Break	
10:15	Narrow and Broad Band Isolation for Uncertain Dynamic Systems on 17	A. von Flotow on 17
10:45	Application of CST to Adaptive Optics	E. Anderson - 3
11:15	Middeck 0-G Dynamics Experiment (MODE)	M. van Schoor -4
11:45	Lunch	
1:00	LABORATORY TOUR (MEET IN 37-372)	
2:00	Shaping System Commands to Reduce Residual Vibration	W. Seering on 17-18-20
2:30	Middeck Active Control Experiment (MACE)	D. Miller - 5
3:00	Break	
3:15	Robust Control for Uncertain Structures	M. Athans - 6
3:45	Cost Averaging Techniques for Robust Structural Control	N. Hagood - 7
4:15	Intelligent Structures Technology	E. Crawley - 8
4:45	Conclusion	



OPTICAL INTERFEROMETER TESTBED

Gary H. Blackwood

MIT Space Engineering Research Center
3rd Annual Symposium

July 1 1991

160323
N93-28168

OPTICAL INTERFEROMETER TESTBED:

OUTLINE

1. Motivation for a laboratory testbed of a space based interferometer
2. Description of testbed in context of Controlled Structures Technology
 - performance metric
 - control hardware
3. Overview of testbed research in context of Controlled Structures Technology
 - structural design
 - disturbances and performance
 - sensor/actuator design
 - local/low authority control
 - global/high authority control

OPTICAL INTERFEROMETER TESTBED PROGRAM

Objective: to provide a versatile environment for well controlled experiments on complete controlled structure systems





Testbed is designed to capture the essential configuration, physics, and performance metric of actual spacecraft

Testbed was designed and constructed by students, staff, and faculty as a facility class experiment

Students will conduct their thesis experiment on the testbed by changing out structural components, control hardware and software

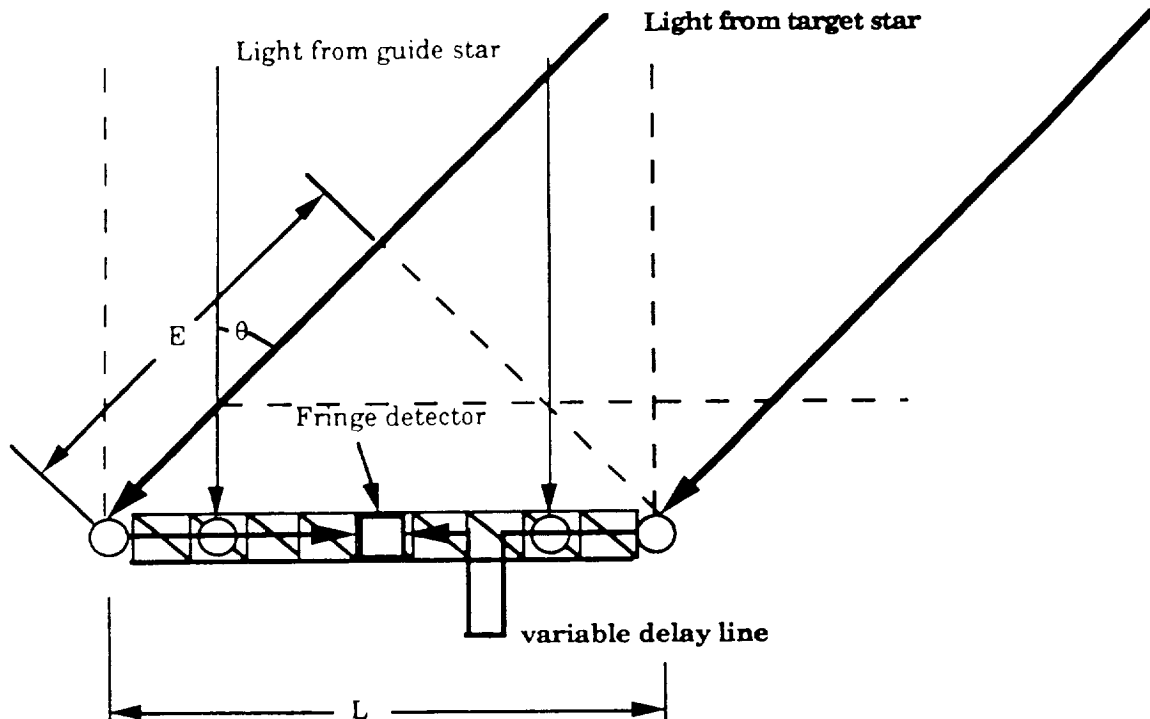
Process provides a realistic evaluation/demonstration of new approaches in *controlled structure design*

A Testbed Based on a Space-Based Optical Interferometer

- CST 
- SERC Scientific Mission Orientation 
 - Candidate Missions 
 - robotics
 - reflectors
 - masking
 - platforms
 - materials proc.
 - Optical Interferometry 
 - Optical Interferometer Testbed Design Project

A Space-Based Interferometer

- used for astrometry:
 - measure baseline and delay lines using metrology system
- used for imaging
 - measure intensity (mag) and phase (via delay line distance) of central fringe of interference pattern
 - vary baseline and rotate siderostats about LOS to target star by rigid body motion
 - reconstruct image from 2-D spatial IFT of the measured intensity



OPTICAL METROLOGY

Unique feature of testbed is multi-axis laser metrology

At 3 mock siderostat locations are precision 3 axis active mirror mounts holding common endpoint retroreflectors (cat's eyes)

Fourth vertex holds laser and other optics

Use commercially available 670 μ Watt laser from Hewlett-Packard

VME based fringe counting provides seamless link to real time controller

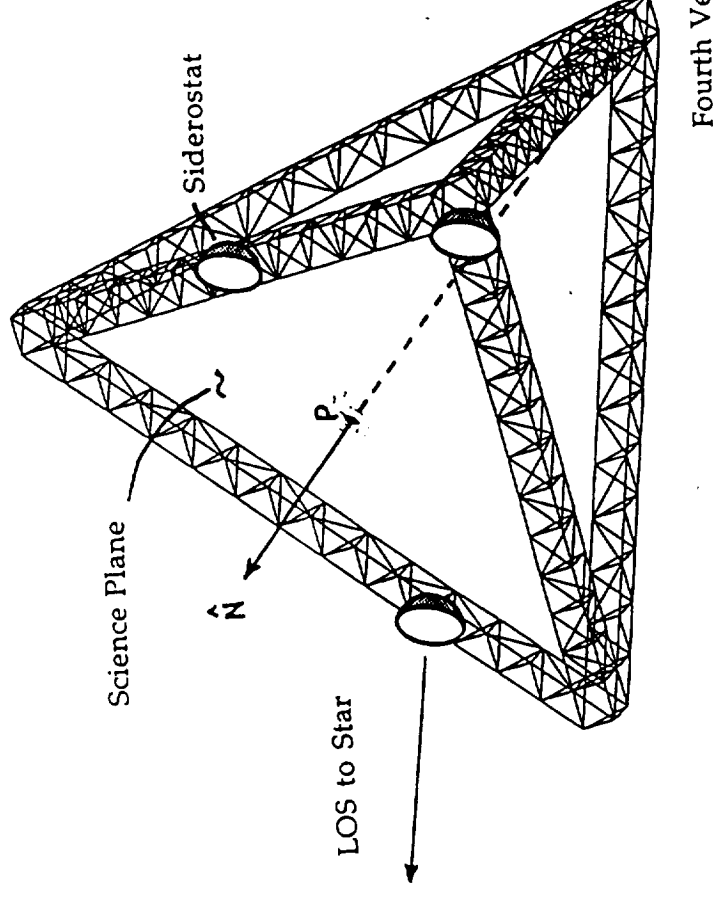
Optical components provide 5 laser pathlength measurements:

- defines baseline for metrology
- define “total starlight differential pathlength error” metric, simulating both internal and external error sources
- a subset of these measurements are available for feedback

OPTICAL INTERFEROMETER TESTBED

(OVERVIEW)

- Testbed based on scientific mission for focus of graduate student theses.
- Testbed modelled on a 35 meter baseline earth-orbiting optical interferometer.
- Precision alignment requirement between three onboard optical elements is 50 nanometers RMS above 1/10th of a hertz.



SENSORS AND ACTUATORS

Sensors for Identification and Control

- 32 Kistler accelerometers for modal identifications testing
- 9 Sunstrand micro-g accelerometers mounted at performance-critical locations
- 5 channels of laser measurement
- strain gages and load cells collocated with active struts

Actuators for Identification and Control

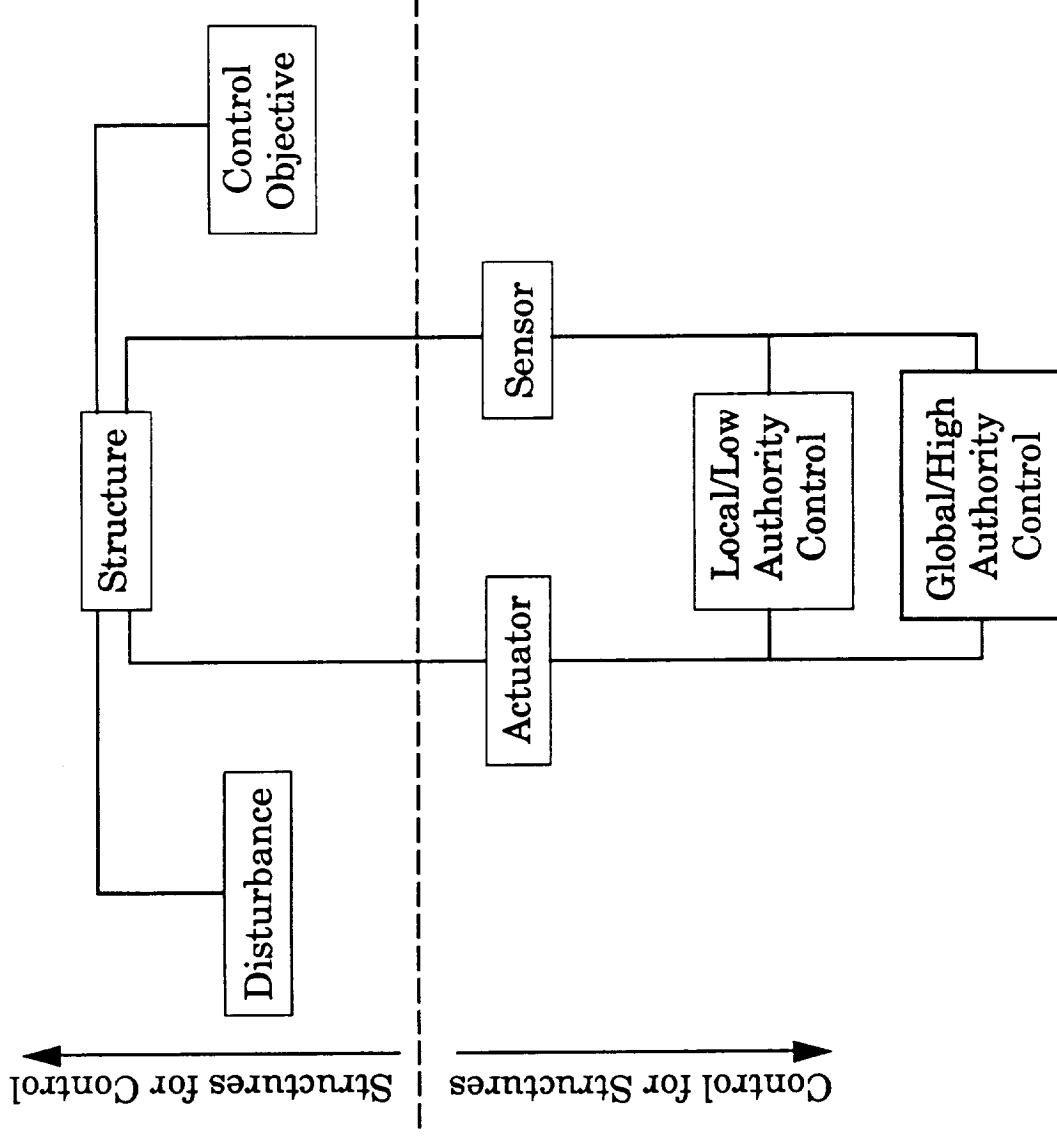
- 3 active struts capable of 60 microns of stroke and 250 Newtons of force at high bandwidth (Physik Instrumente)
- 3 three-axis precision mirror actuators (custom) at each mock siderostat location
- Passively shunted piezoelectric struts

Real Time Control Hardware

- VME based digital control hardware
 - 68030 processor
 - CSPI vector processor
- Capability:
 - 16 inputs
 - 10 outputs
 - 32 states at 1000 Hz; scales by $(n_s + n_i) * (n_s + n_o)$
- Direct link to six HP laser measurement boards
- Control design in MATLAB on Sun SparcStation
- Analog: circuits for displacement and velocity feedback to active struts

A CST DESIGN METHODOLOGY

1. Design structure.
2. Design disturbances and control objective.
3. Design actuator and sensor.
4. Design local/low authority control.
5. Design high authority control.



INTERFEROMETER: EXAMPLE OF CST DESIGN

The interferometer will be used not only as a testbed for the elements of Controlled Structures Technology but also for the evolution of the design process.

Step 0 - Mission Requirement Specification

Disturbance selected from spacecraft experience.

Performance metric established which captures challenge of real spacecraft mission.

Step 1 - Design Structure

Structure chosen for “rigid” alignment of primary performance measures - optical elements of the interferometer

Structure serves as “host” to robust control

Passive damping augmentation for performance and robustness

Step 2 - Design disturbances and control objective

Mount onboard disturbances at locations of lower disturbability

Passive and active isolation at source and output

INTERFEROMETER: EXAMPLE OF CST DESIGN

Step 3 - Design Actuator and Sensor

- pole-zero analysis
- actuator and sensor combinations for active isolation
- induced strain actuators
- actuator and sensor placement for global control
- quasi-static shape control

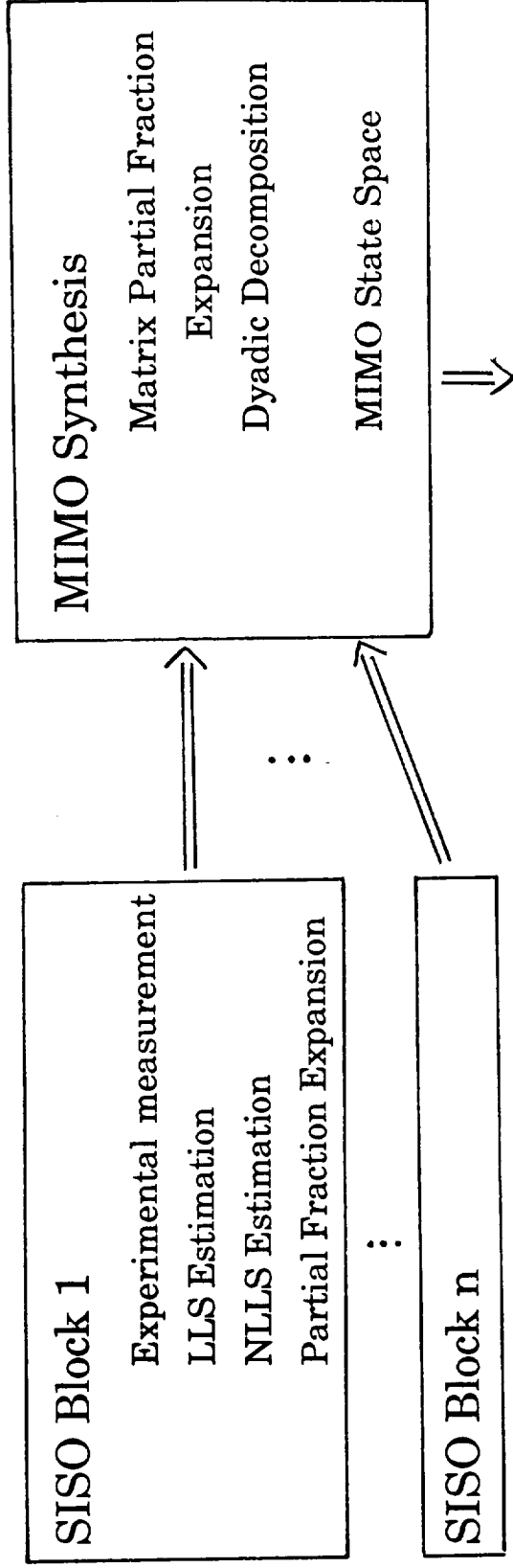
Step 4 - Local/Low Authority Control

- impedance matching
- wave control
- active isolation at disturbance input and at quiet payloads

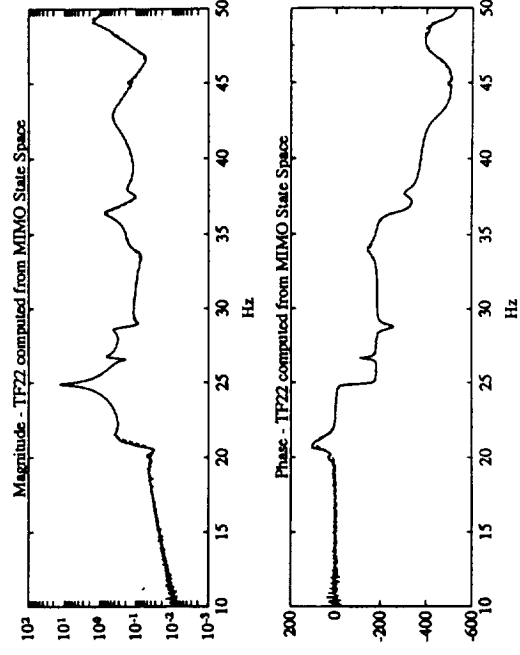
Step 5 - Global/High Authority Control

- modelling and MIMO identification for control
- global control using distributed active struts
- heirarchic control formulation to simultaneously optimize
local and global controllers

IDENTIFICATION FOR MIMO CONTROL



Strut 3 to Accel. 8



Model Validation

— experiment

----- model

FEM/ID CORRELATION FOR THE NAKED TRUSS

<u>Frequencies</u>		<u>Modeshapes</u>
Measured	FEM 1 FEM 2	Overall agreement with FEM modeshapes
31.35 Hz	suspension	<u>Current Issues</u> Assessment of accuracy of measured residues for structure with high modal density Correlation for incomplete ID and degenerated modes Correction , based on ID results, of global parameters, to match the frequencies Correction, based on ID results, of local parameters, to match the modeshapes
31.75 Hz	suspension	
(35.1) Hz	3.5 % 0.4 %	
35.1 Hz	3.5 % 0.4 %	
38.9 Hz	4.7 % 1.8 %	
(38.9) Hz	4.7 % 1.8 %	
39.4 Hz	3.5 % 0.6 %	
43.3 Hz	4.0 % 0.9 %	
43.7 Hz	0.2 % 0.1 %	
(43.7) Hz	3.2 % 0.1 %	
52.1 Hz	3.3 % 0.2 %	
54.7 Hz	3.3 % 0.6 %	
55.2 Hz	2.4 % -0.3 %	
55.6 Hz	2.4 % -0.4 %	
62.7 Hz	suspension	
63.4 Hz	suspension	
94.1 Hz	suspension	
94.8 Hz	suspension	
95.0 Hz	suspension	
100.8 Hz	3.9 % 2.6 %	
101.7 Hz	2.9 % 1.8 %	
102.0 Hz	2.6 % 1.6 %	

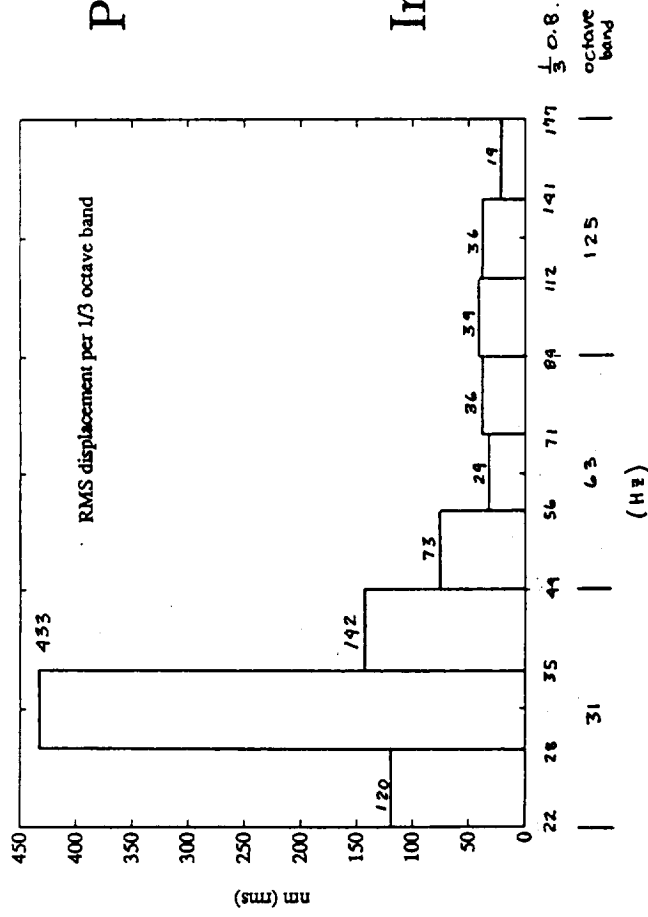
DISTURBANCE MODELLING

Performance degradation due primarily to disturbances from reaction wheels and other on-board machinery. Disturbance level at output expected to be 500 nm (rms) on full scale

Performance metric is not a function of baseline. Scale lab disturbance to same level of 500 nm (rms)

Disturbance source is piezo actuator mounted to vertex; two disturbances modelled are:

- broadband disturbance
- slowly time varying narrowband disturbance



Pathlength error due to broadband disturbance modeled using Statistical Energy Analysis, assuming a typical disturbance input location.

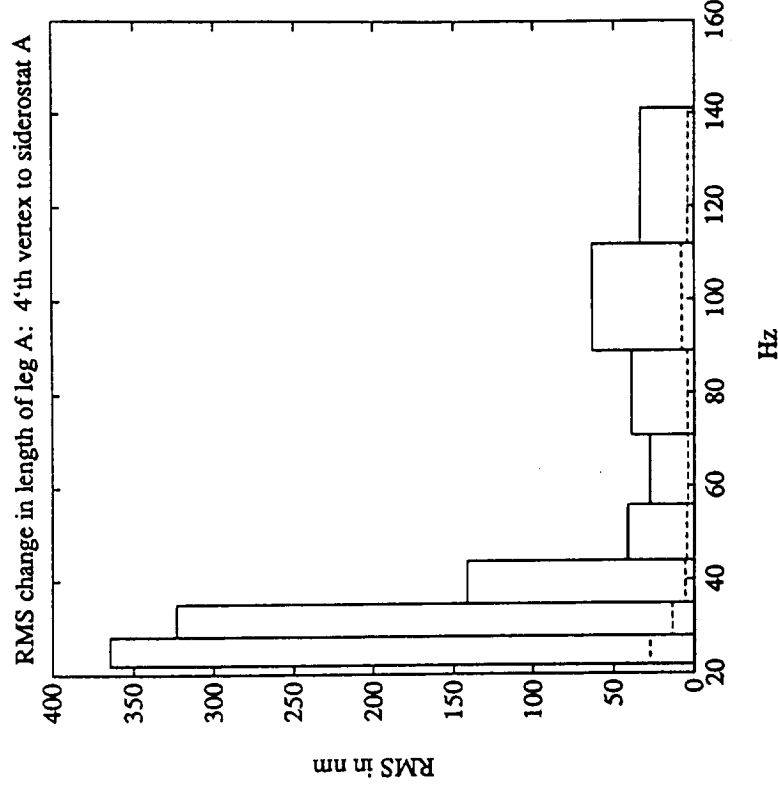
Indicates that 99% of the performance degradation occurs between 20 and 60 Hz.

DISTURBANCE SOURCE IMPLEMENTATION

Goal: Use 3-axis piezoelectric disturbance source to implement the broadband disturbance spectrum resulting in 500 nm (rms) pathlength error

Test: Measured optical pathlength from the fourth vertex to siderostat A with the disturbance source on and off. Computed the RMS change in length over 1/3 Octave bands.

Results: Disturbance source does degrade the pathlength as expected while concentrating energy in vicinity of first few structural modes.

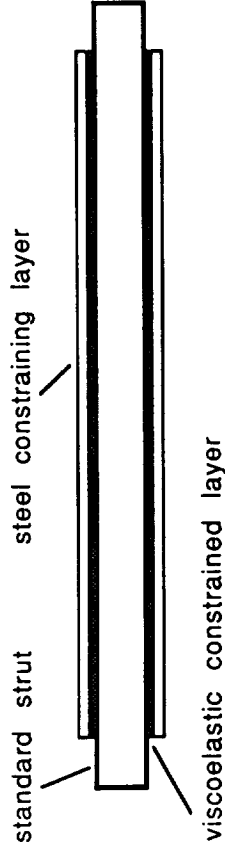


STRUCTURE DESIGN: PASSIVE DAMPING

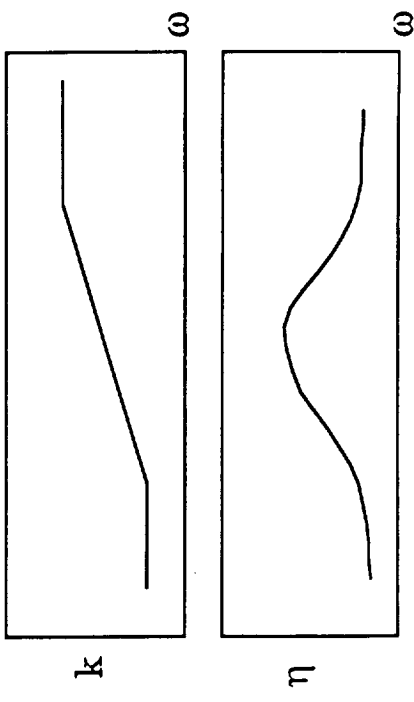
- damping provides some performance within bandwidth
- adds robustness to plant in rolloff region
- improves performance of high authority controllers within bandwidth, which are sensitive to frequency modelling errors

Option: Constrained Layer Viscoelastic struts

- advantages: inexpensive, easy to make
- disadvantages: temperature sensitive, loss factor not high (.05)
many struts are required



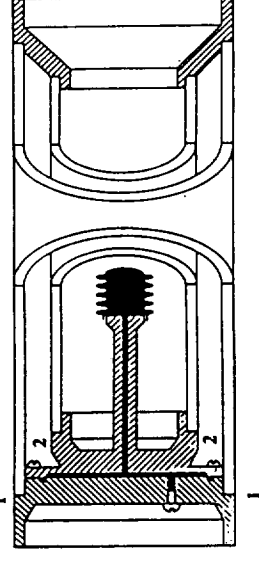
Typical damped strut frequency response



STRUCTURE DESIGN: PASSIVE DAMPING

Option: Honeywell D-Strut Passive Damper

- can be tailored for specific structural impedances
- struts have high loss factor (1.5); fewer struts will be necessary
- analytical study: D-Struts placed in locations of highest weighted strain energy; spectrum of disturbance at pathlength output is improved.



a) Inner-Outer Tube Strut

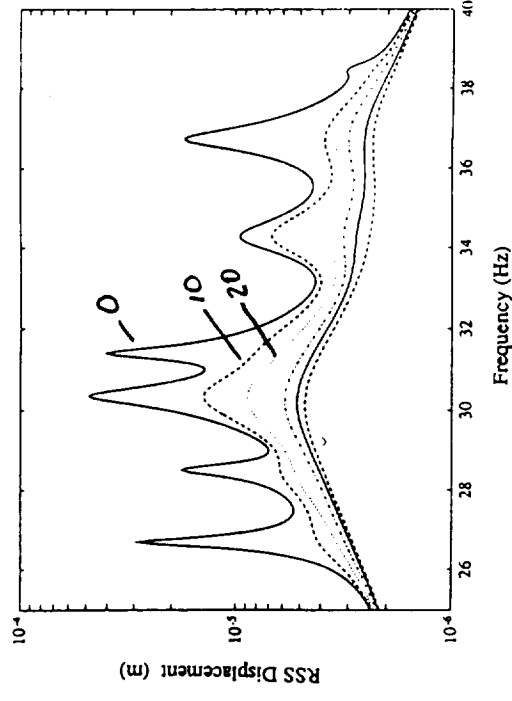
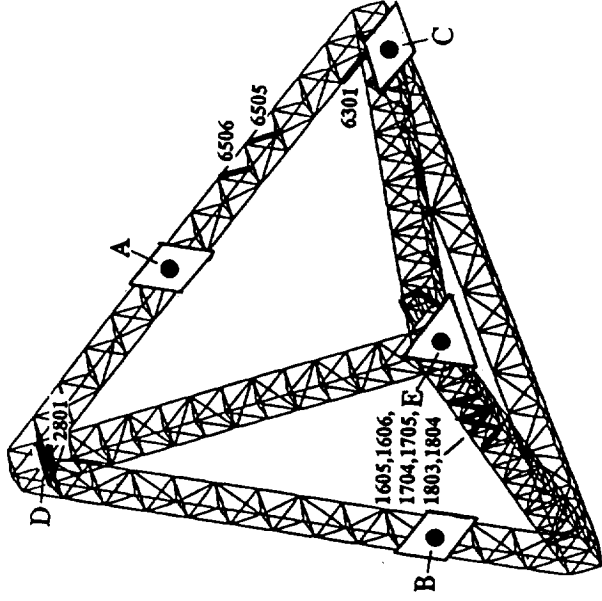
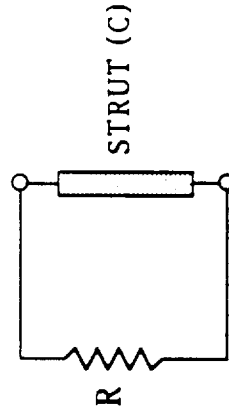
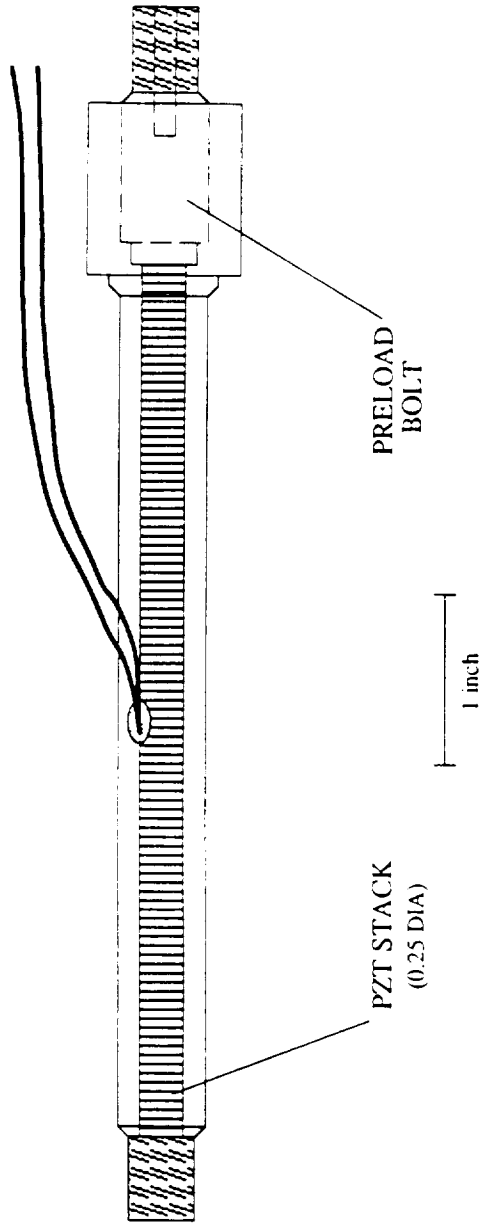
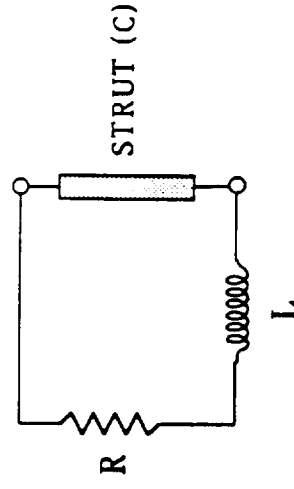


Figure 14: Locations of Struts with Highest Weighted Strain Energies

Shunted Piezoelectric Damping



Resistive Shunting



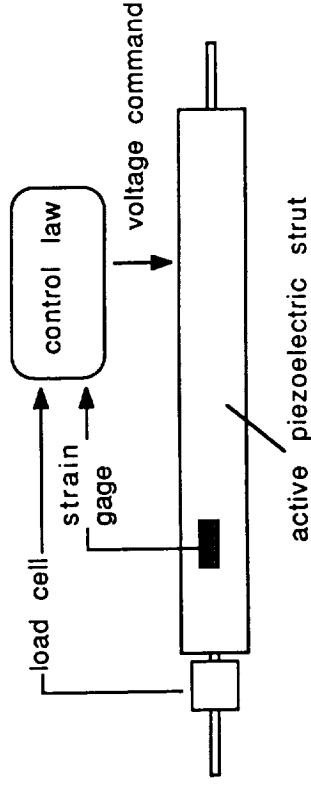
Resonant Shunting

LOW AUTHORITY CONTROL

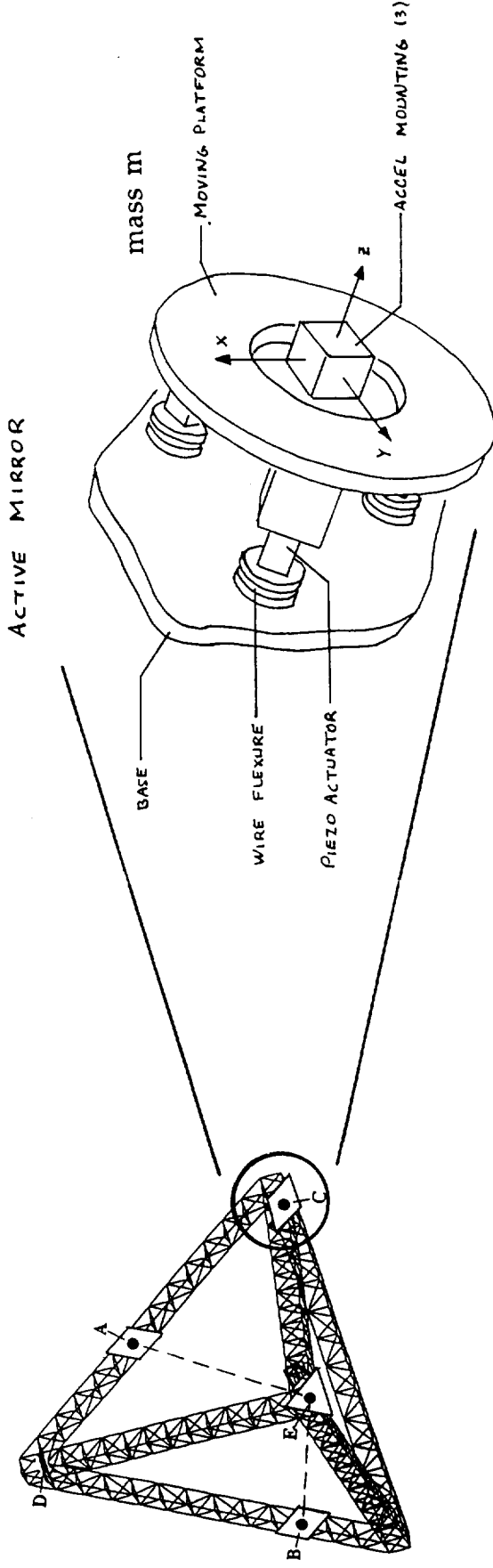
- adds some performance in control bandwidth
- adds robustness in rolloff region of high authority control
- similar benefits to passive damping

Options:

- velocity feedback using active struts
- impedance matching/power flow approaches using external power source
- same formulation, but using passive elements only (shunted piezoelectrics)

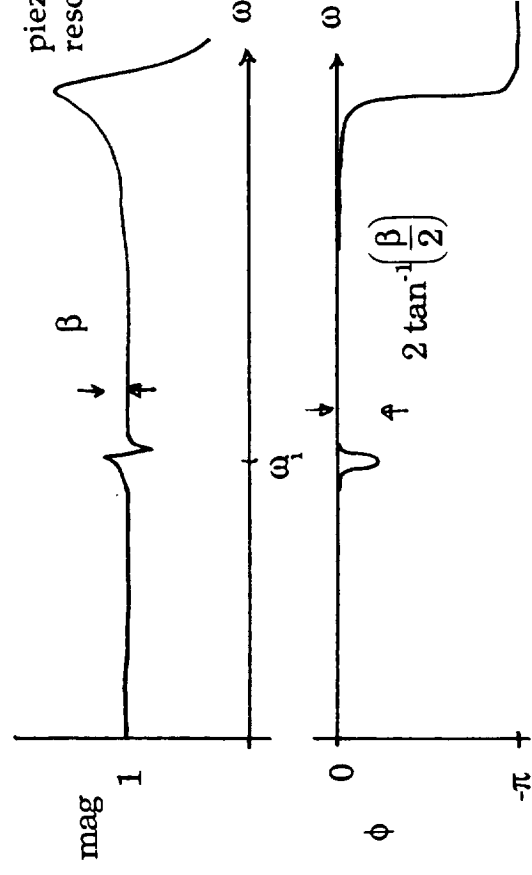


Active Isolation of Lightweight Mirrors on Flexible Structures



- Plant transfer function is $\frac{\text{mirror displacement}}{\text{piezo voltage}}$
- Active mirrors located at locations A, B, C
- Non-dimensional parameter for flex coupling of the i th mode:

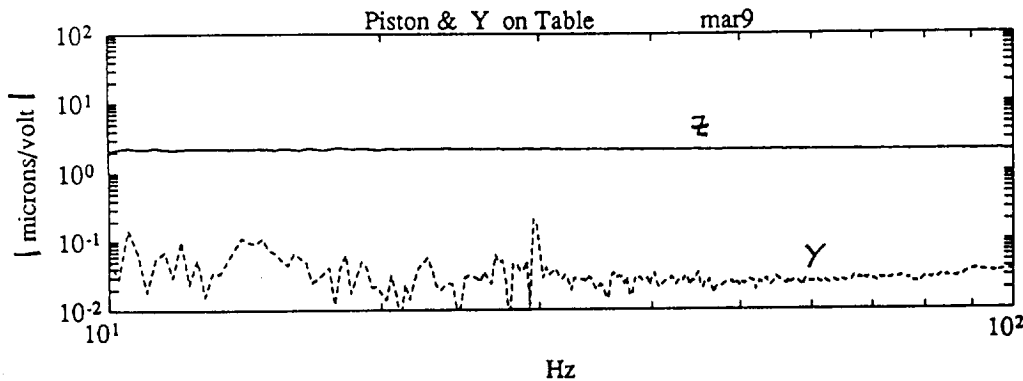
$$\beta = \left(\frac{1}{\zeta_i} \right) \left(\frac{m \phi_i^2}{2} \right)$$



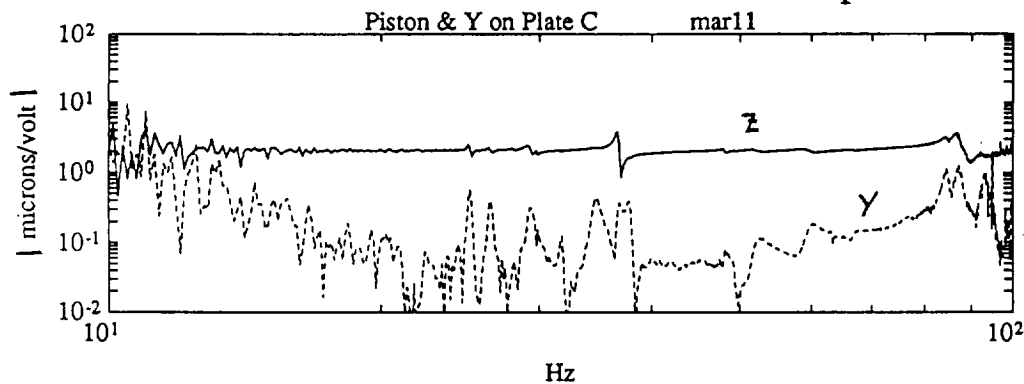
Open Loop Transfer Function of Mirror

- mirror actuated in piston (z) direction only

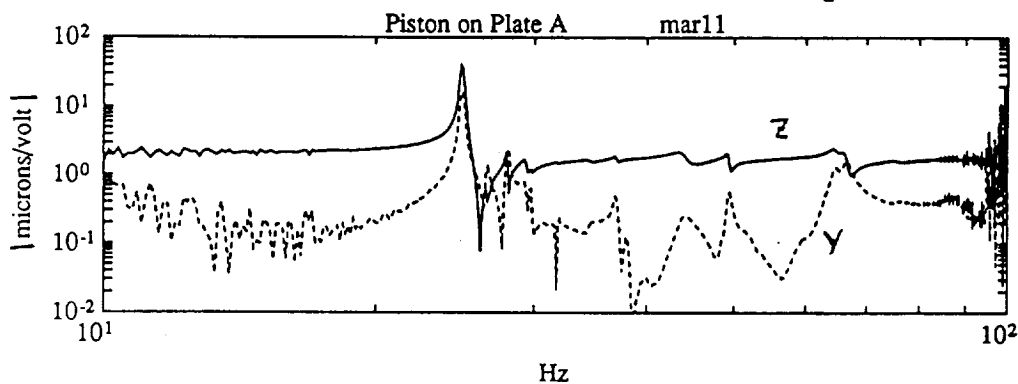
mirror mounted on rigid base



mirror mounted at truss vertex
(plate C)



mirror mounted on truss beam
(plate A)



GLOBAL/HIGH AUTHORITY CONTROL

Current areas of research:

Active strut placement

Sensor placement for control

Static shape control problem

Heirarchic control architectures that combine two or more levels of control design

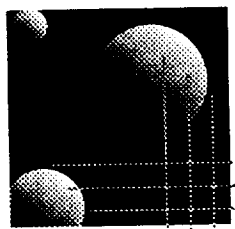
Probabilistic formulation of control design

SUMMARY

Optical Interferometer testbed captures essential configuration, physics, and performance metric of a class of spacecraft

Student theses directed at different aspects of controlled structures design

Near-term plans are demonstration of local and global control approaches on testbed and evaluation with full optical performance metric



MIT
Space
Engineering
Research
Center

Active Impedance Matching of Complex Structural Systems

Douglas G. MacMartin
David W. Miller
Steven R. Hall

July 1, 1991

N93-28169

9.24
155324

p. 19

Goal

- Active broadband control of uncertain modally dense structures.
- Use collocated feedback.
 - Positive real controller guarantees stability.
 - Low authority or local control (“active damping.”)
- Use local acoustic or statistical model of structure.
- Maximize power dissipation.
 - Equivalent to impedance matching.
 - Cannot match impedance exactly at all frequencies due to causality constraint.
- Experimental demonstration on complex structures.

Travelling Wave Model

- Describe junction dynamics using waves.
- Relate physical variables to wave modes:

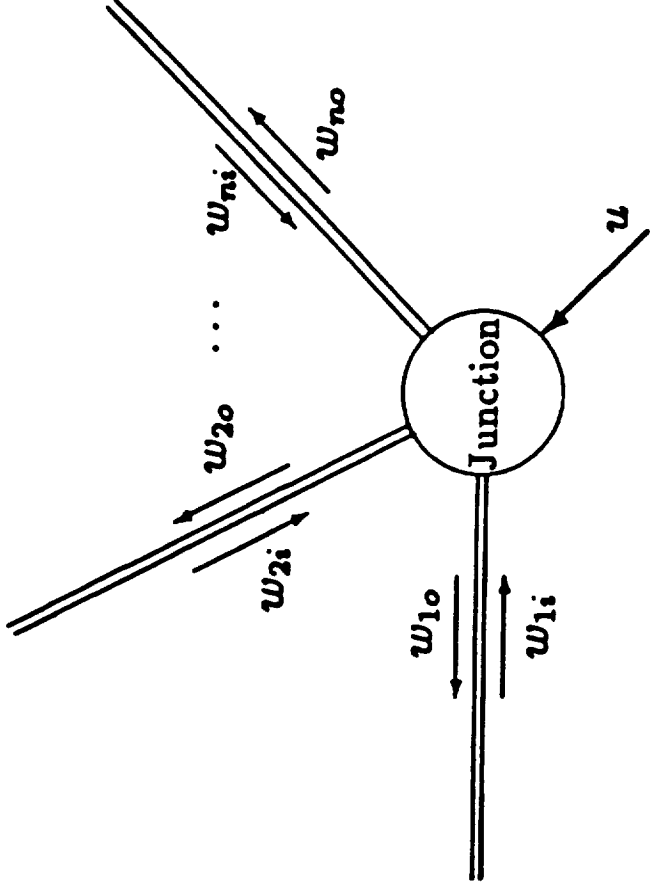
$$\begin{bmatrix} q \\ f \end{bmatrix} = \begin{bmatrix} Y_{qi} & Y_{qo} \\ Y_{fi} & Y_{fo} \end{bmatrix} \begin{bmatrix} w_i \\ w_o \end{bmatrix}$$

- Scattering and generation of waves:

$$w_o(s) = S(s)w_i(s) + \Psi(s)u(s)$$

- Relate physical variables to control:

$$q = (Y_{qo}\Psi)u + (Y_{qi} + Y_{qo}S)w_i$$

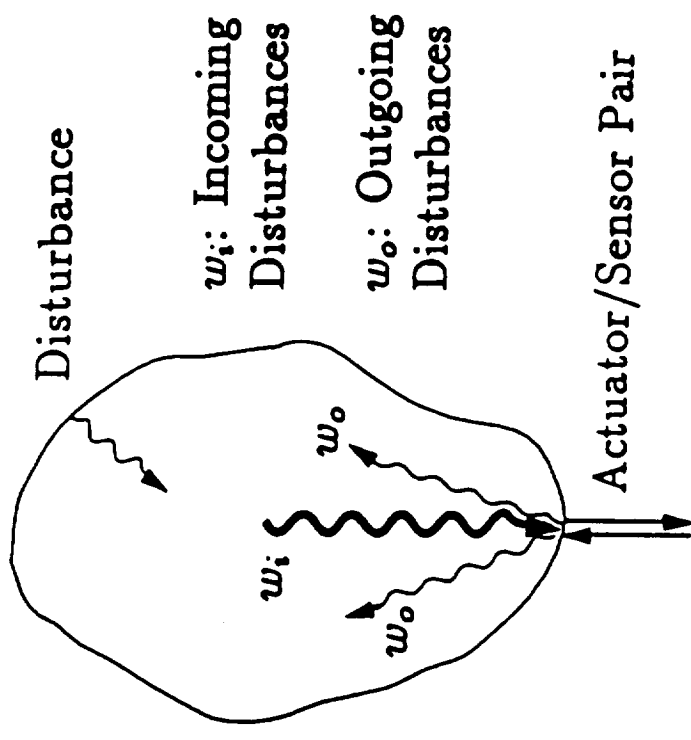


Dereverberated Mobility Model

- Total Response = Direct Field + Reverberant Field
- Response of form:

$$y(s) = G(s)u(s) + d(s)$$

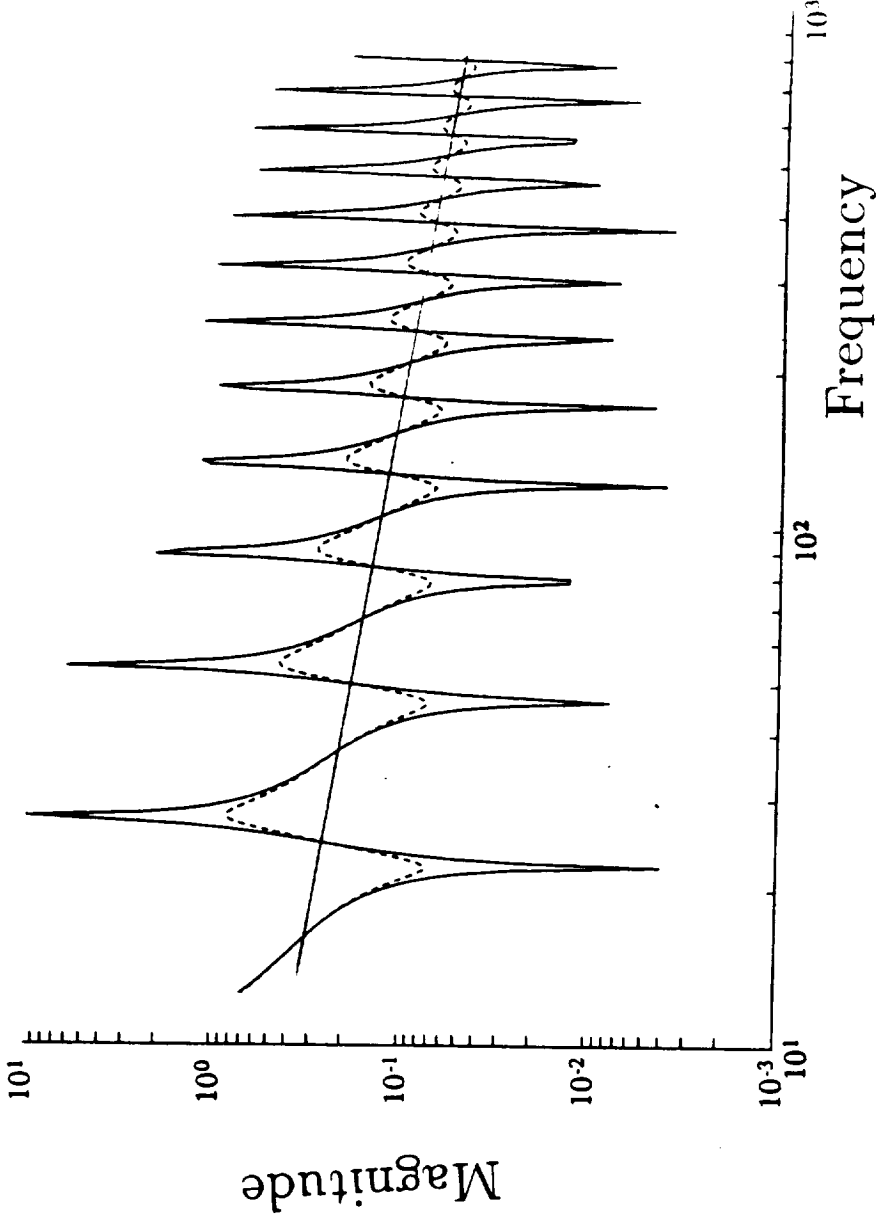
- Gives accurate model of local dynamics.
- Approach applicable to arbitrary structure.



Computation of Dereverberated Mobility

- From wave model:
- From averaging transfer function:

$$G = sT(Y_{qo}\Psi)$$



Control Problem: Optimal Impedance Matching

- Design compensator based on local model and apply to real structure.
- Minimize power flow into structure.

$$\mathbb{P}(\omega) = \text{tr} \{ \Phi_{uy}(\omega) + \Phi_{yu}(\omega) \}$$

- Maximum dissipation is obtained if the compensator is the conjugate of the structural impedance:

$$K(s) = (G(-s)^T)^{-1}$$

- This is noncausal!
- Problem is to match impedance as well as possible, subject to causality.

\mathcal{H}_2 -Optimal Solution

- Minimize rms power flow using Wiener-Hopf or LQG to guarantee causality.

$$\begin{aligned} J &= \int_{-\infty}^{\infty} \mathbb{P}(\omega) d\omega \\ &= \int_{-\infty}^{\infty} \text{tr} \{ \Phi_{uy}(\omega) + \Phi_{yu}(\omega) \} d\omega \end{aligned}$$

- Requires knowledge of disturbance spectrum Φ_{dd} .
- Local model is not conservative: departing energy does not return.
- No guarantee of stability on actual structure.
 - May add power at certain frequencies to achieve greater dissipation at others.

\mathcal{H}_∞ -Optimal Solution

- Guarantee stability by guaranteeing power dissipation at all frequencies:

$$\mathbb{P}(\omega) = \text{tr} \{ \Phi_{uy}(\omega) + \Phi_{yu}(\omega) \} < 0 \quad \forall \omega$$

- Instead, guarantee that the reflected power into the structure is less than the incoming power.
 - This is a standard \mathcal{H}_∞ control problem.
- Guaranteeing $\|T_{zw}\|_\infty < 1$ guarantees power dissipation at all frequencies.
- This also guarantees a positive real compensator.

Statistical Energy Analysis (SEA) Solution

- Model structure with average driving point mobility (a generalization of the dereverberated mobility.)
- Include knowledge that structure conserves energy.
- Guaranteed finite energy \Rightarrow Guaranteed stability.
- Minimize desired rms cost, expressed in terms of power flow.

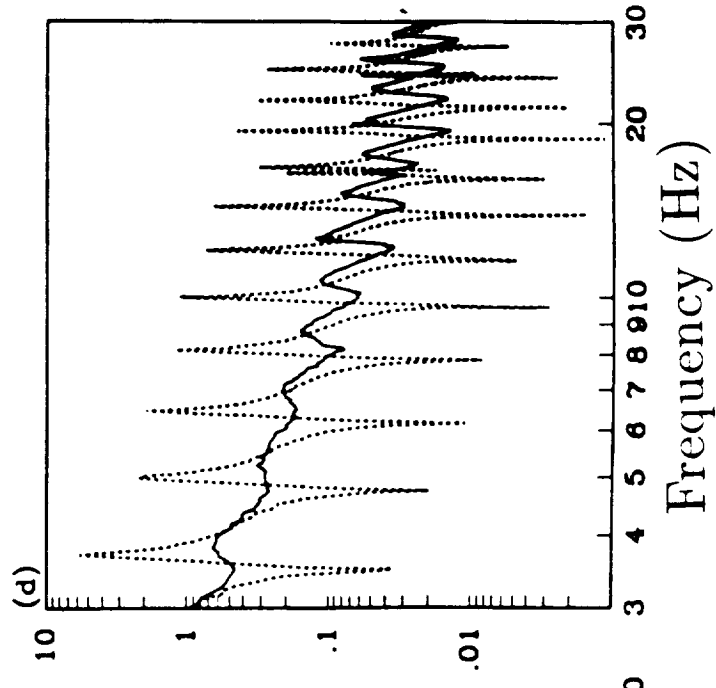
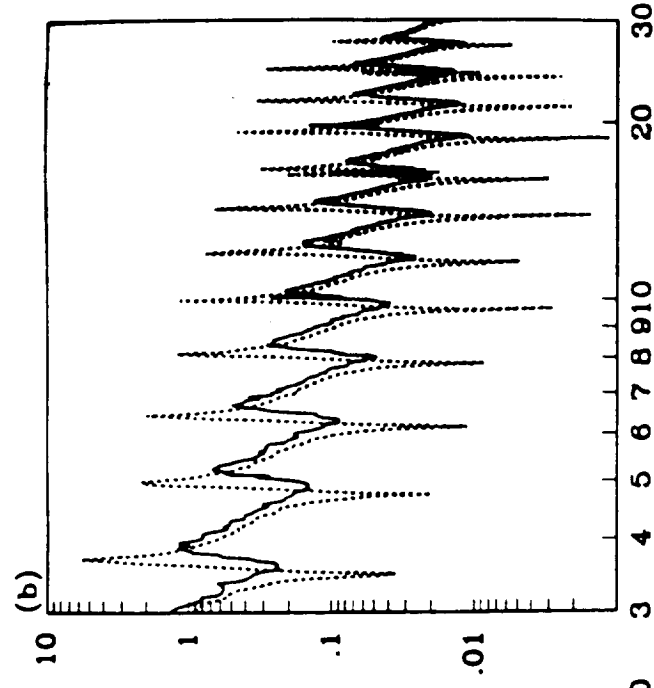
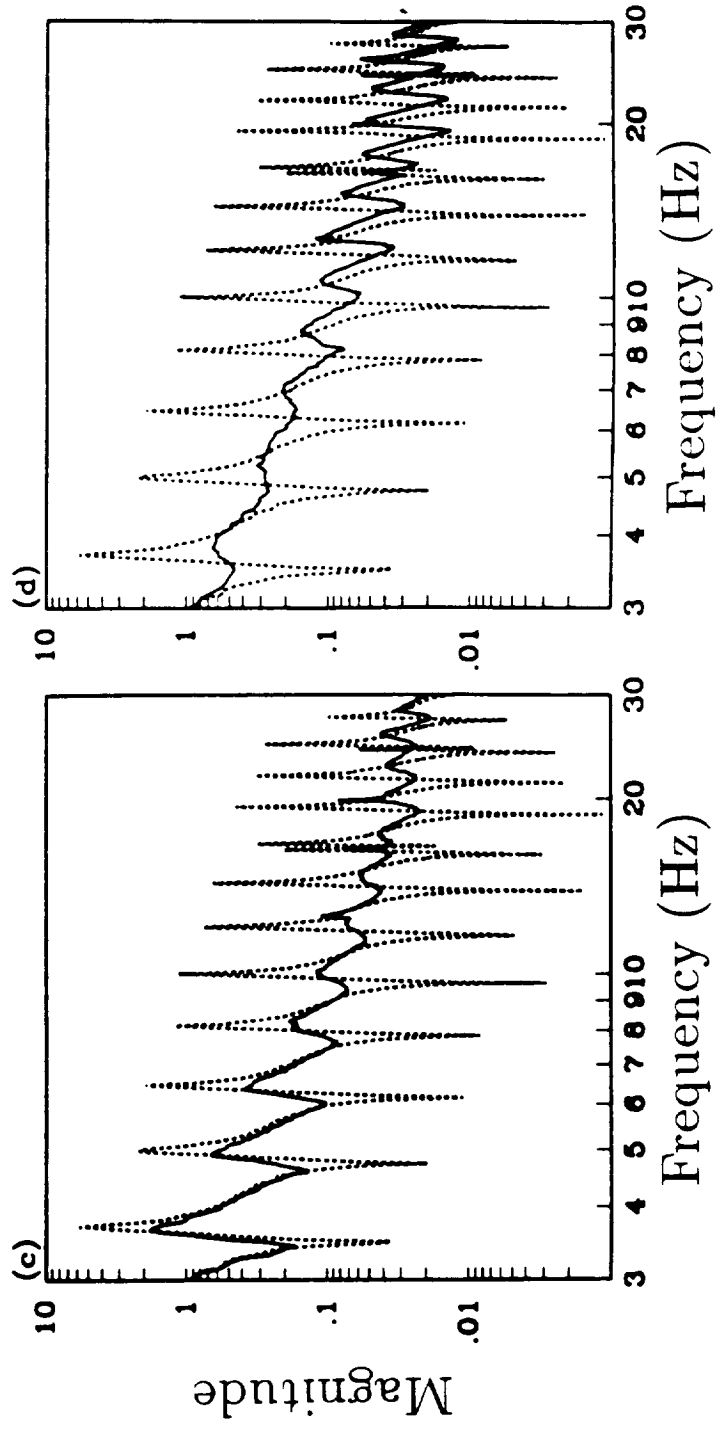
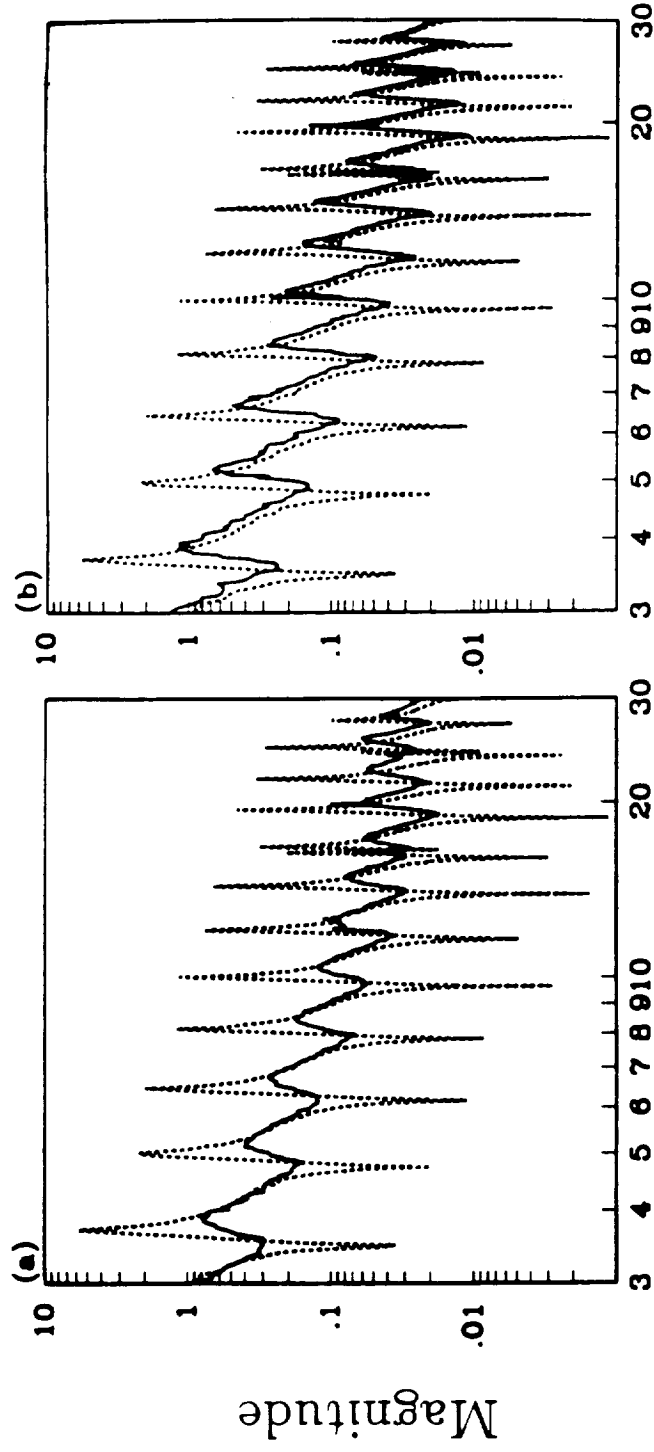
Experimental Transfer Functions

a) Rate

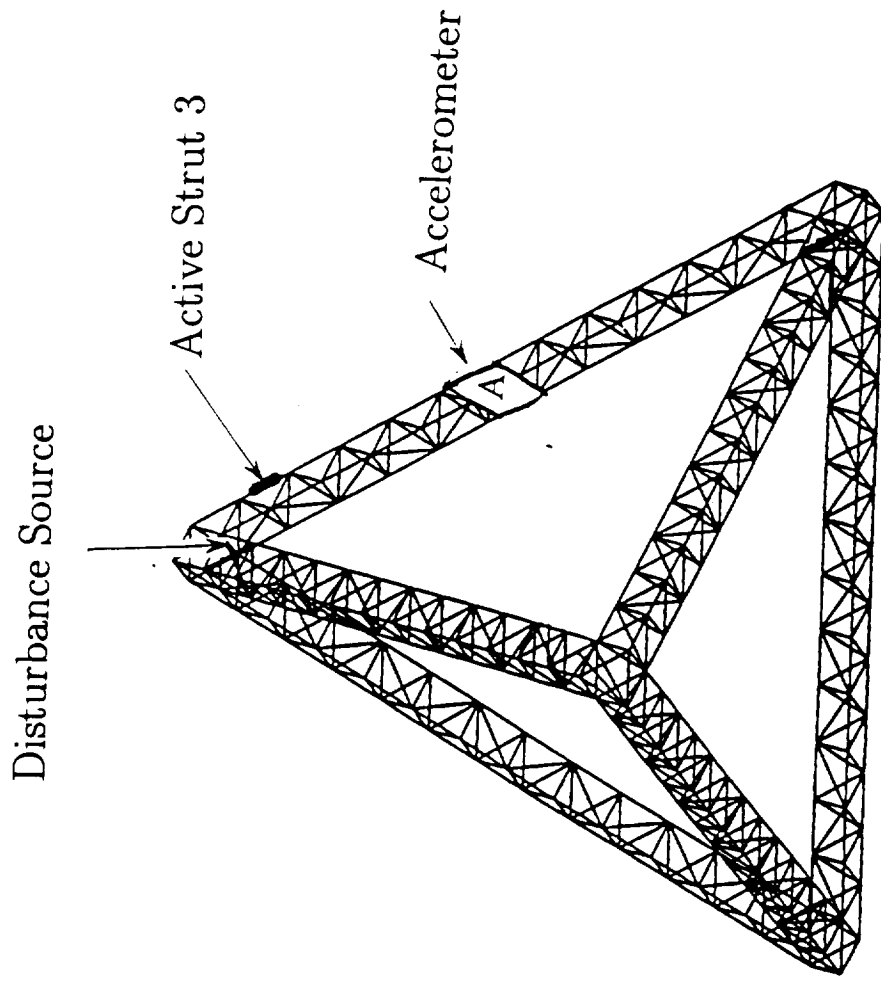
b) \mathcal{H}_∞

c) \mathcal{H}_2

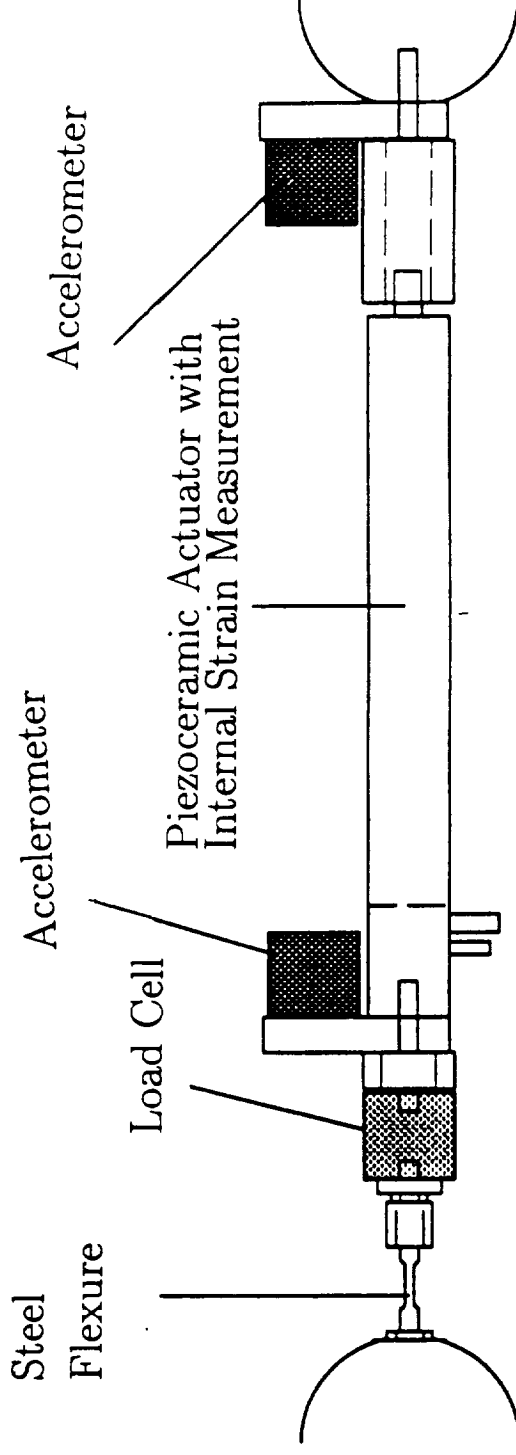
d) Weighted \mathcal{H}_∞



Interferometer Actuator and Sensor Locations



Active Strut Configuration



“Power” Dual Variables

- Force into structure and relative velocity across active strut are dual.
- Piezo stack stiffness is high \Rightarrow commands displacement.
 - Can also command relative velocity.
- Want compensator $K(s)$ such that

$$\begin{aligned}\dot{x} &= K(s)f \\ \Rightarrow x &= K(s)\left(\frac{f}{s}\right)\end{aligned}$$

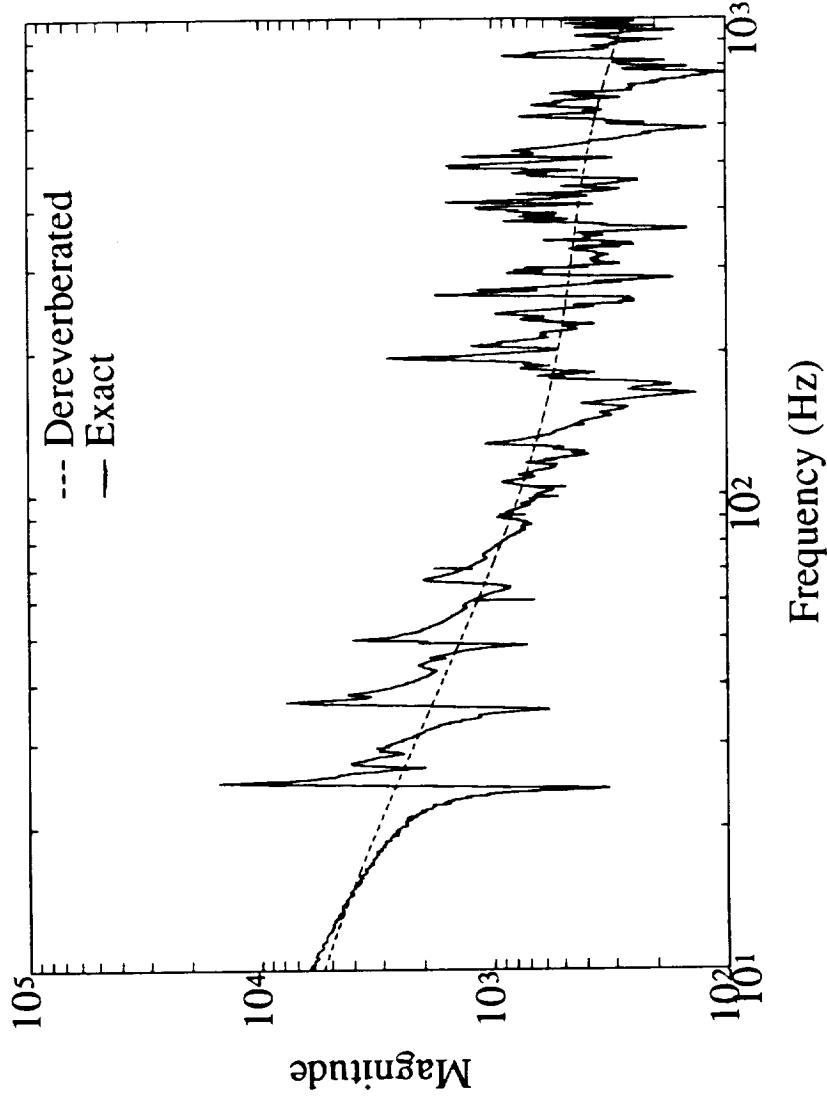
- Use integral of force feedback.

Dereverberation of Complex Structure

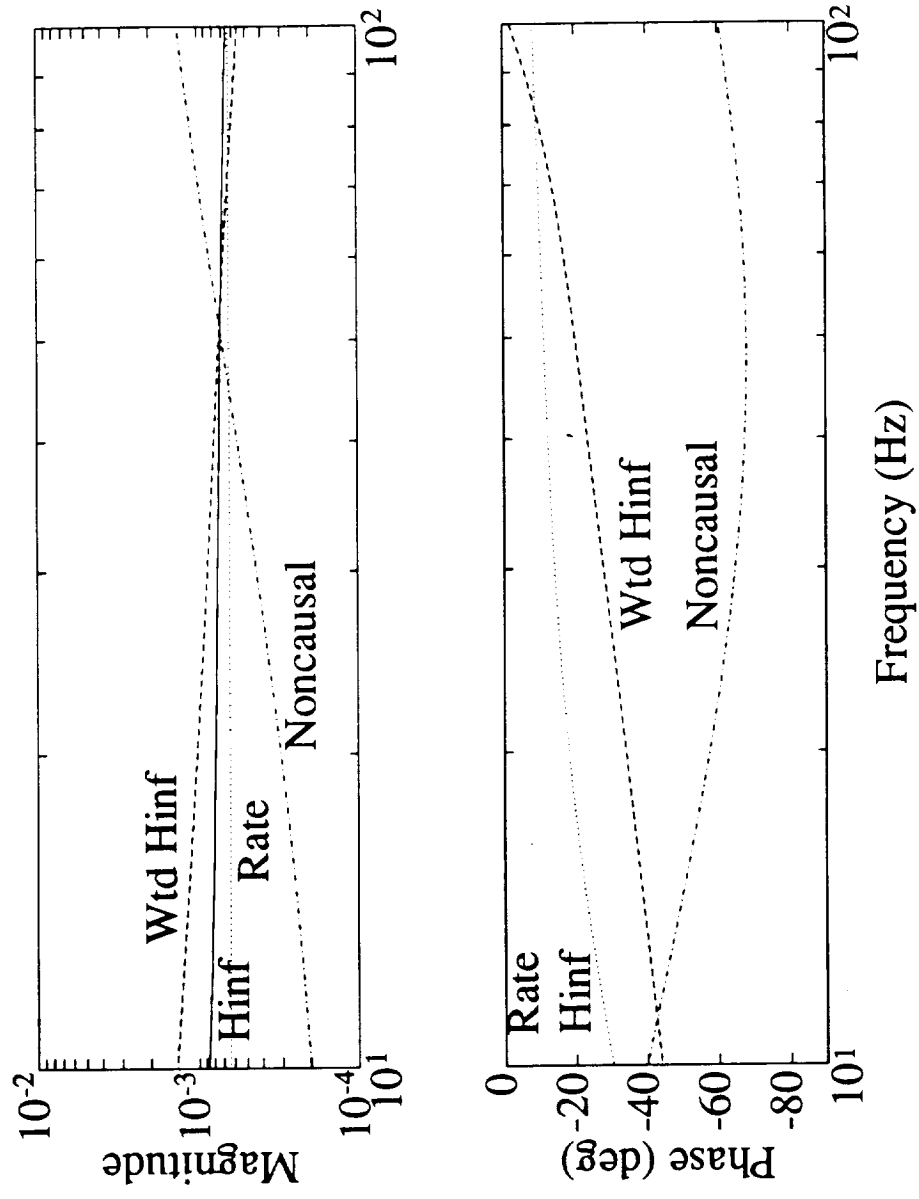
- Wave approach: truss behaves like a beam at low frequencies.
- Compute “best” fit of log magnitude using only real poles and zeroes.
- Fit transfer function using complex poles and zeroes, and add damping to resulting model.

Dereverberated Transfer Function

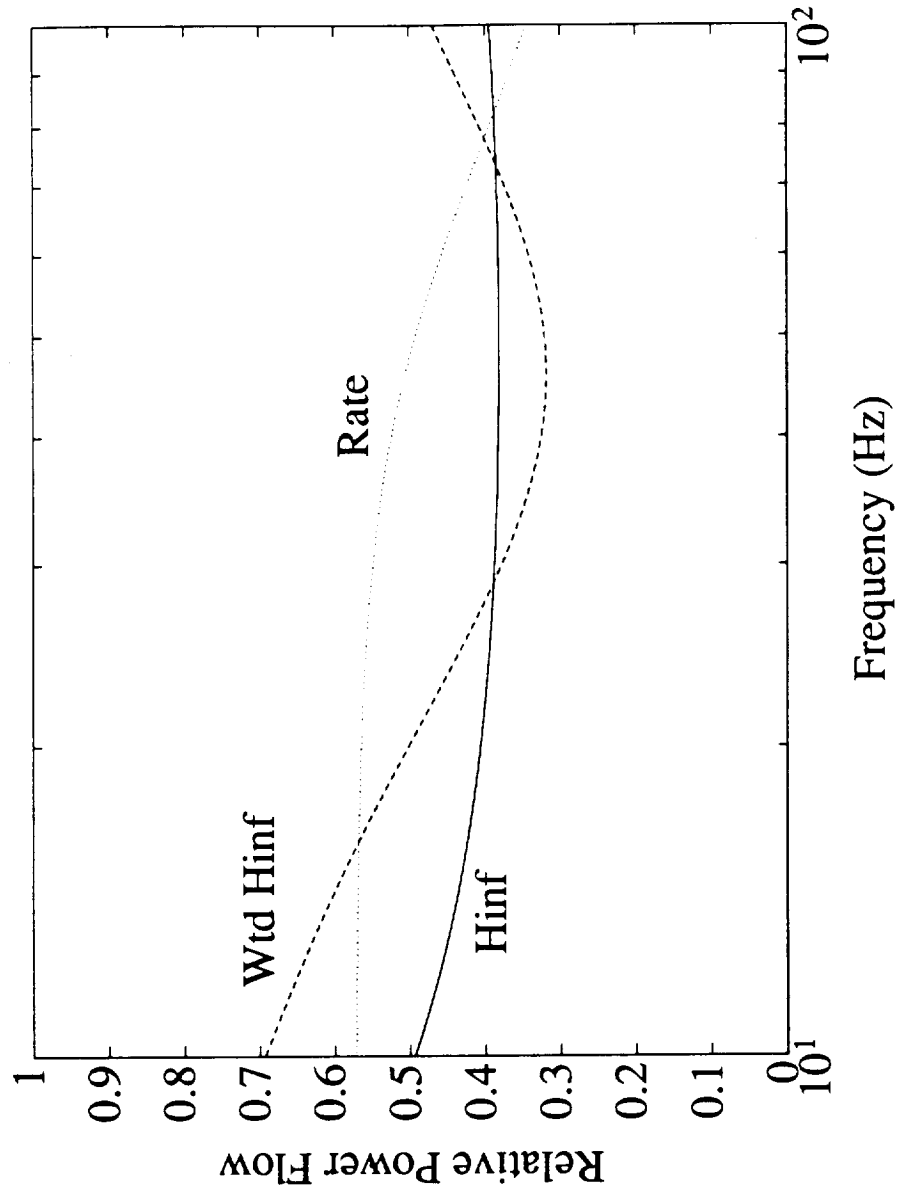
- Open loop transfer function from displacement to integrated force.
- Three (real) pole fit of log magnitude.



Compensators

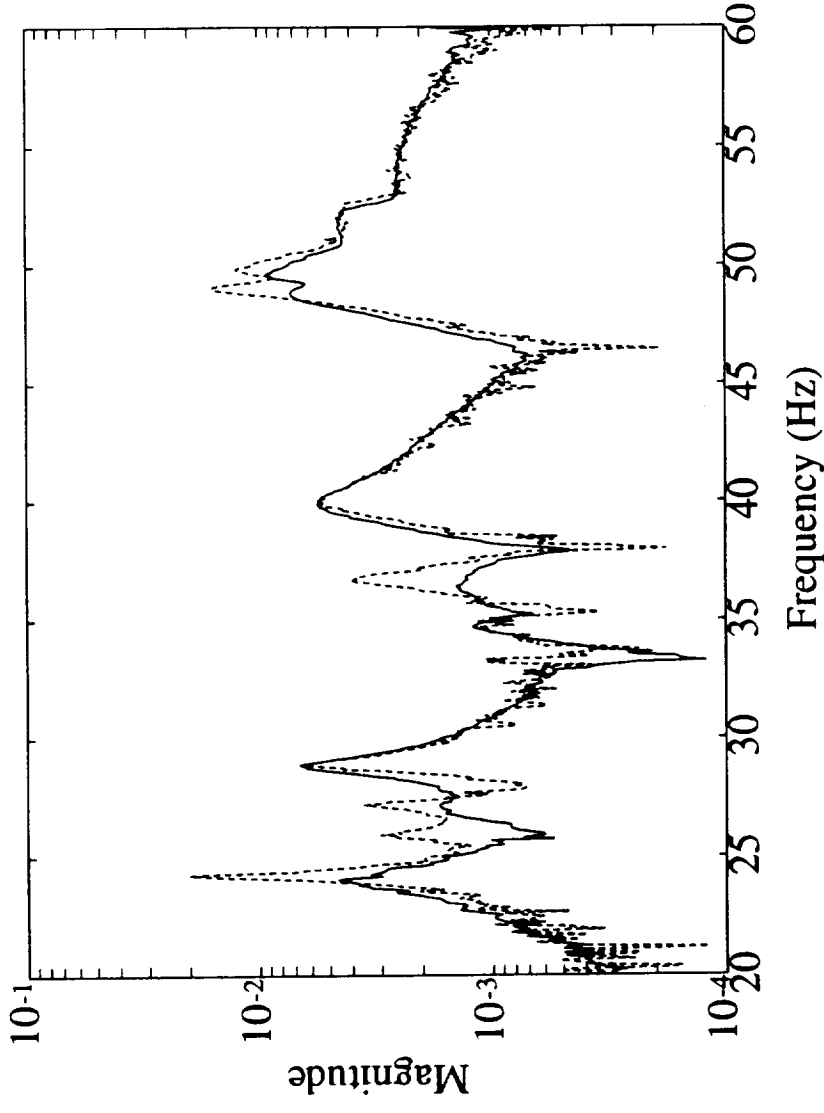


Relative Power Flow



Preliminary Experimental Results

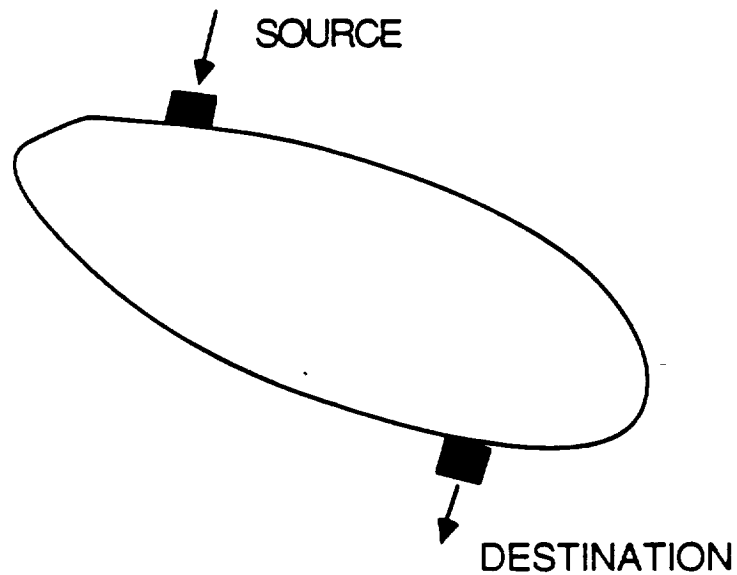
- Open and closed loop transfer functions from disturbance source to siderostat acceleration.
- Single constant gain loop closed around active strut # 3.



Conclusions

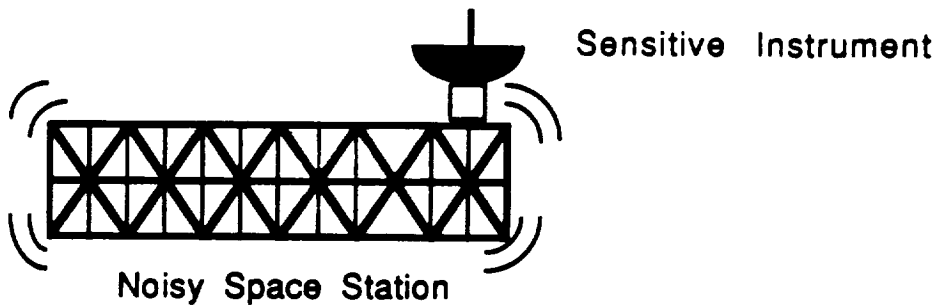
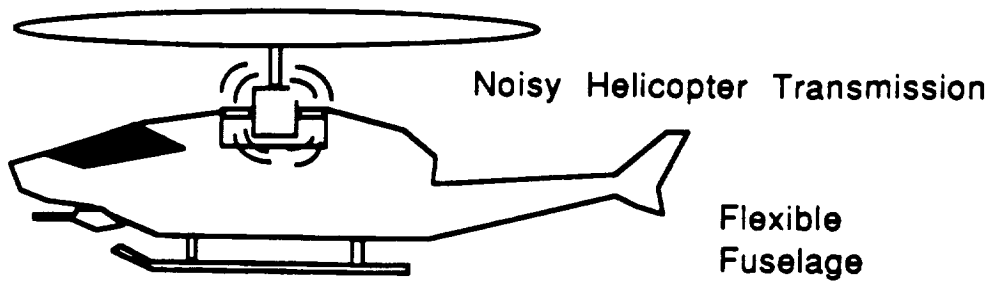
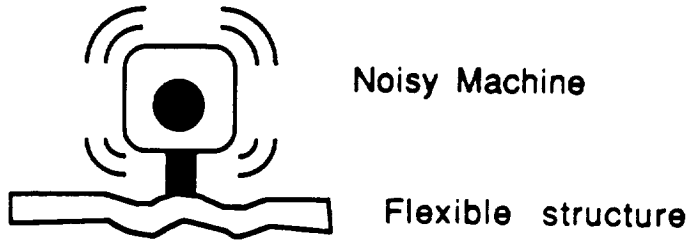
- Local model can be used for control design for uncertain modally dense systems.
 - Travelling wave or dereverberated mobility model.
- Ideal compensator for power dissipation is usually noncausal.
 - This is an impedance matching problem.
- \mathcal{H}_2 or \mathcal{H}_∞ optimal matches give good performance.
 - \mathcal{H}_∞ approach guarantees stability.
 - Weighting functions introduce flexibility.
- Concepts can be applied to arbitrarily complex structural systems.
 - Some damping added with simple compensator.
 - Expect more damping possible with better impedance match.

ACTIVE VIBRATION ISOLATION



- NOISY SOURCES, SENSITIVE DESTINATIONS
- OPPORTUNITIES FOR ACTIVE CONTROL
- CURRENT WORK / FORECAST

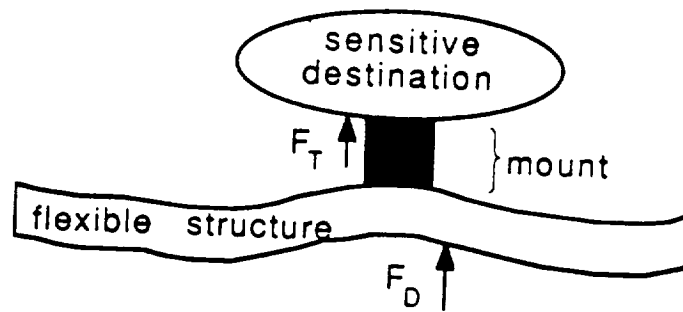
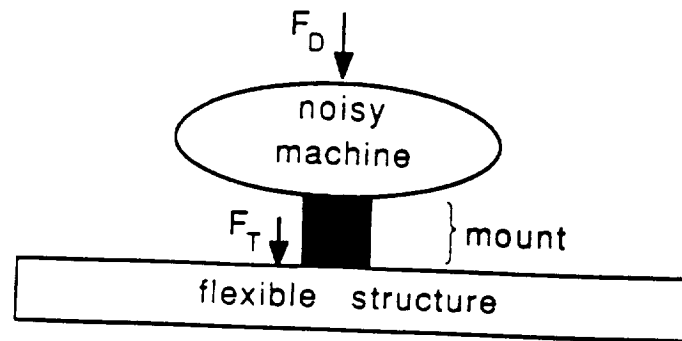
Applications



Common Features:

- The mount represents a "bottle neck" in the disturbance path.
- Structural Response is poorly known.

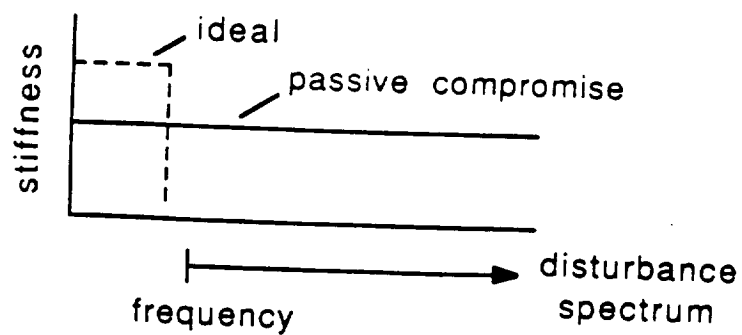
DYNAMIC MACHINERY ISOLATION



F_D = disturbance force

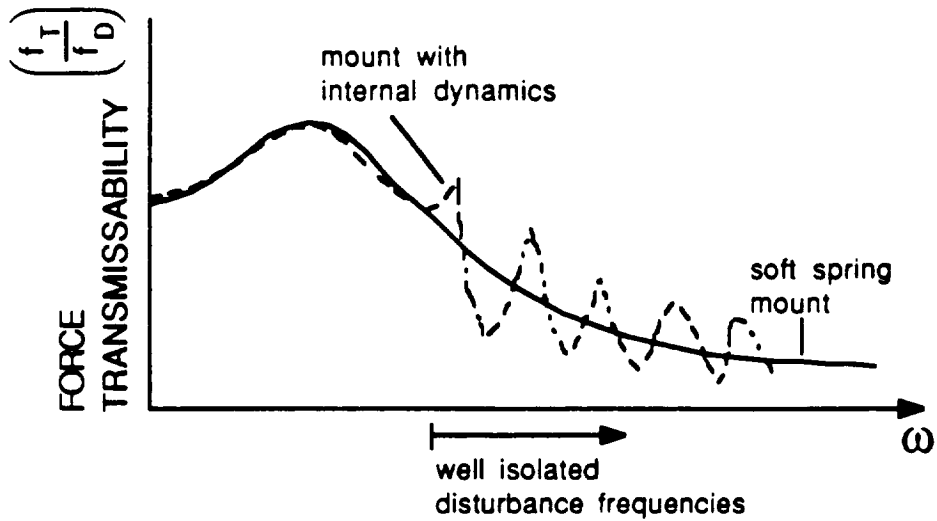
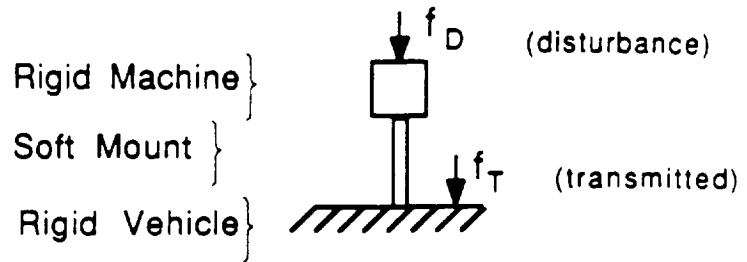
F_T = transmitted force

STIFFNESS OF MOUNT

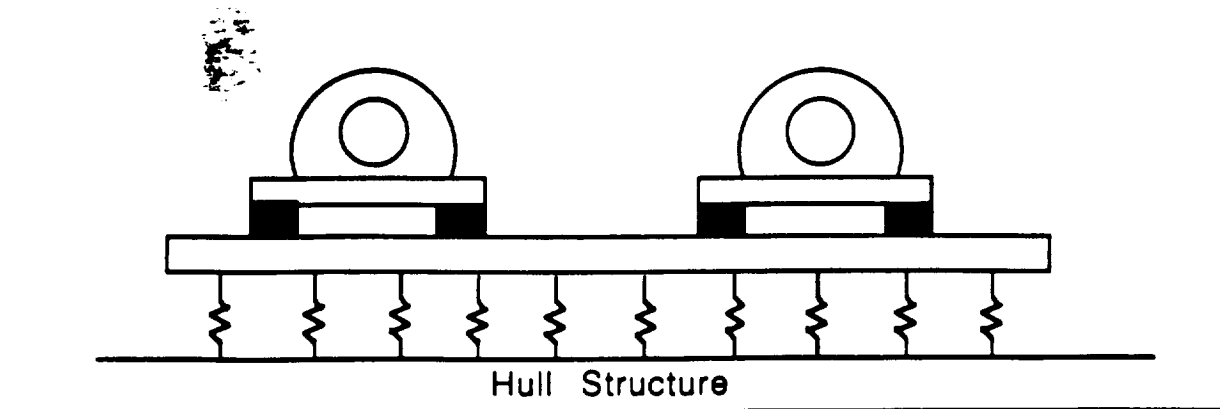


TRADITIONAL PASSIVE MOUNT DESIGN

DESIGN MODEL:

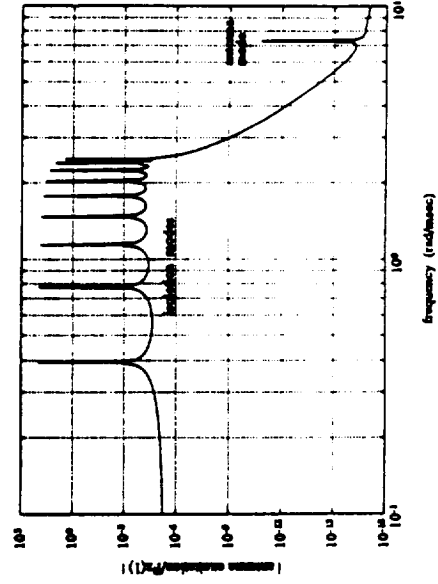
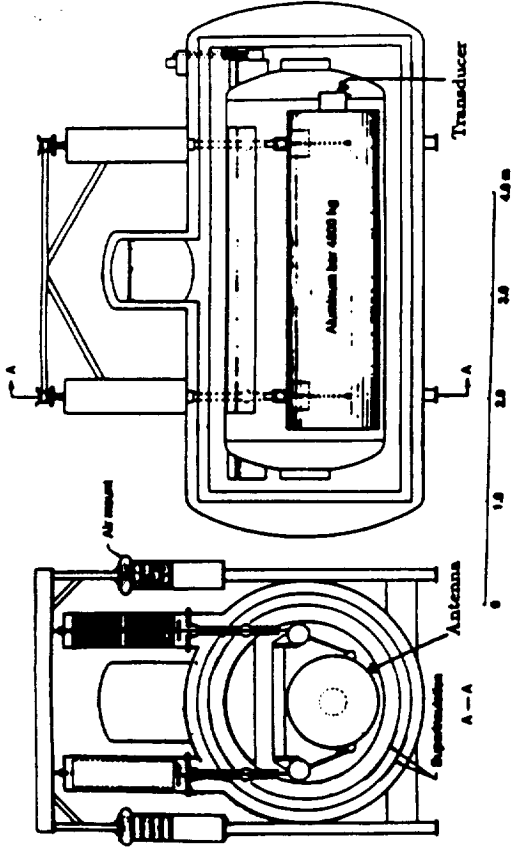


EXAMPLE: Naval Machinery Raft



EXAMPLES OF PASSIVE ISOLATION

GRAVITY WAVE INTERFEROMETER



Space
Station
PPS

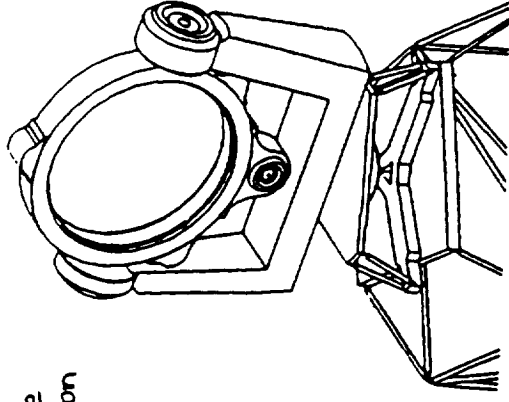


Fig 4 Configuration of Gimbal Pointer Model with Passive Base Isolator

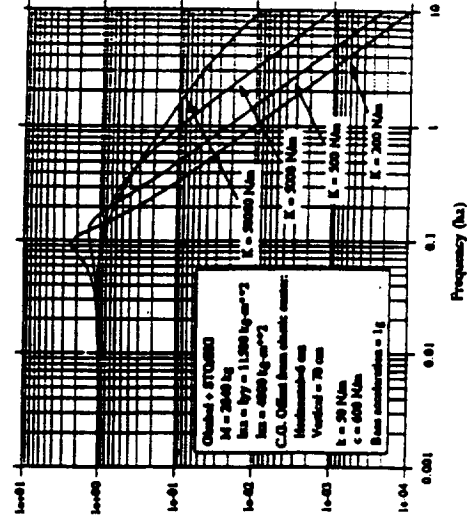


Fig 6 Isolator Performance vs Secondary Stiffness K

RESPONSE FREQUENCIES:

Machine:



Mount:

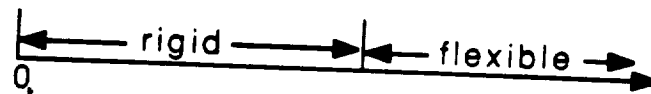


Vehicle



MODELING APPROACHES:

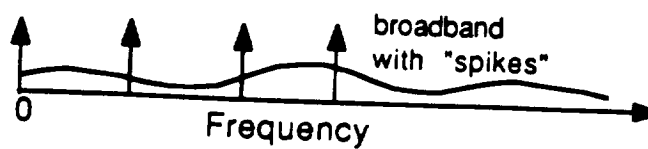
Machine:



Vehicle

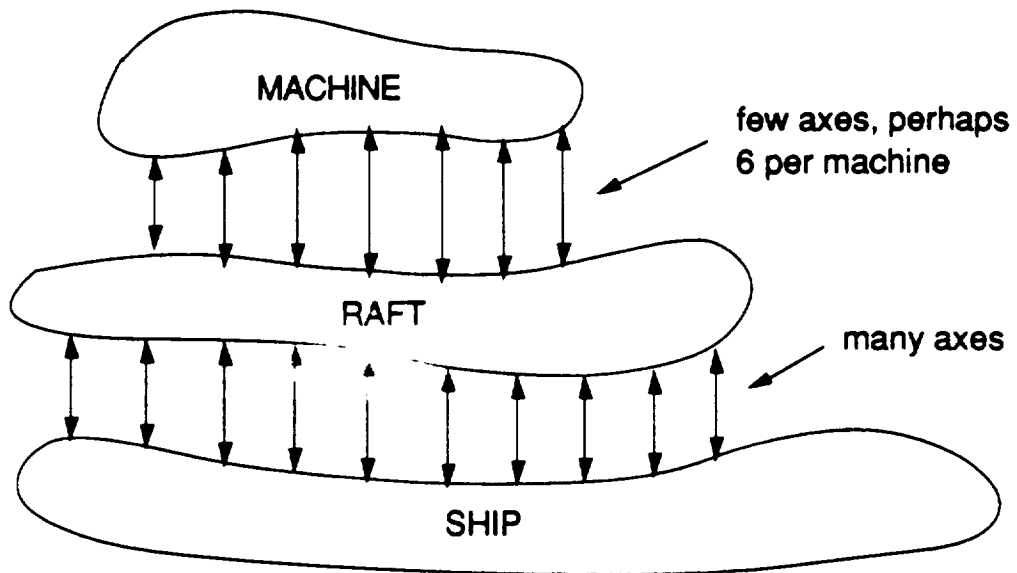


DISTURBANCE SPECTRUM



HOW MANY INDEPENDENT MOUNT AXES?

If $\omega_{Dist} < \omega_{Flex}$, then a flexible body is rigid.



OVERVIEW OF ACTIVE APPROACHES FOR MACHINERY ISOLATION

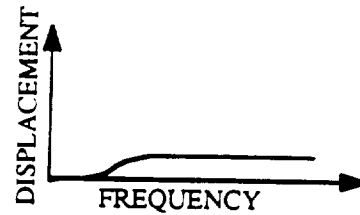
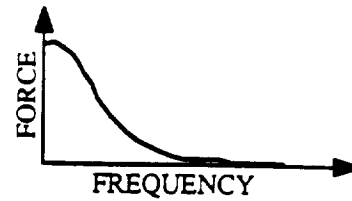
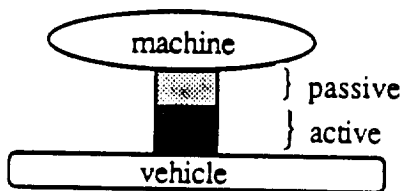
- Broadband / Semi-passive
- Narrowband

ACTUATOR OPTIONS

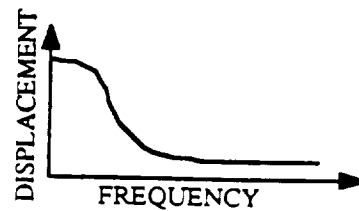
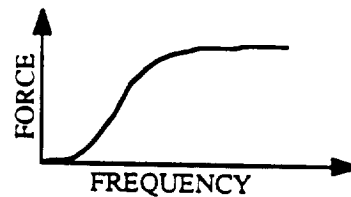
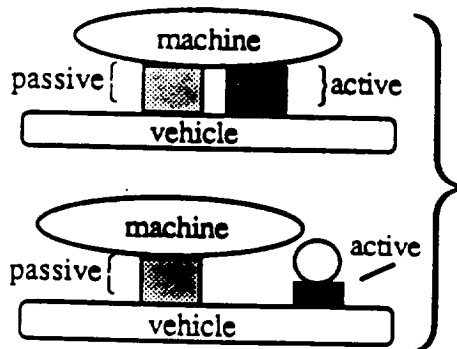
GEOMETRY

ACTUATOR REQUIREMENTS

ACTUATOR IN THE LOAD PATH:

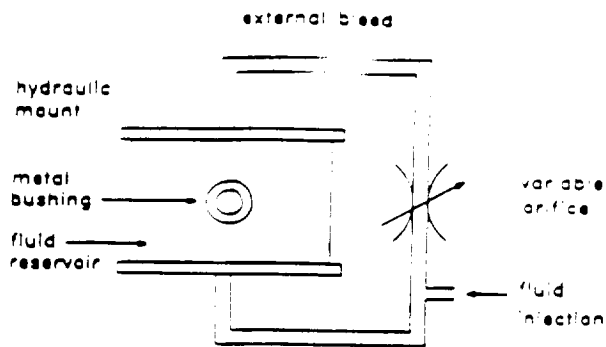


ACTUATOR PARALLEL TO THE LOAD PATH



BROADBAND/SEMI-PASSIVE

1) Variable viscous damping:



Graf & Shoureshi, 1987
(also much work on
vehicle suspensions)

Figure 1a The Semi-Active Hydraulic Mount

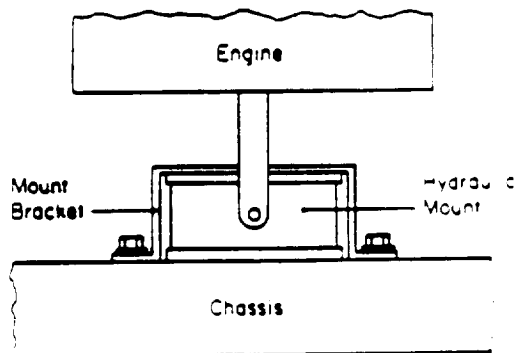


Figure 1b Installation of a Hydraulic Mount

BROADBAND/ACTIVE

Newport Corp EVIS Vibration Table (1988)

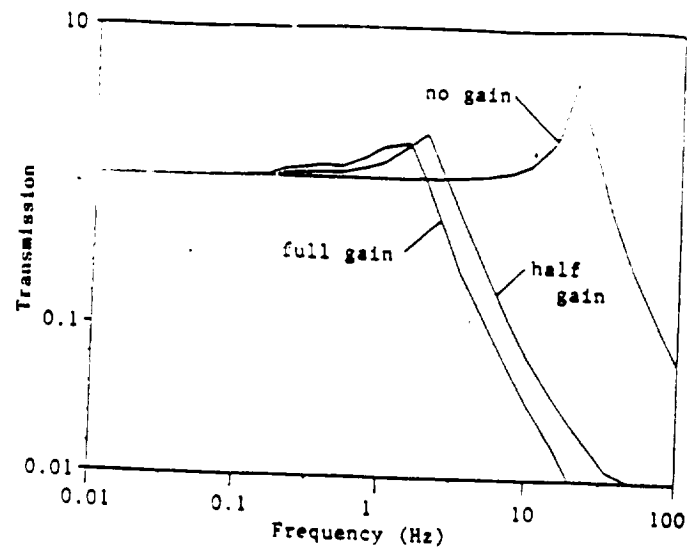


Figure 2. Transmission by EVIS of vibrations from the support to the working surface as a function of frequency.

Sperry Corp. FEAMIS Magnetic Isolation System

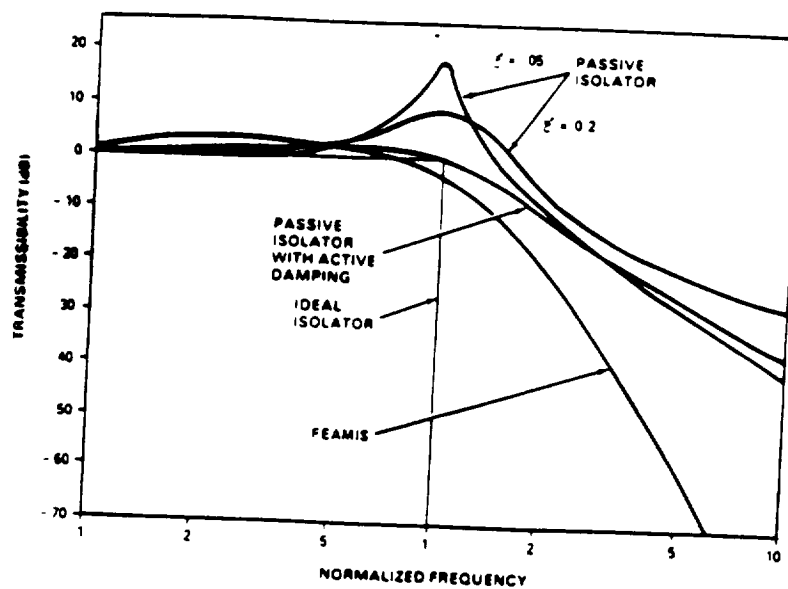
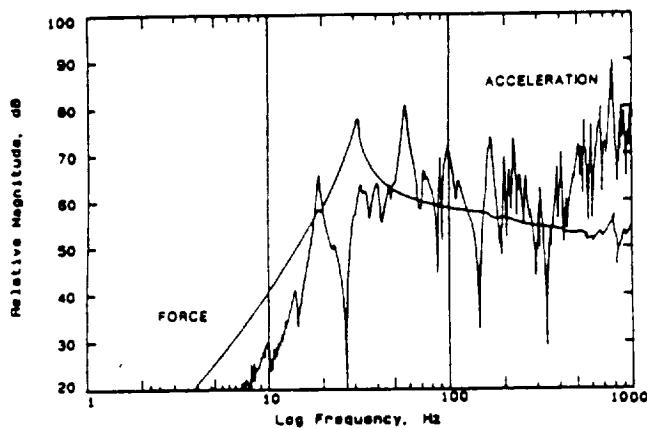
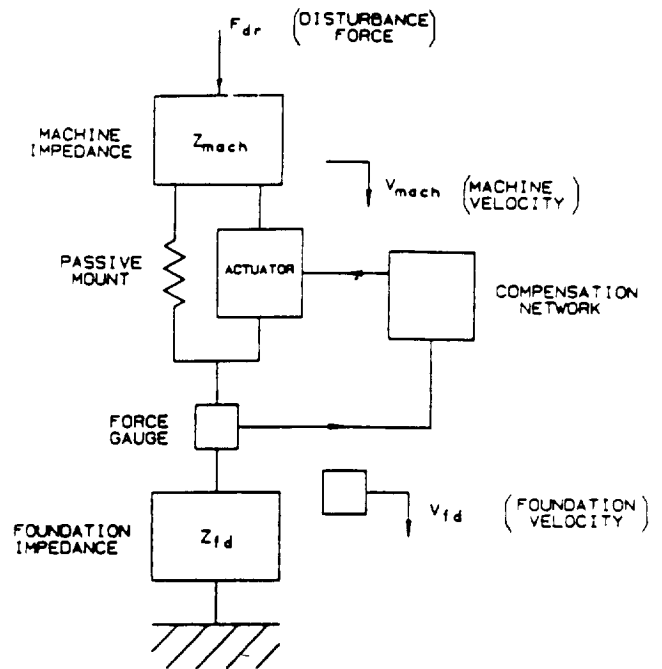
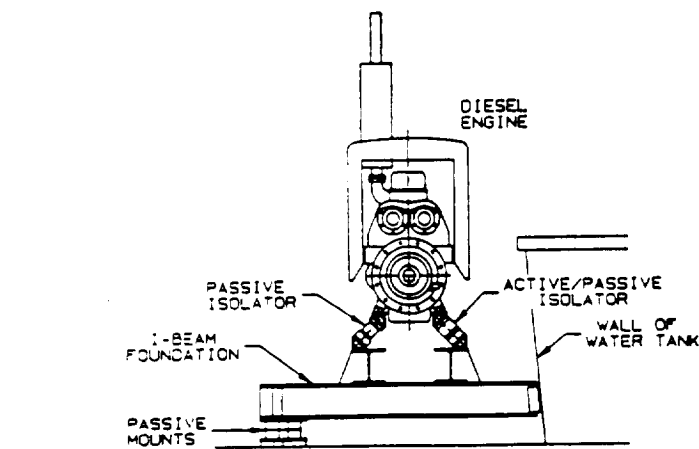
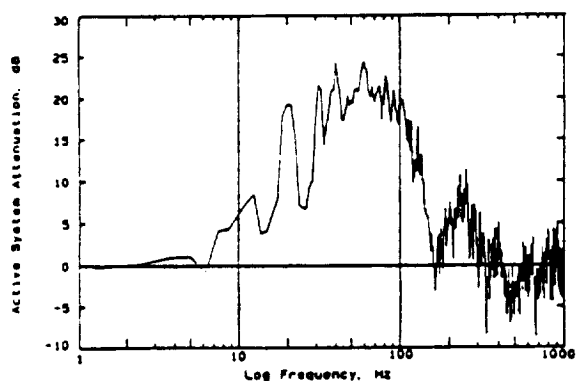
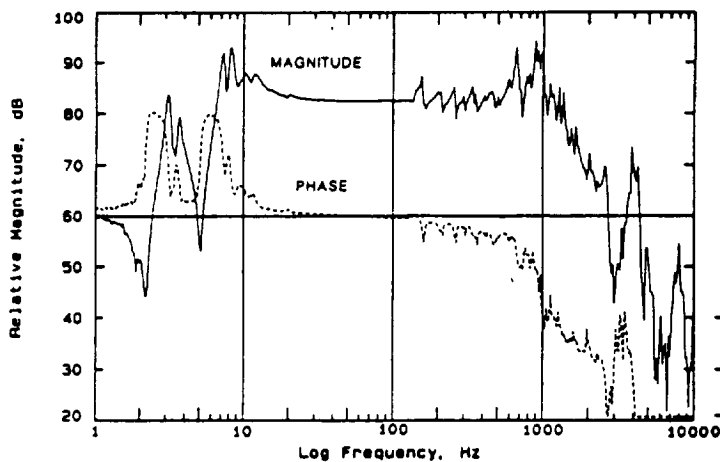


Fig. 5 Isolator Response Comparison

BROADBAND SINGLE AXIS FEEDBACK (WATERS ET. AL. 1989)



THE MOUNT FORCE SENSOR
IS A BETTER FEEDBACK
SENSOR THAN ACCERATION



10. Ratio of Transmitted Force into Foundation for Active/Passive Mount Relative to Passive Mount

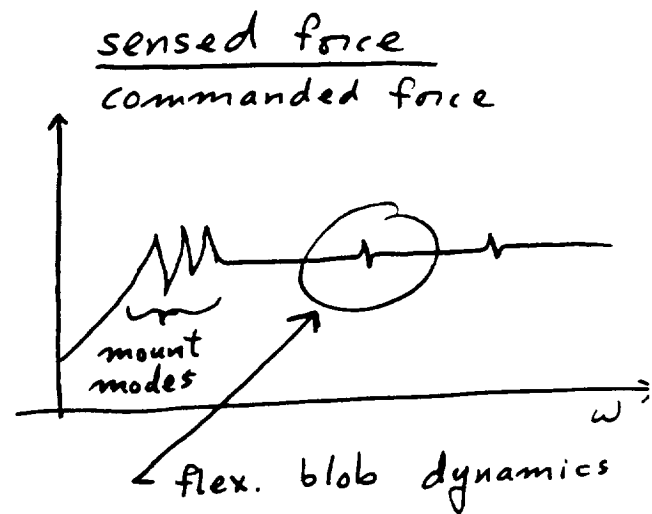
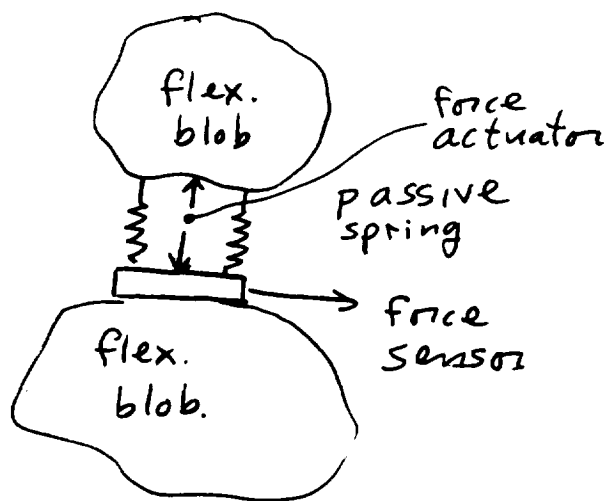
Fig. 7. Open-Loop Frequency Response for Uncompensated System

BROADBAND FEEDBACK DOES NOT SELECTIVELY
ATTENUATE NARROWBAND DISTURBANCES

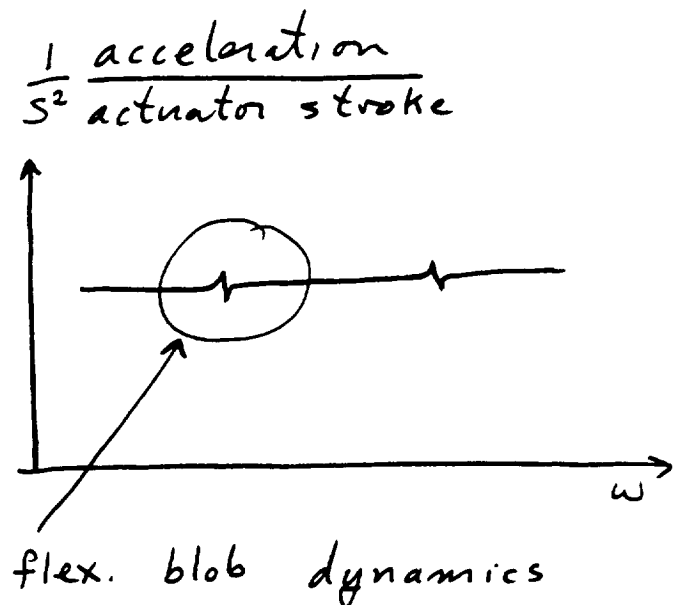
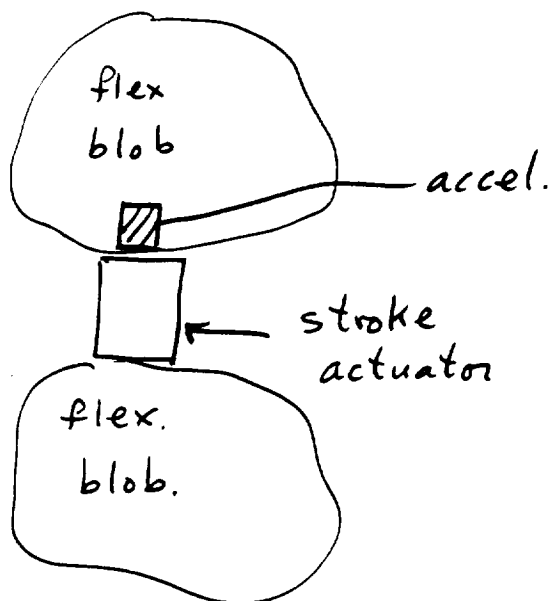
IMPEDANCE MATCHED SENSOR / ACTUATORS

(FOR ROBUST BROADBAND
ACTIVE ISOLATION)

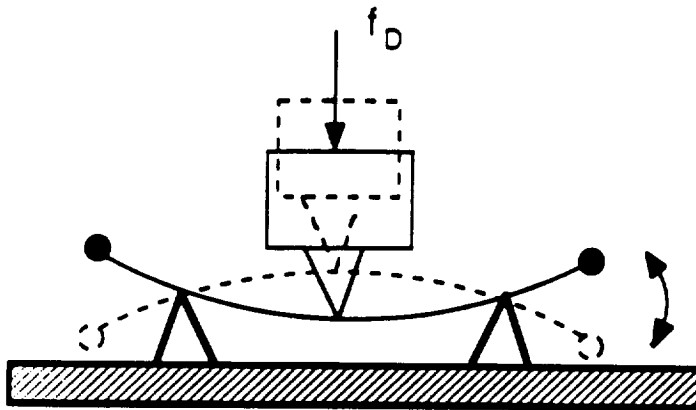
FORCE (ZERO IMPEDANCE)



DISPLACEMENT (INFINITE IMPEDANCE)

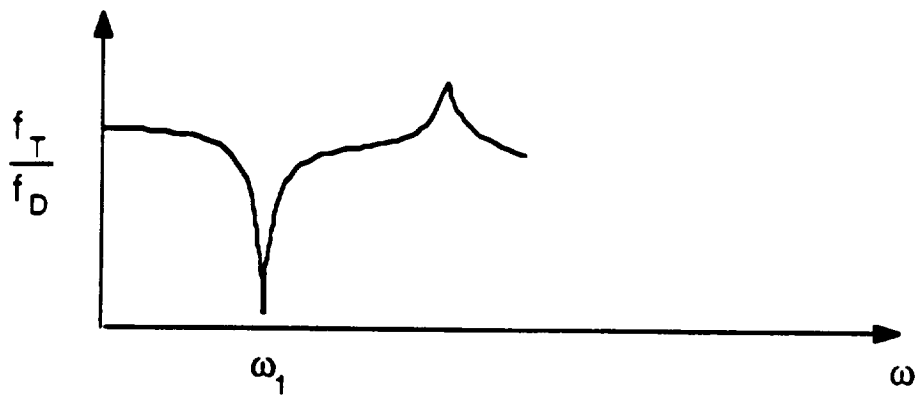


A PASSIVE NARROW BAND ISOLATION MOUNT



$$f_D = \sin(\omega_1 t)$$

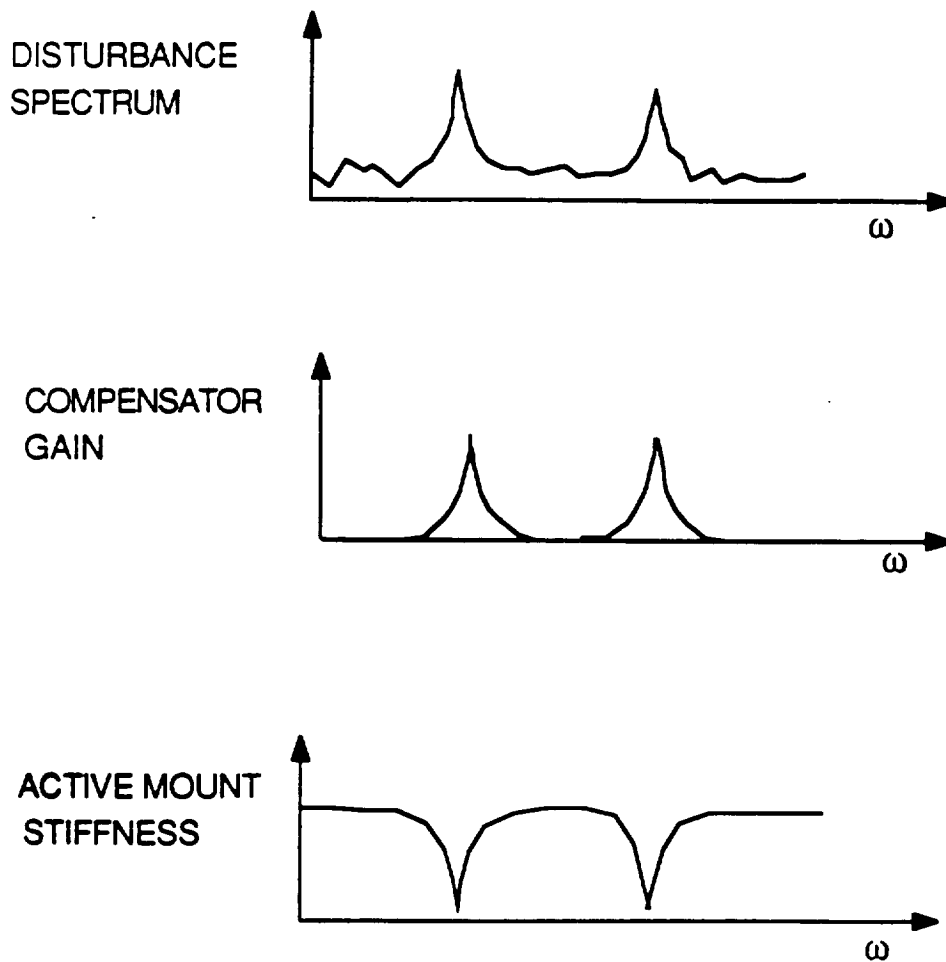
(A tip-weighted beam
in bending)



USE: VIBRATION ISOLATION MOUNTING OF A
HELICOPTER FLOOR

NARROWBAND/ACTIVE

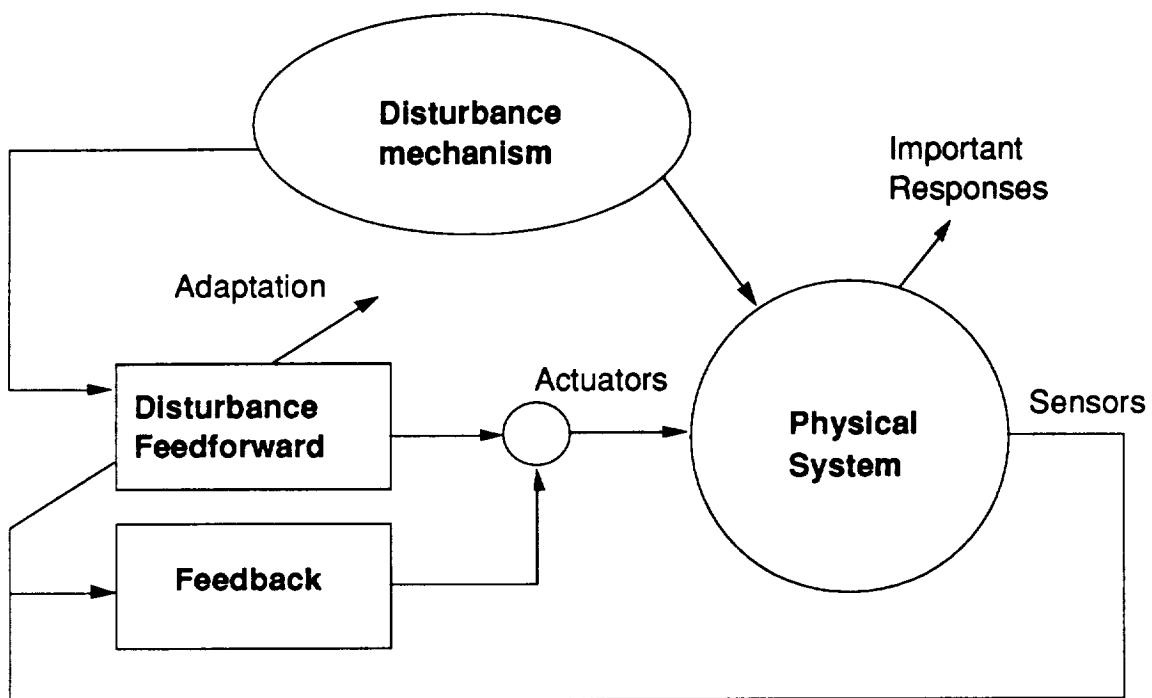
Basic principle: Provide compensator gain only at (well-known) disturbance frequency. Avoid destabilizing unmodelled dynamics.



MIMO implementation?

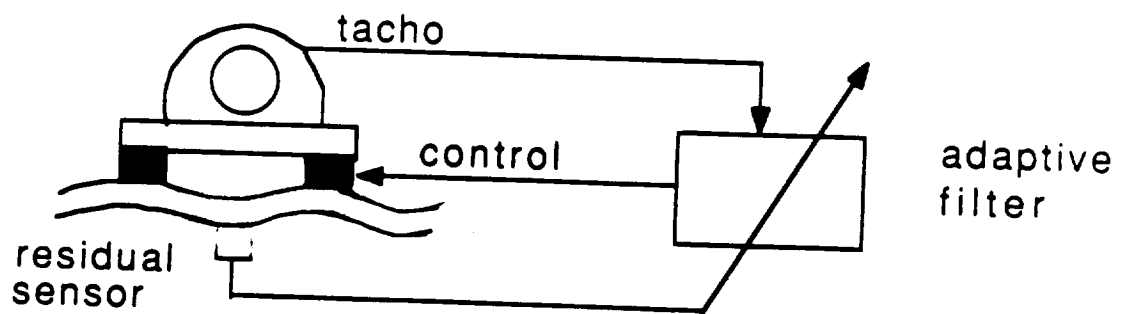
CLASSIFICATION OF APPLICATIONS AND ACCOMPLISHMENTS

Generic

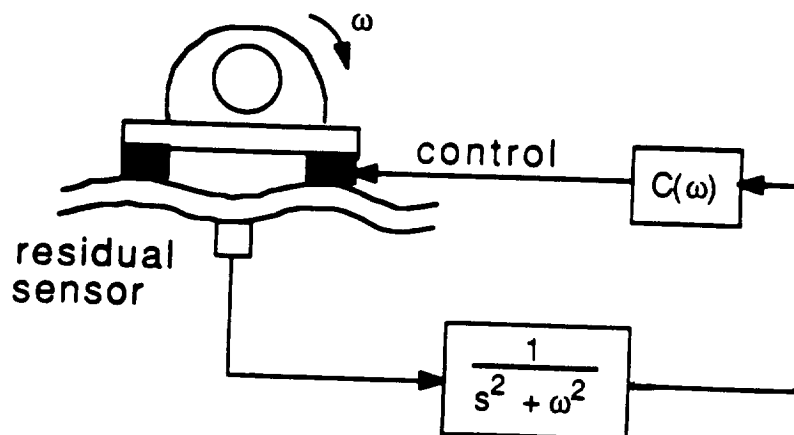


NARROWBAND/ACTIVE CONTROL SYNTHESIS TECHNIQUES

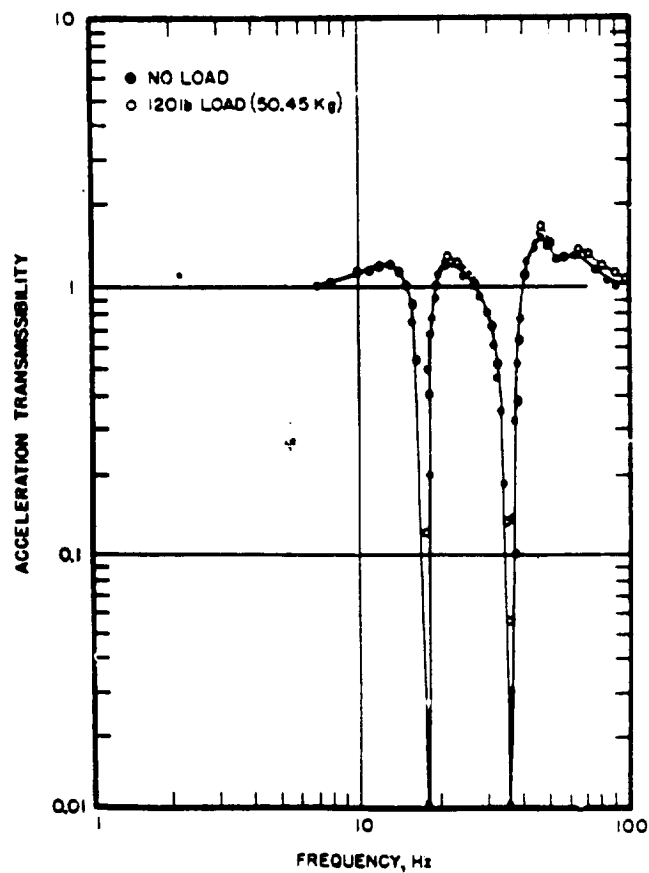
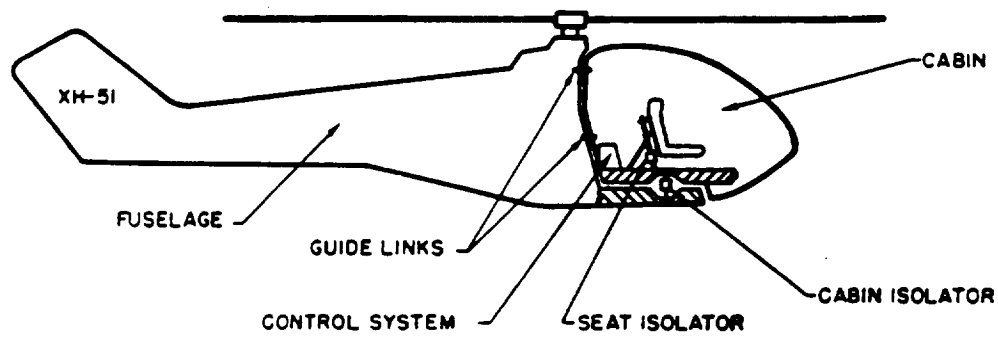
Adaptive Signal Processing:



Tuned Oscillator in Feedback Loop:



NARROWBAND/ACTIVE



Allen & Calcaterra
(1972)

Figure 21: Vertical Transmissibility of Active Seat Isolator in Isolate Mode Measured During Laboratory Tests

NARROWBAND/ACTIVE

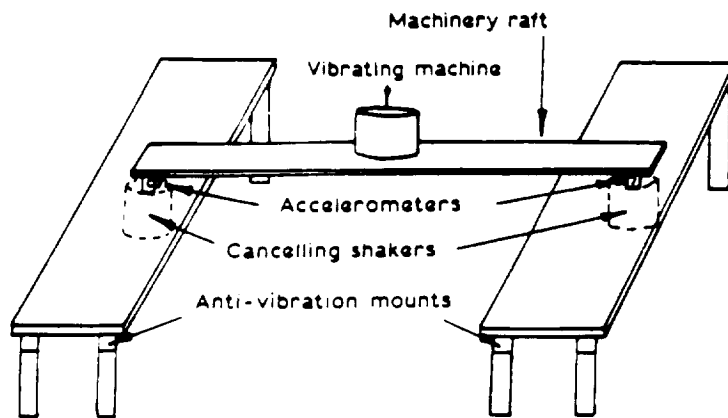


Fig. 3.

White & Cooper
(1984)

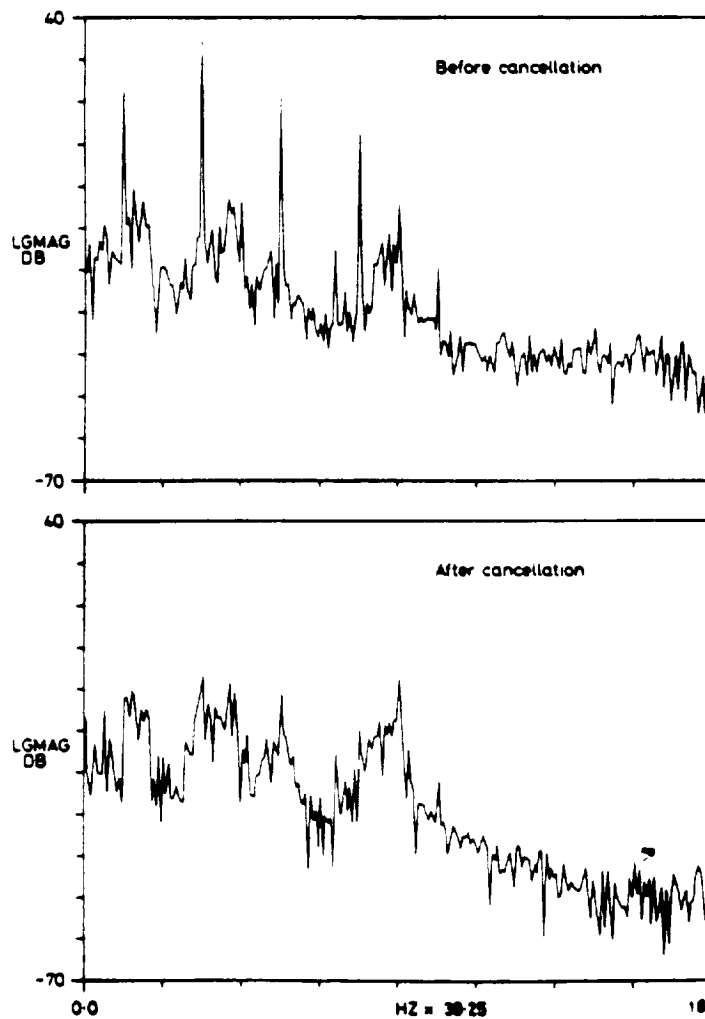


Fig. 7. Sensor 1 autopower spectra.

NARROWBAND/ACTIVE

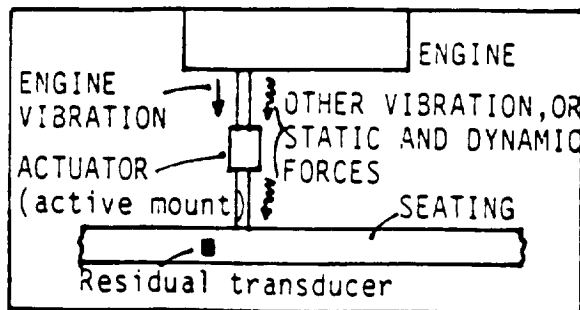


Fig. 5 The active engine mount prevents engine vibration reaching the seating but ignores all other forces. It thus holds the engine rigidly aligned. Any vibration from other parts of the structure which may be transmitted via the seating to the mount (ie, the reverse direction) is treated identically — it is ignored and not cancelled. This is an essential feature of any active mount since cancellation would not be occurring at "source" and would result in actual enhancement in other parts of the structure.

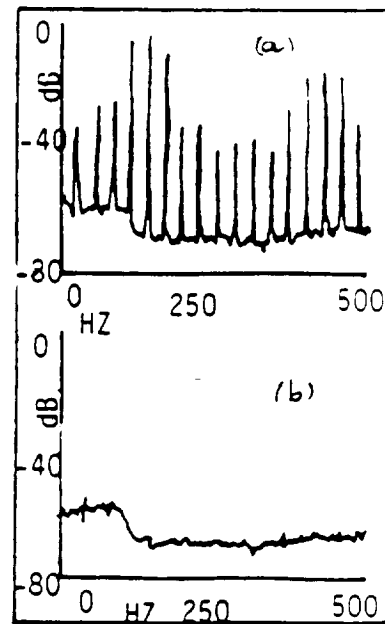
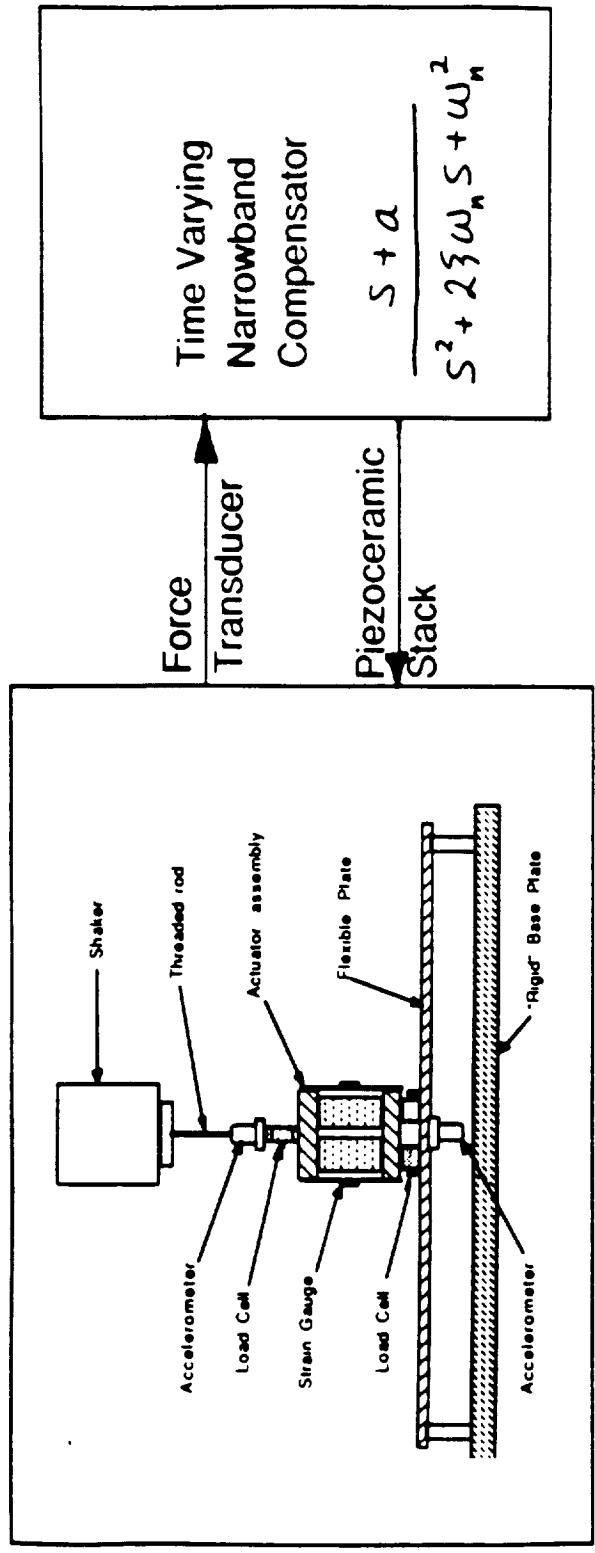


Fig. 6 Typical periodic spectrum from the active vibration cancellation rig — (a) before cancellation, (b) after cancellation.

EGHTESADI & CHAPLIN (1987)

TRACKING A TIME-VARYING PERIODIC DISTURBANCE

Narrowband Vibration Isolation

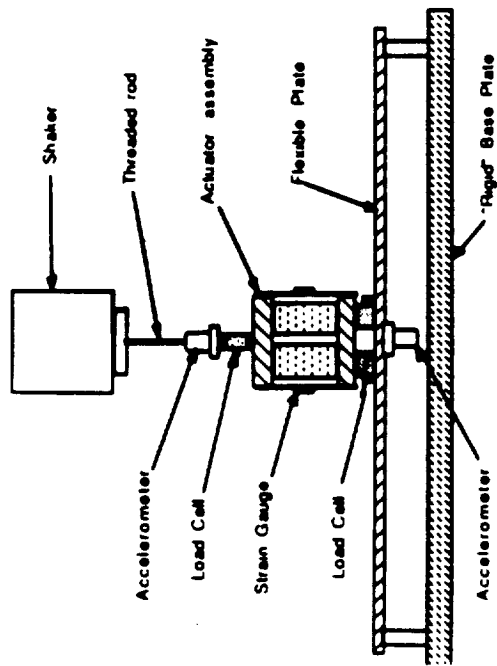


$$\omega_n = \omega_{\text{dist}} \text{ (time-varying)}$$

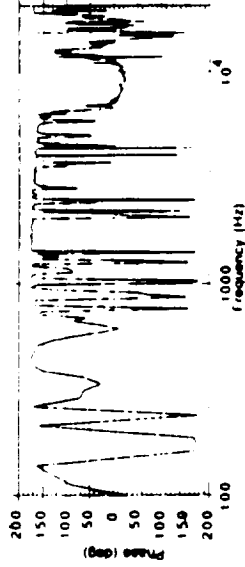
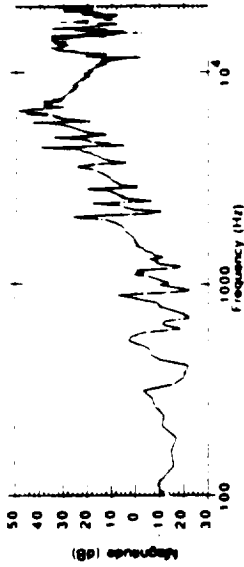
$$\zeta = \zeta_{\text{plant}} \text{ (best)}$$

(TRACK THE DISTURBANCE
FREQUENCIES THROUGH
RESONANCES)

Narrowband Vibration Isolation

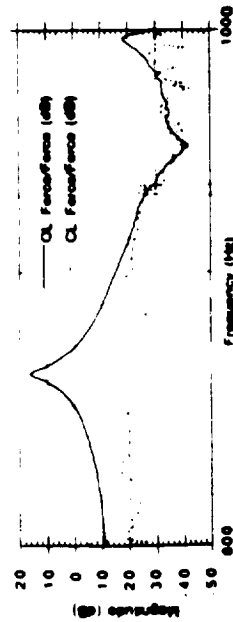


Apparatus



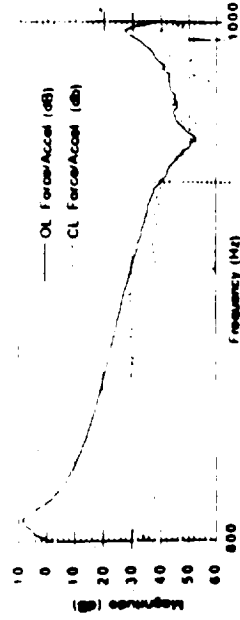
Measured Plant Transfer Function

Active Isolation Performance: (Time Varying Sinusoidal Disturbance)



Light Machine

→ swept in
one second →



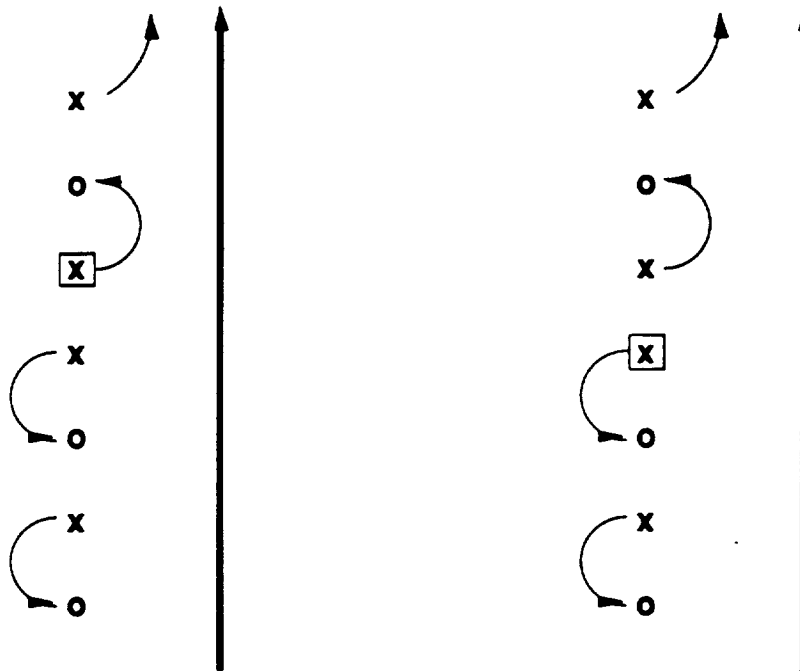
Massive Machine

→ swept in
one second →

UNKNOWN PLANT PHASE

Compromise between performance and stability:

Possible root - loci (local):



(Collocated force sensor, piezo actuator)

Compromise:

Make compensator damping ratio equal to plant damping ratio

(Limits theoretical active disturbance attenuation to $1/\zeta$)

A STUDY OF ERROR SENSORS AND IMPORTANT AXES

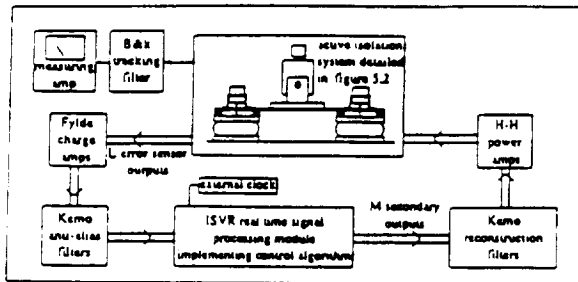
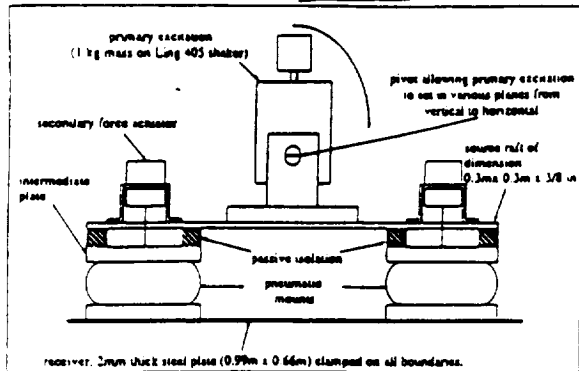
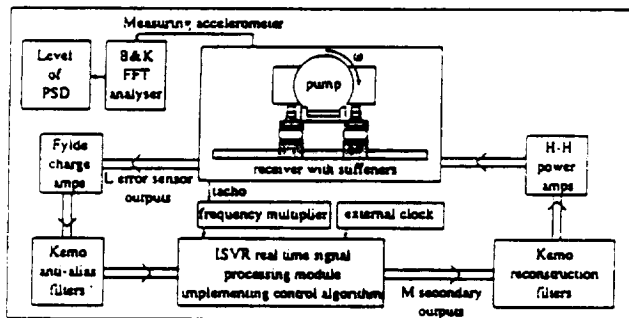


Figure 1. Details of the mount design and laboratory experimental rig



3.66 m

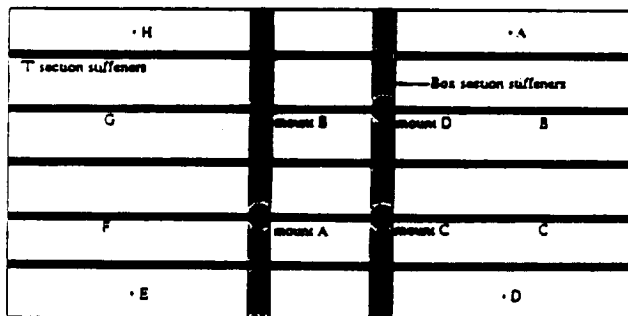


Figure 2. Section of the experimental system used to measure the reductions in PSD for the diesel installation, also shown is a plan view of the receiver and measurement locations

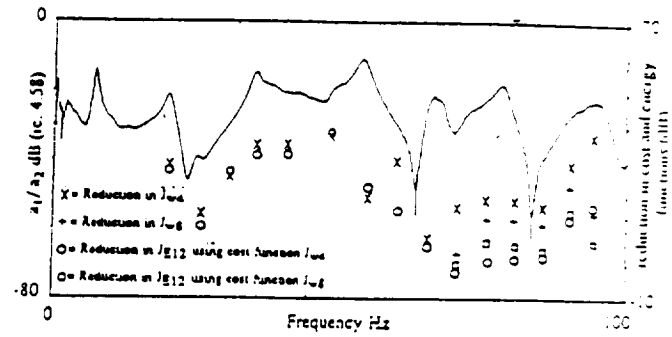


Figure 3. Reductions in cost and energy functions for the system with vertical primary excitation.

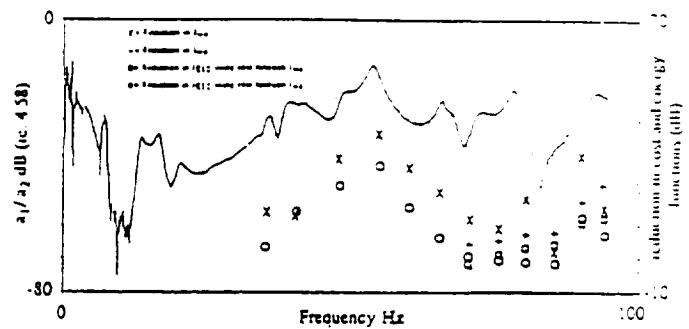


Figure 4. Reductions in cost and energy functions for the system with horizontal primary excitation.

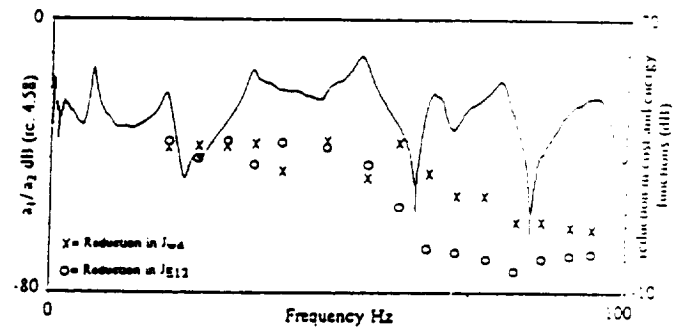


Figure 5. Reductions in cost and energy functions for the system with vertical primary excitation and the error sensors located on the intermediate plates.

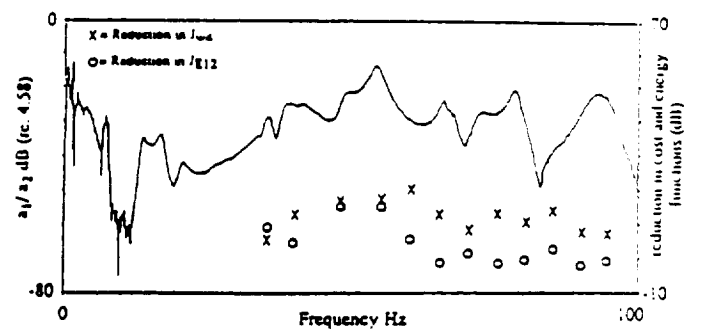


Figure 6. Reductions in cost and energy functions for the system with horizontal primary excitation and the error sensors located on the intermediate plates.

SUMMARY

- Error sensors should be carefully selected
- Colocated force transducers make good error sensors
- Flanking paths may be important
- Uncontrolled axes are flanking paths
- Active isolation of periodic disturbances is ready for widespread implementation:

Each application:
how many axes?
flanking paths?
actuators?
sensors?
plant dynamics?

MOUNTING OF INSTRUMENTS

The influence of disturbances on the cost can be written in terms of modal parameters

$$J = \frac{1}{4\beta\omega_0} \left(\phi^T \bar{\beta}_u \omega^T \beta_u^T \phi \right) r_{\dot{q}}$$

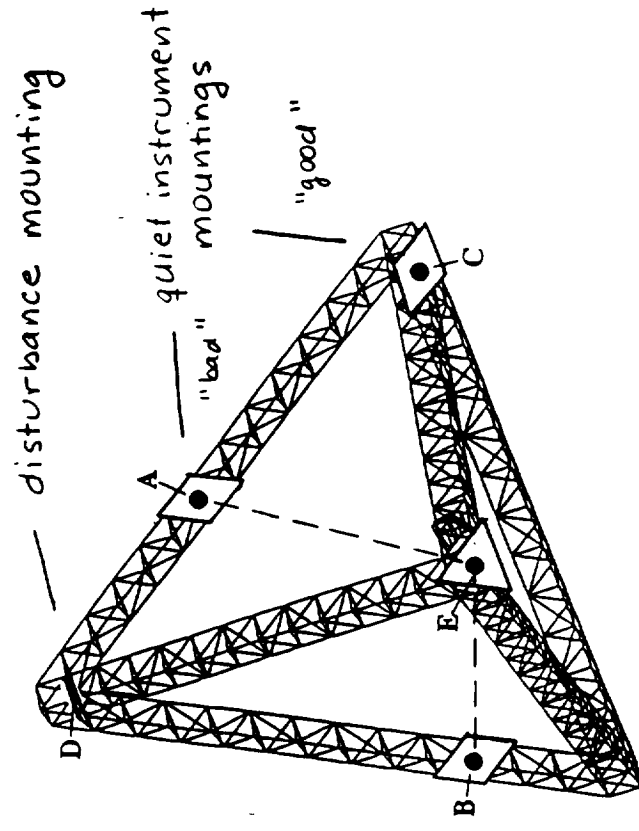
ϕ mass normalized eigenvector at input location

$r_{\dot{q}}$ state penalty at output location

Sensible mounting locations are those for which ϕ is small (nodes) for the appropriate coupling degrees of freedom

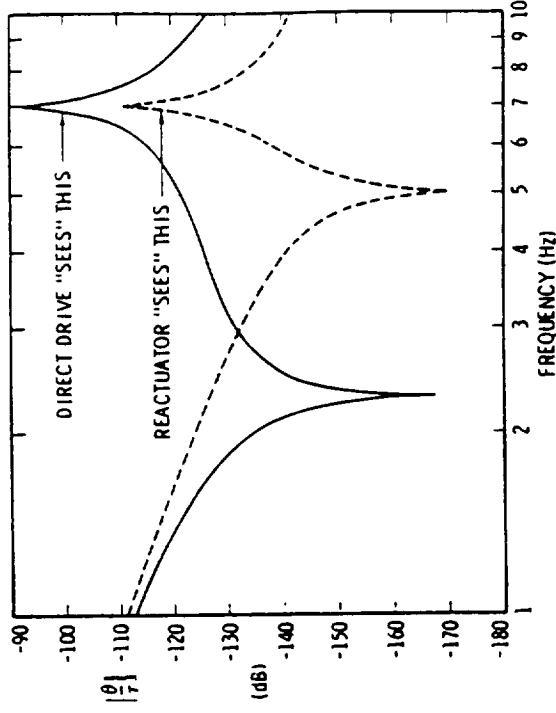
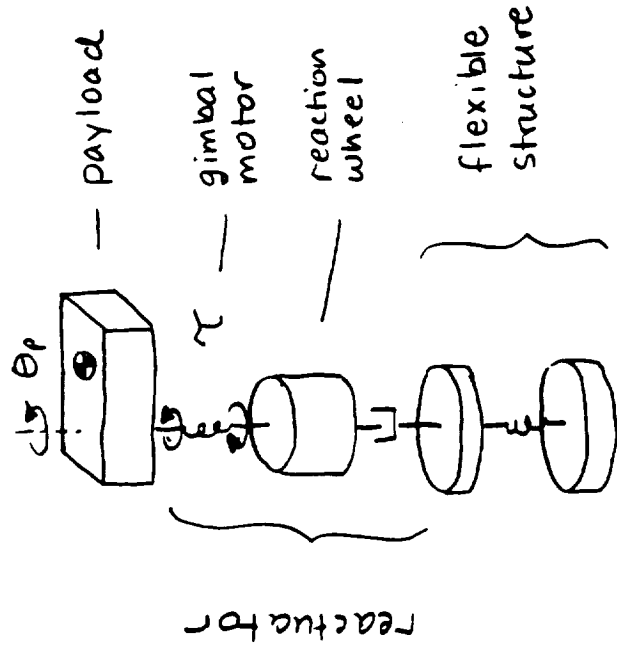
The MIT SERC interferometer testbed:

- closed tetrahedral topology
- vertices provide good mounting locations (20 dB improvement)
- midspan of beams exhibit flexible coupling



REACTUATION OF GIMBALLED PAYLOADS

- used to articulate a payload with minimal reaction torques on base structure
- payload is pointed by reacting against a rigid reaction wheel using gimbal motor
- in ideal situation, no net torque is applied to structure
- in real situation, gimbal friction, cabling stiffness limit torque reduction

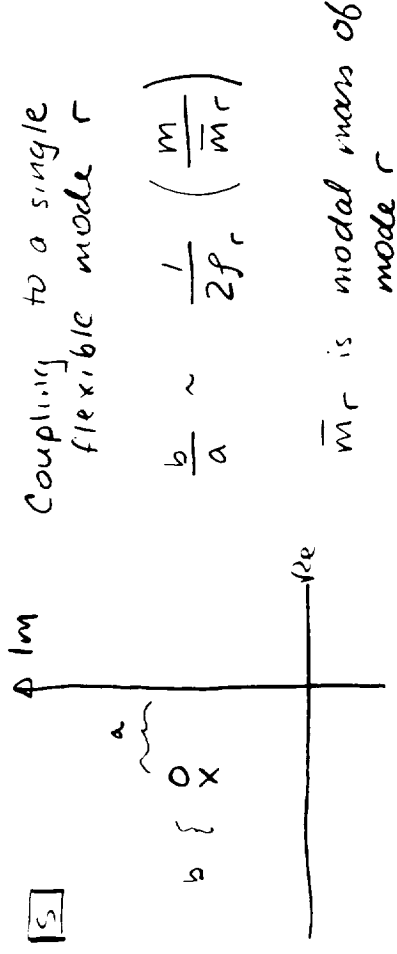
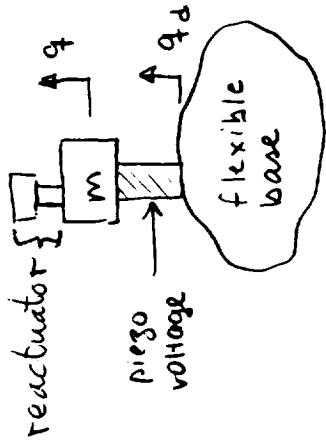


ref: Laskin et. al., AAS, 1987

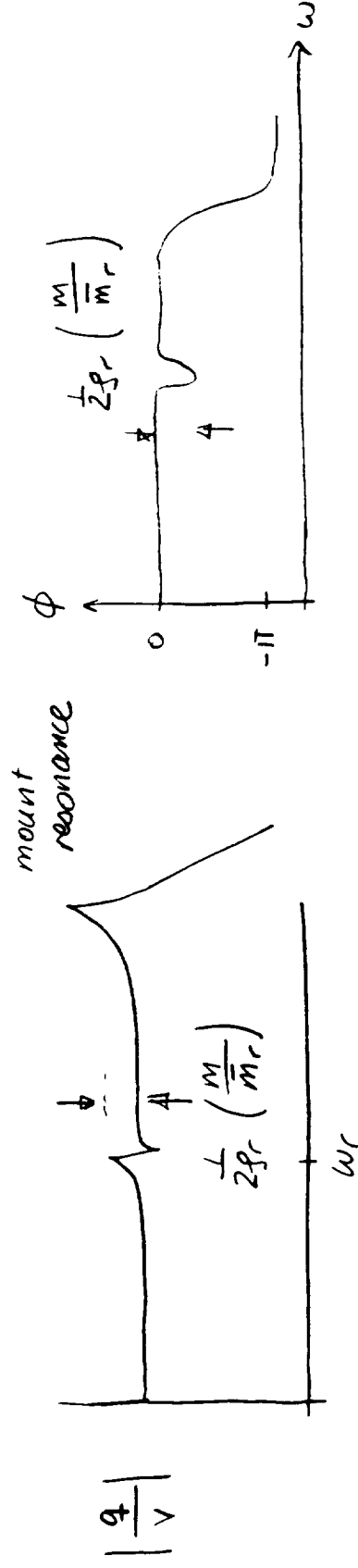
(with mass center offset)

BROADBAND ACTIVE ISOLATION

Problem: isolate lightweight mirror from a broadband base disturbance. The base is also flexible.

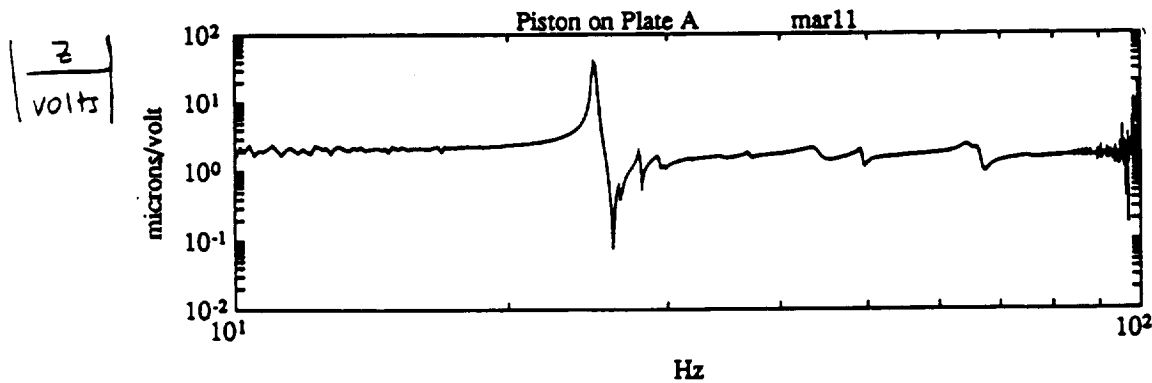
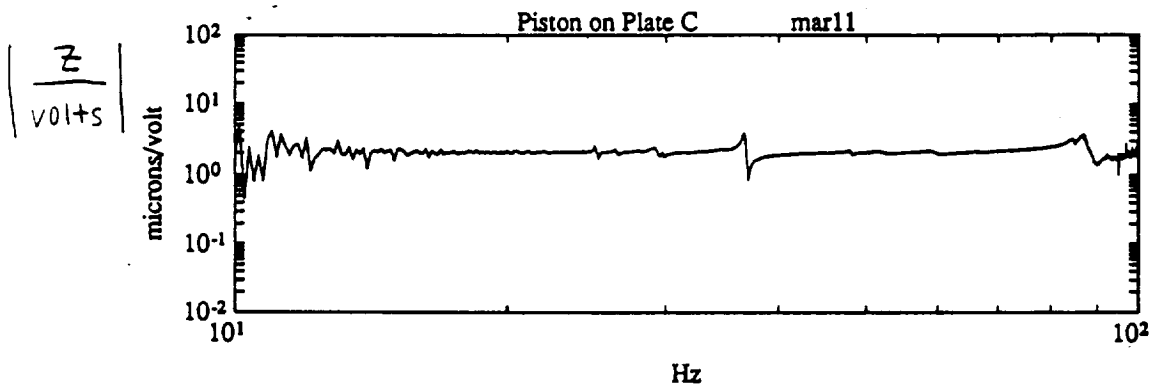
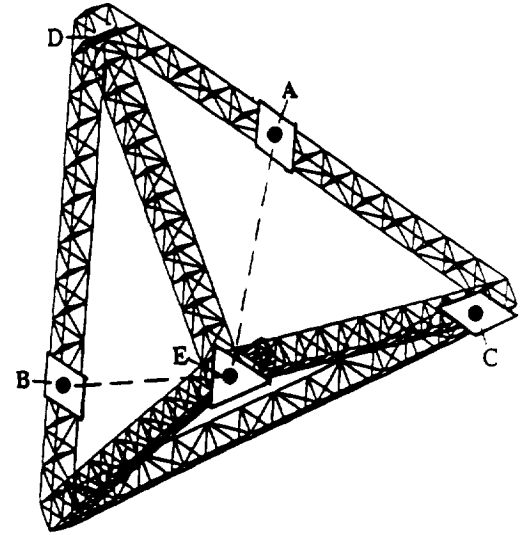
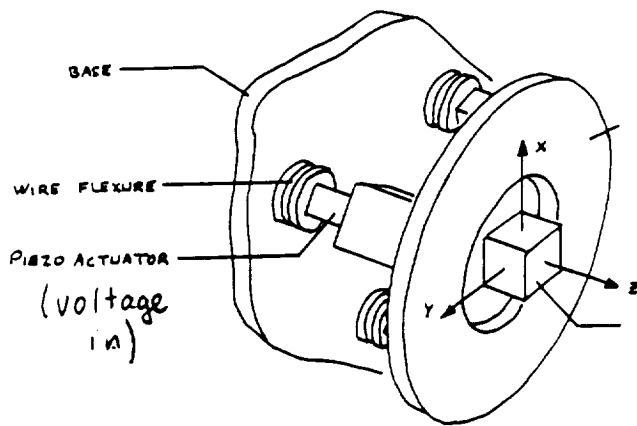


- wish to design controllers that can ignore the flexibility of the base
- take advantage of a mass ratio that is small compared to the damping ratio to bound gain and phase excursion in the control loop



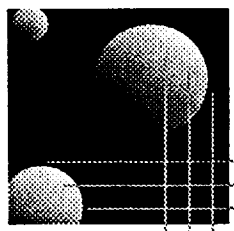
Lightweight Mirror Positioning on Interferometer Testbed

ACTIVE MIRROR



FORECAST: (ACTIVE VIBRATION ISOLATION)

- Active control of periodic noise (narrowband) is easy and important
- Active techniques will have major impact upon narrowband *machinery isolation* when
 - Design requirements prohibit soft mounts
 - Performance demands justify cost and maintenance
- Broadband isolation will remain passive or quasi-passive, particularly in presence of important plant dynamics.
- *Clever sensor/actuator selection enables broadband active isolation; structural dynamics do not contribute to plant*



MIT
Space
Engineering
Research
Center

The Application of Controlled Structures Technology to Adaptive Optics

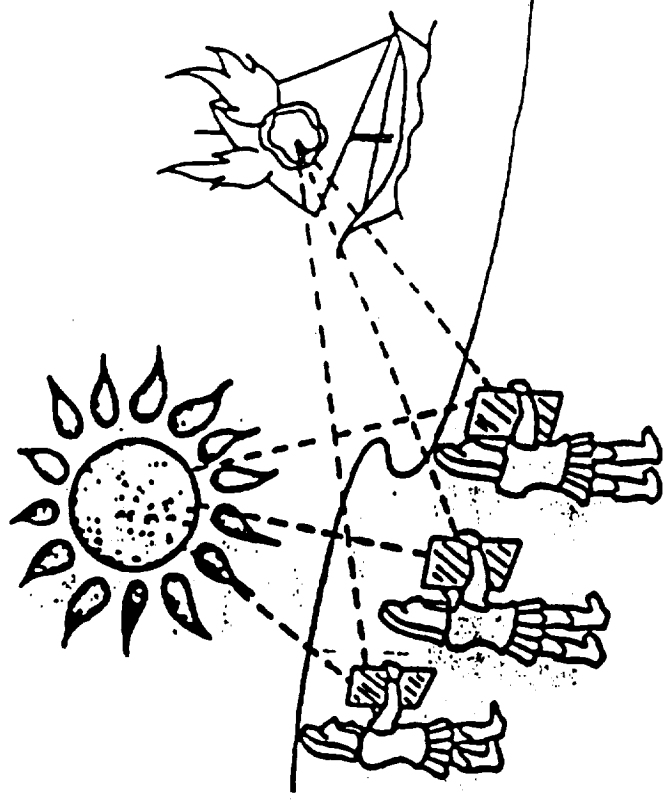
Eric H. Anderson
Jonathan P. How

3rd Annual SERC Symposium
July 1, 1991

52 37
160365
P. 27
N93-28170

Historical Note

- Archimedes (287-212 BC)
- Roman warships burned during siege of Syracuse
(open to historical debate)



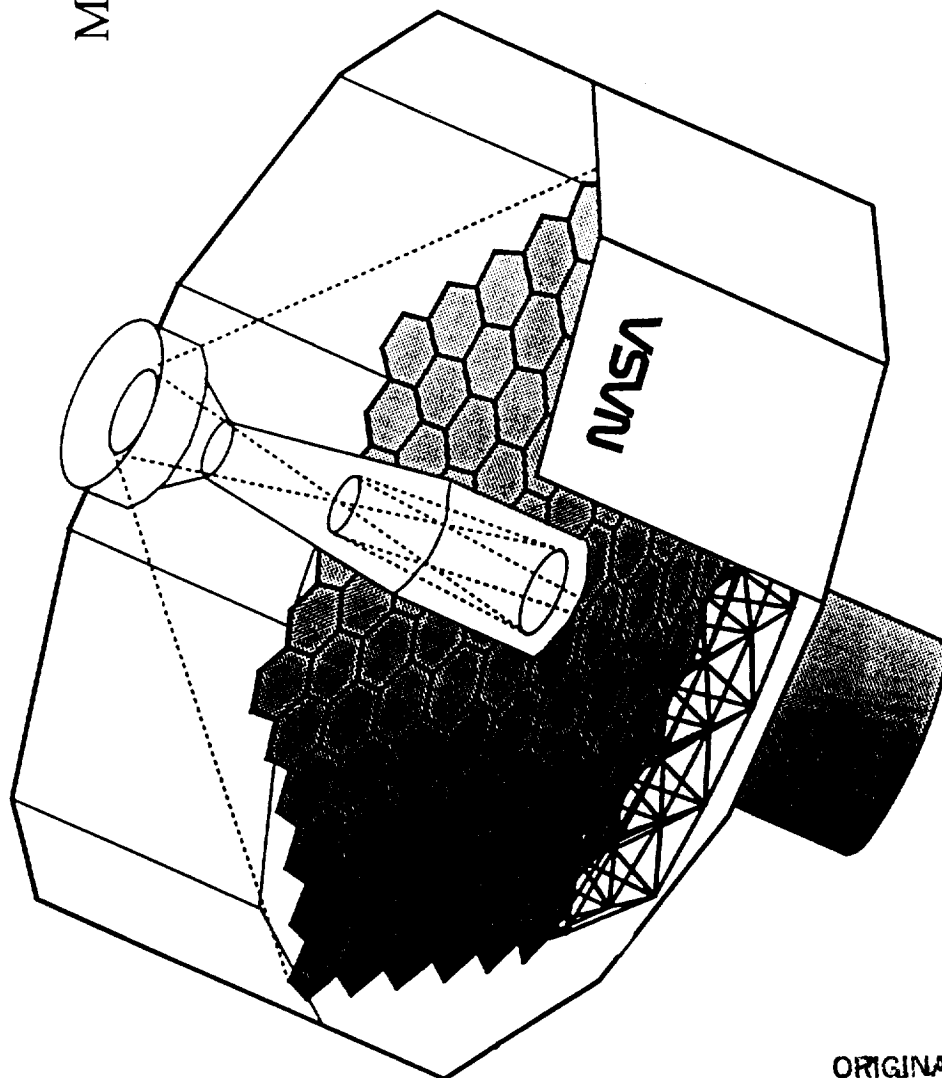
Outline

- Objectives
- Review of current approaches to optics
- Constraints on weight and performance imposed by control-structure interaction (CSI)
- Potential benefits of CST methodology
- Testbeds for demonstration of approach
- Experimental results from a simple testbed
- Open issues and conclusions

Objectives

- Understand current approaches in optics
- Investigate potential limitations imposed by flexibility in existing and planned optical systems
- Determine and demonstrate benefits of designing large optical systems within the Control Structures Technology (CST) framework.
 - Deformable surfaces
 - Flexible support structures

A Typical Large Optical System (LDR)



Major components:

- Primary
- Secondary / other optics
- Support structure

ORIGINAL PAGE IS
OF POOR QUALITY

Overview of Current Optical Programs

- Current design methodologies
 - mirror and support structure designed to avoid interaction of flexible modes with disturbances
 - controller bandwidth limited to avoid any interaction with flexible modes
- Note on terminology
 - Adaptive control
 - Active and adaptive structures
 - Active and adaptive optics

Current Approaches

- Passive devices
 - designed for mechanical and thermal stability
 - typically heavy, thick, very stiff (high natural frequency)
 - not directly designed to perform active or adaptive optics
 - possible gravity sag in secondary support structure
 - recent advance: large lightweight mirror (borosilicate and thin meniscus)
- Example: Hale Observatory/Mt. Palomar (1949)

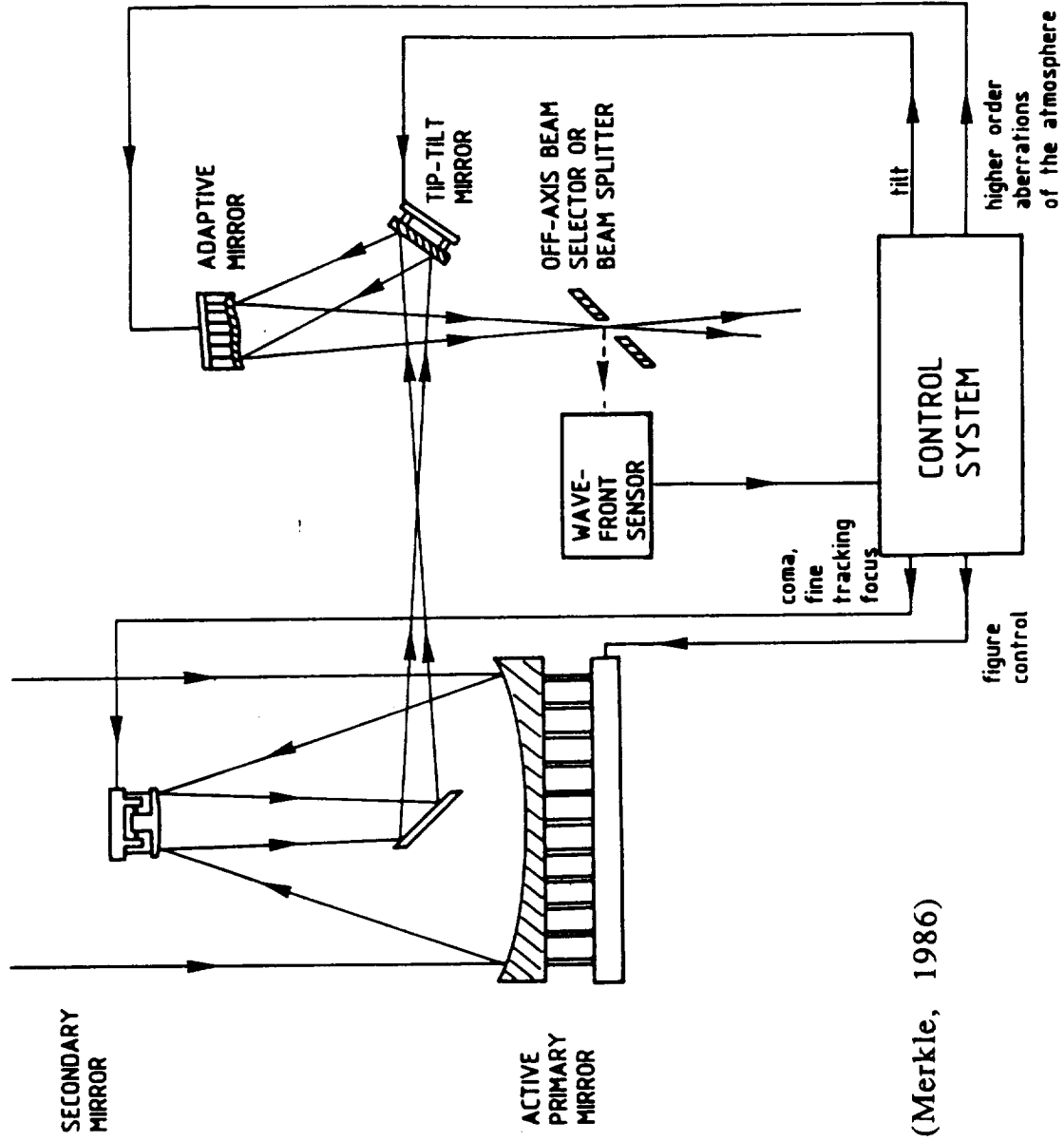
Current Approaches, cont.

- Active devices
 - quasistatic shape correction
 - demonstrated benefits over passive devices:
 - improved performance with wind disturbances.
 - requires smaller blanks and less stringent polishing
 - backplane stiffness (weight) major issue for monolithic mirrors (depends on actuator type)
 - control has proved effective for segmented mirrors (Keck), but CSI limits bandwidth and performance
 - employ thin meniscus mirrors (40:1)
- Examples: HST, Keck, New Technology Telescope (NTT)

Current Approaches, cont.

- Adaptive devices
 - atmospheric compensation requires very high frequency control.
 - current design methodology results in structures with natural frequencies of kHz.
 - leads to size and weight restrictions
 - pixel processing limit exists as well
 - recent innovation: laser guide star beacon (Starfire)
- Examples: SDI, Very Large Telescope (VLT)

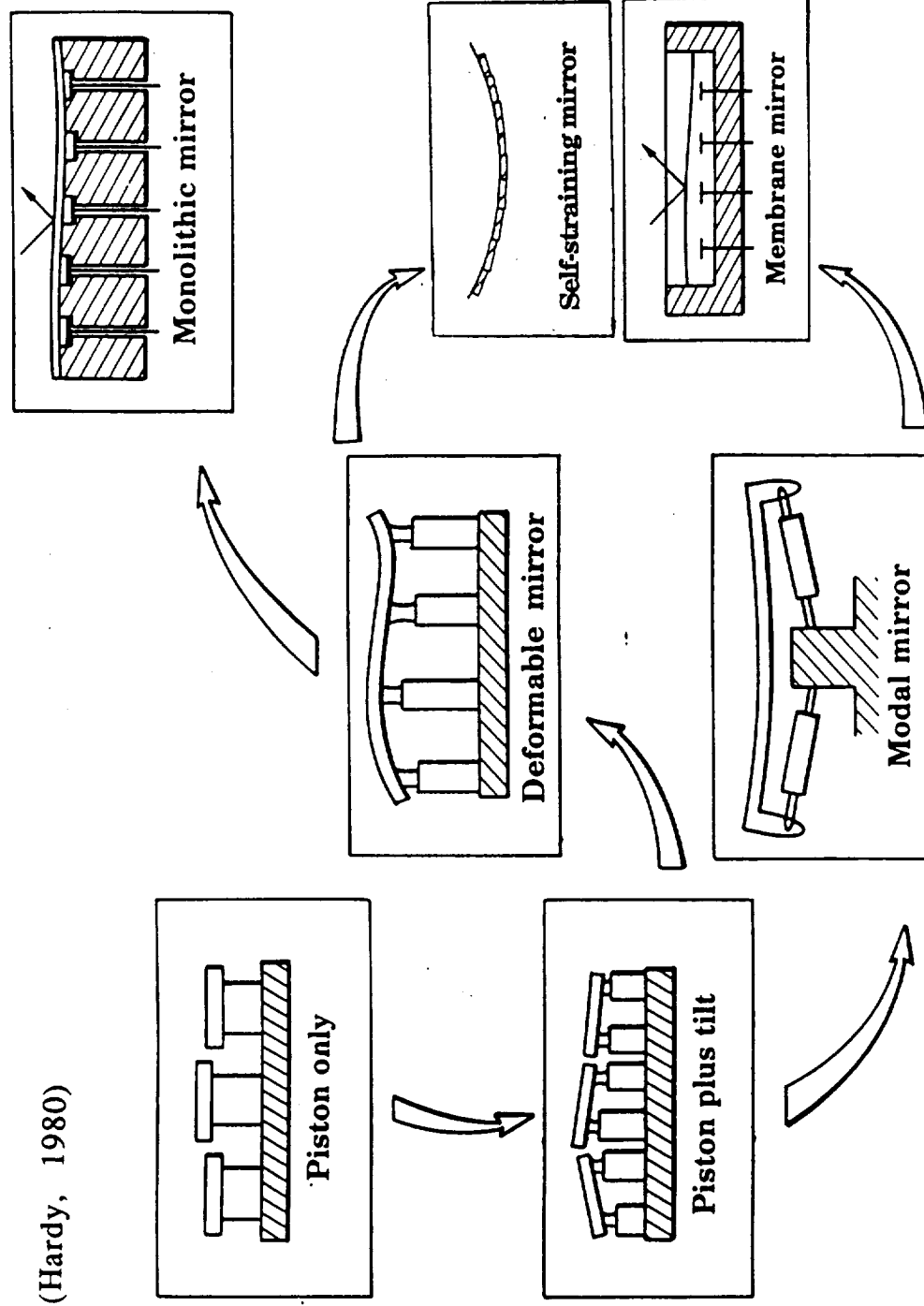
Typical Adaptive Optics System



(Merkle, 1986)

Actuation Approaches for Deforming a Mirror

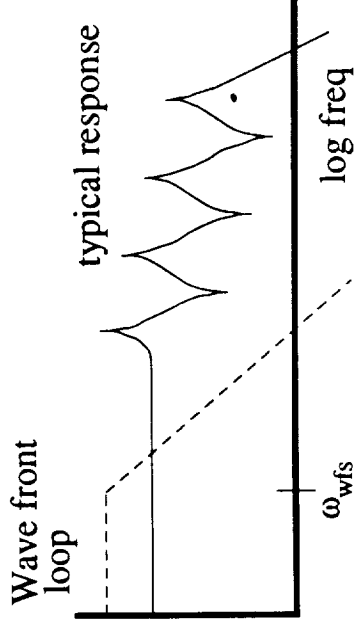
(Hardy, 1980)



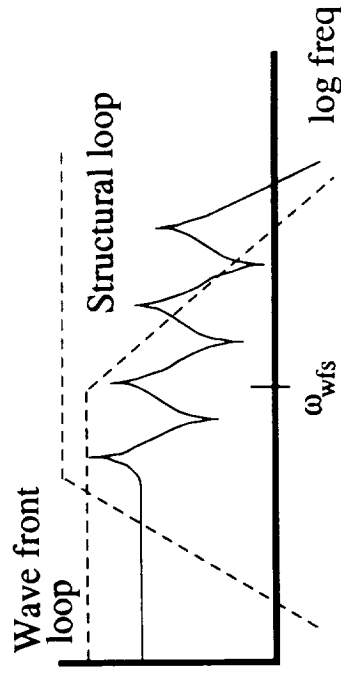
Control Approach Comparison

- Current design:
 - stiff structure
 - static displacement feedback

Control
authority

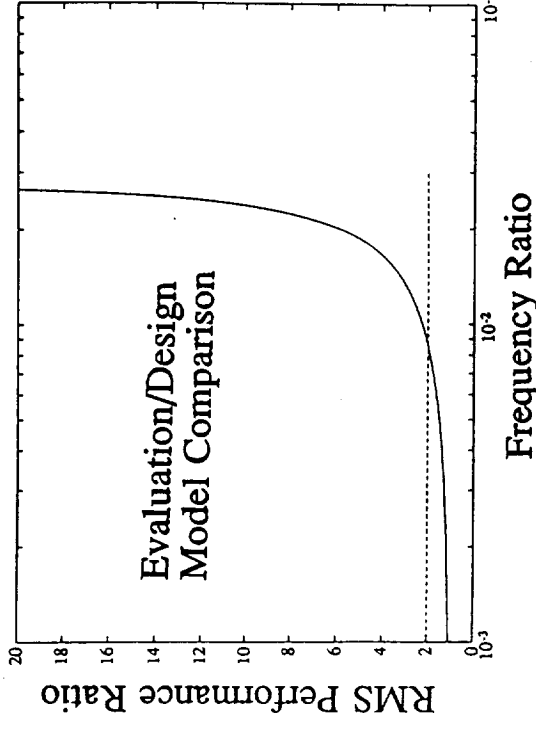
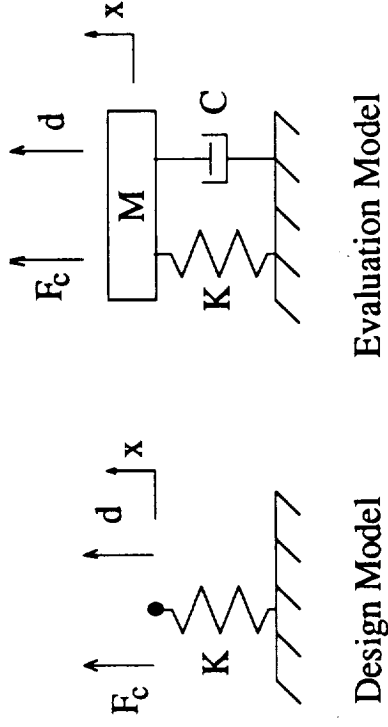


- CST approach:
 - performance demands lead to higher bandwidths
 - weight limitations lower natural frequency
 - design structural loop to augment WFS, using passive and active feedback



CSI Control Bandwidth Limitations

- Simple models [Hardy 1977], [Robertson 1970] can predict CSI instability from displacement feedback.



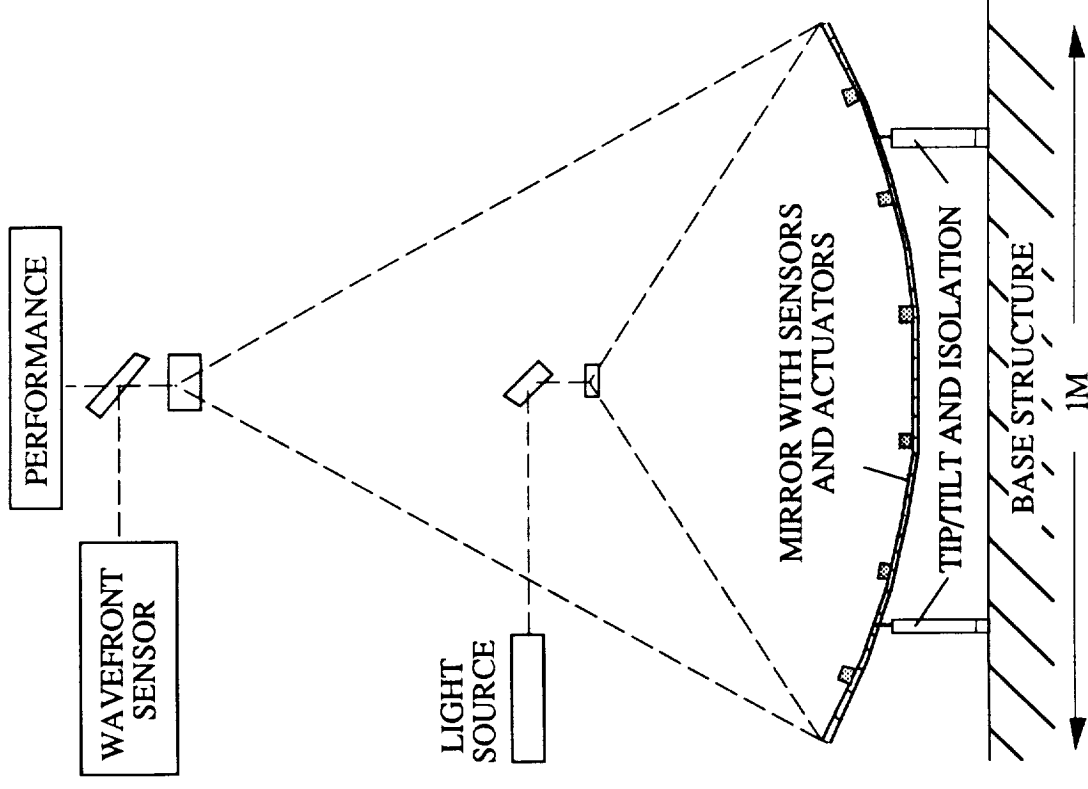
- In this case, can increase control bandwidth by including rate feedback and/or passive damping [Pearson and Hansen].
 - CST design methodology provides unified approach to control design for significantly more complex structures
- ==> potential performance improvements.

Applications of CST Concepts to Optics

- Examples from literature:
 - Pearson and Hansen [1977] - viscous damping oil extends control bandwidth beyond first mode
 - Greene and Pope [1980] discuss importance of flexible modes on optical performance
 - Perkin Elmer JOSE proposal - truss control bandwidth includes natural frequency of primary mirror
 - segmented mirror designs with active elements in support structure [Chen et al., 1989]
 - ASCIE - closed loop verification of CST on a segmented precision optical device
 - Combined CST/optics modelling (Redding)
- Emphasis of previous CST work has been on support structure
- Application to flexible mirror surface control not fully explored.

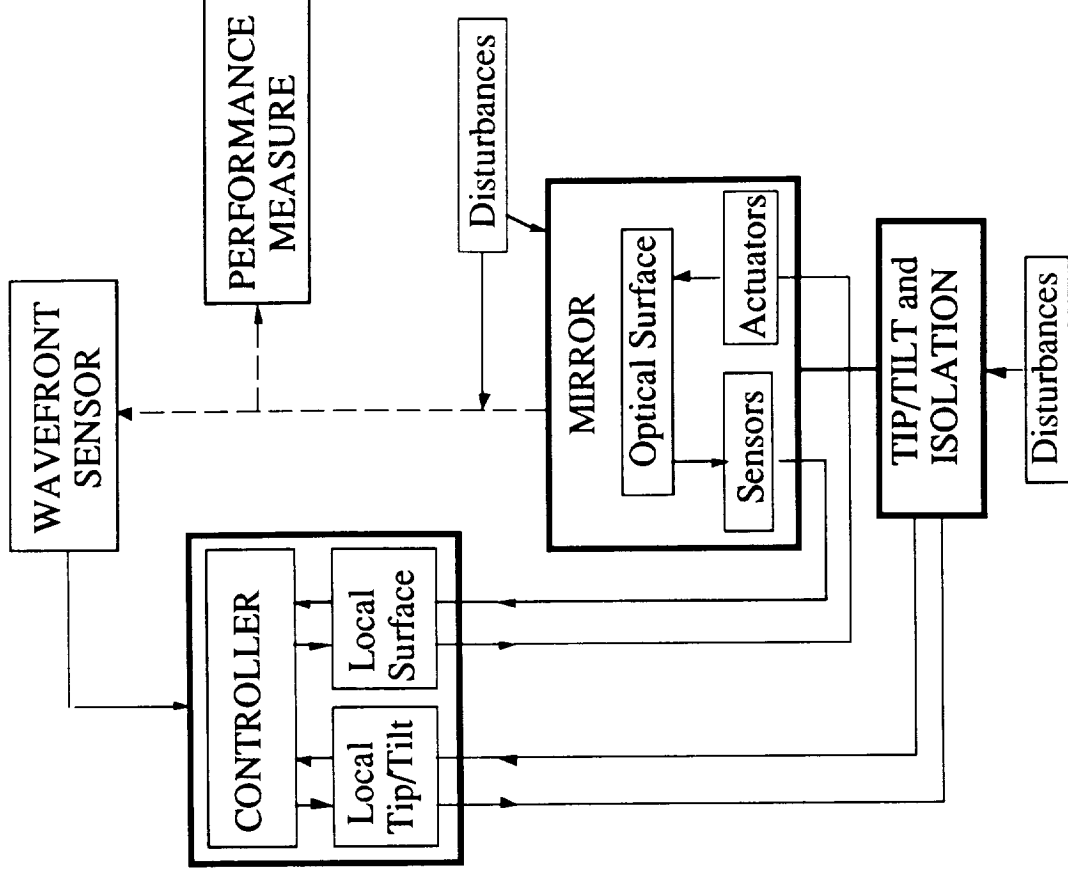
Deformable Mirror Testbed Concept

- Main features:
 - self-straining lightweight mirror surface, no backplane
 - elliptical shape for nearby source and sensor (or use distrib. point retroreflectors)
 - 1D testbed captures some relevant science and dynamics.
 - tip/tilt and isolation from supporting truss structure (not shown)

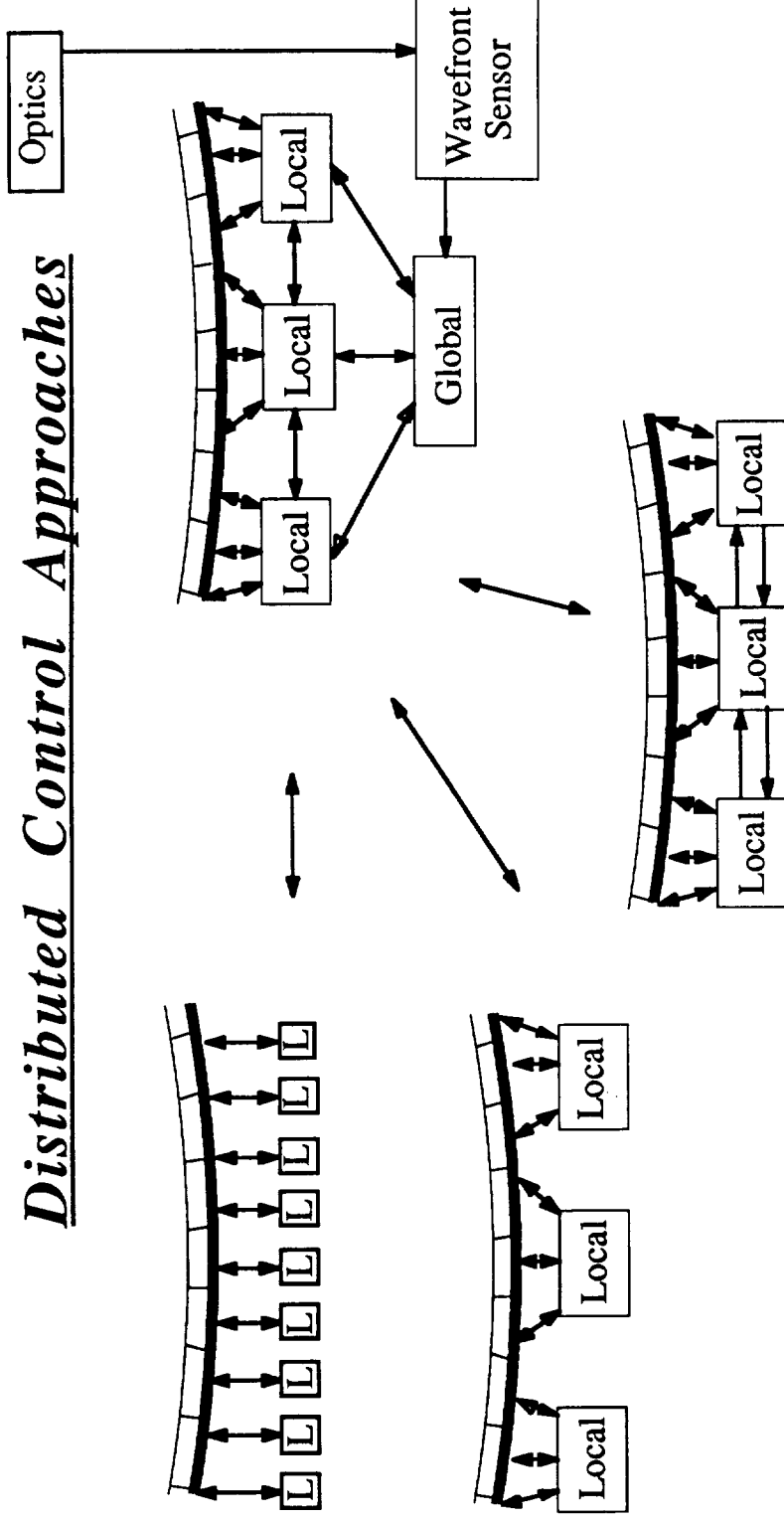


Testbed Functional Block Diagram

- Main components:
 - mirror (actuators/sensors)
 - isolation and controller
 - optical measurement and performance evaluation
- For design flexibility, disturbances enter acoustically, mechanically, and optically.



Distributed Control Approaches



- Distribute control to complement dynamic behavior of structure.
- Efficiency and performance of multi-level architecture required to handle large number of sensors and actuators.
- Low authority controllers designed for stability robustness and local performance.

Available Testbeds

- Phase 0 deformable mirror testbed
 - Initial step towards more comprehensive testbed
 - Self-straining (PZT actuators)
 - Optical and structural (PVDF) measurements
- Interferometer multi-point alignment testbed



ORIGINAL PAGE IS
OF POOR QUALITY

DEFORMABLE MIRROR TESTBED

C.2

Results from the DMT

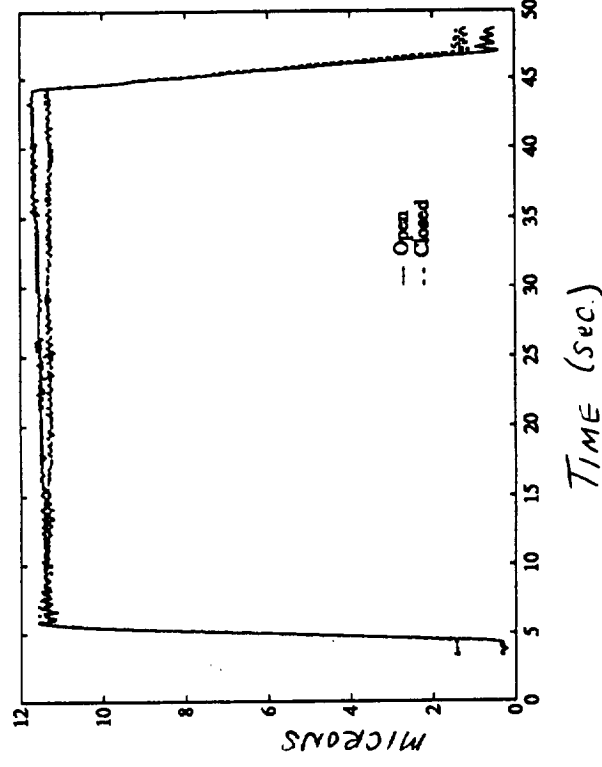
- Static and quasistatic considerations
- Noncollocated transfer functions and non-minimum phase zeros (Fleming, Spector and Flashner)
- Overall approach to dynamic control
 - Passive damping (resistive shunting)
 - Low authority control (collocated strain rate feedback)
 - High authority control (reduced order LQG, noncollocated optical measurement, low bandwidth)
- RMS performance

Test	Description	Tip RMS (microns)	Perf. Ratio
A	Open Loop	23.0	1.0
B	Shunt	21.9	.95
C	CRF(1,2)	19.9	.86
D	CRF(1,2), HAC(2)	16.8	.73
E	CRF(1), HAC(1,2)	11.8	.51

Table 1: Test summary. Numbers in correspond to sensor/actuator pairs for collocated rate feedback (CRF), or the actuator used for high authority control (HAC).

Quasistatic Error Correction

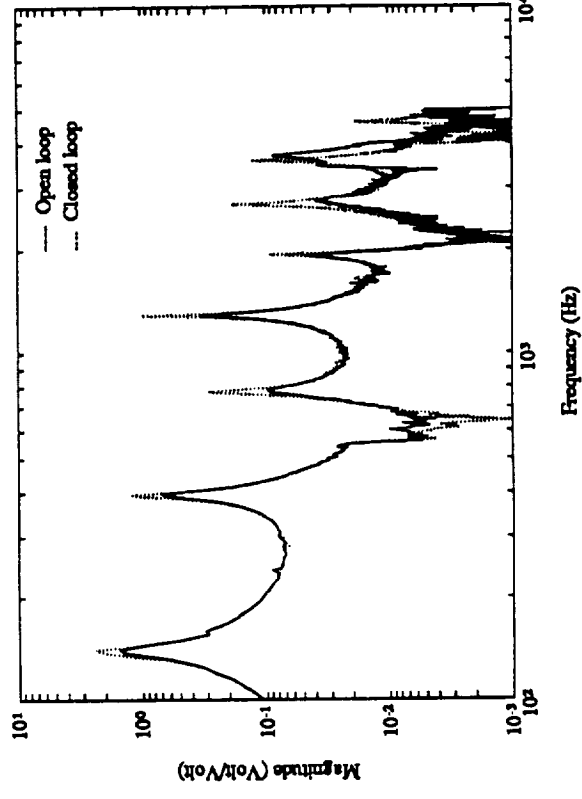
- Sources of error: initially wrong shape; thermal distortion; actuator material nonlinearities
- Solutions: alternative actuators; charge control; linearizing feedback



proportional feedback / actuator 3

Low Authority Control (LAC)

- Measuring strain rate with PVDF
- Rolloff issues
- Implemented at locations 1 and 2
- Target 3rd and 4th modes (400 Hz, 780 Hz)
- Disturbance at actuator 3

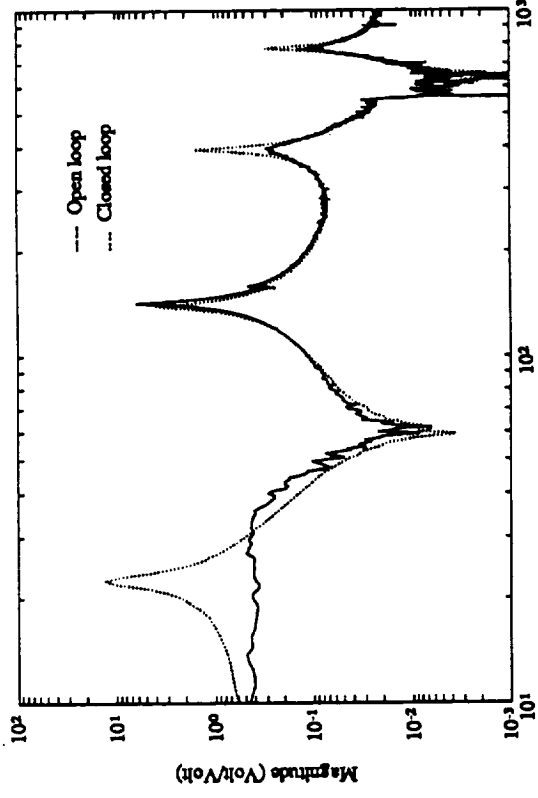


High Authority Control (HAC) Design Methodology

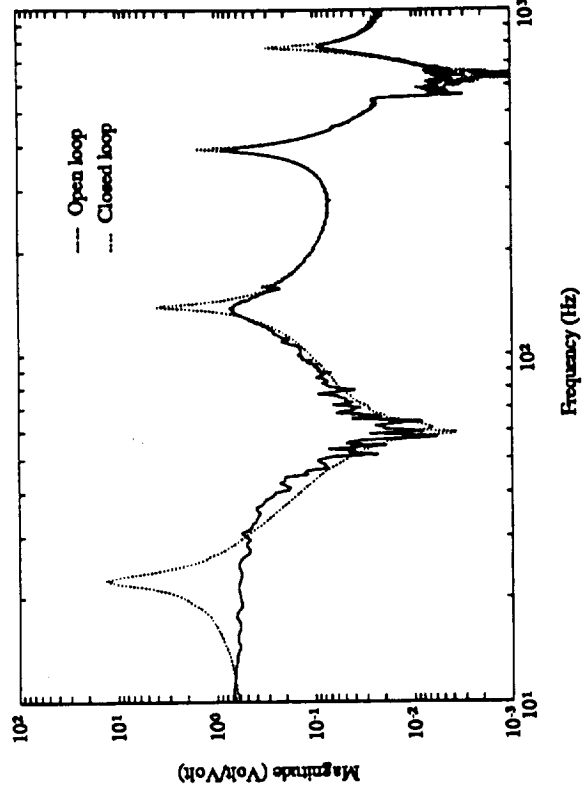
- Designed for first 2 modes (freq.-weighted rms performance)
- 10th order design model based on measured data
- Reduced order LQG
 - Technique developed by Mercadal
 - Possible robustness improvement
 - 2nd and 4th order compensators
- Disturbance at actuator 3

Results of HAC

- Implemented on "stealth" real-time control computer at 4 kHz



HAC: actuator 2
CRF: locations 1,2



HAC: actuators 1,2
CRF: location 1

Open Issues

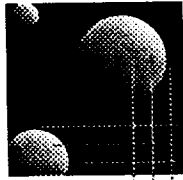
- Must demonstrate concepts on a realistic optical system
 - 2-D mirror
 - wavefront sensor
 - disturbances
 - aircraft borne, atmospheric, wind, thermal, gravity gradient
- Structural sensor options
 - number, location, size, shape
 - fiber optics, strain gauges, piezo-polymers (PVDF), piezo-accelerometers
 - resolution for small surface deflections
 - benefits of “ganging”
- Actuator options
 - number, location, size, shape
 - amplifier power consumption and potential of charge storage devices.
 - membrane mirrors/electrostatic actuation

Open Issues

- Control
 - efficient architecture for numerous sensors
 - implementation: digital/digital vs. digital/analog
 - integration of WFS information into control loop

Conclusions

- Deformable mirrors built to date have been constrained by flexibility.
- Optical systems/deformable mirrors can benefit immediately from application of CST.
- Both weight reduction and performance improvement are possible.
- Application to surface control complements multi-point alignment goal

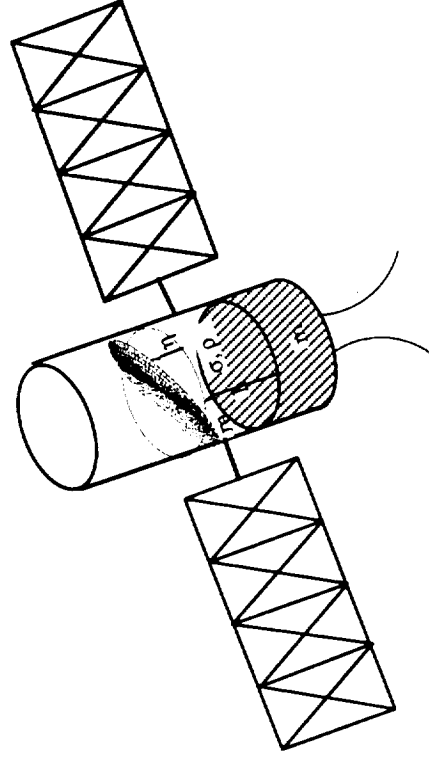


MIDDECK 0-GRAVITY DYNAMICS EXPERIMENT (MODE)

Marthinus C van Schoor

MIT Space Engineering Research
Center
3rd Annual Symposium

July 1991



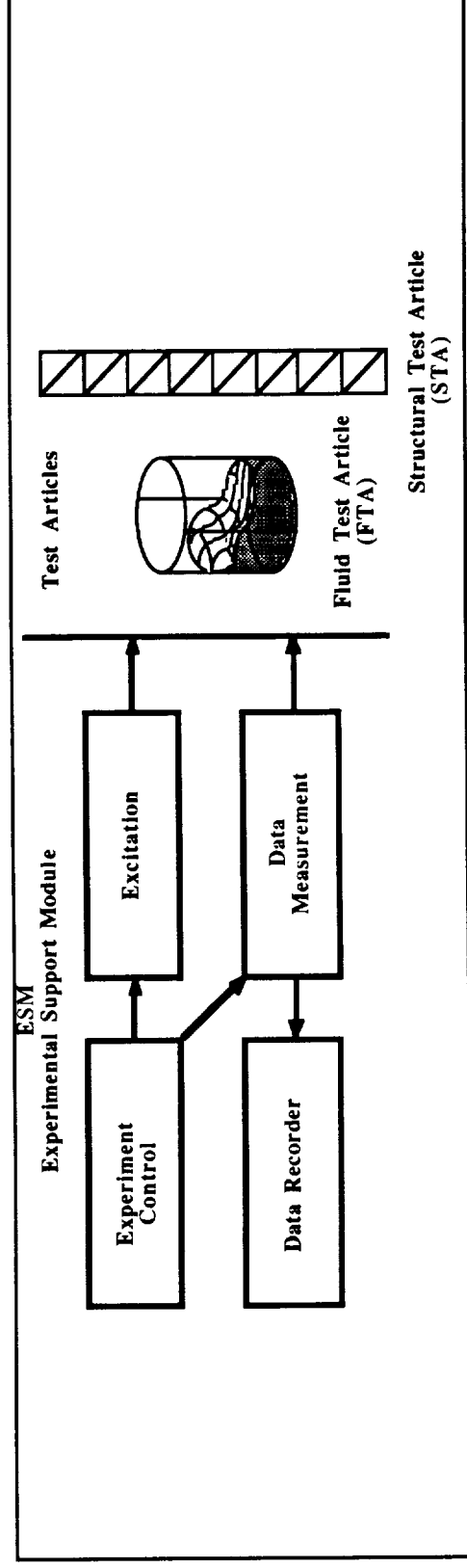
54-51
103326
N93-28171

OUTLINE

- MODE and its Rationale
- Program Objectives
- Science Overview
 - Truss structures
 - Contained fluids
- Experimental Design
 - Structures
 - Contained Fluids
- Progress to date
 - Component Tester
 - ESM, STA and FTA
 - Schedule

MODE and its Rationale

- An experiment that investigates the nonlinear characteristics of two important components of spacecraft
 - Nonlinear dynamics of truss structures
 - Nonlinear dynamics of contained fluids



MODE

- Why investigating the dynamics of truss structures ?
 - Nonlinear dynamics of jointed space structures can alter the vibrational/acoustical characteristics of a space structure
 - This behavior is important for:
 - On-board micro-gravity experiments
 - Passive damping characteristics of “open-loop” structures
 - Closed-loop stability and performance of controlled structures
 - Little experimental data is available on how gravity effects the dynamic characteristics of jointed space structures and models are not verified

MODE and its Rationale (Continued)

- Why investigating the dynamics of contained fluids ?
 - Large fluid/spacecraft mass fractions are desirable
 - Dynamics of contained fluids in space are inherently different from their behavior in 1-g
 - The traditional “linearized or small amplitude” approach , cannot be used since
 - The motion resulting from large amplitude vibrations significantly departs from the linear behavior
 - Bifurcation instabilities and non-deterministic motion also exist
 - Nonlinear fluid motion interacts with the spacecraft degrees-of-freedom to yield nonlinear spacecraft modal behavior
 - The existing linear/quasi-nonlinear models are inadequate and new nonlinear models are not validated for zero-gravity conditions. This leads to conservative attitude control designs for spacecraft’s with on-board fluids to avoid instabilities

Program Objectives

- For space structures ?
 - To establish a database of the dynamic response behavior of structures with typical space structure-components
 - To develop a nonlinear model for the spacecraft's zero-gravity nonlinear structural resonant and transient response characteristics
 - To use the results/model to understand and model how the nonlinear characteristics will alter the spacecraft's vibration/acoustics characteristics
 - Identify the limitations of earth modal testing given the influence of gravity effects on the modal characteristics
 - Use the knowledge and models to design optimal structures and robust and optimal structural controllers.

Program Objectives (Continued)

- For the contained fluids ?
 - To obtain the “missing” data point. The measurement of the nonlinear dynamic characteristics of contained fluids in zero-gravity
 - To understand how the nonlinear fluid dynamics interact with the motion of the spacecraft
 - To use the experimental results to verify the nonlinear model developed at MIT
 - To establish a design tool with which designers can with confidence design optimal and robust attitude controllers - even for spacecraft with high fluid/spacecraft mass fractions

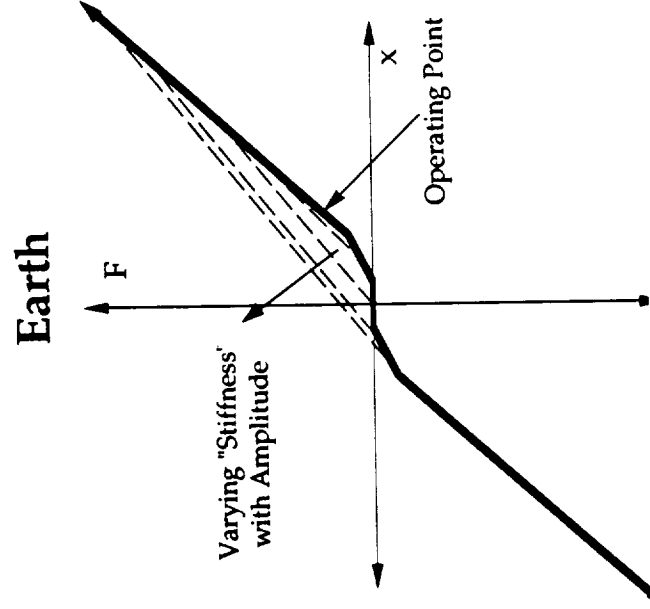
Science Overview (Truss Structures)

Gravity effects that alter the modal characteristics of truss structures

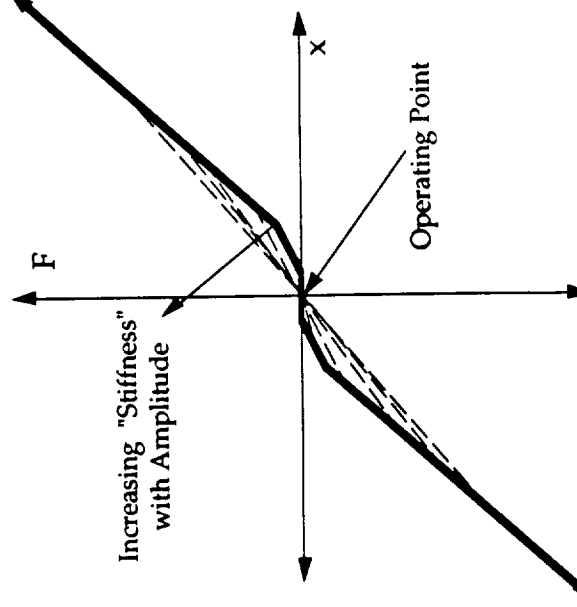
- Gravity loading which scales with:

$$\frac{\text{Gravity Load}}{\text{Pre - Load}}$$

Nonlinear Joint



Space



Gravity alters the operating point and, therefore, the apparent stiffness and damping of joints and tensioning wires;

- Similar for tensioning wires

- Gravity field also alters the modal characteristics (frequency and mode shapes) of the structure. This effect scales with:

$$\frac{g / L_{Suspension}}{\omega^2} = \frac{\omega_{Pendulum}^2}{\omega_{1st}^2}$$

where ω_{1st}^2 is the 1 st modal frequency of interest.

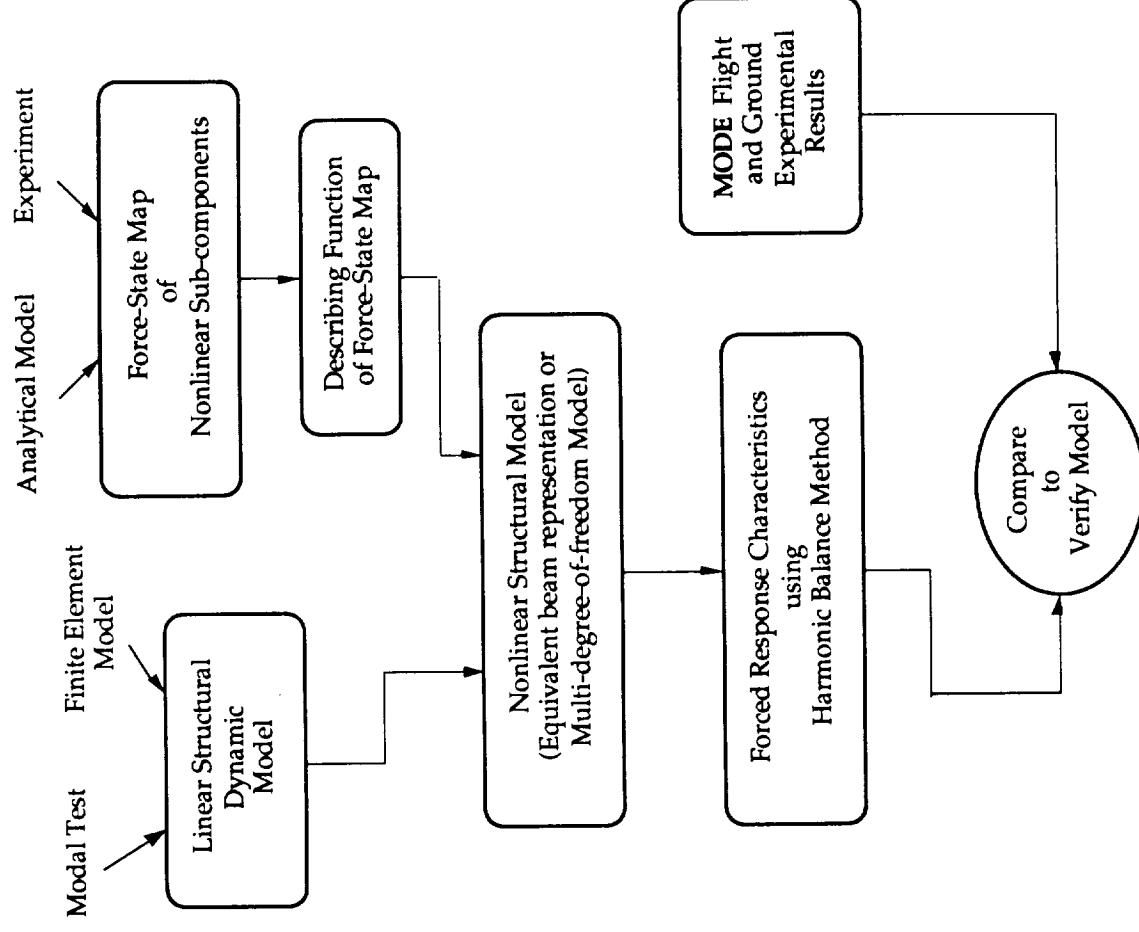
For example; significant changes in the modal characteristics are observed for a 6 foot long structure if the natural frequency is less than 1 Hz.

- Suspension of the structure changes the boundary conditions:
 - On earth, free-free boundary conditions are simulated by suspending the structure with a very flexible suspension system.
 - Effect scales with:

$$\frac{\omega_{Suspension}}{\omega_{1st}}$$

- Need suspension frequency 1 order of magnitude lower than 1 st natural frequency of structure.
- 0.1 Hz suspension frequency can be achieved with state-of-the-art suspension systems.

Modelling Approach

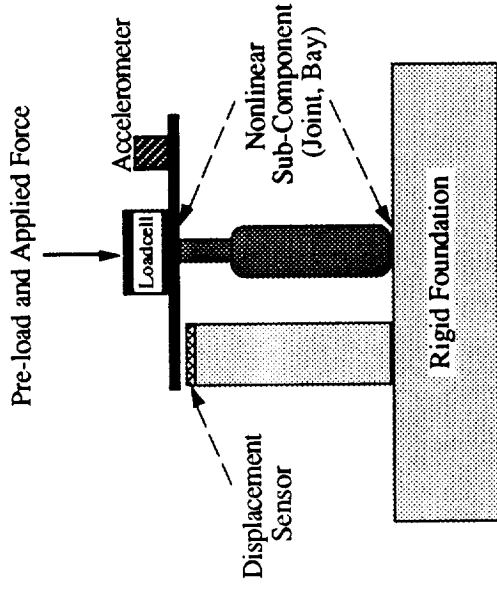


Characterization of the Nonlinear Components

- Force transmitted by a nonlinear structural component is:

$$F_t(x, \dot{x}) = F - M\ddot{x} = D(x, \dot{x})\dot{x} + K(x, \dot{x})x$$

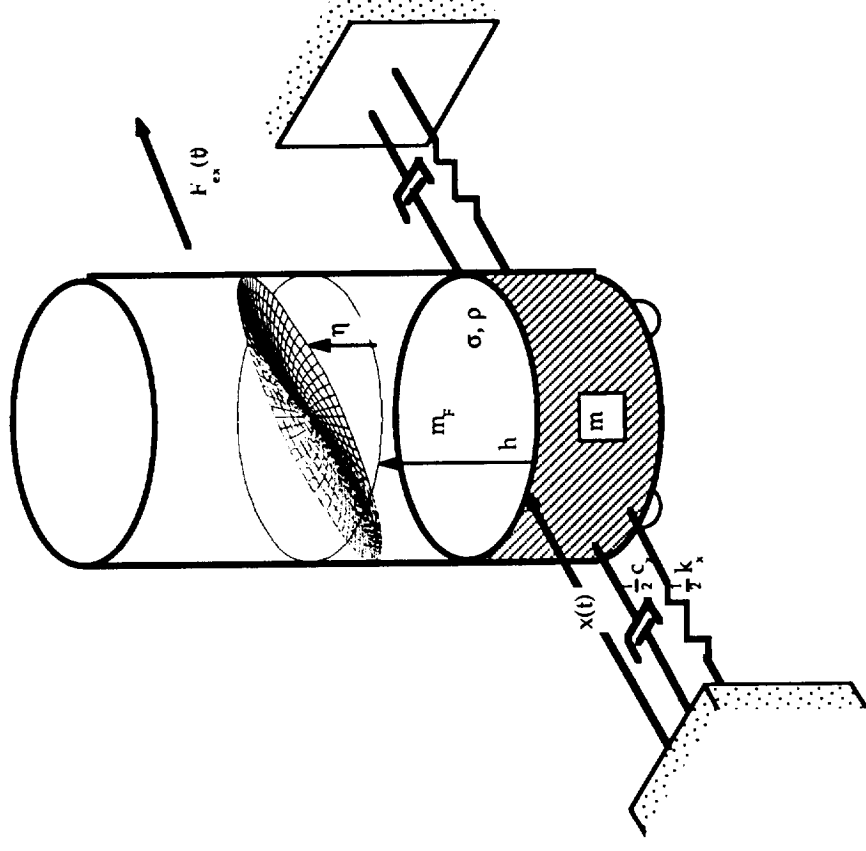
- Model requires a force-state map (Force transmitted as a function of the states of the component) of nonlinear sub-components
- Typical measurement of the force-state characteristics



Science Overview (Contained Fluids)

Major sources of nonlinearities in the dynamics of contained fluids

- 1 Potential energy stored in surface tension is a nonlinear function of the amplitude of motion



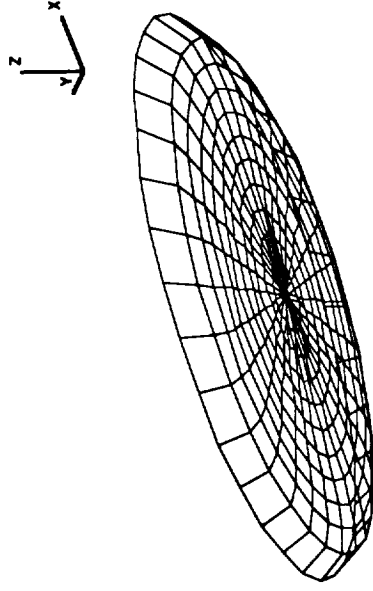
Simplified Nonplanar Model

Let $\eta(r, \theta, t) = f(r, \theta) + \eta_d(r, \theta, t)$

f is the function that describes the equilibrium free surface

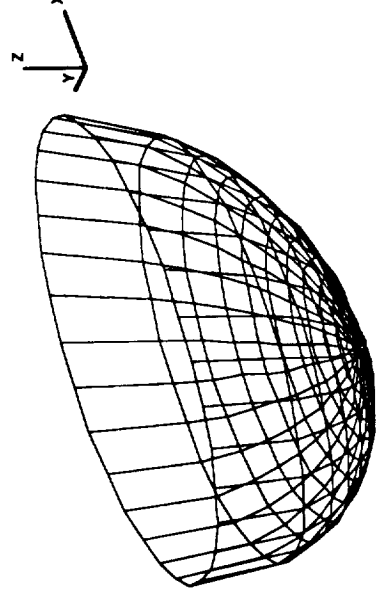
For example the equilibrium fluid shape of Silicone Oil in a 3.1 cm cylindrical tank

Silicone Oil: 1-Gravity (Earth)



Earth

Silicone Oil: 0-Gravity (Space)



Space

The surface tension potential energy is given by

$$U_{\sigma} = \sigma \iint_S \sqrt{1 + \nabla(f + \eta_d) \cdot \nabla(f + \eta_d)} dS$$

$$\text{Effect scales with the Bond number } Bo = \frac{\rho g a^2}{\sigma}$$

2 Convection forces at the free surface

$$\frac{\partial \eta}{\partial t} + \nabla \phi \bullet \nabla \eta \Big|_{z=\eta} = \frac{\partial \phi}{\partial z} \Big|_{z=\eta}$$

Dirichlet or Neumann time dependent boundary condition

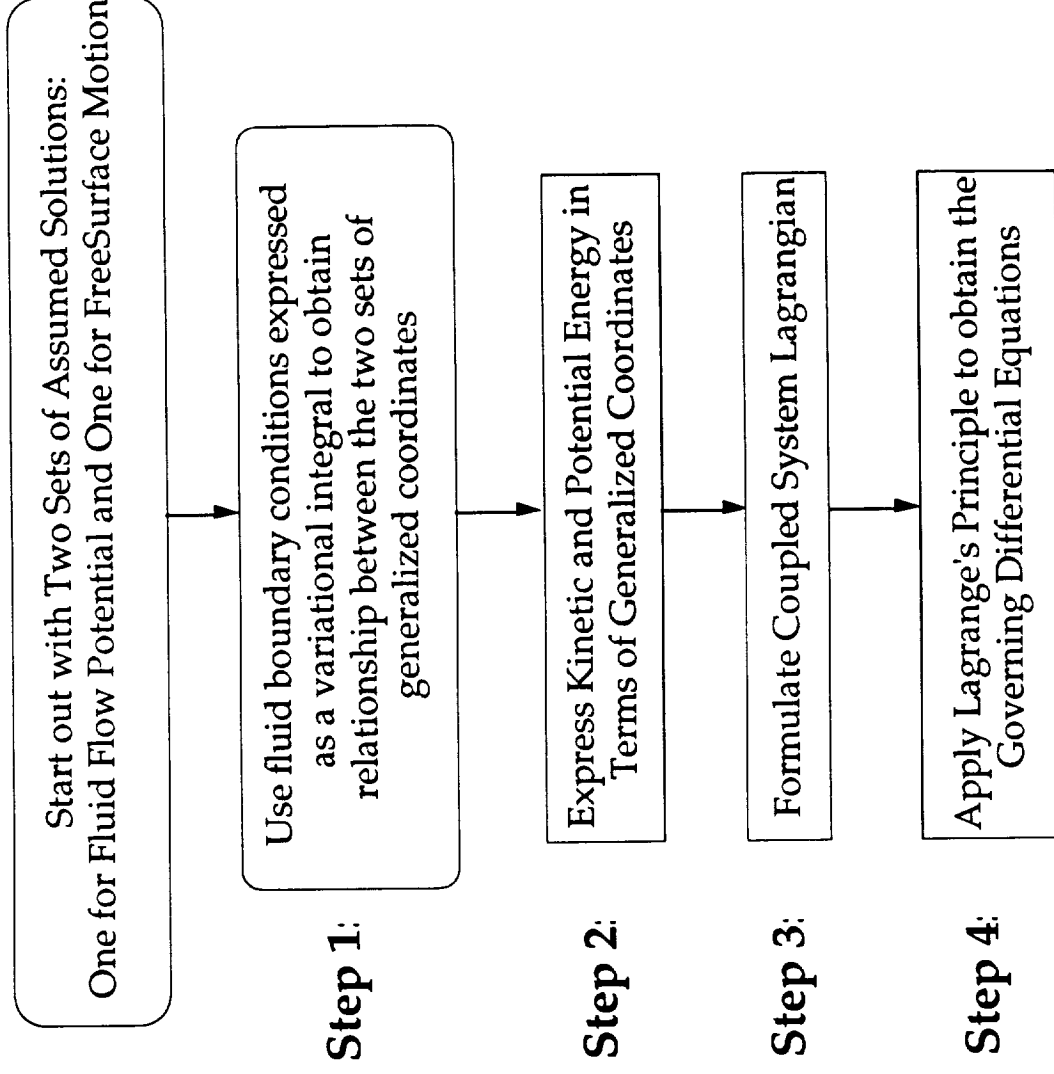
“The internal fluid must follow the motion of the free surface”

- This boundary condition is also dependent on the equilibrium free surface

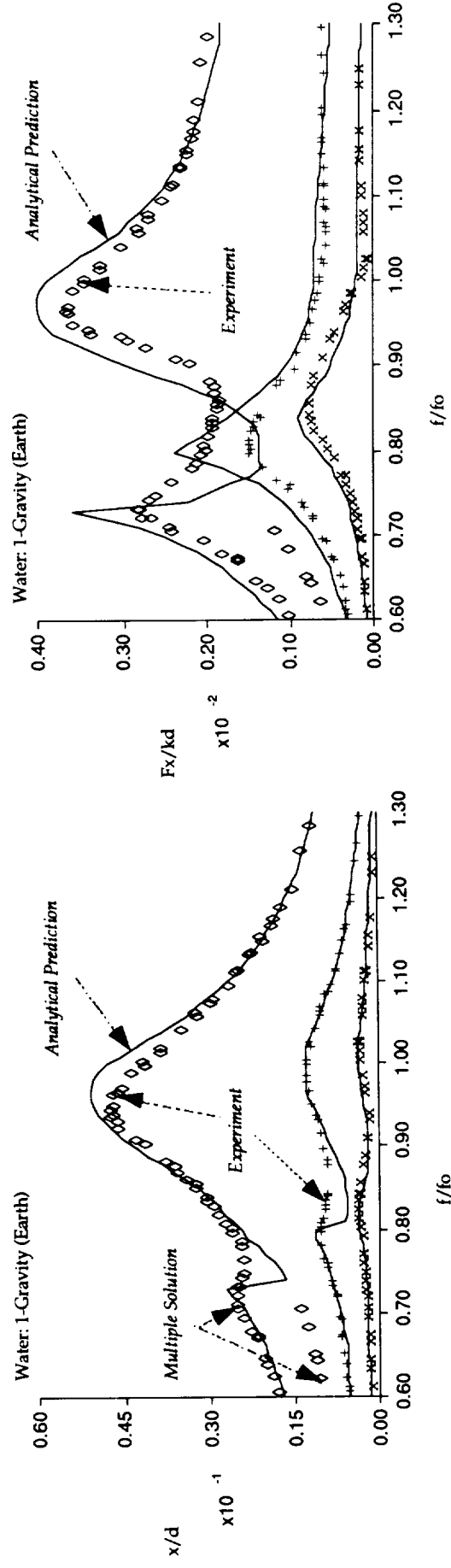
$$\frac{\partial \eta}{\partial t} = \frac{\partial \phi}{\partial z} \Big|_{z=\eta} - \nabla \phi \bullet \nabla (\eta_d + f) \Big|_{z=\eta}$$

- Even when linearized $\frac{\partial \eta}{\partial t} = \frac{\partial \phi}{\partial z} - \frac{\partial f}{\partial r} \frac{\partial \phi}{\partial r}$

Modelling Approach



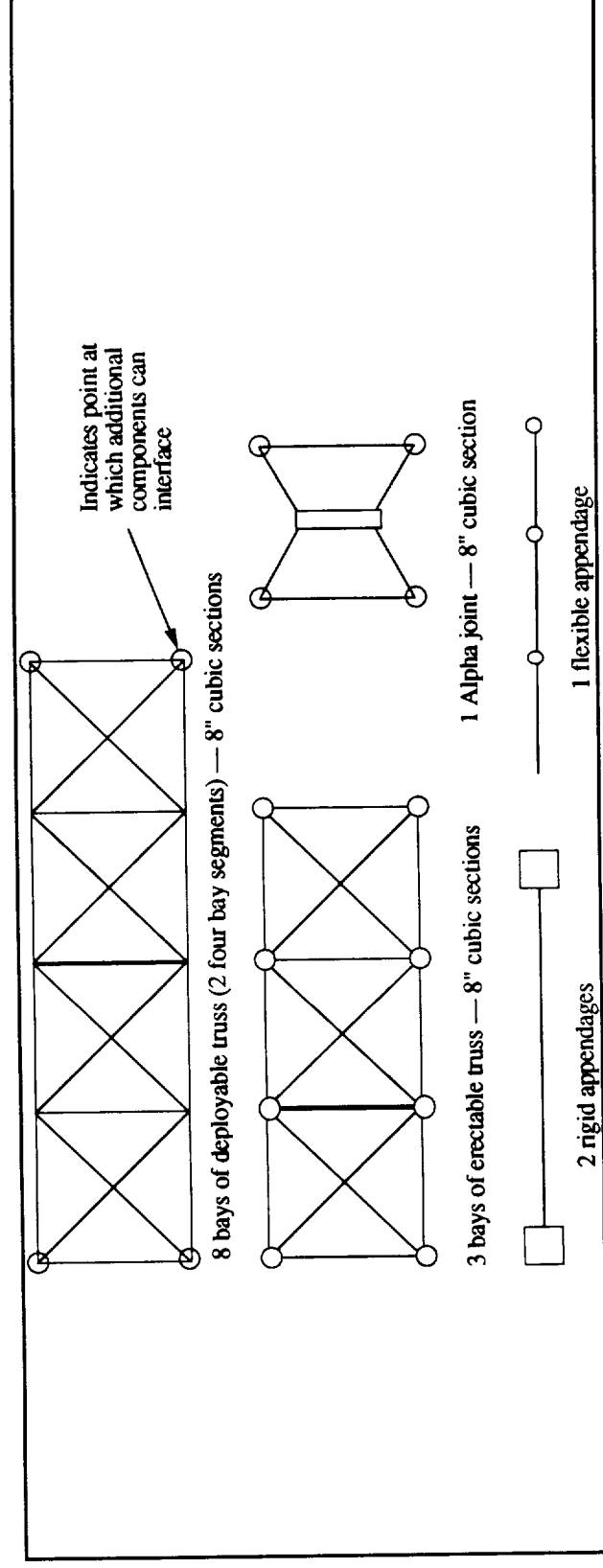
Typical Ground Test Experimental and Predicted Results



Measured and Predicted One-Gravity Results for a Cylindrical Tank with Water. Tank Diameter=3.1 cm. $\mu=0.16$, $\nu=0.89$, $\zeta=9.1\%$, $Bo=33$, $fo = 7$ Hz)

Experimental Design (Structures)

- Scaled models of prototypical space truss structures
 - Deployable bays with a bay with variable pre-tension and nonlinear joints
 - Erectable bays
 - Scaled Alpha (α) joint
 - Very flexible appendage (1 Hz)



Component Testing

Bay testing
Single joint testing

Analytical Model

Use force-state results to generate nonlinear model

Use results to verify nonlinear on component level or to build "component" nonlinear model

Use to update FEM

Use to verify analytical model

Identify limitation of earth testing

Ground Modal Testing

Determine linear modal characteristics

Determine Nonlinear Modal characteristics

Understand suspension effects

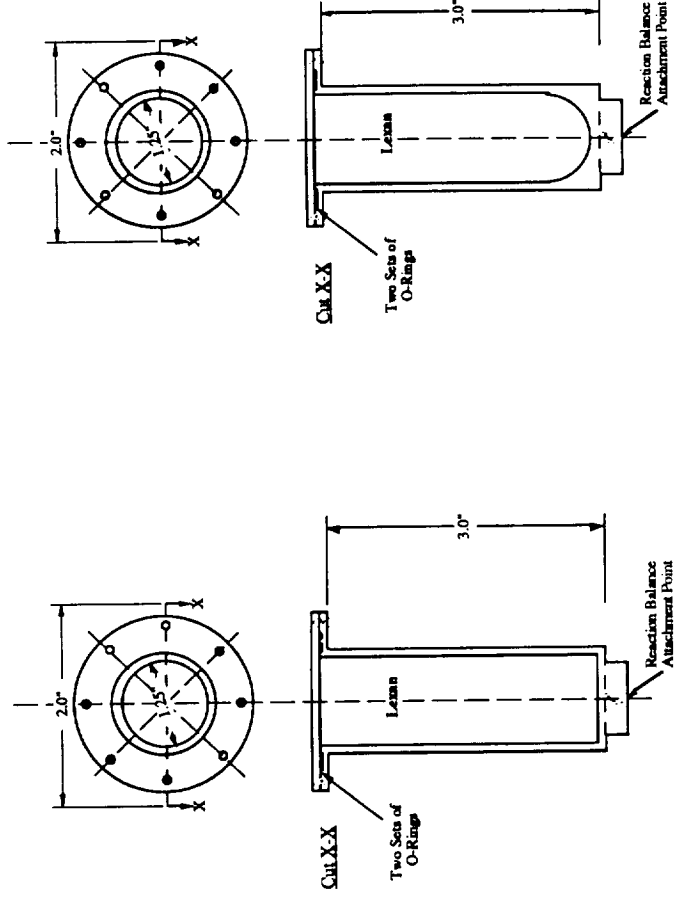
Space Modal Testing

Determine linear modal characteristics

Determine Nonlinear Modal characteristics

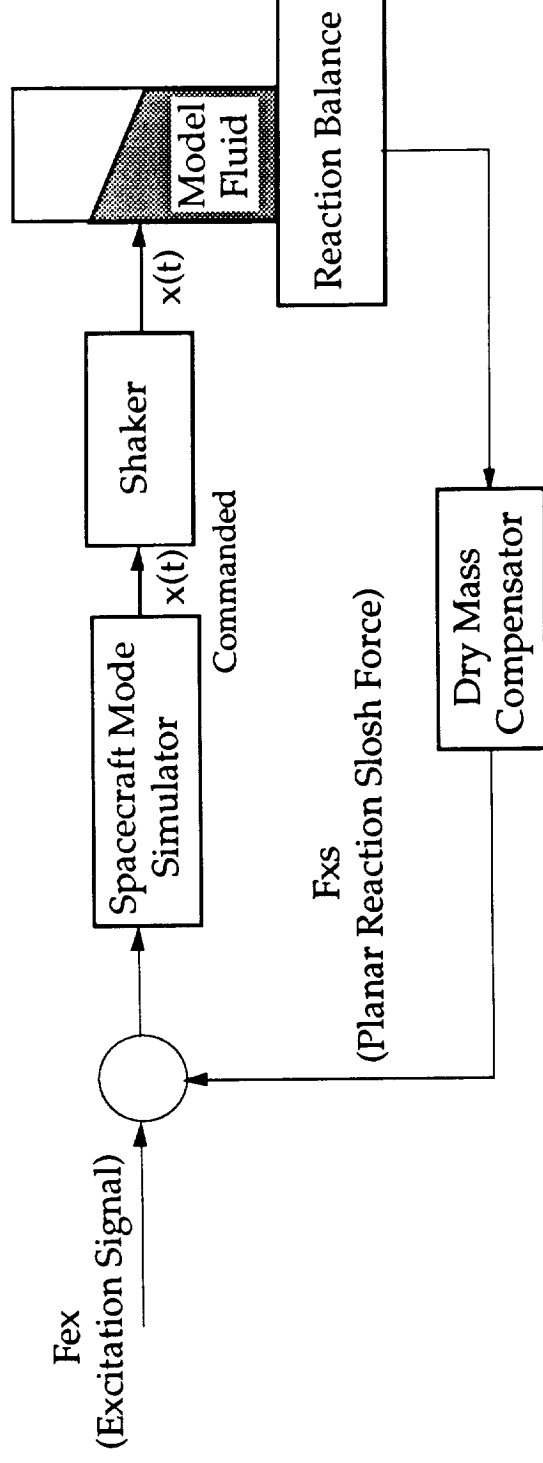
Experimental Design (Contained Fluids)

- Scaled tanks of prototypical spacecraft fluid containers
 - Cylindrical tank with a flat bottom
 - Cylindrical tank with a spherical bottom
- Fluids matching the properties of typical cryogenics
 - Silicone oil (Potential stability problem)
 - Water as a backup
 - Both are non-toxic and non-flammable

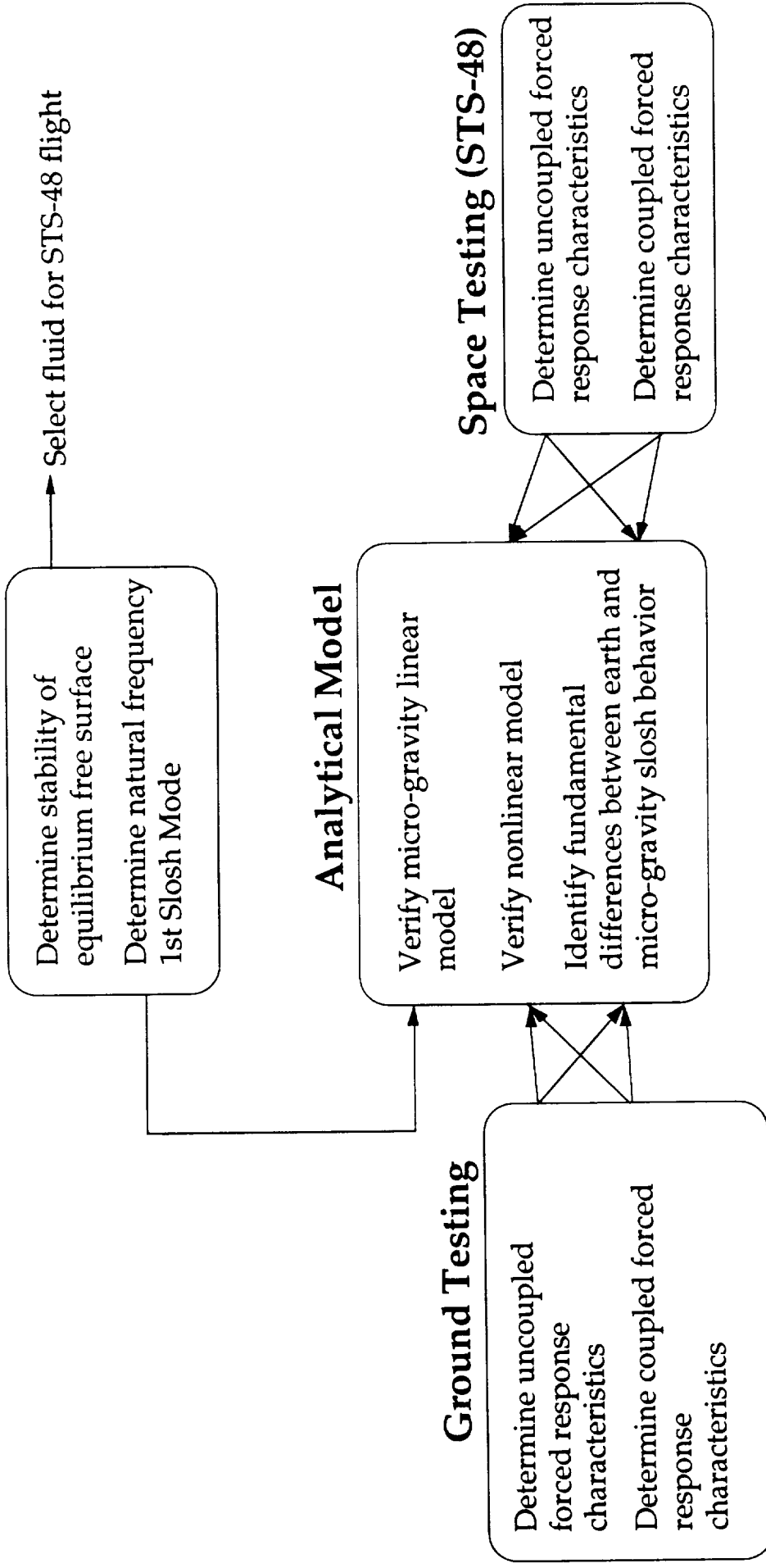


Experimental Design (Contained Fluids - Cont.)

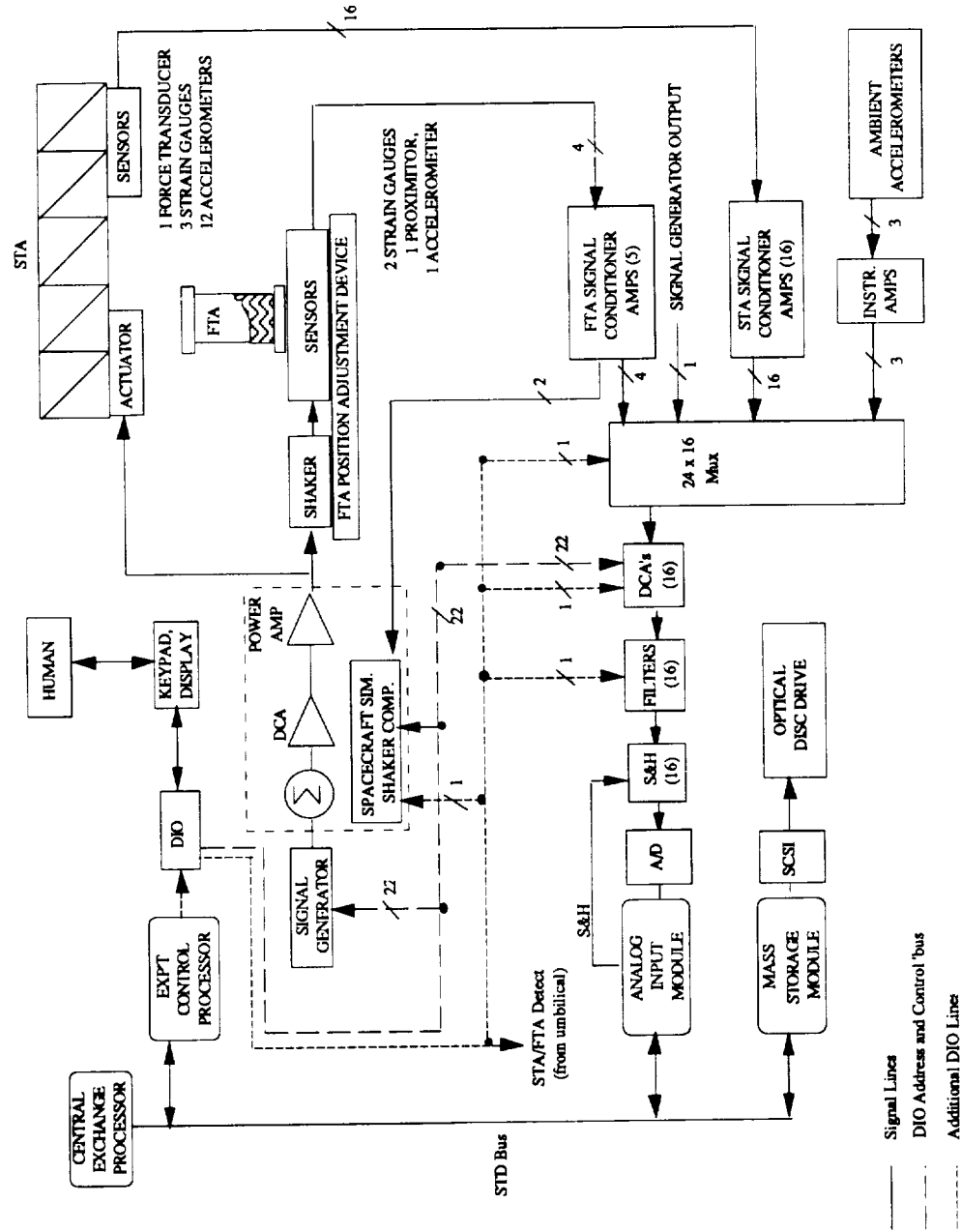
- Fluid/Spacecraft interaction studied by including an analog simulation of a spacecraft's mode



MODE-0 (STS-40)

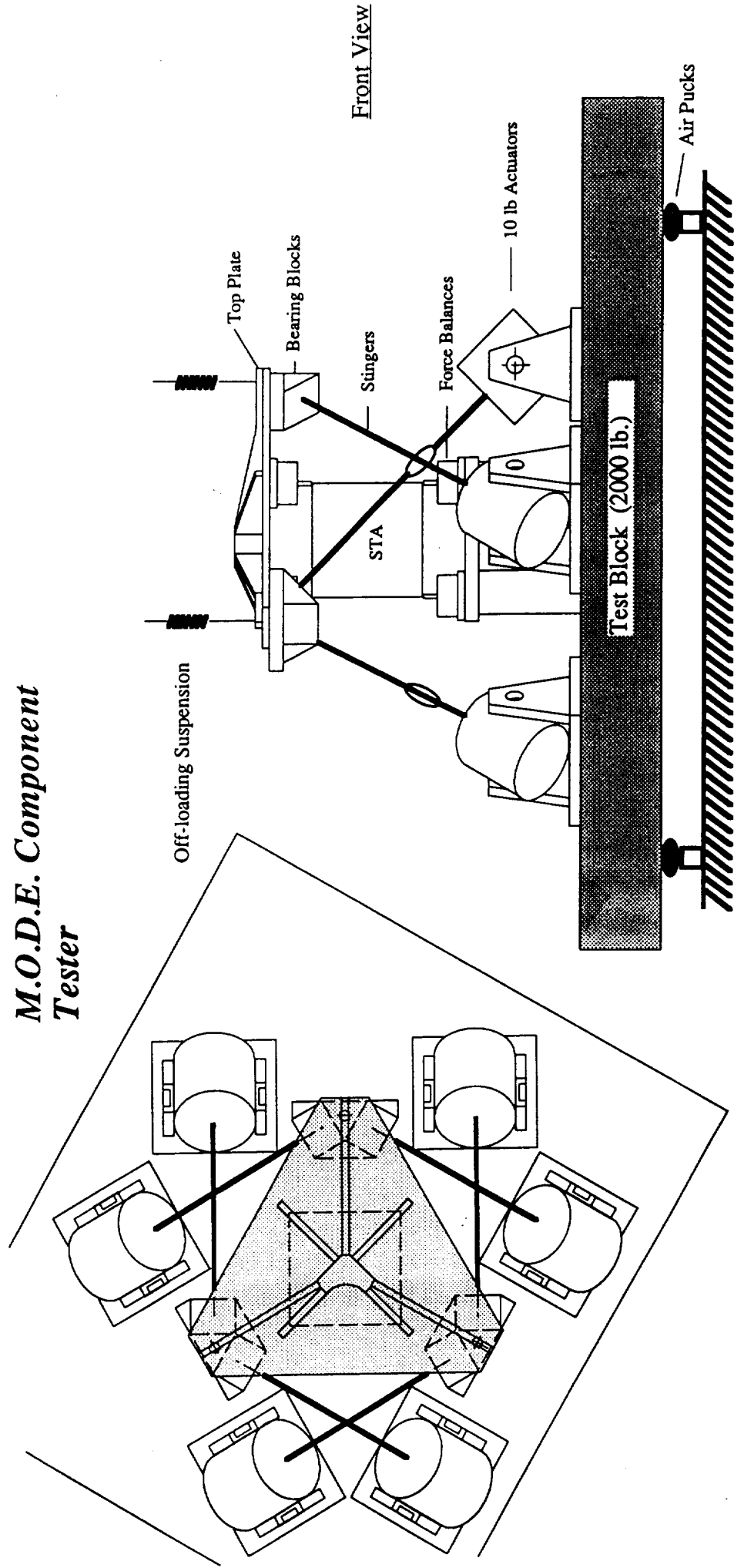


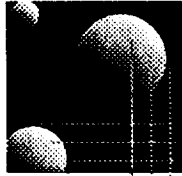
Progress to Date



Progress to Date (Continued)

M.O.D.E. Component Tester





INHIBITING MULTIPLE MODE VIBRATION IN CONTROLLED FLEXIBLE SYSTEMS

James M. Hyde
Kenneth W. Chang
Prof. Warren P. Seering

Massachusetts Institute of Technology

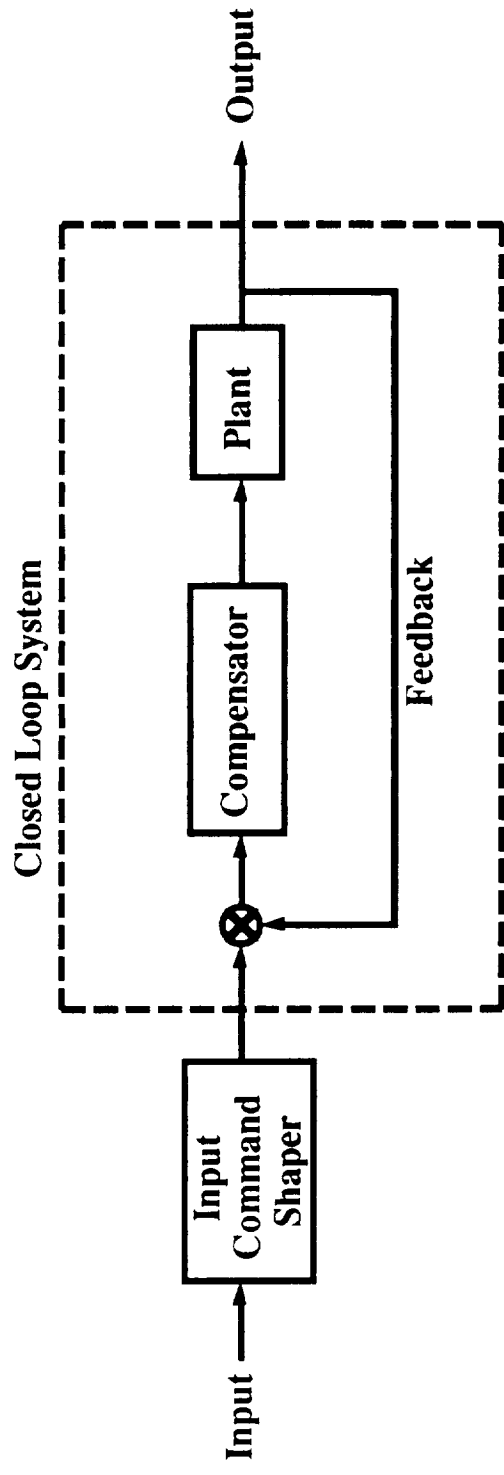
July 1, 1991

639
165327
p. 19
N93-28172

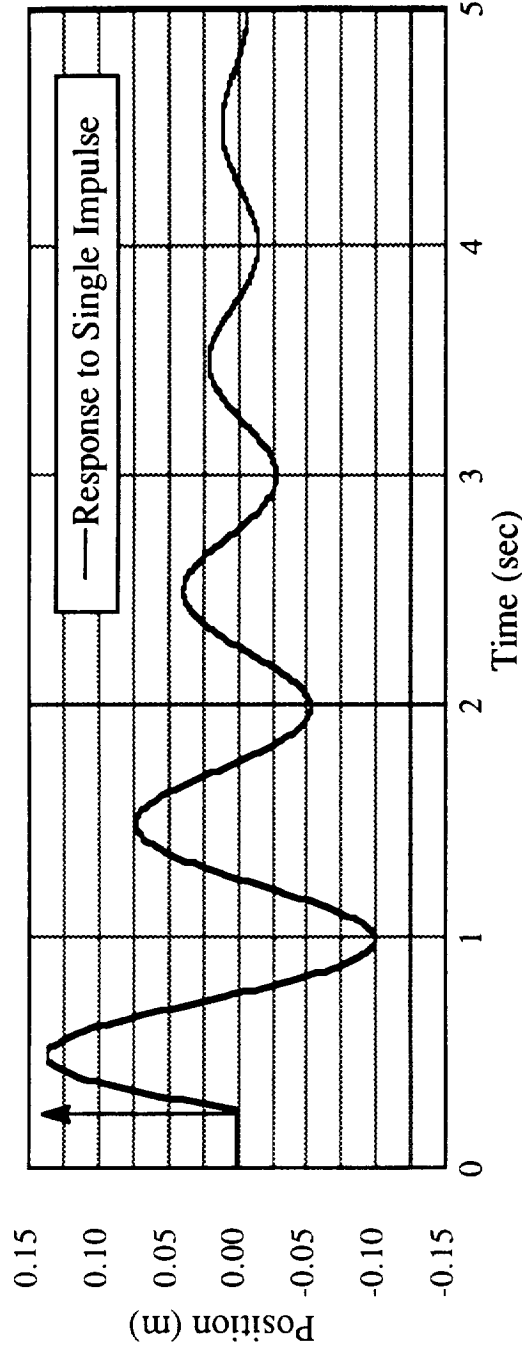
OUTLINE

- Input Pre-Shaping Background
- Developing Multiple-Mode Shapers
- The MACE Test Article
- Tests and Results

SHAPER POSITION IN CONTROL SYSTEM



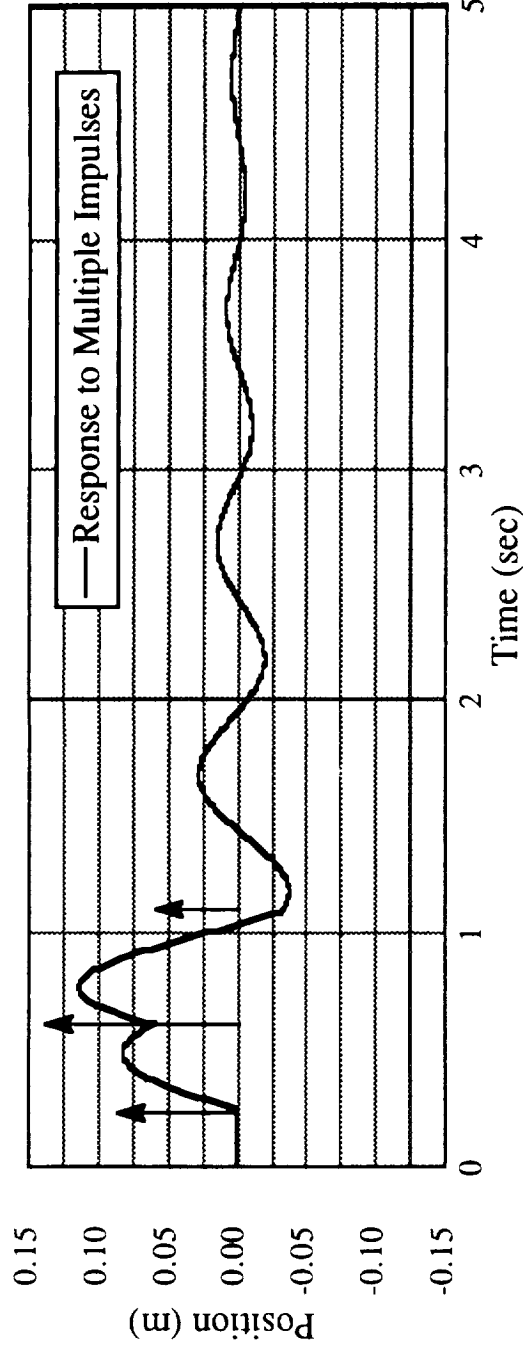
LINEAR SYSTEM IMPULSE RESPONSE



$$y_i(t) = A_i e^{-\zeta \omega (t - t_i)} \sin((t - t_i) \omega \sqrt{1 - \zeta^2})$$

y_i	Response to Impulse i
A_i	Magnitude of Impulse i
t_i	Time of Impulse i
ω	System Natural Frequency
ζ	System Damping Ratio

RESPONSE TO "N" IMPULSES



$$y_i(t) = \sum_{i=1}^N A_i e^{-\zeta \omega (t - t_i)} \sin((t - t_i) \omega \sqrt{1 - \zeta^2})$$

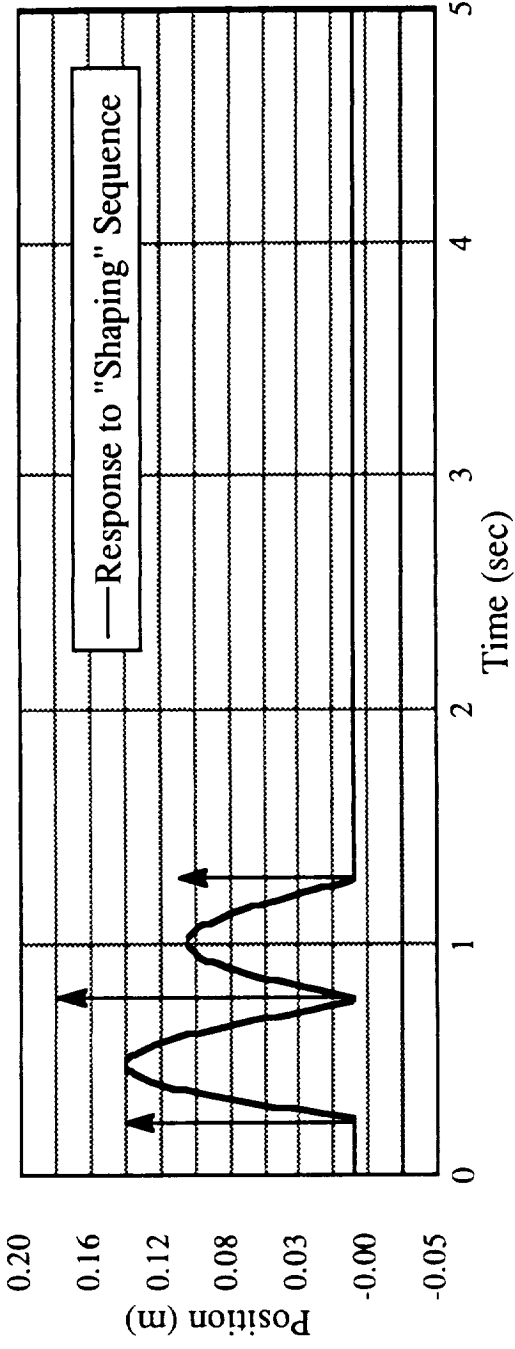
i Impulse Counter
 N Number of Impulses

AMPLITUDE OF THE MULTIPLE-IMPULSE RESPONSE ENVELOPE

$$Amp = \left[\left(\sum_{i=1}^N A_i e^{-\zeta \omega (t_N - t_i)} \sin(t_i \omega \sqrt{1 - \zeta^2}) \right)^2 + \left(\sum_{i=1}^N A_i e^{-\zeta \omega (t_N - t_i)} \cos(t_i \omega \sqrt{1 - \zeta^2}) \right)^2 \right]^{1/2}$$

Expression for envelope amplitude at t_N ,
the time of the final impulse.

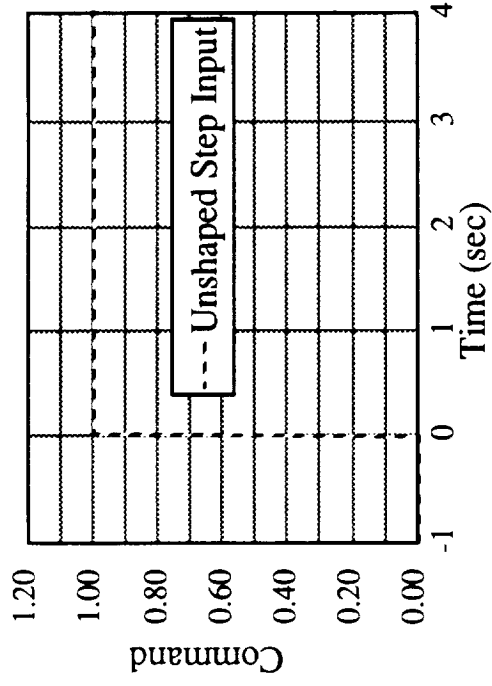
ELIMINATING RESIDUAL VIBRATION



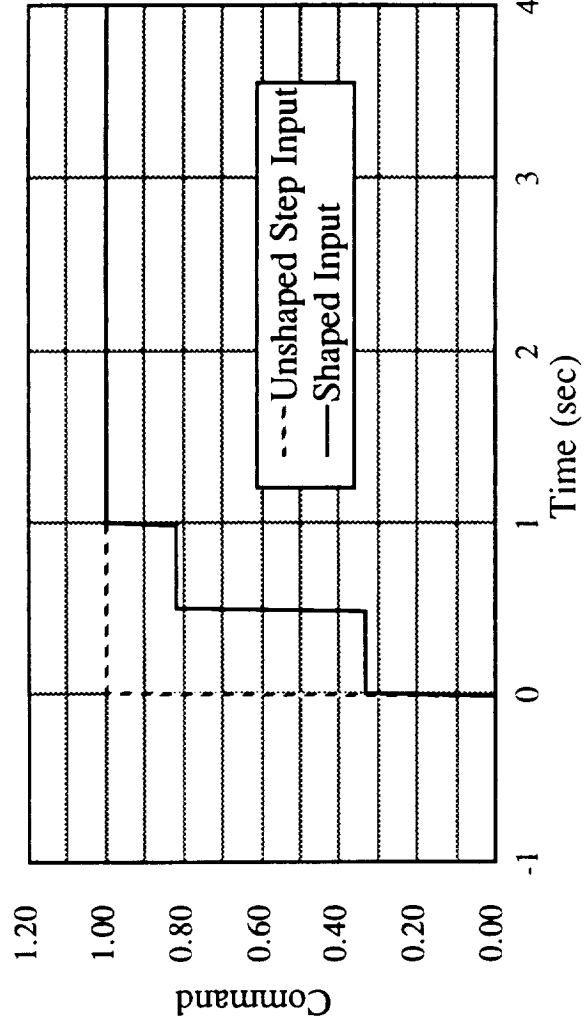
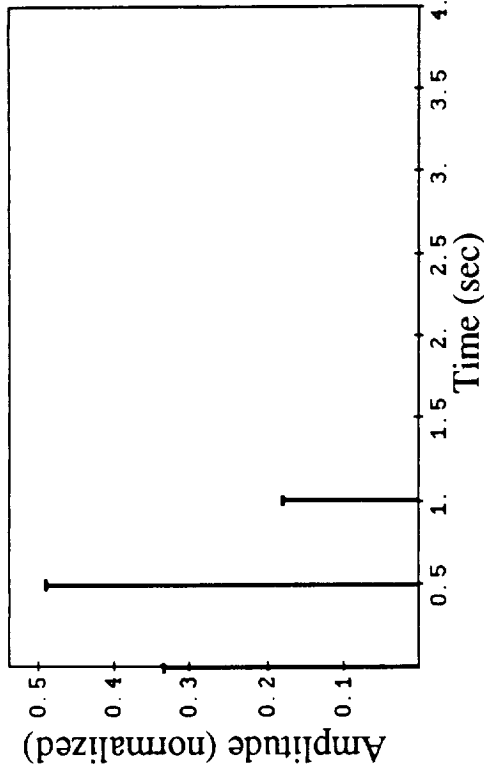
$$\sum_{i=1}^N A_i e^{-\zeta \omega t_i} \sin(t_i \omega \sqrt{1 - \zeta^2}) = 0 \quad \sum_{i=1}^N A_i t_i e^{-\zeta \omega t_i} \sin(t_i \omega \sqrt{1 - \zeta^2}) = 0$$

$$\sum_{i=1}^N A_i e^{-\zeta \omega t_i} \cos(t_i \omega \sqrt{1 - \zeta^2}) = 0 \quad \sum_{i=1}^N A_i t_i e^{-\zeta \omega t_i} \cos(t_i \omega \sqrt{1 - \zeta^2}) = 0$$

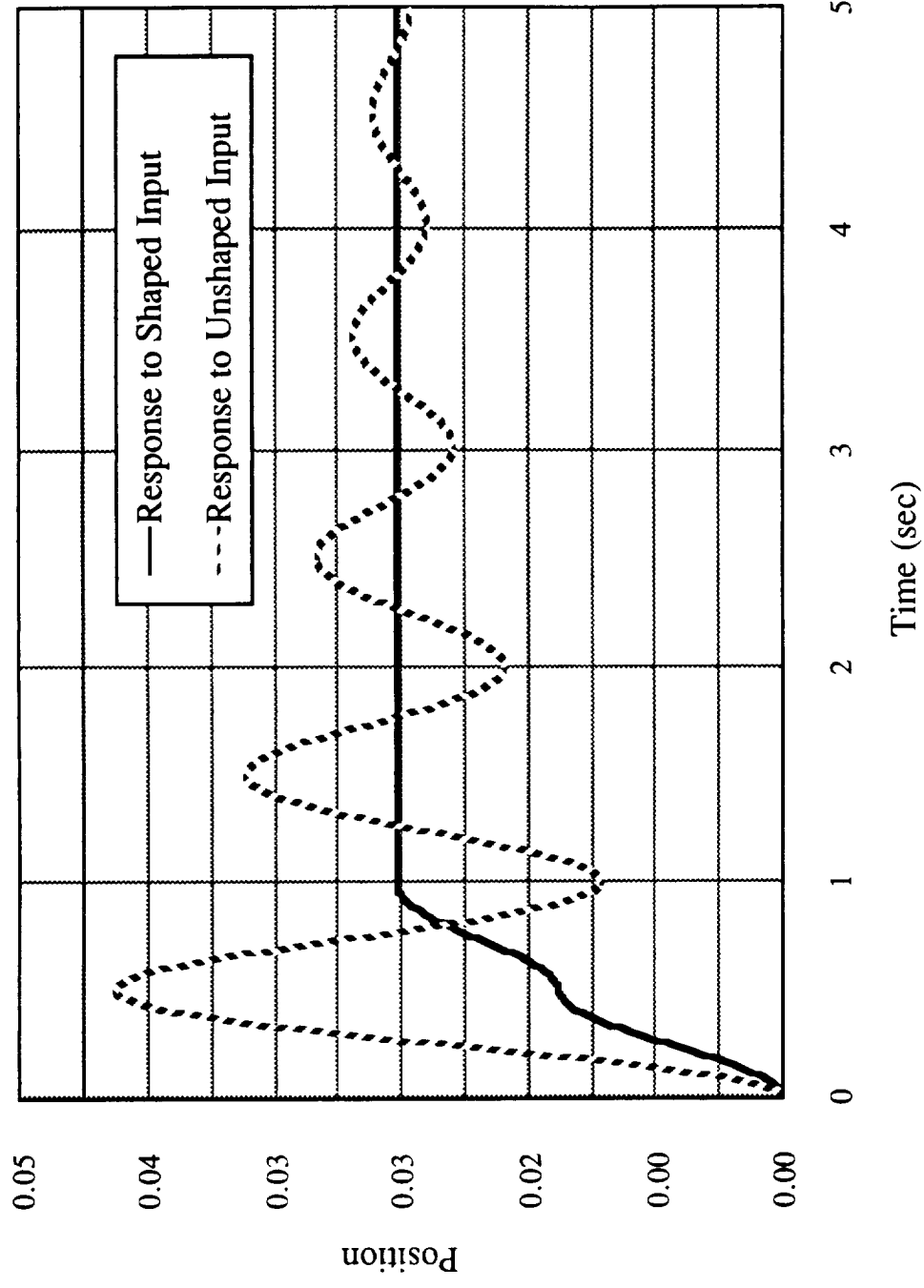
USING THE IMPULSE SEQUENCE



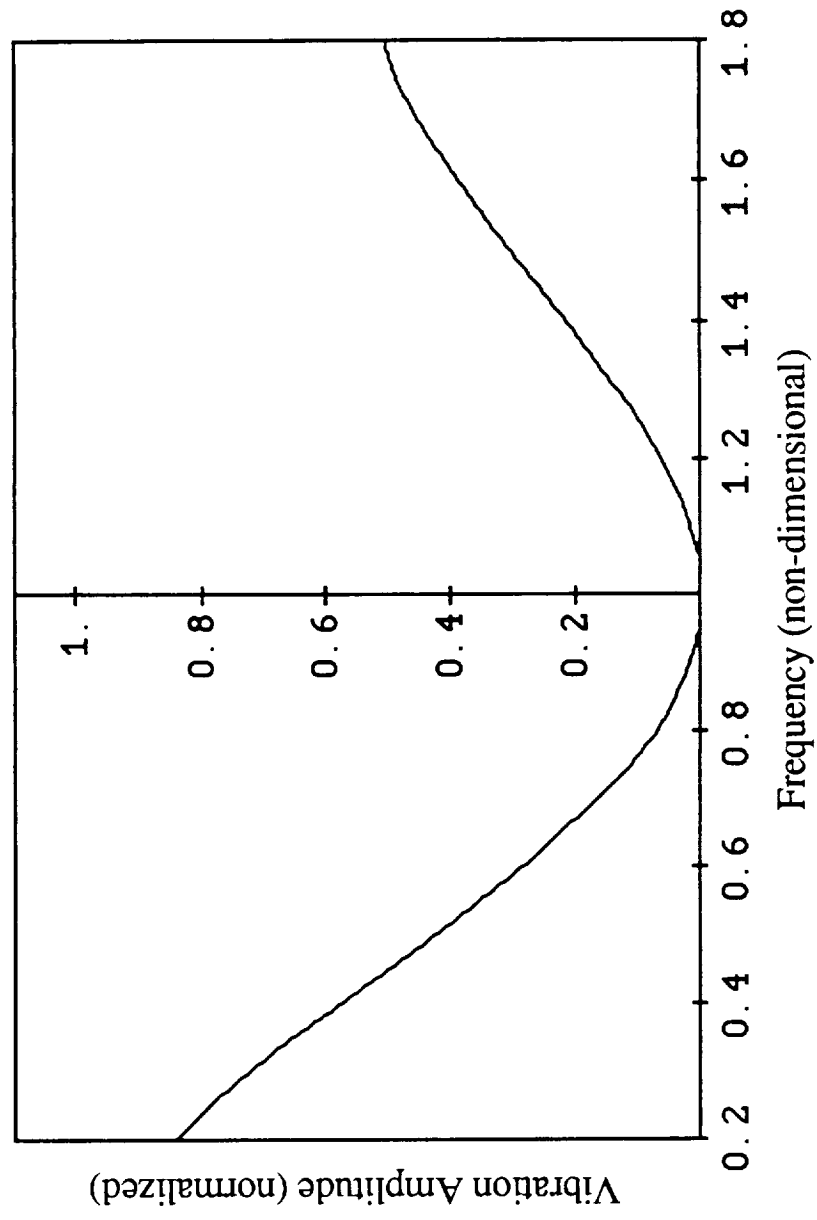
*



RESPONSE TO INPUTS

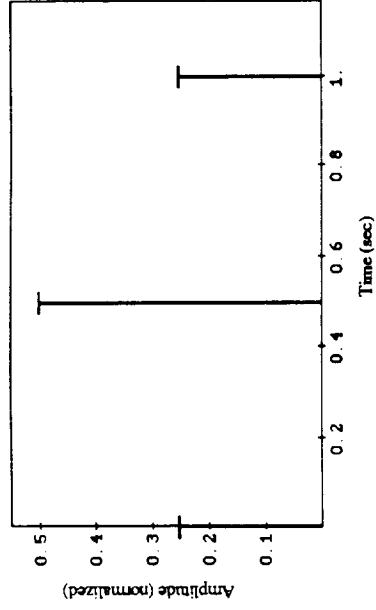


INSENSITIVITY OF THREE-IMPULSE SEQUENCE

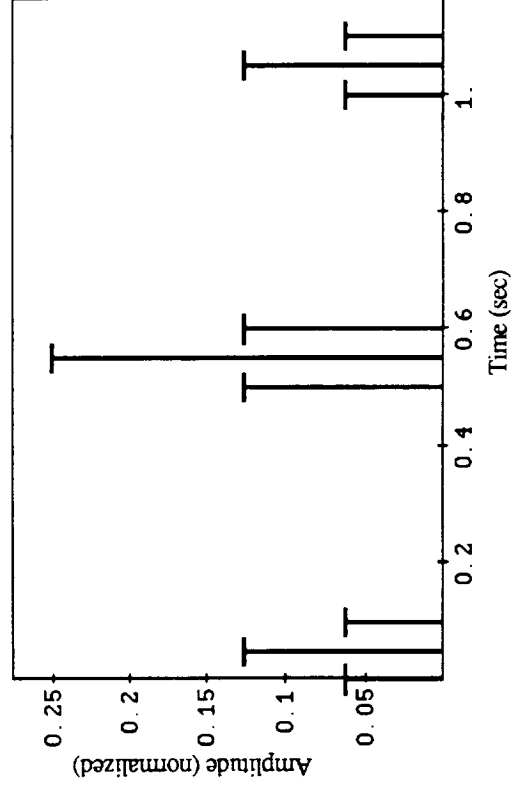
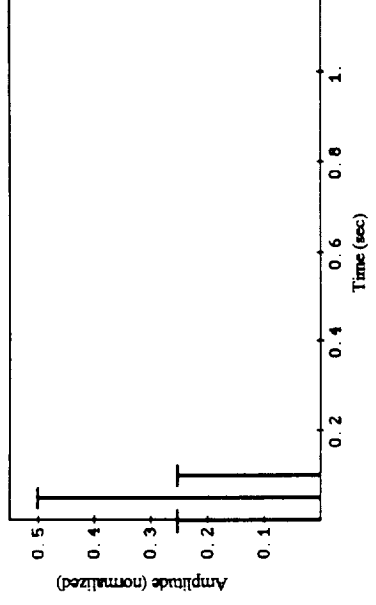


EXTENDING TO MULTIPLE MODE PROBLEMS

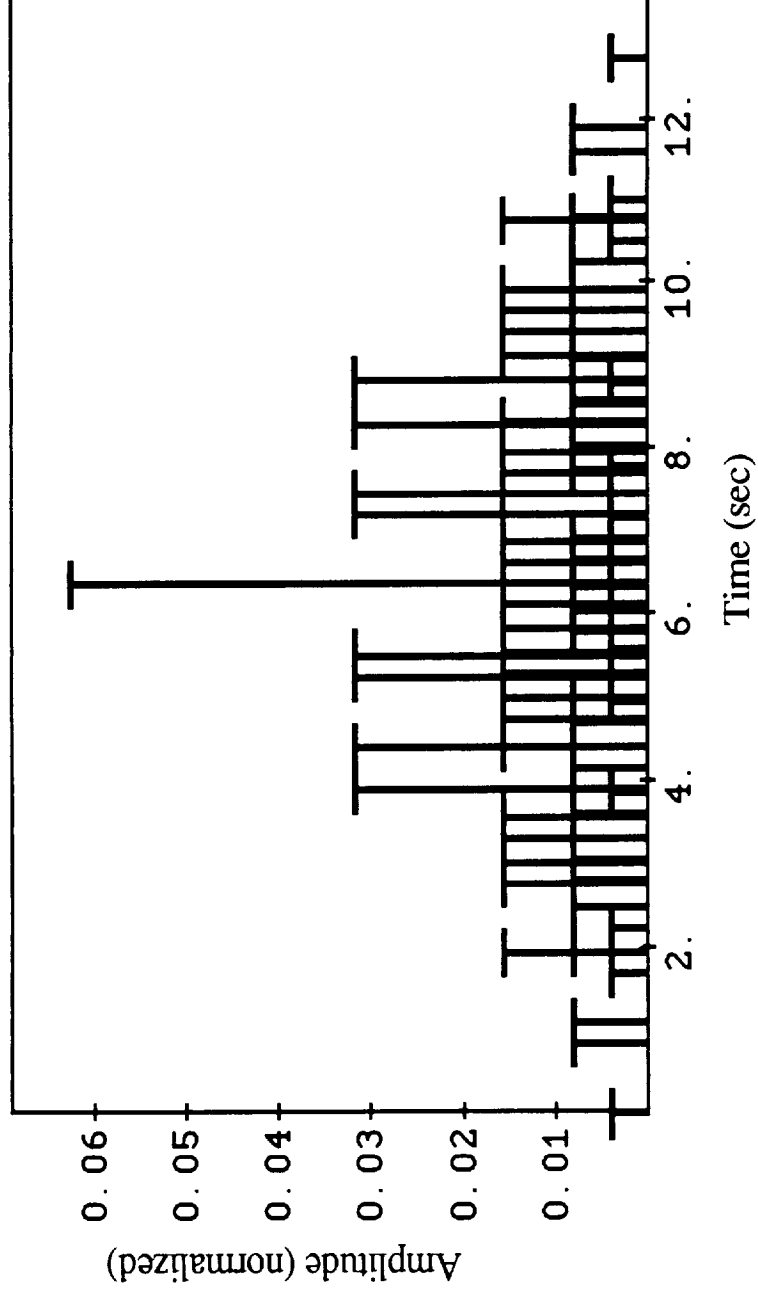
CONVOLUTION



*



CONVOLUTION SEQUENCE PROBLEMS



$$\omega_1 = 0.20 \text{ Hz}$$

$$\omega_2 = 0.26 \text{ Hz}$$

$$\omega_3 = 0.45 \text{ Hz}$$

$$\omega_4 = 0.59 \text{ Hz}$$

DIRECT SOLUTION CONSTRAINT EQUATIONS

$$\sum_{i=1}^N A_i e^{-\zeta_j \omega_j t_i} \sin(t_i \omega_j \sqrt{1 - \zeta_j^2}) = 0$$

$$\sum_{i=1}^N A_i e^{-\zeta_j \omega_j t_i} \cos(t_i \omega_j \sqrt{1 - \zeta_j^2}) = 0$$

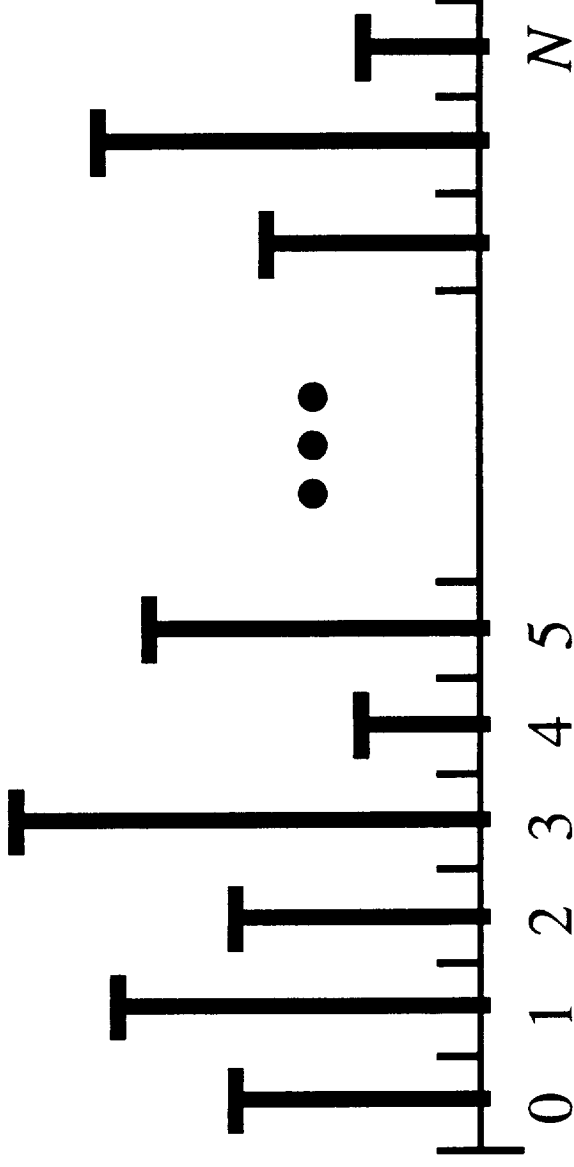
$$\sum_{i=1}^N A_i t_i e^{-\zeta_j \omega_j t_i} \sin(t_i \omega_j \sqrt{1 - \zeta_j^2}) = 0$$

$$\sum_{i=1}^N A_i t_i e^{-\zeta_j \omega_j t_i} \cos(t_i \omega_j \sqrt{1 - \zeta_j^2}) = 0$$

These four equations are repeated for each mode "j"

LINEARIZING THE EQUATIONS

Define time mesh with N slots



Impulse times (t_i) : Known

Impulse amplitudes (A_i) : Unknown

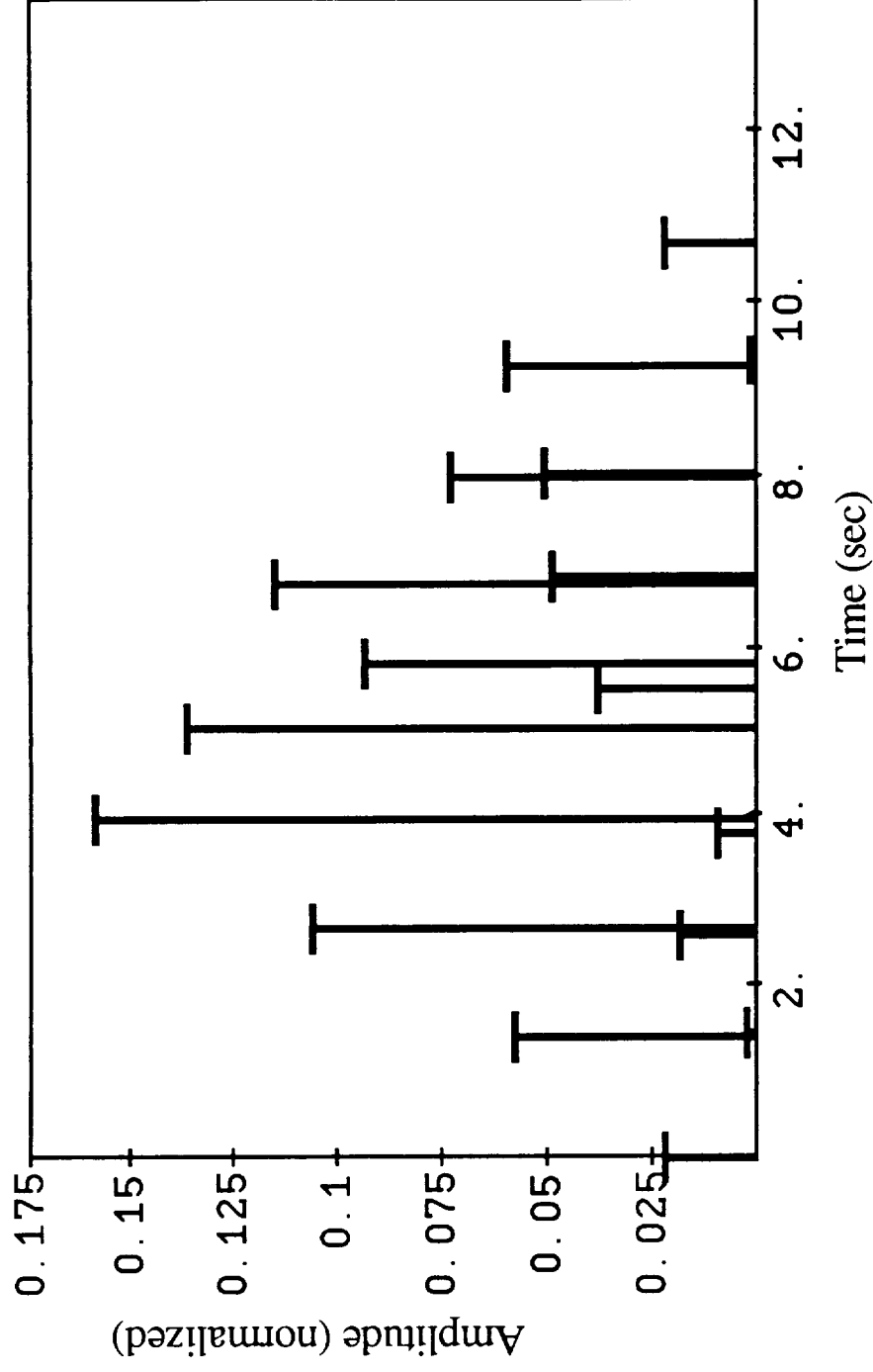
COST FUNCTION

$$Cost = \sum_{j=1}^M \left[\left(\sum_{i=1}^N A_i t_i^2 e^{-\zeta_j \omega_j t_i} \sin(t_i \omega_j \sqrt{1 - \zeta_j^2}) \right)^2 + \right.$$

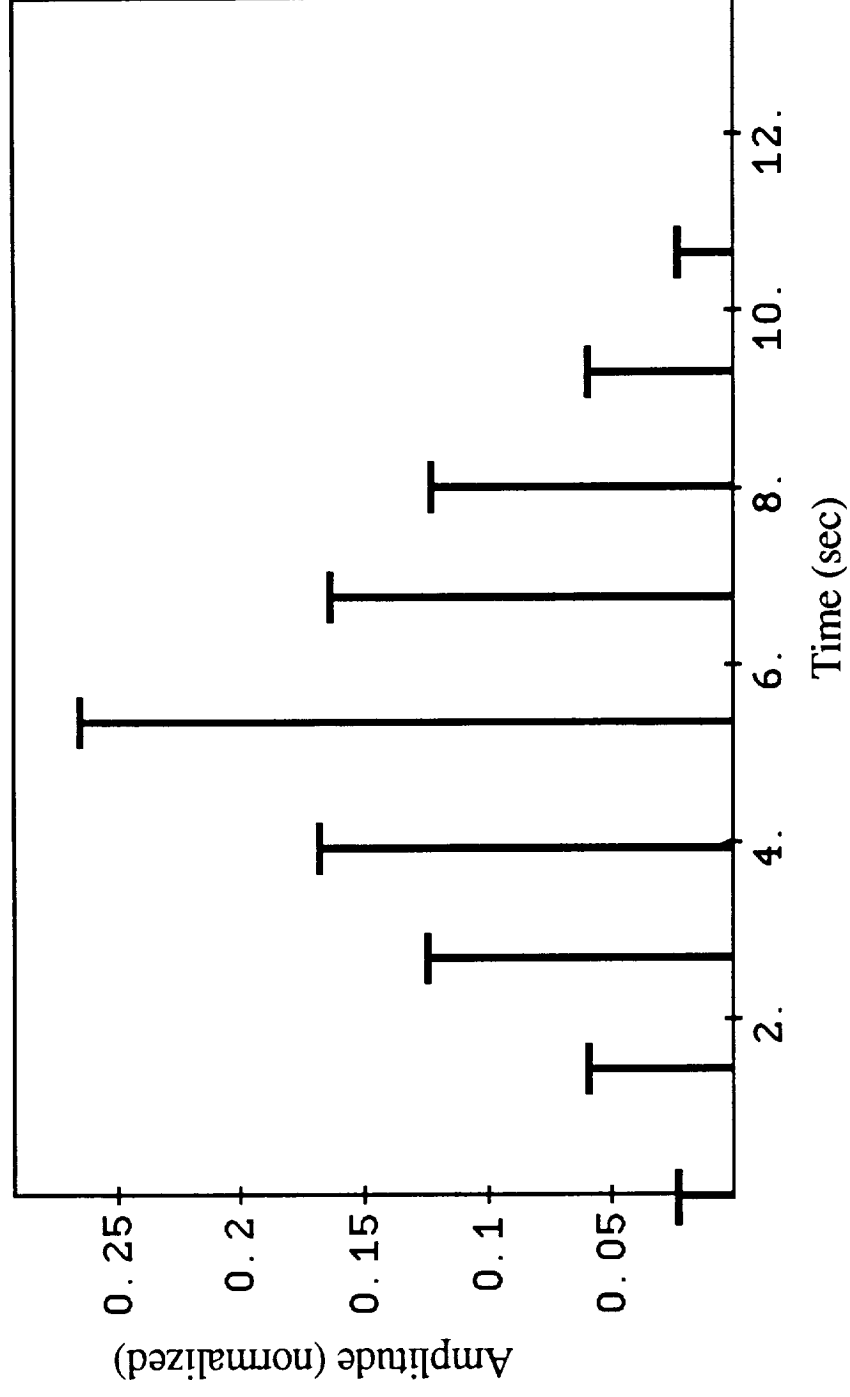
$$\left. \left(\sum_{i=1}^N A_i t_i^2 e^{-\zeta_j \omega_j t_i} \cos(t_i \omega_j \sqrt{1 - \zeta_j^2}) \right)^2 \right]$$

M Number of modes
 j Modal index

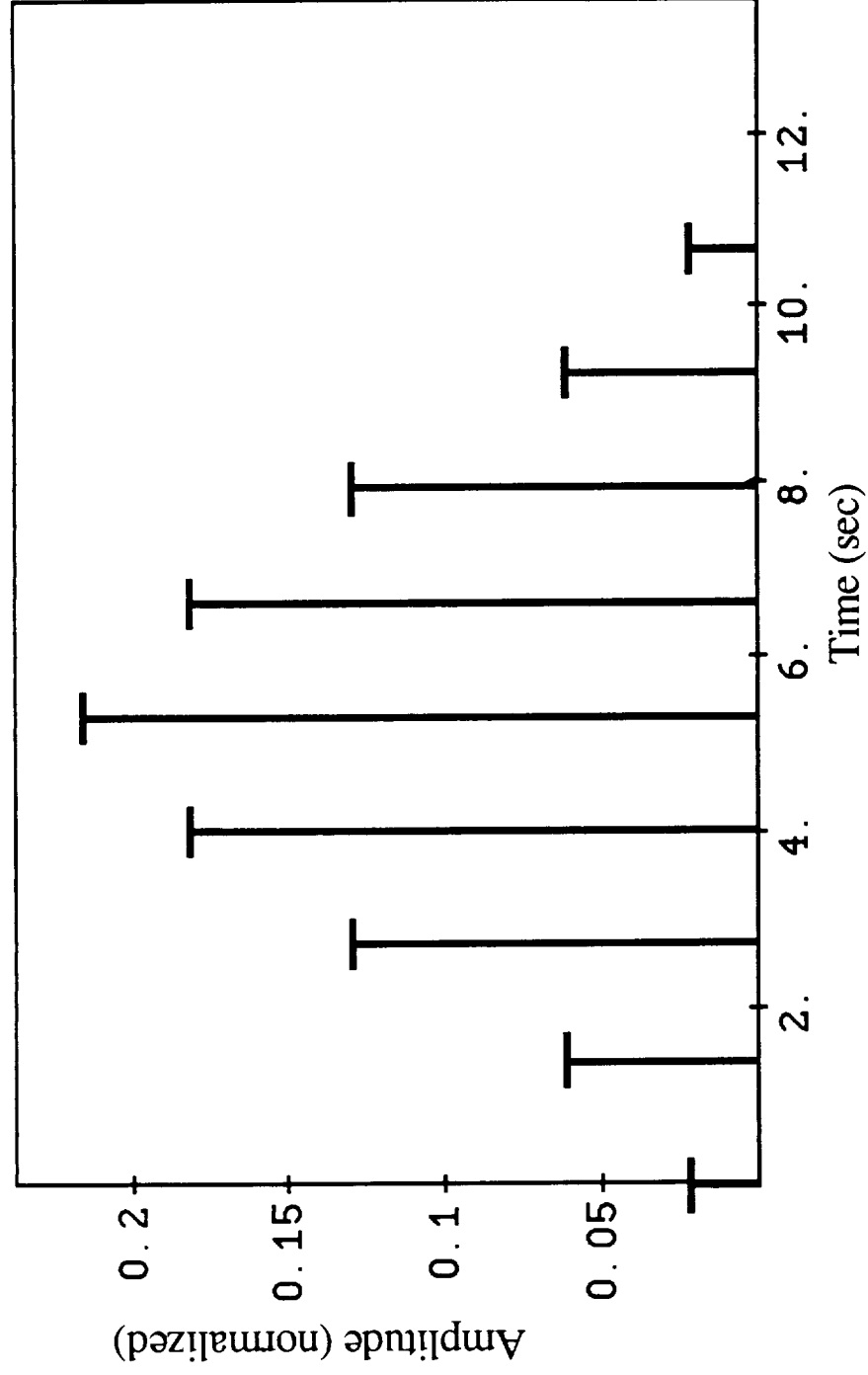
LINEAR APPROXIMATION SEQUENCE



INTERPRETED LINEAR SEQUENCE

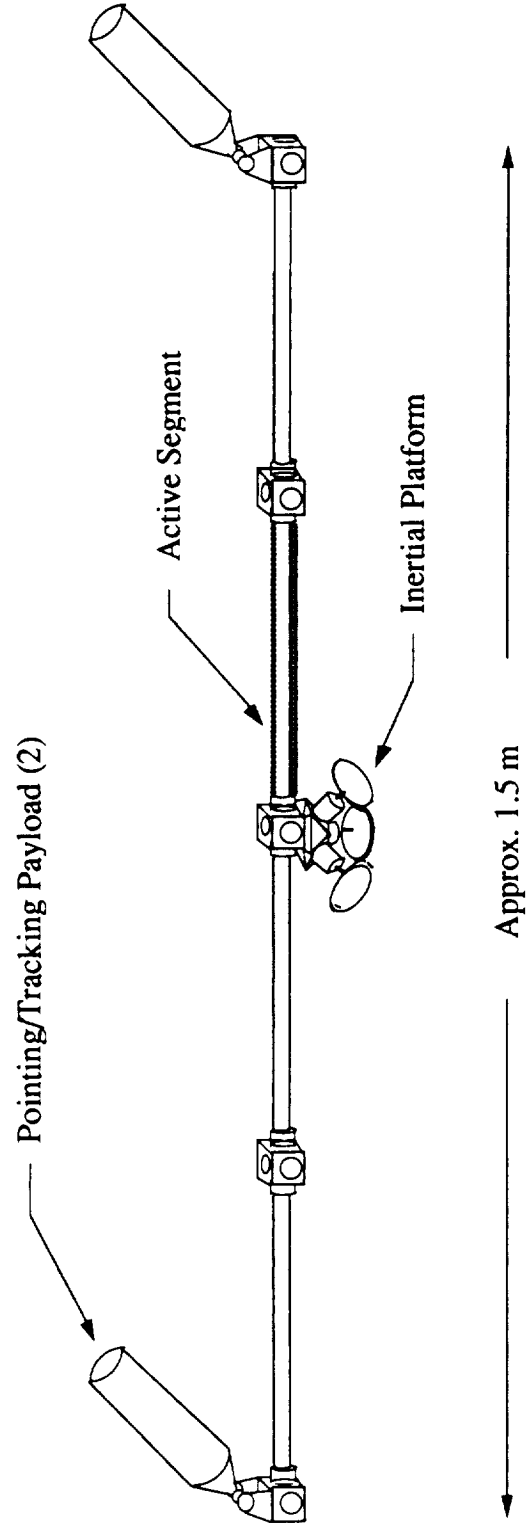


EXACT DIRECT SOLUTION SEQUENCE



THE MID-DECK ACTIVE CONTROL EXPERIMENT
(MACE)

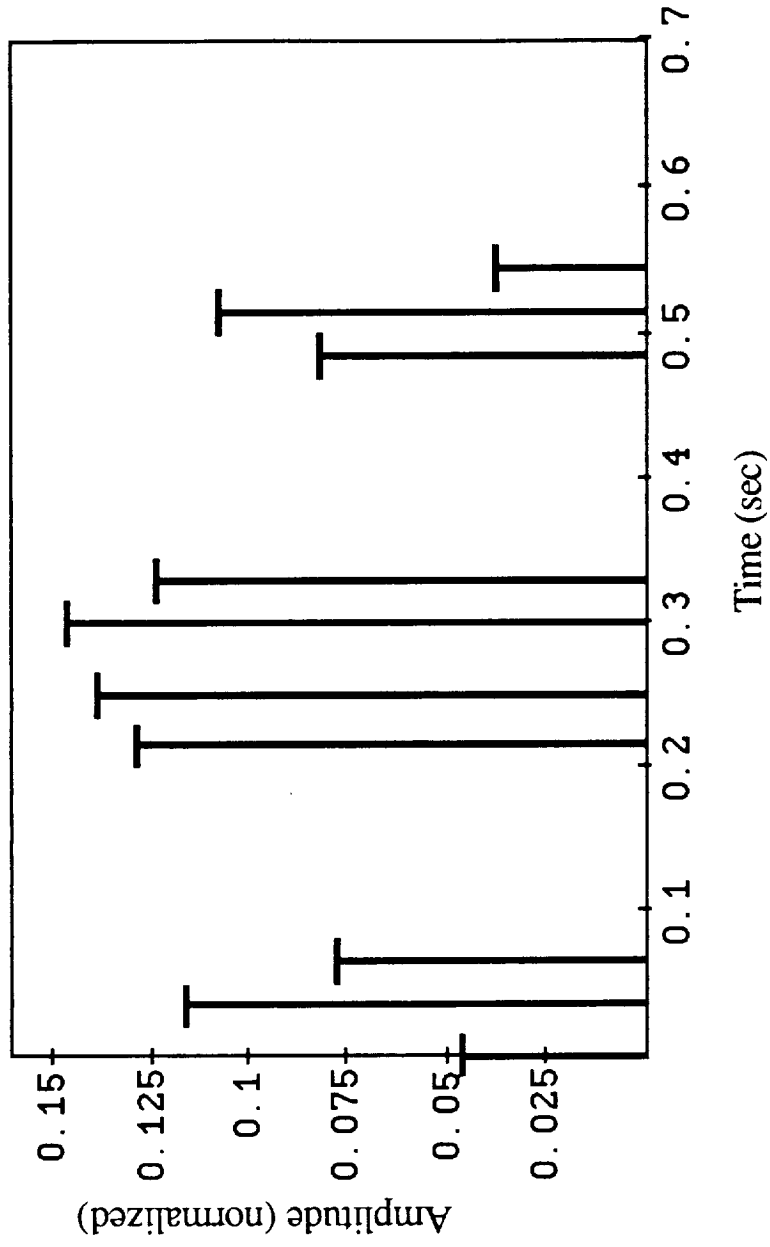
MACE SYSTEM SCHEMATIC



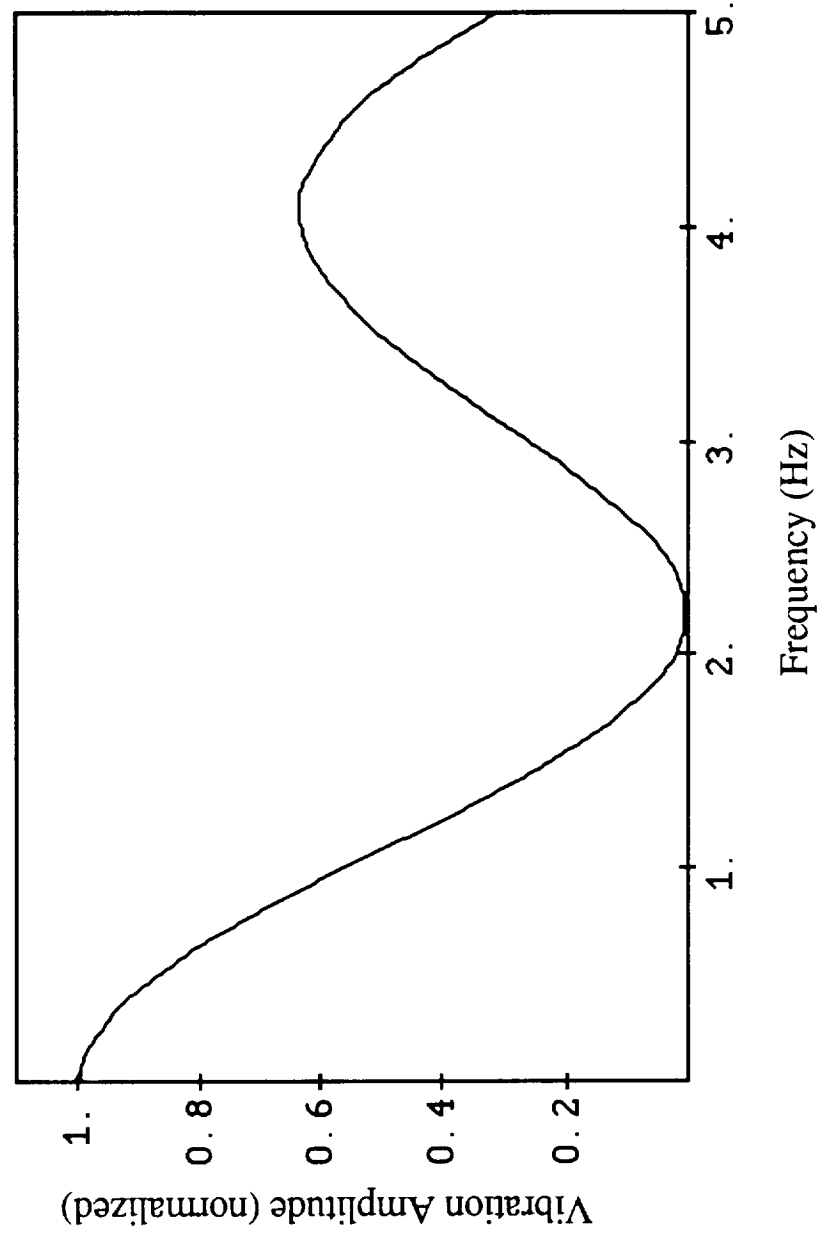
IDENTIFIED CLOSED LOOP FREQUENCIES (NON-LINEAR DISCOS MODEL)

60° Outboard (Hz) (Beginning of 120° Slew)	60° Inboard (Hz) (End of 120° Slew)
2.18	1.88
14.25	13.40
15.25	14.20
15.90	15.90

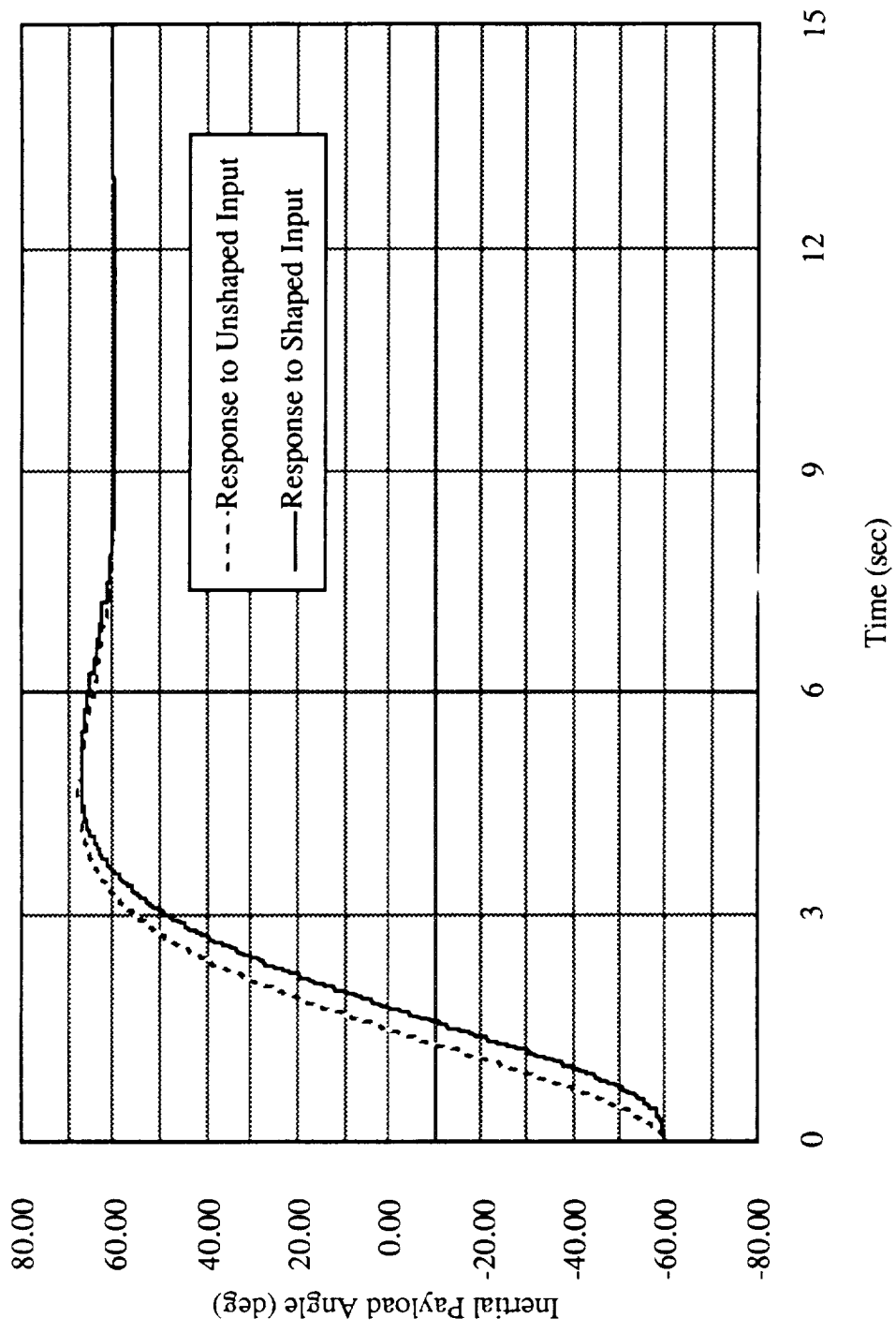
SHAPER DESIGNED FOR "BEGINNING FREQUENCIES"



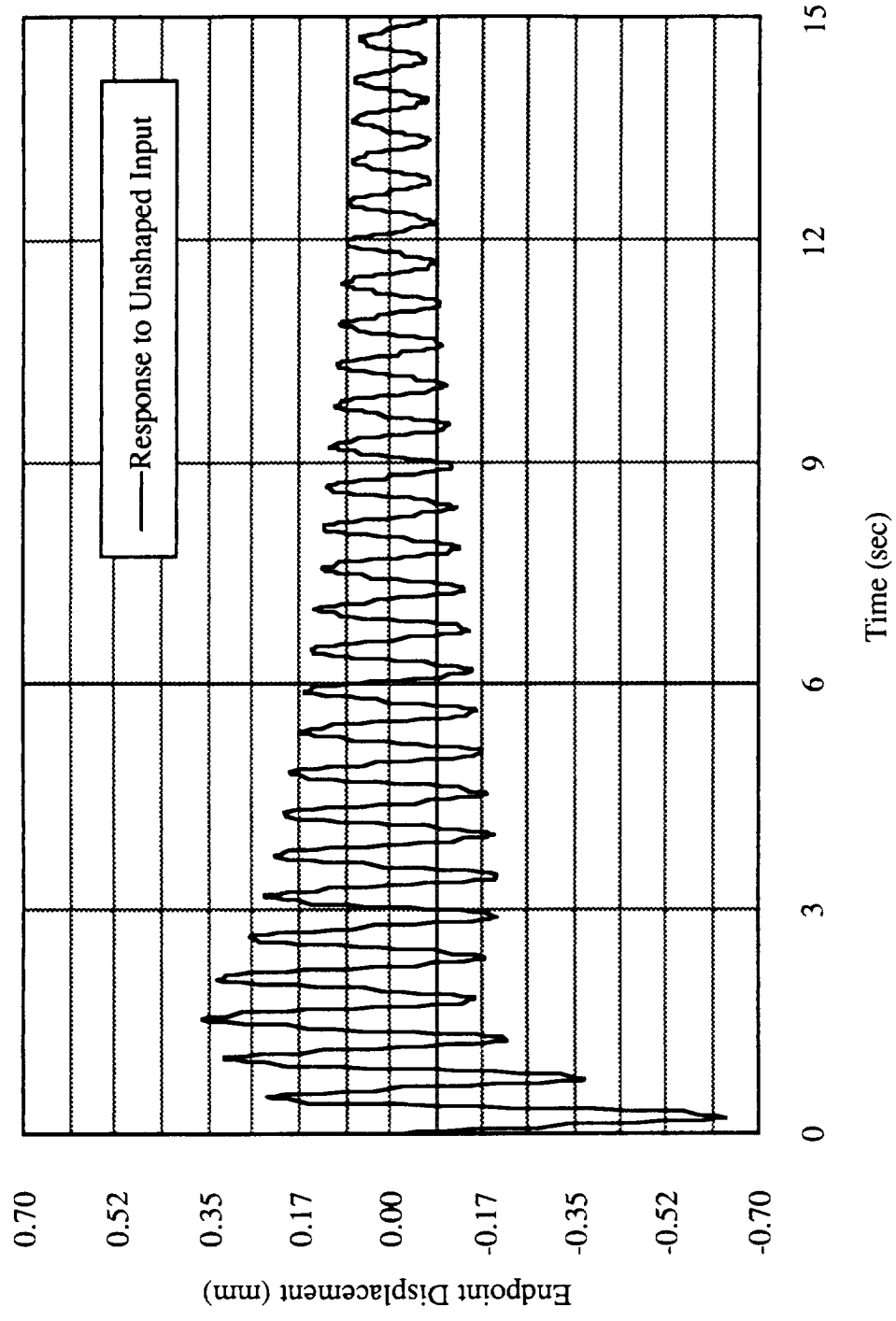
INSENSITIVITY CURVE FOR "BEGINNING FREQUENCIES SHAPER"



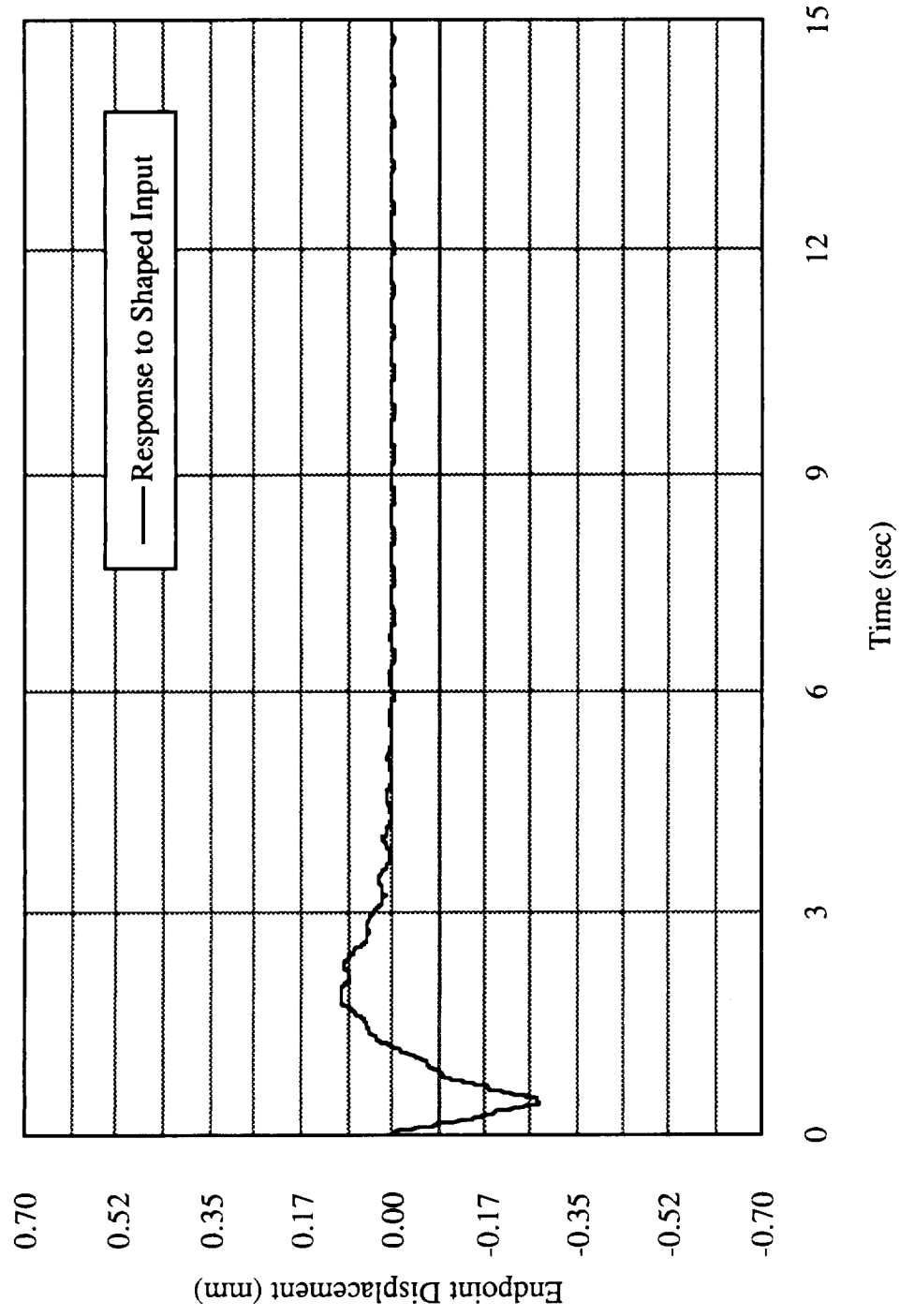
120° CLOSED LOOP PAYLOAD SLEW



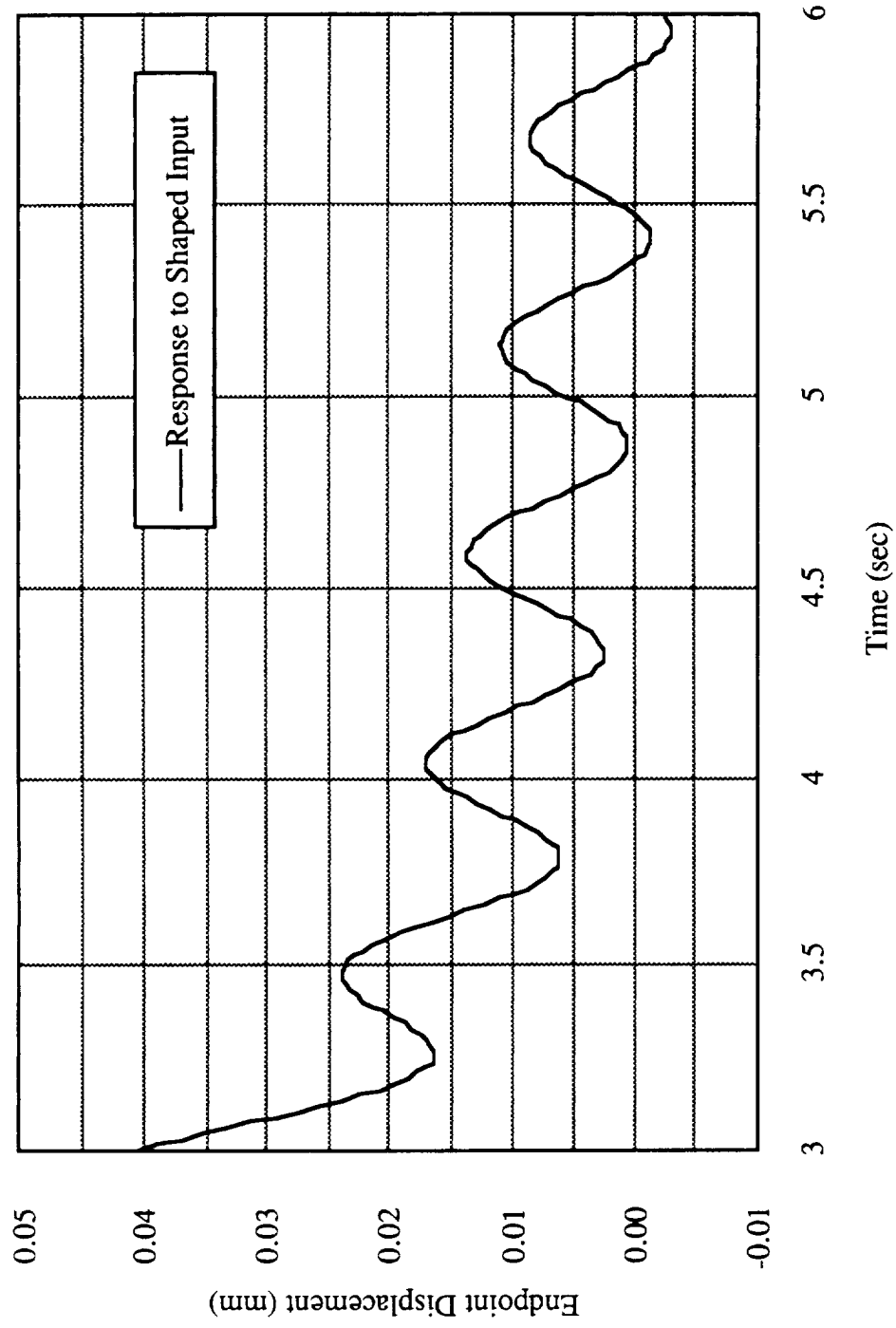
ENDPOINT RESPONSE TO UNSHAPED SLEW



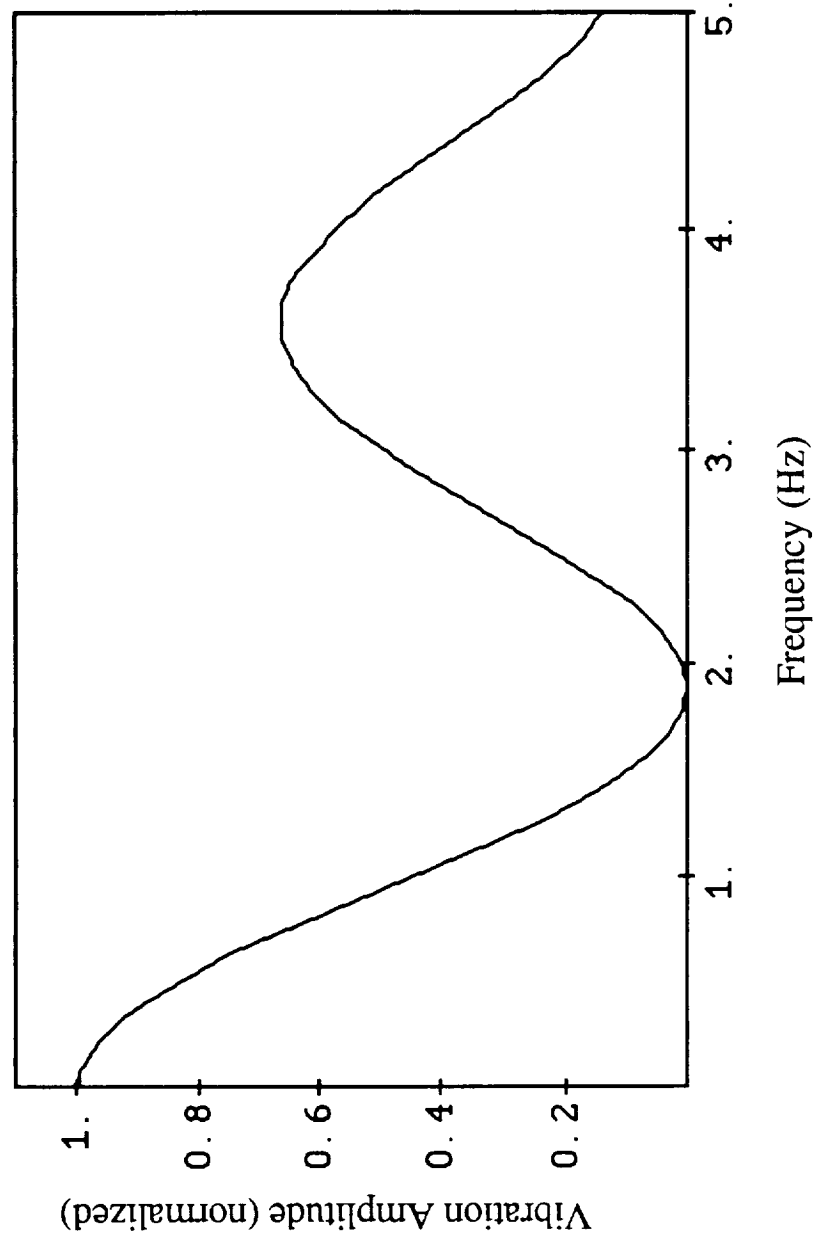
ENDPOINT RESPONSE TO SHAPED SLEW



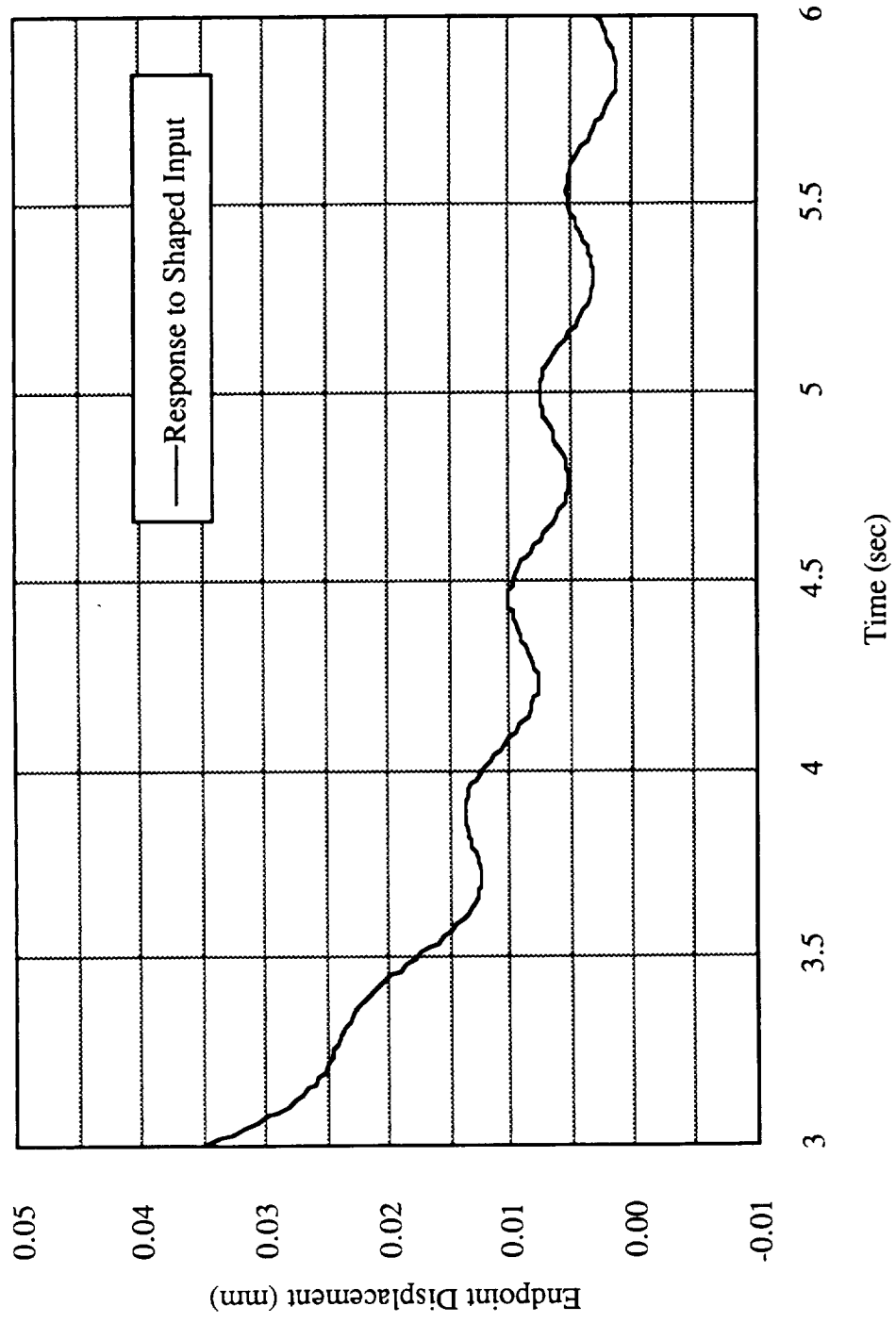
SHAPED RESPONSE DETAIL



INSENSITIVITY CURVE FOR "ENDING FREQUENCIES SHAPER"

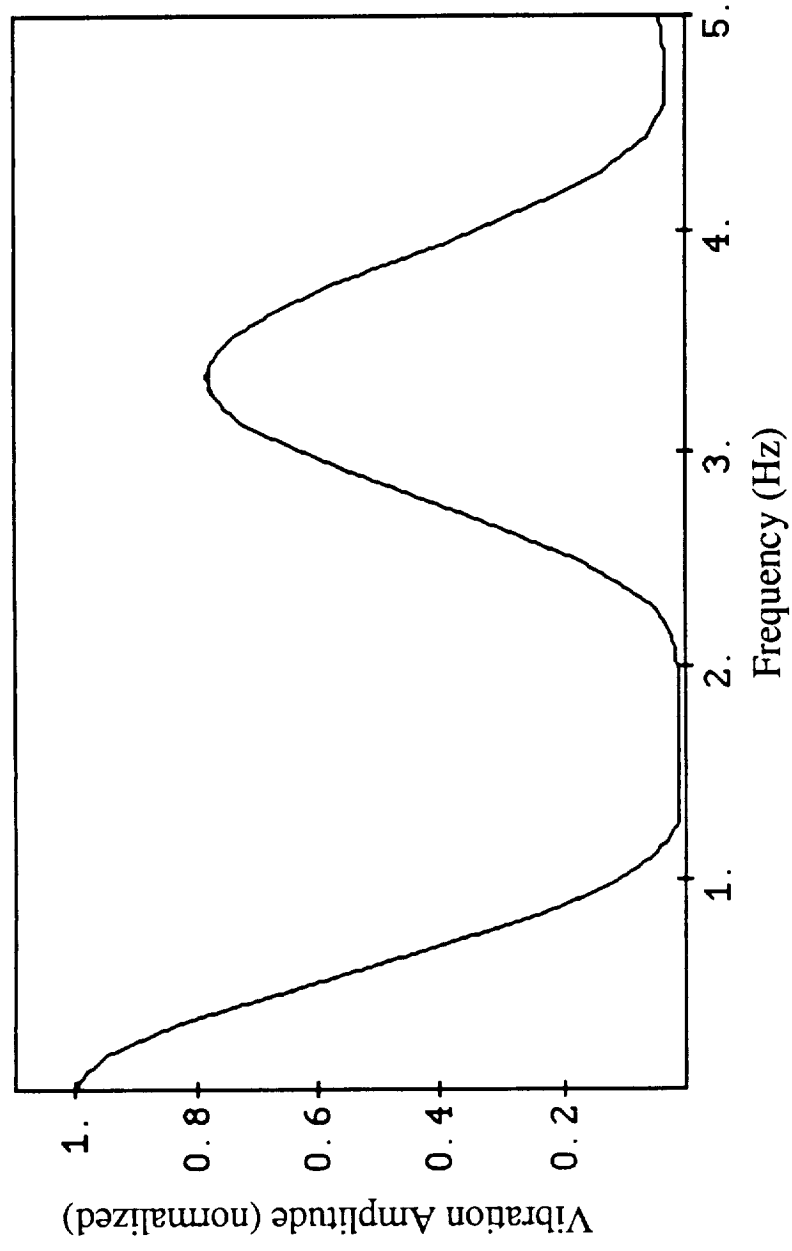


SHAPED RESPONSE DETAIL

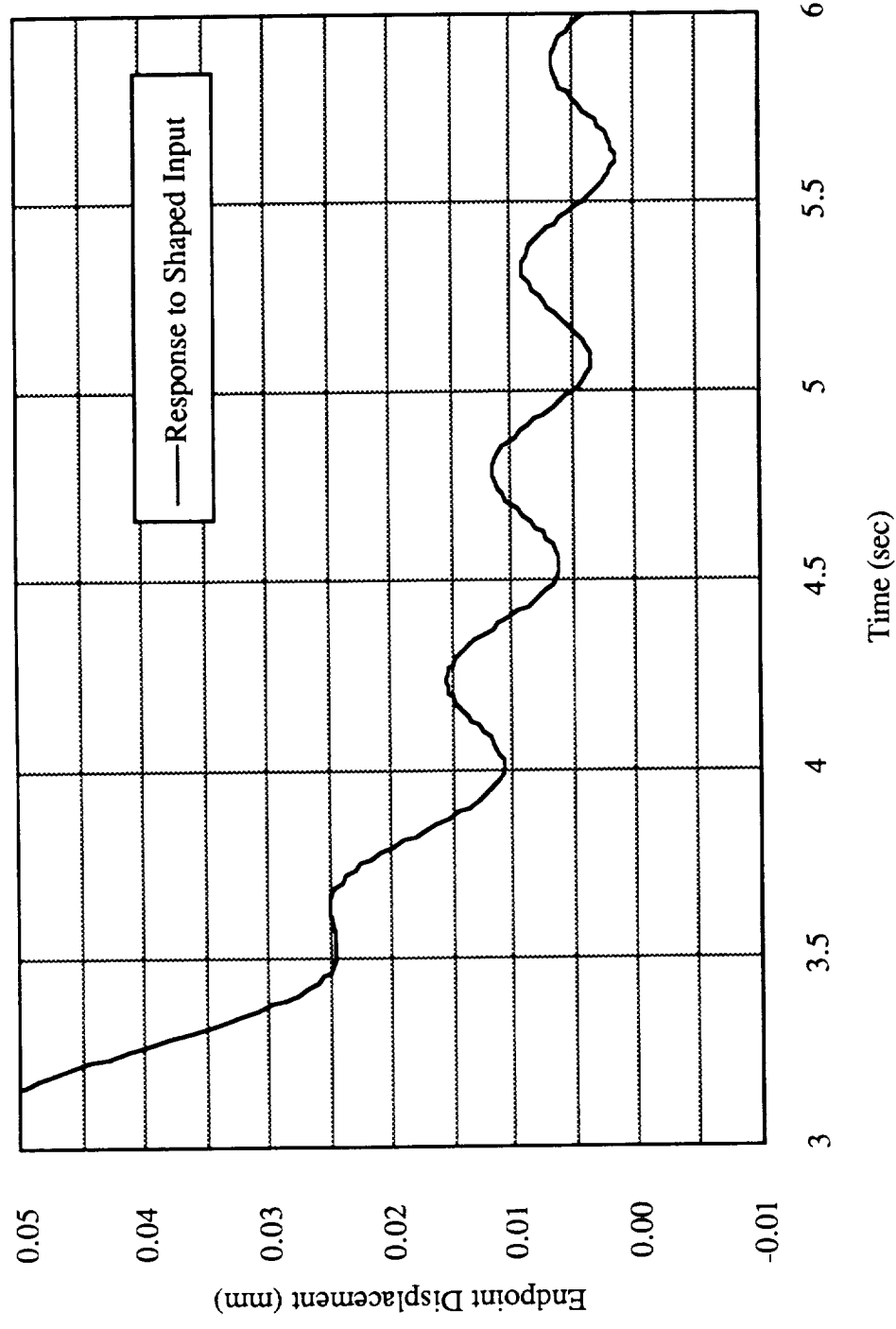


**SHAPING FOR ADDITIONAL FREQUENCIES
TO FURTHER REDUCE RESIDUAL VIBRATION**

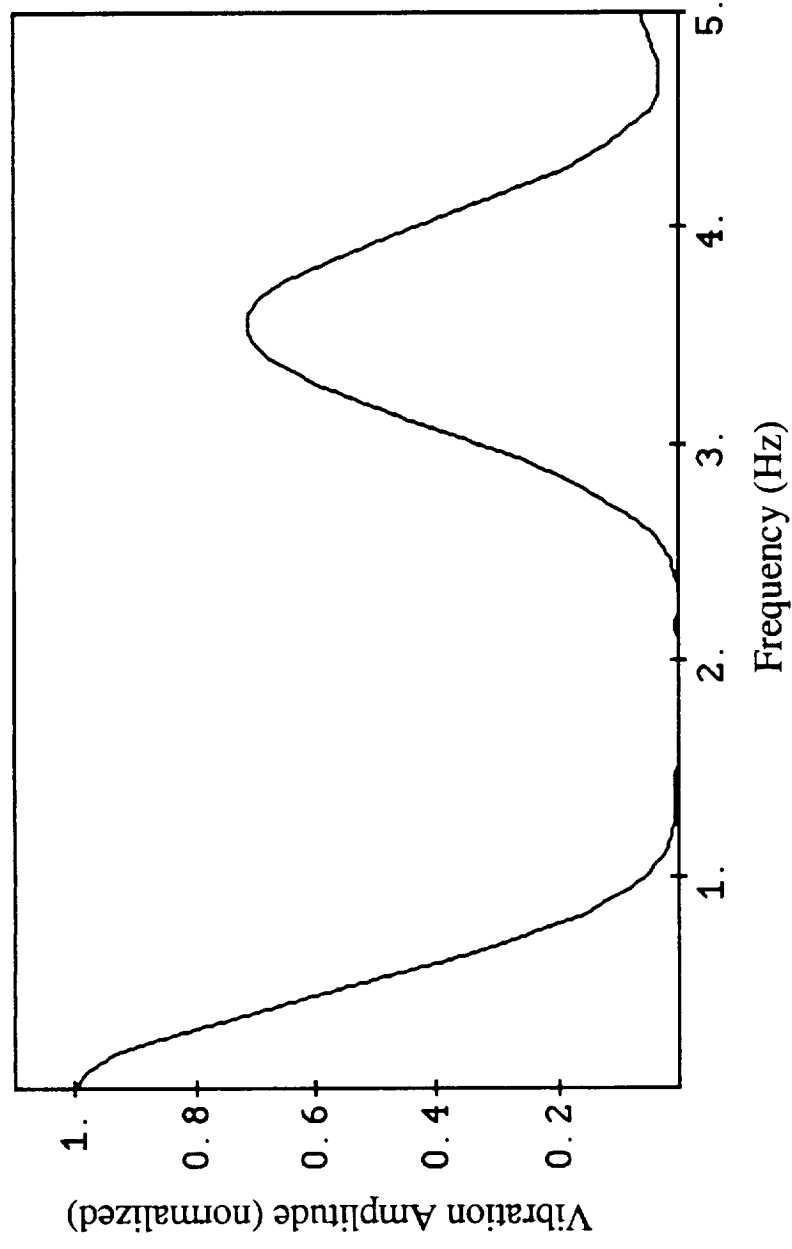
INSENSITIVITY CURVE FOR 1.5, 1.88HZ



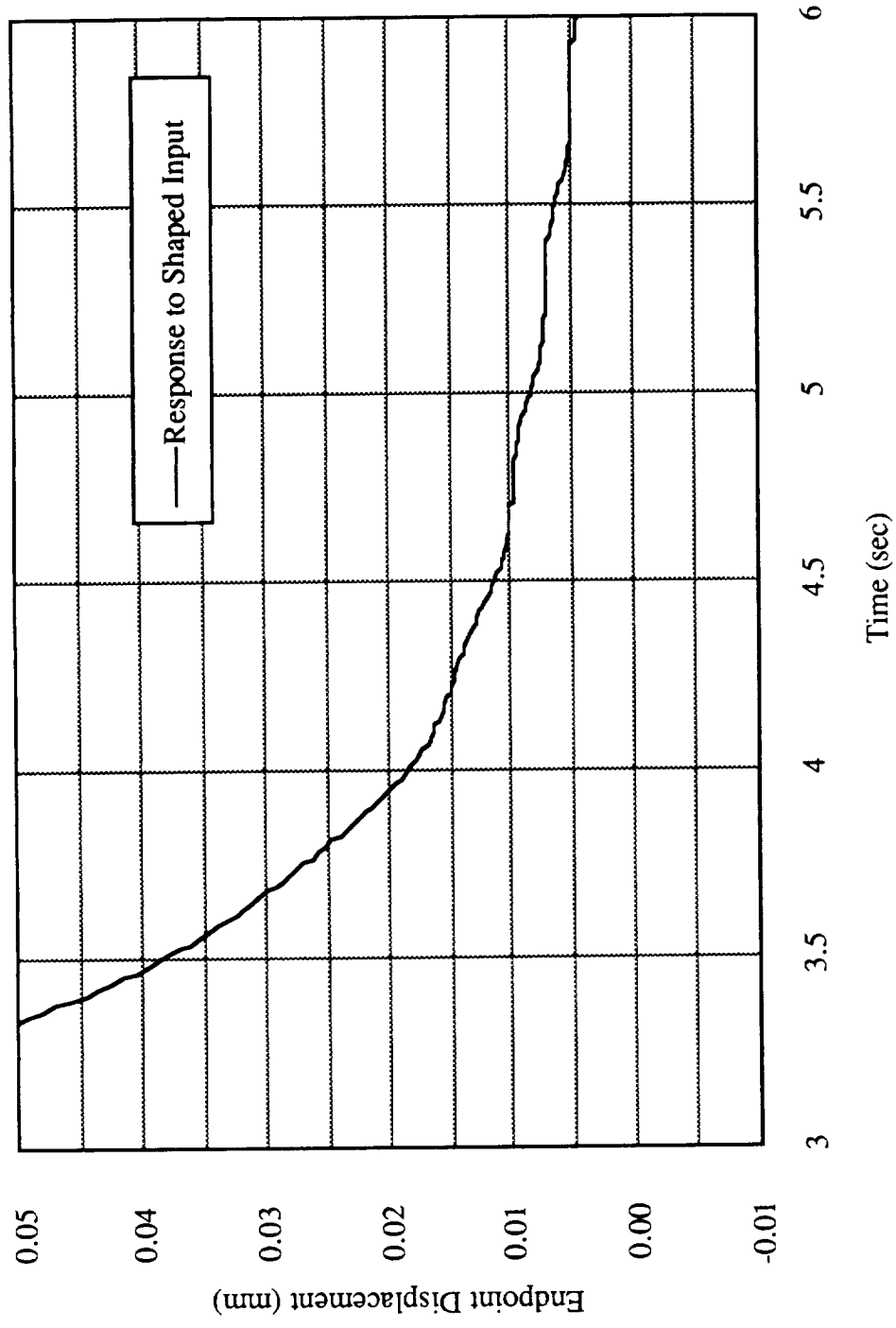
SHAPED RESPONSE DETAIL



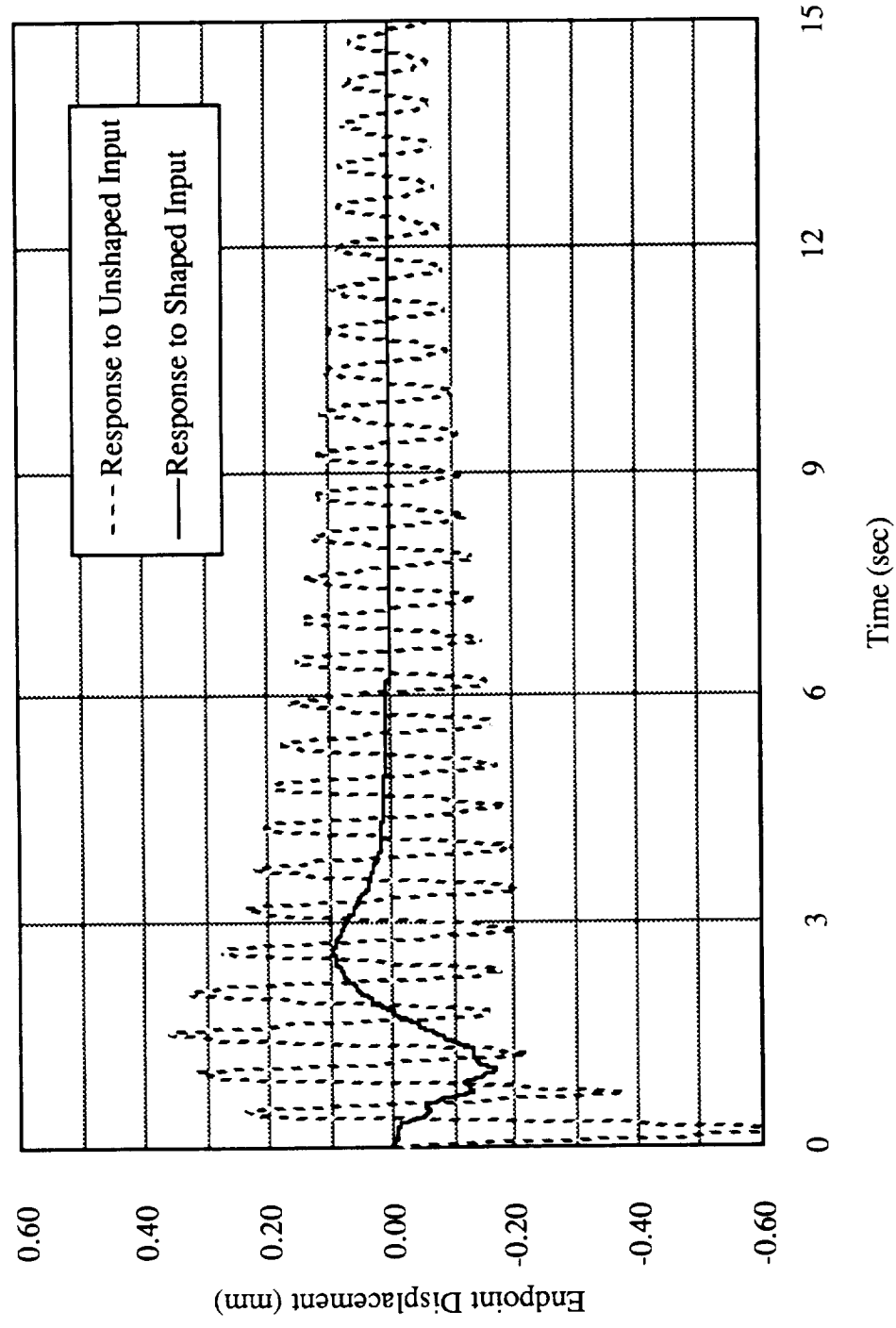
INSENSITIVITY CURVE FOR 1.5, 1.88, 2.0 HZ



SHAPED RESPONSE DETAIL

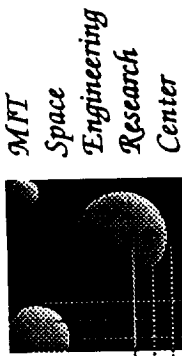


FINAL UNSHAPED/SHAPED COMPARISON



CONCLUSIONS

- Input Shaping Can Suppress Residual Vibration Even in Systems with Changing Natural Frequencies.
- Future: Test Shaping Methods on Physical MACE Structure, Coming on Line in Mid-Summer.



THE MIDDECK ACTIVE CONTROL EXPERIMENT (MACE)

Dr. David W. Miller MIT

1991 Summer Symposium

N 9 3 - 2 8 1 7 3

36-47
16-328
1 24

Space Engineering Research Center

OUTLINE

MODE Family of Experiments

MACE

Team: Participating Organizations

Science Program

Objectives and Rationale

Science Requirements

Capturing the Essential Physics

Science Development Approach

Hardware Development

Development Model Hardware

Development Model Test Plan

Flight Hardware and Operations

Schedule

Summary

THE MODE FAMILY OF EXPERIMENTS

**Fluid Test Article
(FTA)**

**Coupled Non-Linear
Dynamics of Fluids and
Structures in Zero
Gravity**

**Structural Test Article
(STA)**

**Non-Linear Dynamics of
Jointed Truss Structures in
Zero Gravity**

MACE Test Article

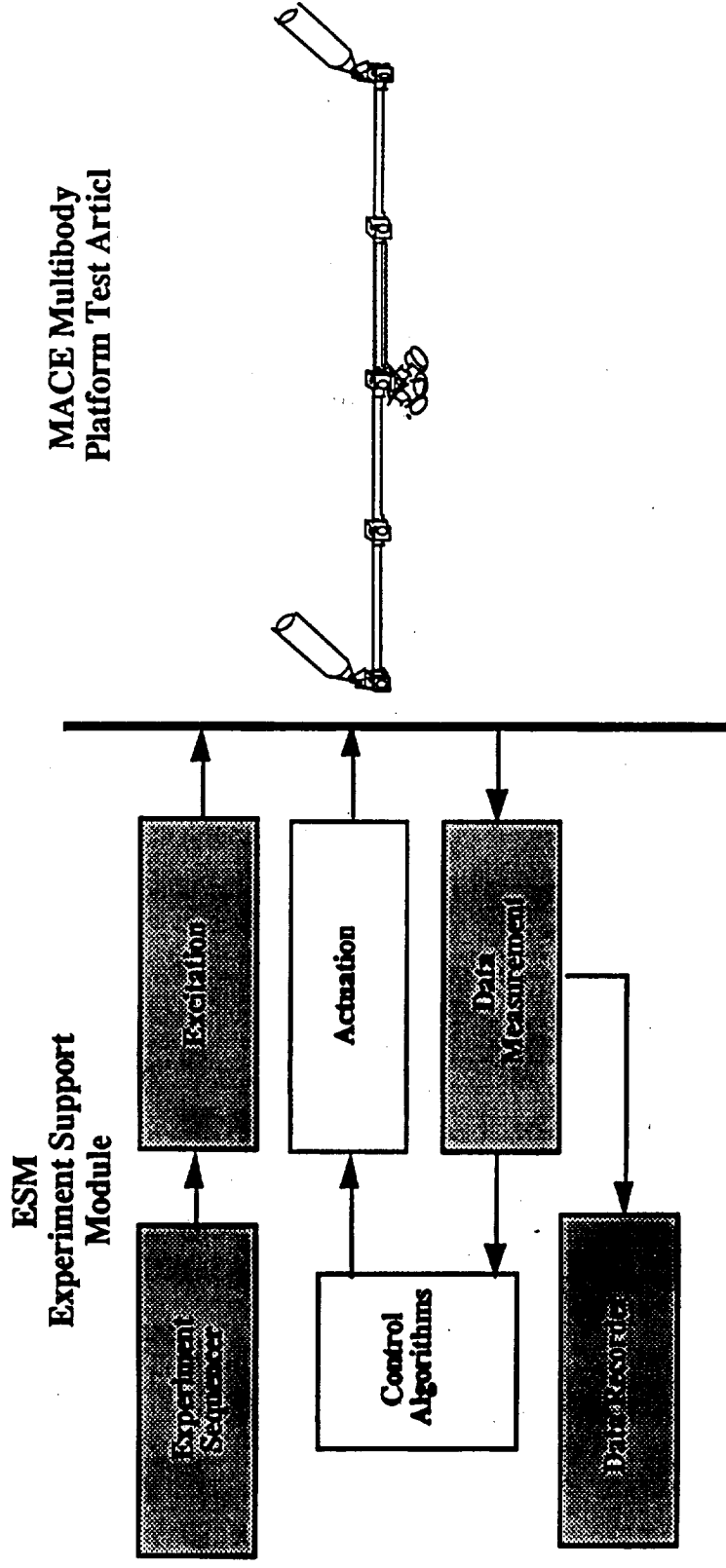
**Influence of Gravity on the
Active Control of a
Multibody Platform**

**Flight # 1:
September 1991**

**Flight # 2:
June 1994**

MACE is part of a logical sequence of cost-effective flight experiments designed to advance technology of interest to NASA in the area of controlled structures.

THE MIDDECK ACTIVE CONTROL EXPERIMENT (MACE)



- Substantial commonality of ESM hardware/software
- Significant savings in integration/certification process.

TEAM: PARTICIPATING ORGANIZATIONS

Organization	Roles
MIT Space Engineering Research Center	Science, Modelling, EM Fabrication
Payload Systems Inc.	Exp. Support, Flight Hardware Fab., Integration
Lockheed Missiles and Space Co.	Science, Modelling, EM Fabrication
Sonitech International	DSP Development
MIT Center for Space Research	Financial Oversight

OBJECTIVES AND RATIONALE

Objective: To develop a well verified set of CST tools that will allow designers of future CST spacecraft, which cannot be dynamically tested on the ground in a sufficiently realistic on-orbit simulation, to have confidence in the eventual orbital performance of such spacecraft.

- Since the model fidelity required for stability and performance robustness is intimately related to the level of applied control authority, closed-loop testing is required.
- Vehicle qualification testing will most likely occur on the ground where suspension and direct gravity effects will cause the 1-g and 0-g dynamics to differ.
- Differences between the ground and on-orbit environment cause perturbations which can substantially alter closed-loop behavior.
- Therefore it is essential to perform on-orbit closed-loop testing for comparison with ground testing and analytical predictions to develop these tools.

MACE SCIENCE REQUIREMENTS

The test article must be representative of a mission or vehicle architecture so that the developed technology has clear application.

- The test article must be representative of expected near-term missions.
- The test article geometry, performance metric and disturbances must be representative of expected near term missions.
- Improvement in the performance must be representative of that predicted for CST spacecraft under sensor, actuator and processor dynamic range constraints. Assuming unstaged actuator dynamic range to be 40 db and sensor dynamic range to be 60 db, a performance improvement of 40 db is required.

MACE SCIENCE REQUIREMENTS

The test article must exhibit differences in its dynamic behavior between ground based and on-orbit testing.

- The test article must be difficult to test on the ground because of the effect of gravity and suspension on its flexibility.
- Detailed modeling of gravity and suspension effects on the test article flexibility is required to properly predict closed-loop behavior on the ground.
- At a 20 db performance level, gravity/suspension effects on flexibility will distinguish closed-loop behavior between ground and on-orbit tests when the same active controller is applied.
- The test article must have a performance improvement in the selected performance metric of a minimum of 20 db which must be verified by experiment on the ground.

MACE SCIENCE REQUIREMENTS

A comprehensive series of coherent ground and on-orbit tests must be performed which identify current limitations and develop plausible alternative approaches.

- Control algorithms will be implemented on orbit which are identical to those implemented on the ground. These tests identify current limitations.
- Control algorithms will be implemented on orbit which are derived from the ground model with suspension and gravity effects removed. These tests identify predictive ability.
- Control algorithms will be implemented on orbit which are derived from on-orbit dynamic test data. These tests identify the ability to fine tune the control once on orbit.

CAPTURING THE ESSENTIAL PHYSICS: TEST ARTICLE REQUIREMENTS

The simulation of a vehicle with payloads and articulating appendages with pointing and positioning requirements, necessitates a test article with the following attributes:

- appropriately scaled to fit in the middeck while preserving the essential performance requirements.
- two gimballed payloads to enable implementation of multiple interacting control systems with independent objectives.
- two rigid payloads and a flexible appendage, representative of compact high mass fraction devices and a robotic servicer.
- flexible bus with resonances within the controller bandwidth and to exhibit suspension coupling, gravity stiffening and droop.
- sufficiently complex geometry such that the test article undergoes full 3-D kinematic and coupled flexible motion.

SCIENCE DEVELOPMENT APPROACH:

CONTROL OBJECTIVES

Control Objectives:

- **Pointing** performance of single and multiple payloads.
- **Scanning** performance of single and multiple payloads.

Performance Metrics:

- **Stability**--RMS 2-axis angular position about pointing line of sight or scanning reference profile.
- **Jitter**--RMS 2-axis angular rate about pointing line of sight or scanning reference profile.
- **Slew response time**--time required to complete maneuver.
- **Percent degradation**--reduction from single payload performance associated with addition of an interacting, controlled payload.

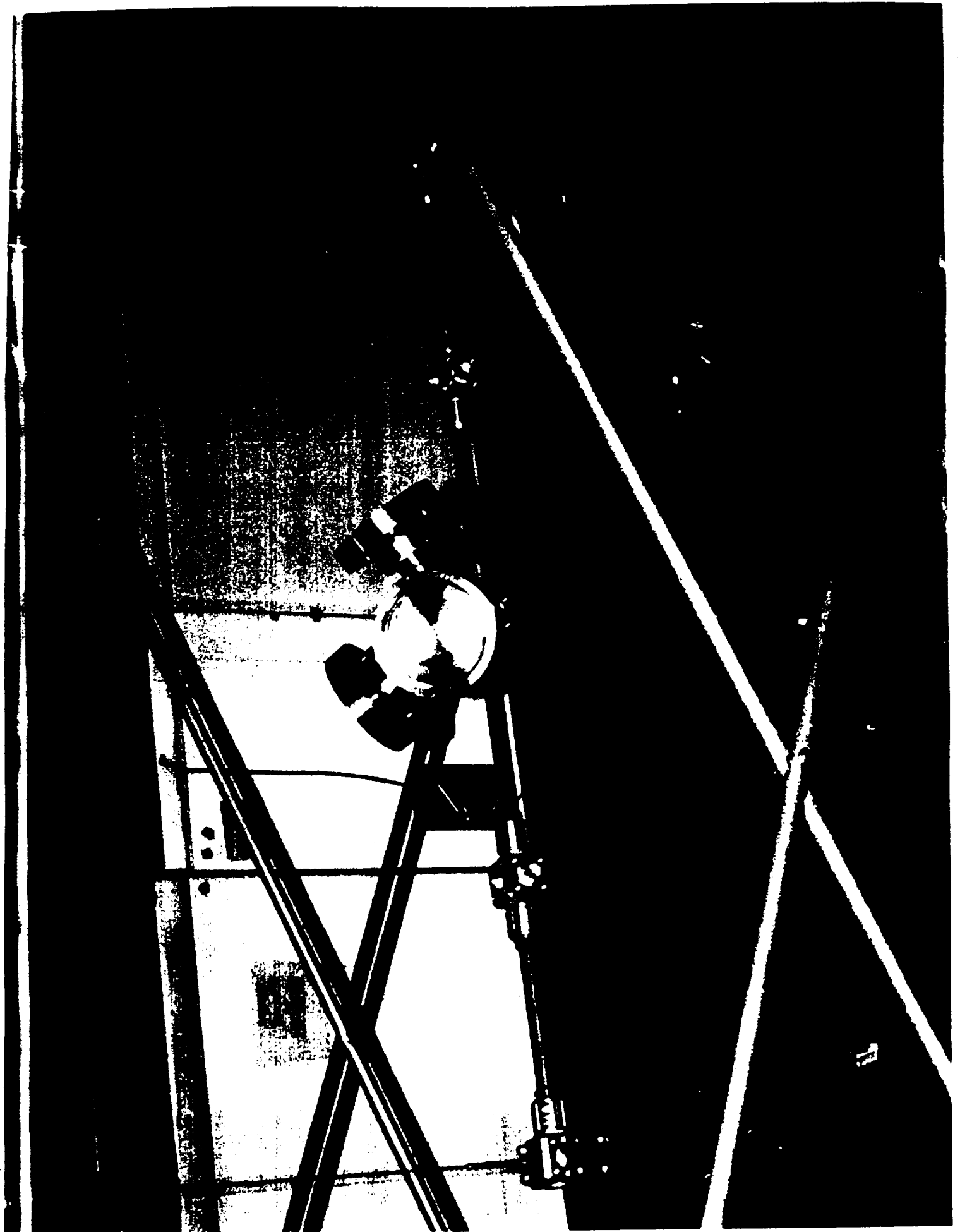
SCIENCE DEVELOPMENT APPROACH: GRAVITY INFLUENCES

Objective: Identify and quantify the magnitude of the perturbation effects of a gravity field and a suspension system on the dynamics of a suspended test article.

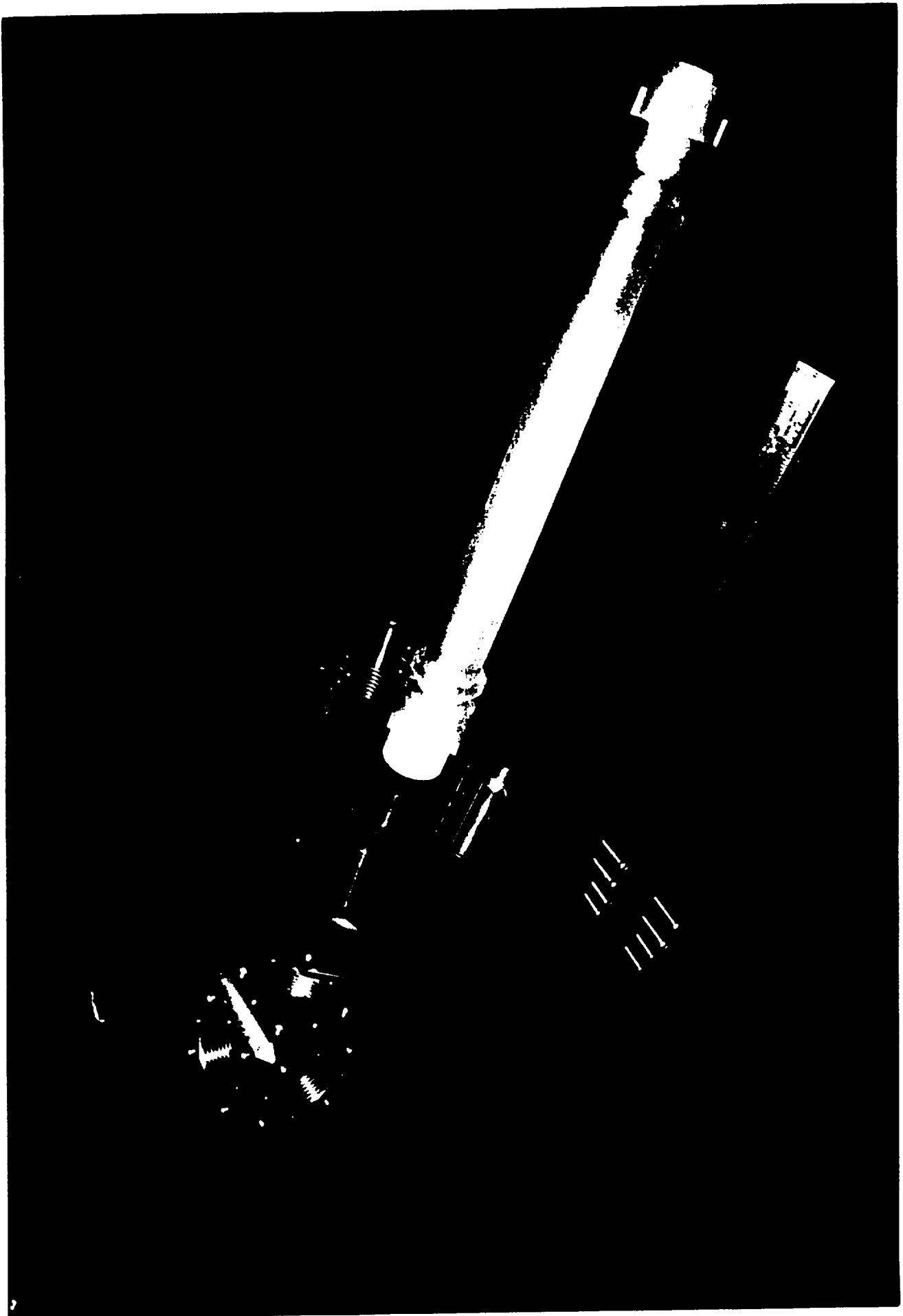
GRAVITY FIELD EFFECTS	SUSPENSION SYSTEM EFFECTS
<p>1) GRAVITY STIFFENING/DESTIFFENING</p> <ul style="list-style-type: none"> changes in membrane energy due to small deformations and loading of the structure can be modelled as system stiffness perturbations. 	<p>3) STATIC B. C. PERTURBATIONS</p> <ul style="list-style-type: none"> static translational stiffnesses in the horizontal and vertical directions are prescribed by the suspension system at each attachment point.
<p>2) FINITE DEFLECTIONS</p> <ul style="list-style-type: none"> finite deflections require a redefinition of the reference structure; stiffness modifications do not capture the perturbation to the eigenstructure. 	<p>4) DYNAMIC B.C. PERTURBATIONS</p> <ul style="list-style-type: none"> modal coupling with the suspension dynamic modes results in dynamic impedances at the attachment points.
<p>5) DYNAMIC LOADING DUE TO GRAVITY FIELD AND SUSPENSION CONSTRAINTS</p> <ul style="list-style-type: none"> dynamic torques which result from center of mass axis offsets with respect to the suspension support plane(s). 	

HARDWARE DEVELOPMENT

- Three sets of hardware are being developed under the MACE program:
 - The Development Model for science development
 - The Engineering Model for prototyping flight hardware
 - The Flight Hardware for actual flight
- The purpose of the Development Model is to develop the science associated with the MACE program by validating theory through experimental implementation.
- The purpose of the Engineering Model is to attempt to redesign the DM and its support equipment to operate within the constraints of the STS middeck.
- The purpose of the Flight Hardware is to provide one unit for crew training and spare parts and one unit for flight.

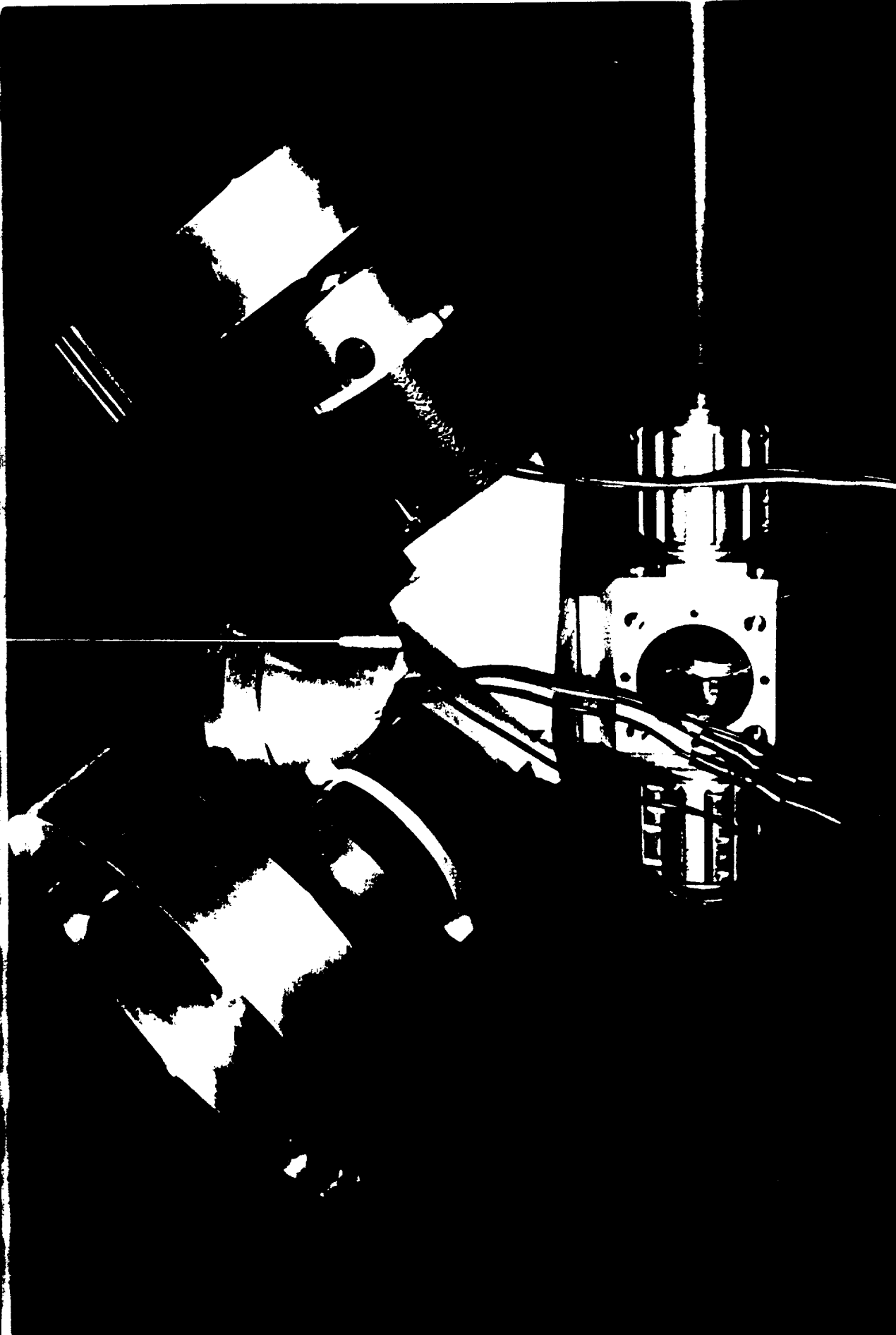


ORIGINAL PAGE IS
OF POOR QUALITY



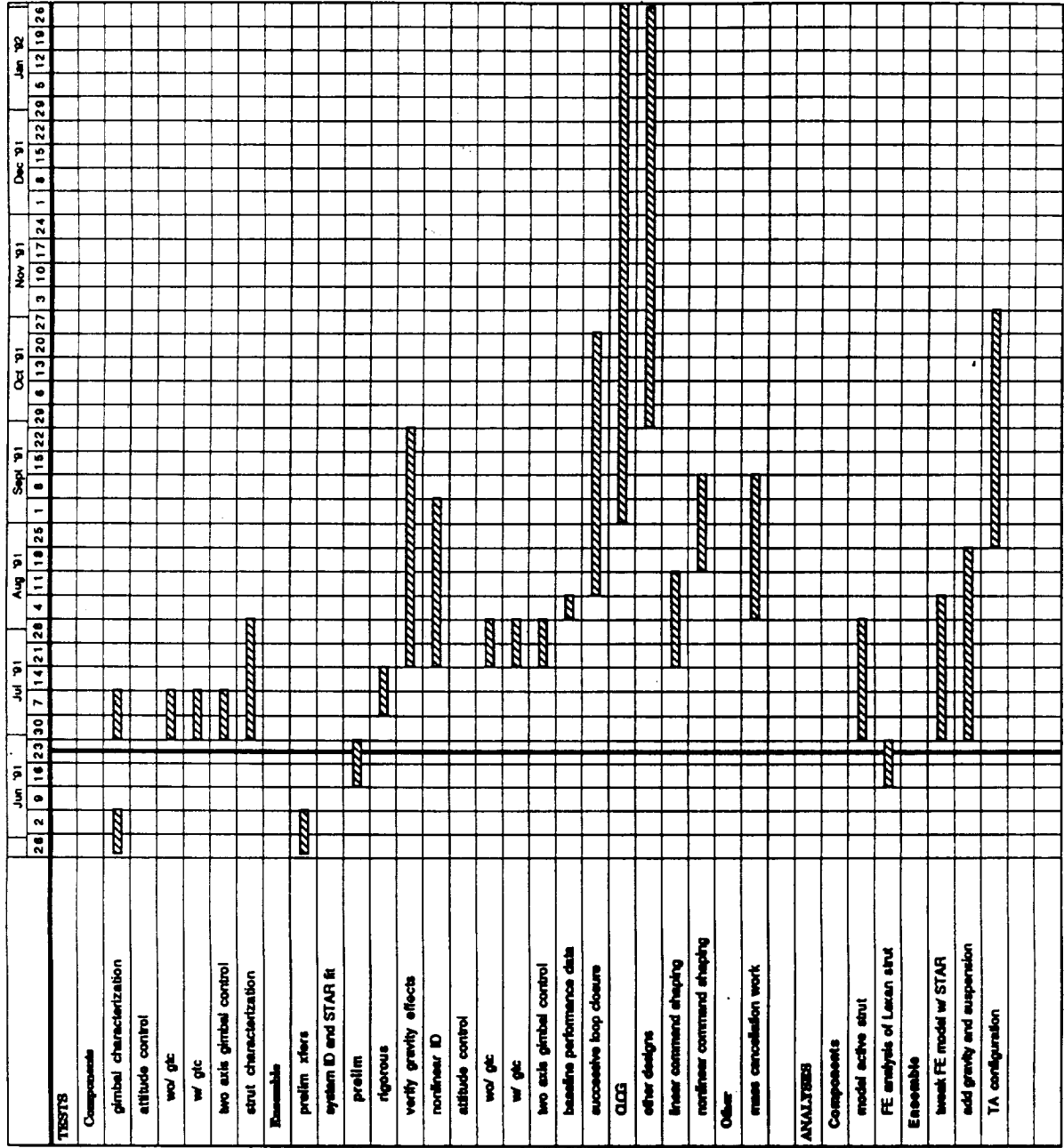


ORIGINAL PAGE IS
OF POOR QUALITY

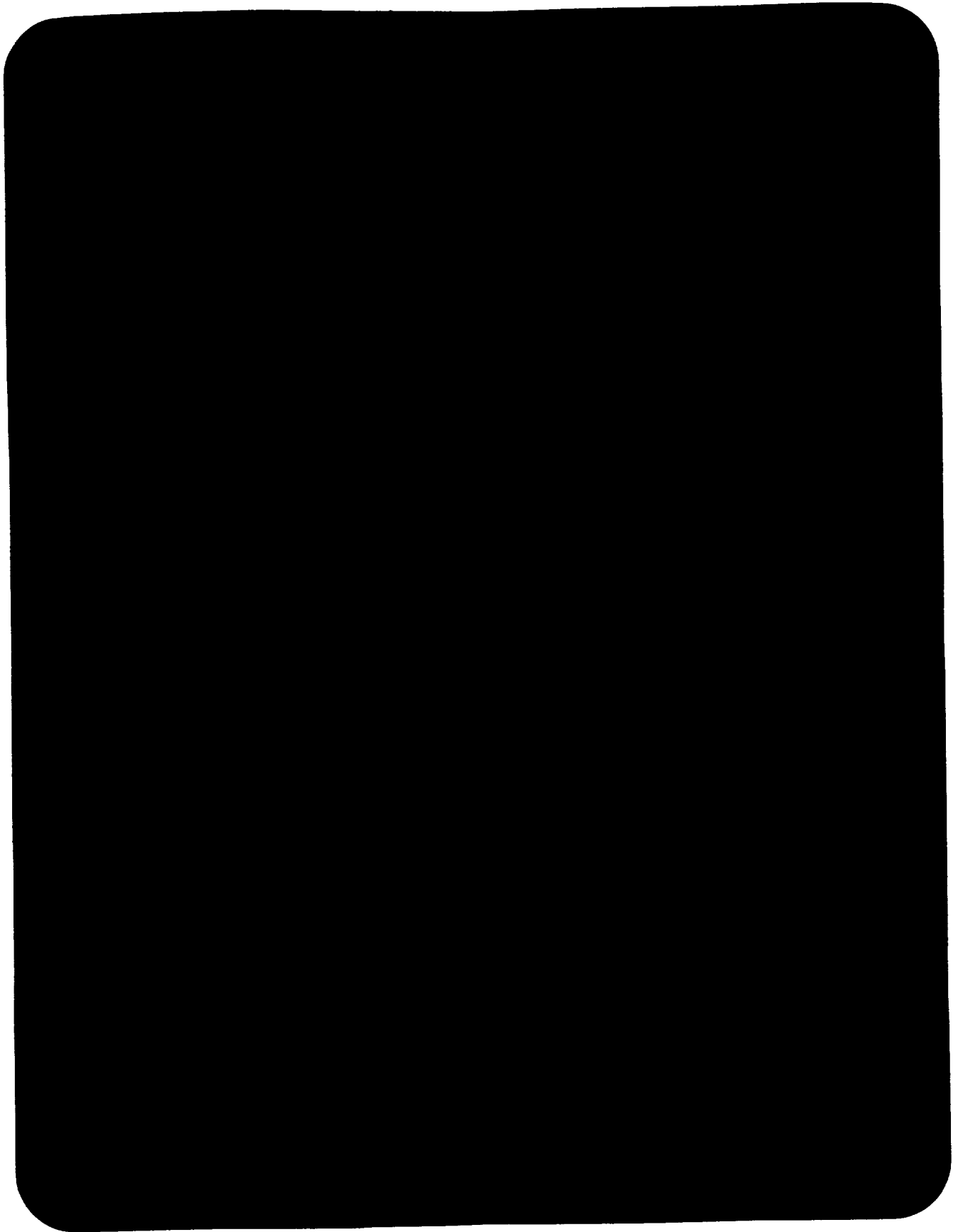


A high-contrast, black and white photograph of a mechanical assembly, possibly a pump or engine component. The image is dominated by dark, silhouetted parts against a bright background. In the upper left, a large, curved, cylindrical component, likely a tank or a large valve, is visible. Below it, a complex network of pipes, hoses, and smaller mechanical parts is arranged. A prominent horizontal pipe runs across the middle of the frame. To the right, a vertical pipe or structure extends upwards. The overall impression is one of a dense, industrial machine with various functional components.

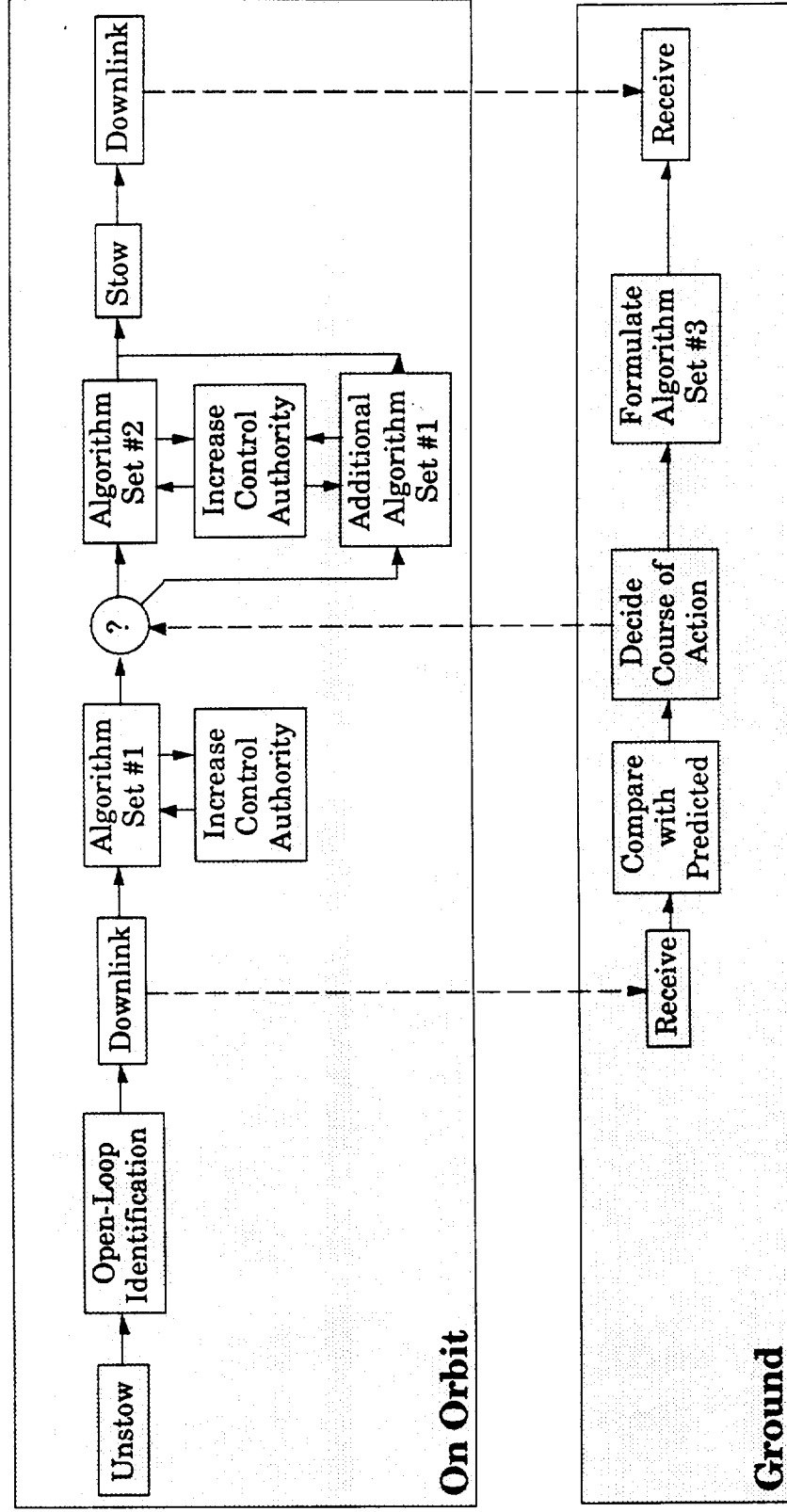
DEVELOPMENT MODEL TEST PLAN



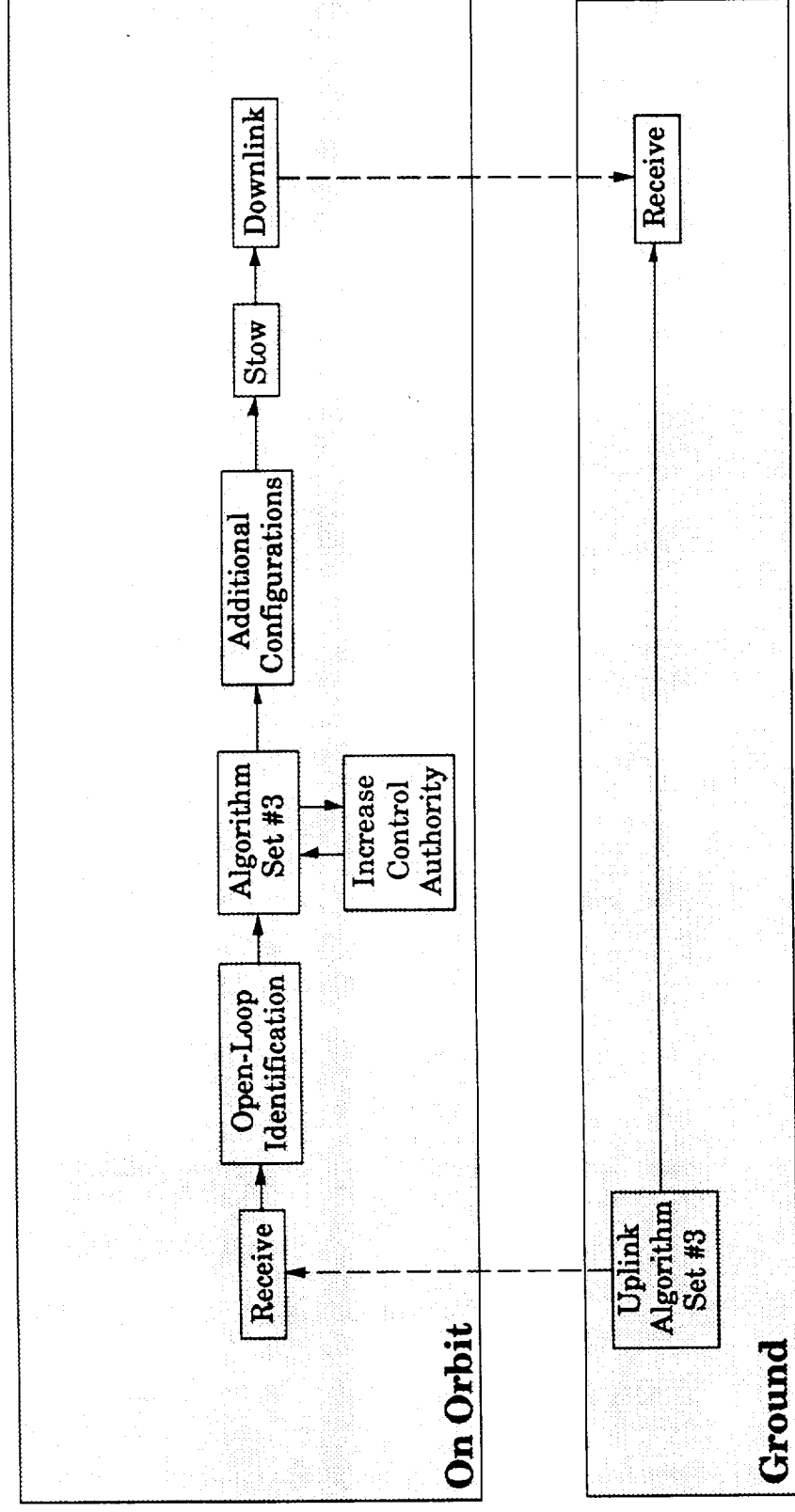
ORIGINAL COPY IS
OF POOR QUALITY



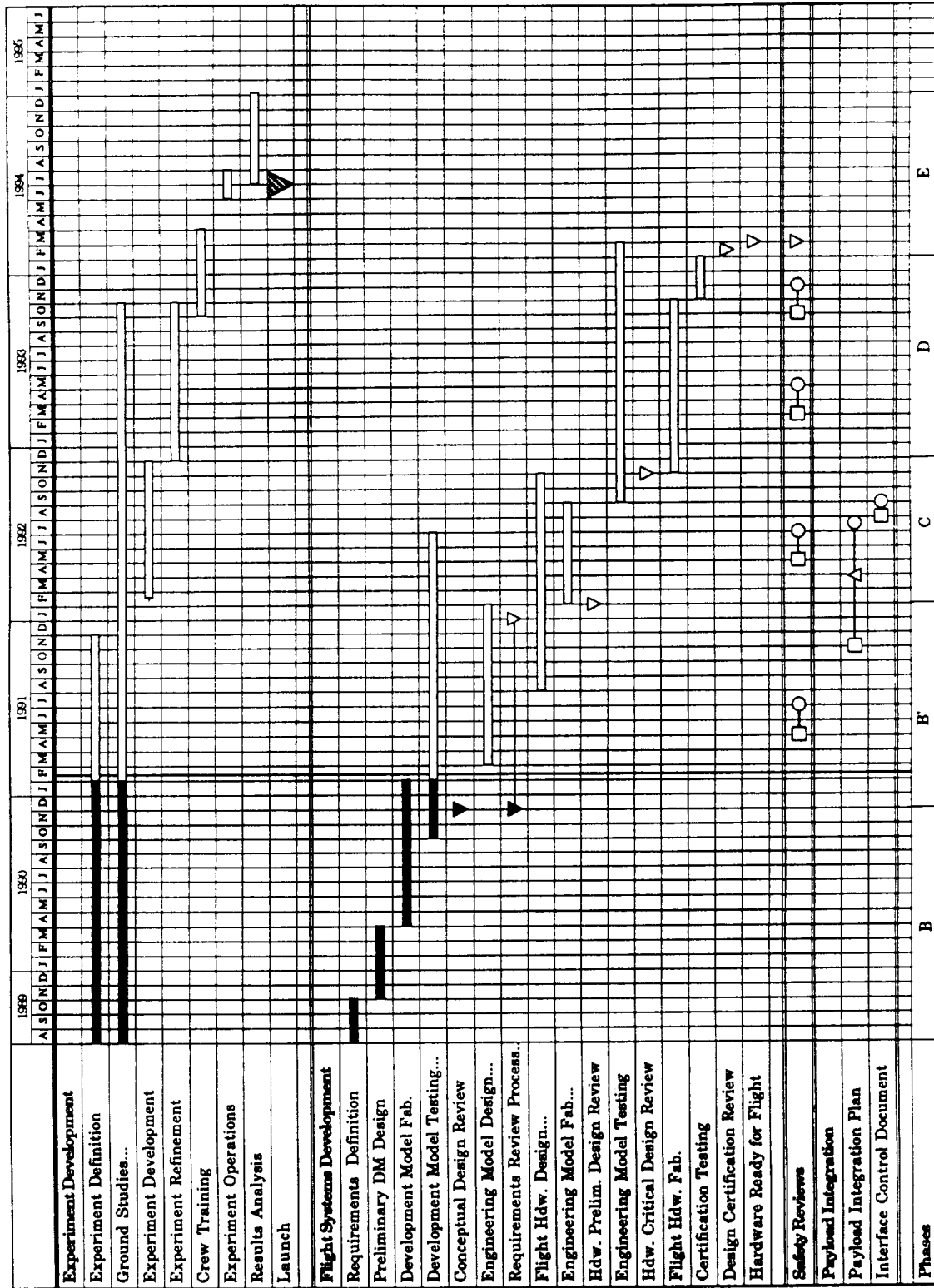
EXPERIMENT OPERATIONS: DAY ONE



EXPERIMENT OPERATIONS: DAY TWO

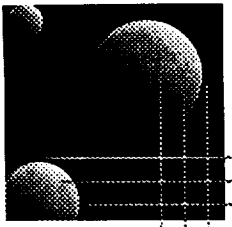


SCHEDULE: EXPERIMENT DEVELOPMENT



SUMMARY

- The MODE family of flight experiments is designed to verify analytical tools developed to predict the gravity dependent behavior of proposed space structures.
- The MODE family of flight experiments uses reusable dynamic and control tests facilities and exploits the unique environment on the STS middeck.
- MACE investigates gravity dependent phenomena pertinent to the closed-loop dynamics of proposed space structures.
 - By comparing performance as a function of control authority between ground and on-orbit testing, perturbations in the dynamics due to the change from 1 to 0-g will be identified.
 - By noting the level of control authority where these performance deviations occur, either analytical predictive capabilities or on-orbit identification procedures can be refined.
- The MACE program consists of a strong consortium of university, government and industry to develop a CST flight experiment which is technically relevant, mission relevant and cost effective.



MIT
Space
Engineering
Research
Center

ROBUST CONTROL FOR UNCERTAIN STRUCTURES

Joel Douglas
Michael Athans

Massachusetts Institute of Technology

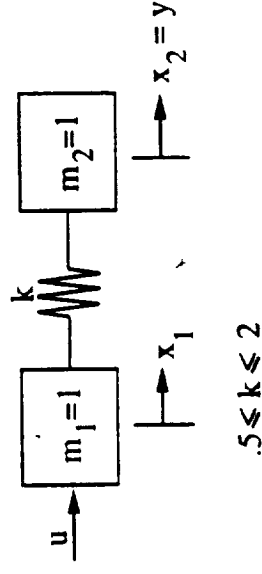
July 1, 1991 (SERC Symposium)

N 9 3 - 2 8 1 7 4

57 27
166329
1. 17

APPROACH

- Assume full-state feedback
- Try to guarantee stability and performance robustness of classical LQR design
 - Guaranteed stability
 - Reasonable guaranteed robustness (gain and phase margin properties)
- Apply to benchmark problem to see interesting properties



ROBUST LQR FORMULAS

- Standard LQR design when there is no uncertainty

$$J = \int_0^\infty (x^T(t)Q_0x(t) + \rho u^T(t)u(t))dt$$

$$PA_0 + A_0^TP + Q_0 - \frac{1}{\rho}PBB^TP = 0$$

- Apply Petersen-Hollot bounds to derive robust Riccati Equation

$$A = A_0 + \sum_{i=1}^p q_i E_i \quad |q_i| \leq 1$$

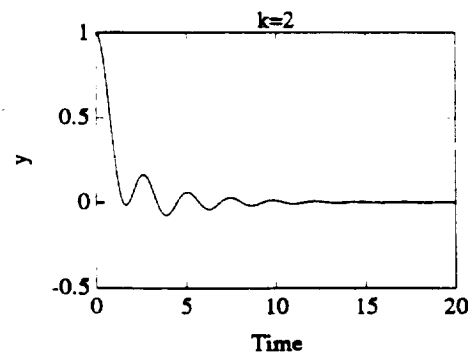
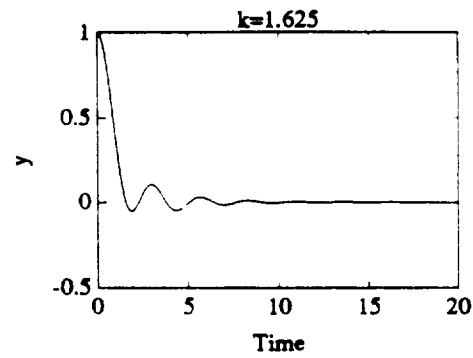
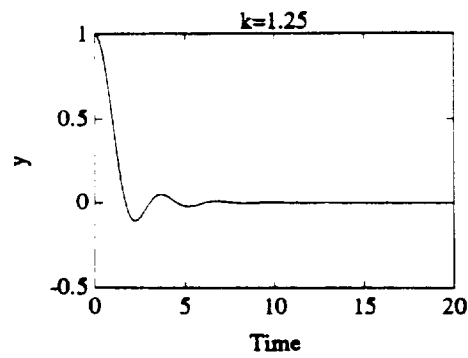
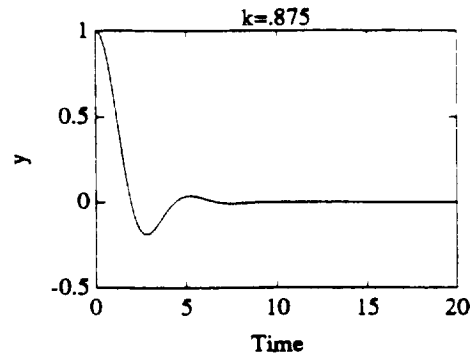
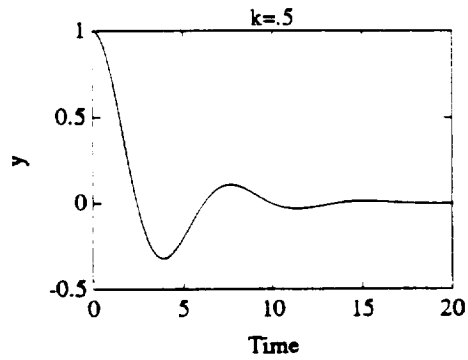
$$E_i = l_i n_i^T \quad L = [l_1 \ l_2 \ l_3 \dots]; \quad N = [n_1 \ n_2 \ n_3 \dots]$$

$$PA_0 + A_0^TP + (Q_0 + \gamma NN^T) - P(\frac{1}{\rho}BB^T - \frac{1}{\gamma}LL^T)P = 0$$

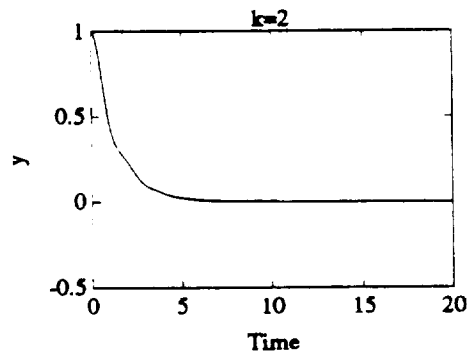
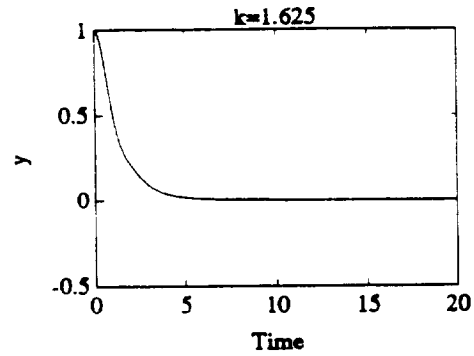
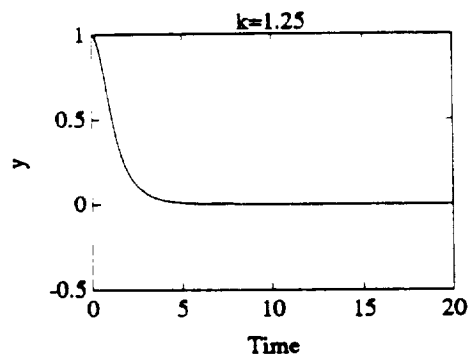
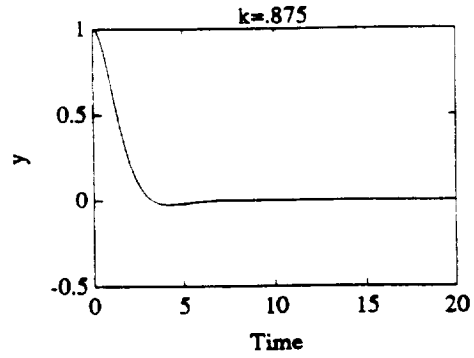
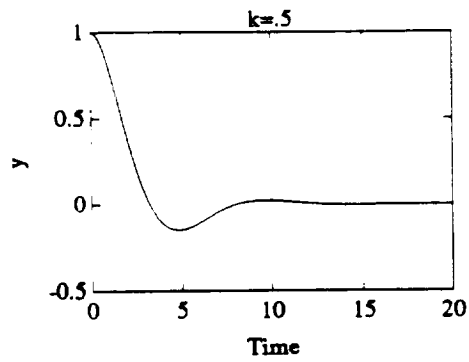
- Control

$$G = \frac{1}{\rho}B^TP \quad u = -Gx$$

MISMATCHED LQR DESIGN



RLQR DESIGN

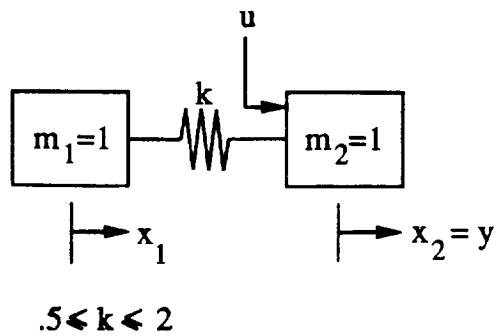


INTERPRETATIONS OF RLQR DESIGN

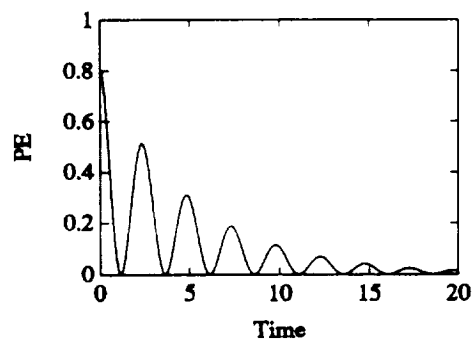
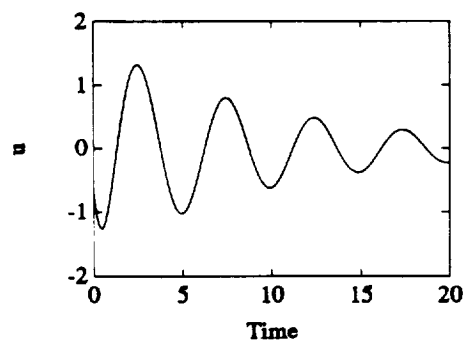
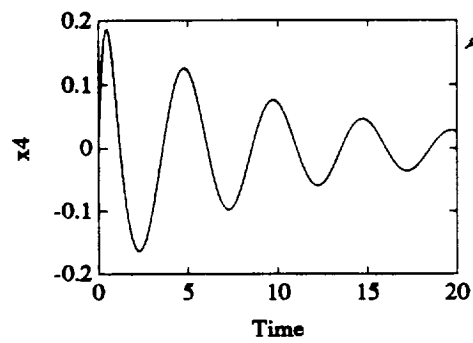
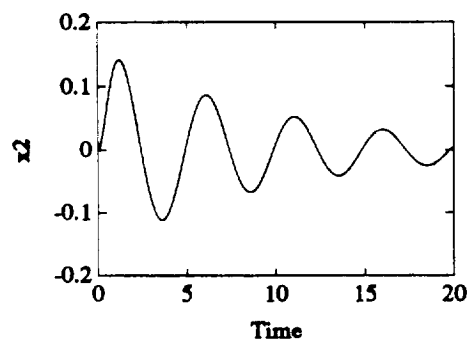
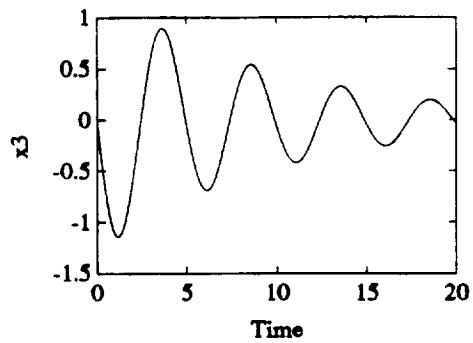
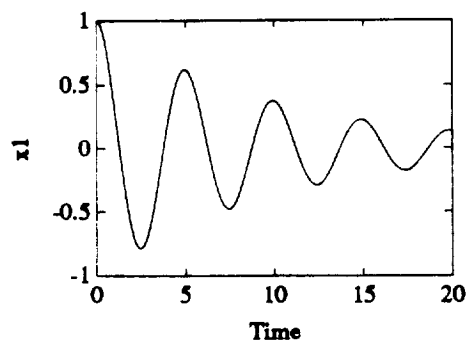
- Equivalent to an optimal design where we minimize the cost functional

$$J = \int_0^\infty (x^T(t)Q_0x(t) + x^T(t)\gamma NN^Tx(t) + \underbrace{x^T(t)\frac{1}{\gamma}PLL^TPx(t) + \rho u^T(t)u(t)}_{-\beta d^T(t)d(t)})dt$$

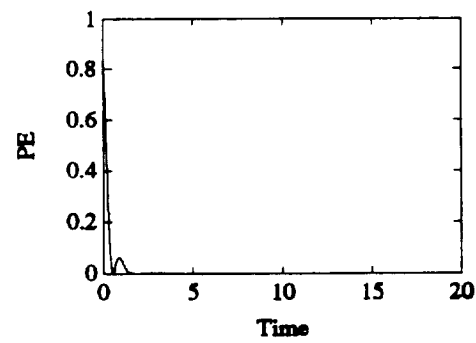
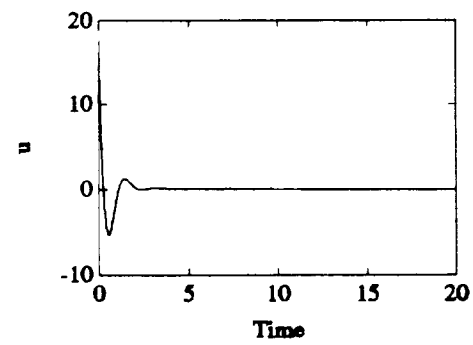
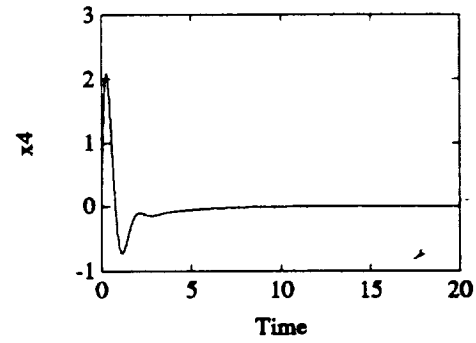
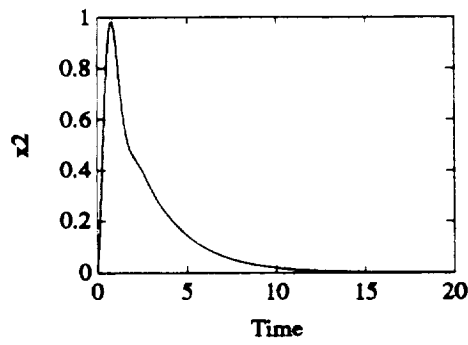
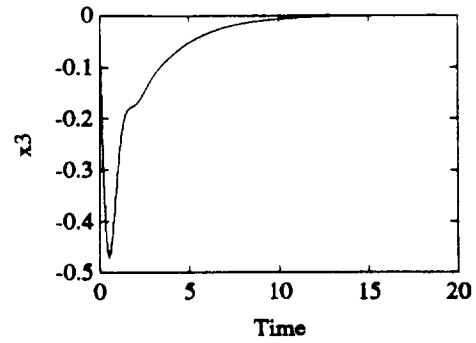
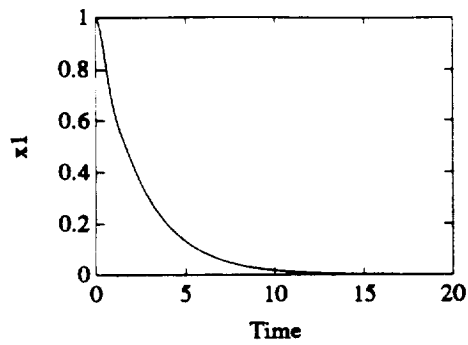
- $x^T(t)Q_0x(t)$ is the state weighting
- $x^T(t)NN^Tx(t)$ has been shown to be uncertain potential energy of an uncertain spring (or rate of dissipation for a damper)
- $x^T(t)PLL^TPx(t)$ is an equivalent \mathcal{H}_∞ term.
- Parameter γ is therefore a tradeoff between minimizing unknown uncertain energy and worst case disturbance arising from forces due to parameter errors.



$$K = 1.625$$

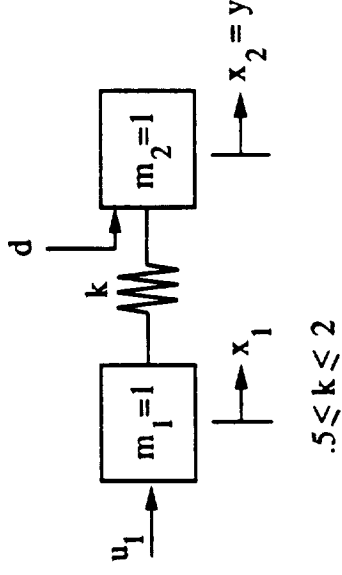


$K = 1.625$ (RLQR)

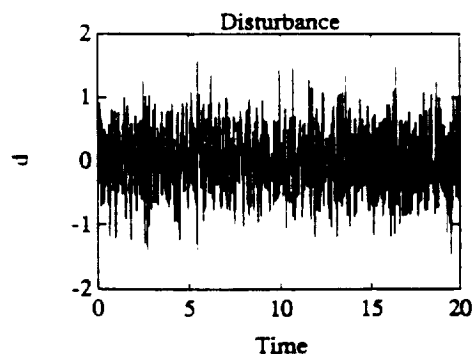
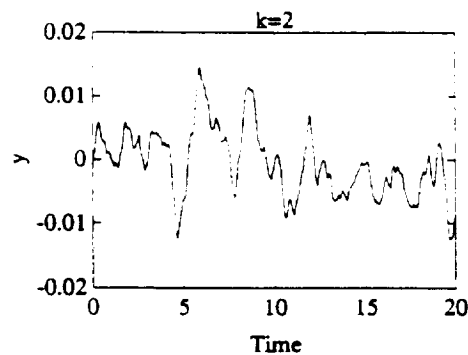
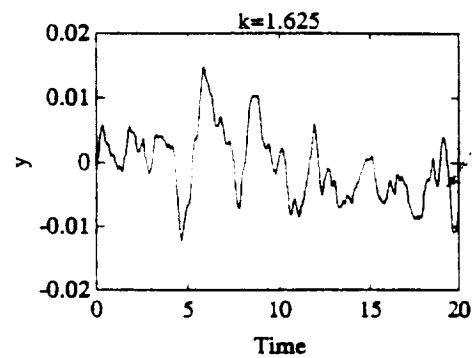
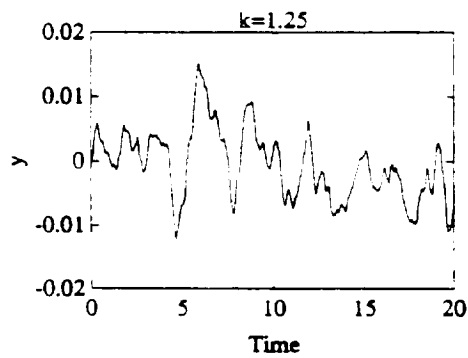
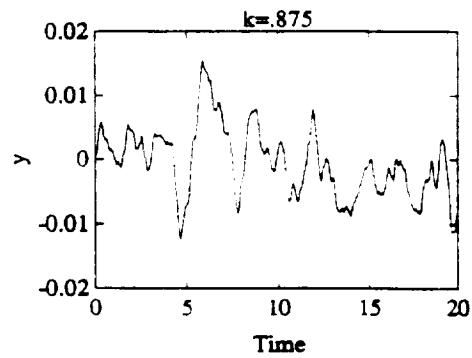
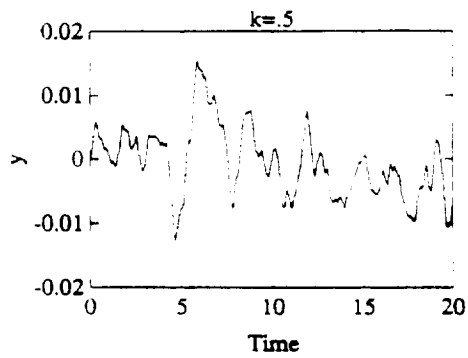


DISTURBANCE REJECTION

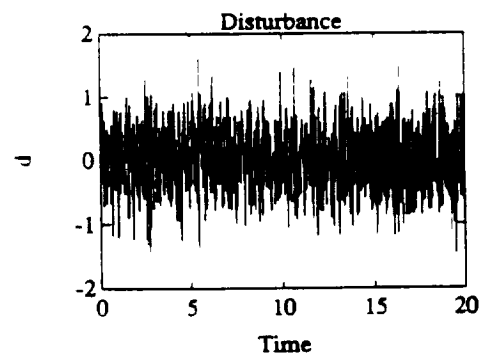
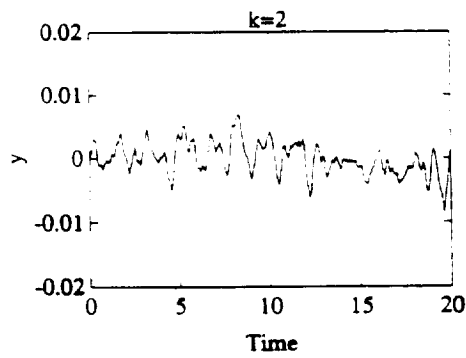
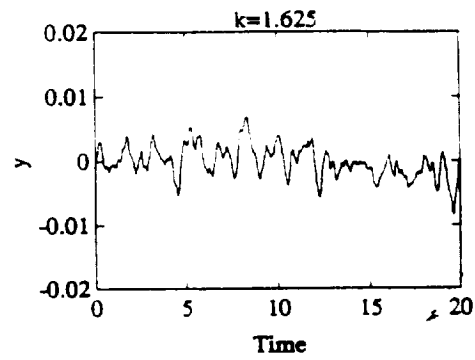
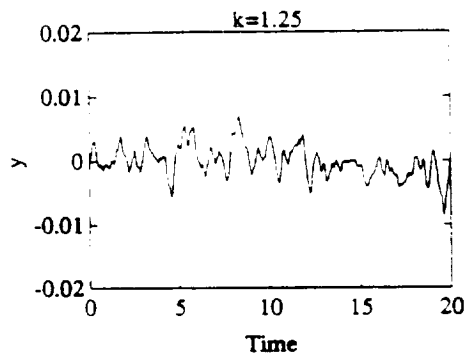
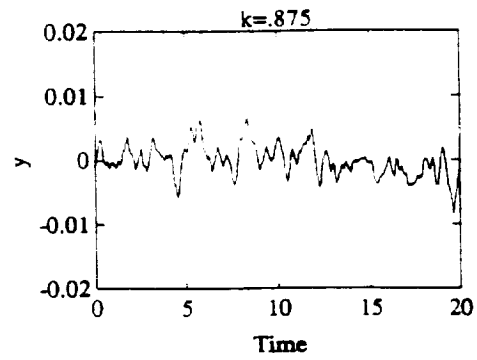
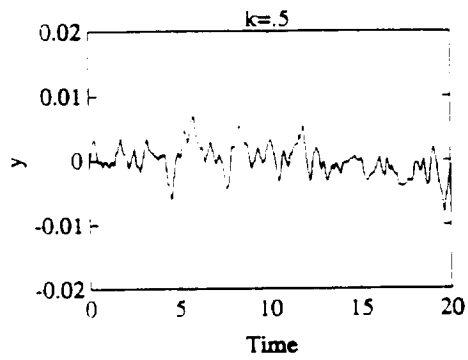
- Does the RLQR controller reject disturbances?
- Add a white noise disturbance at the output
- Apply both mismatched LQR and RLQR designs

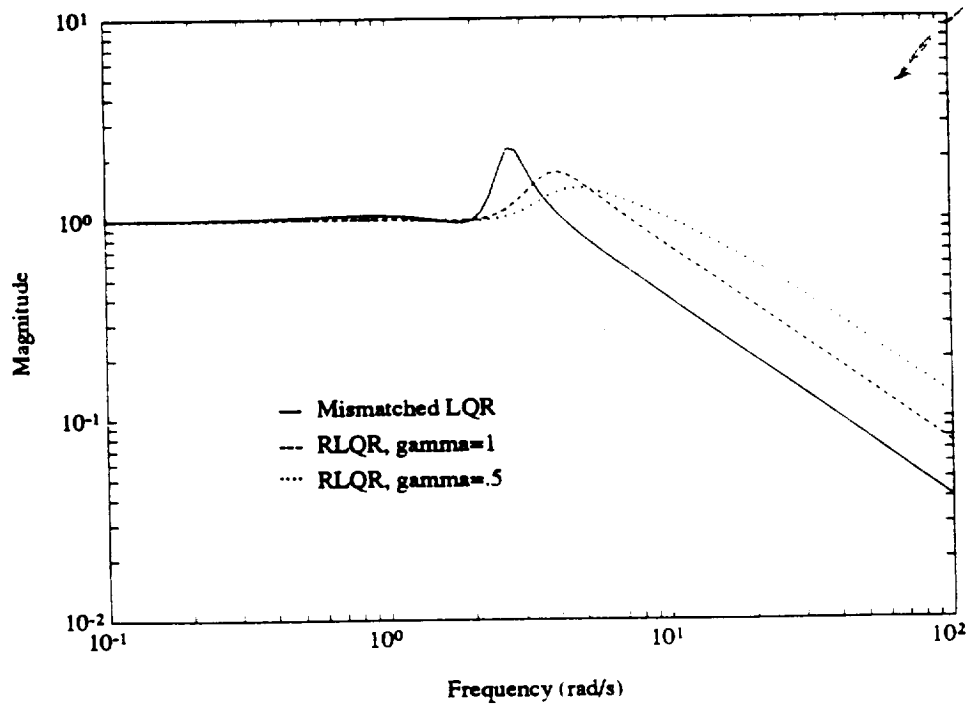
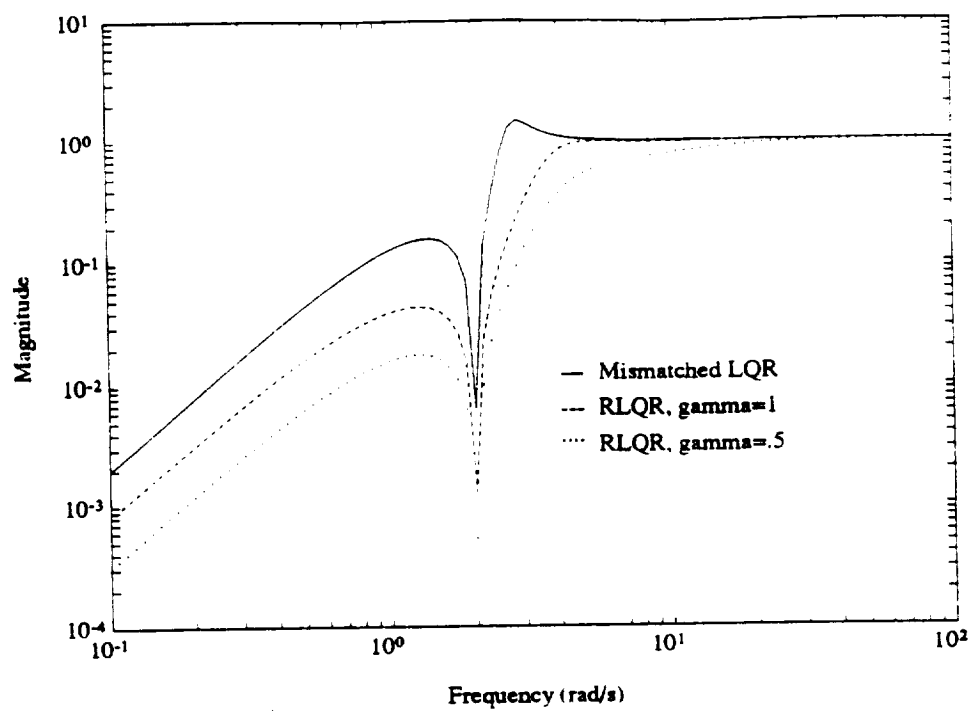


MISMATCHED LQR DESIGN

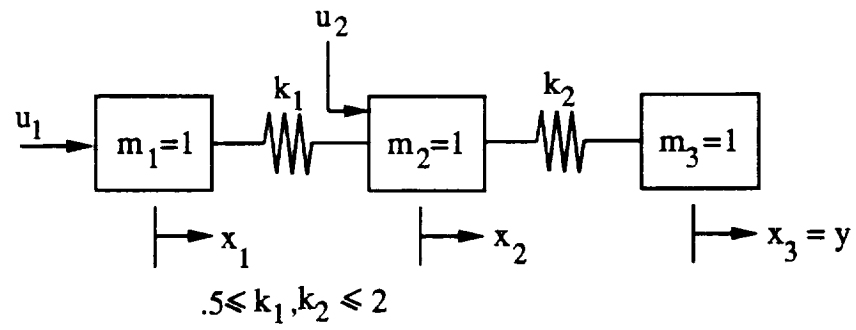


RLQR DESIGN

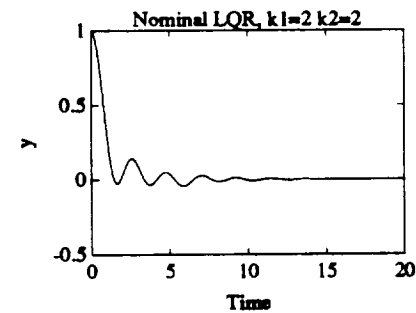
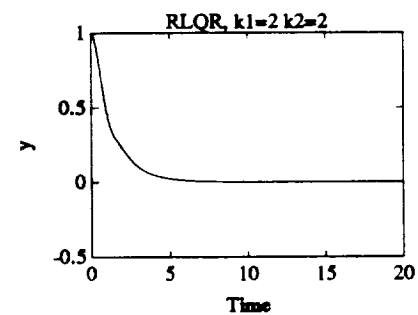
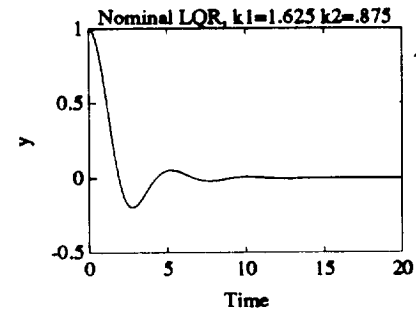
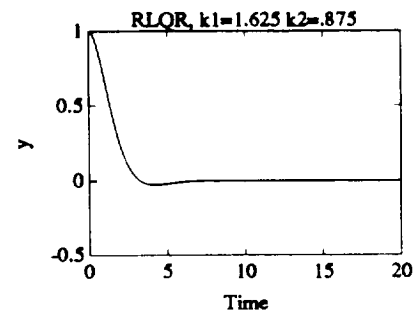
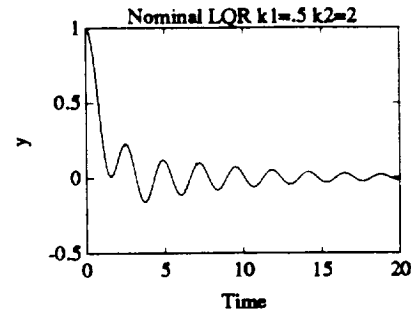
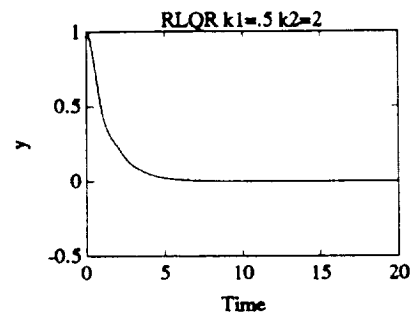
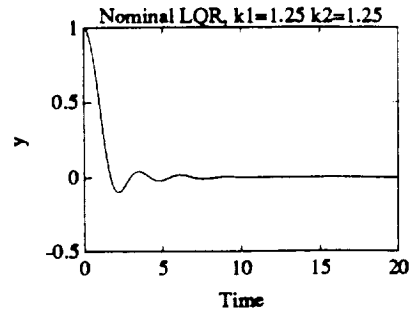
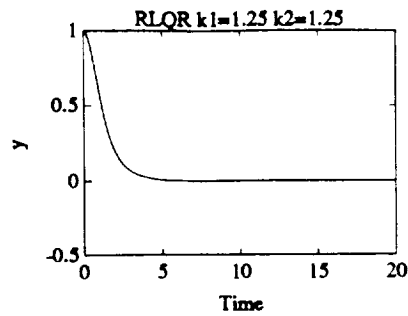




THREE-MASSSES, TWO UNCERTAIN SPRINGS

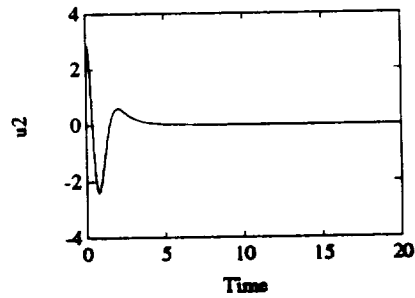
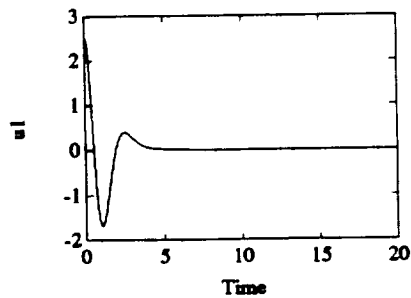
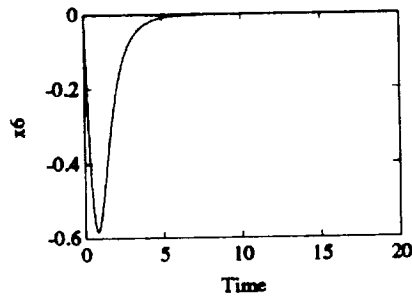
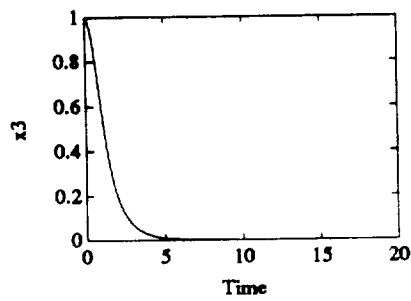
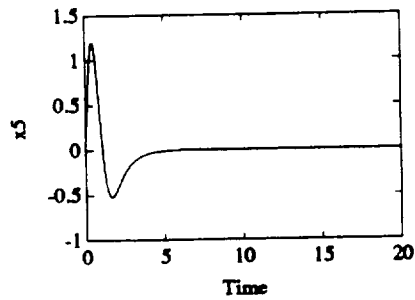
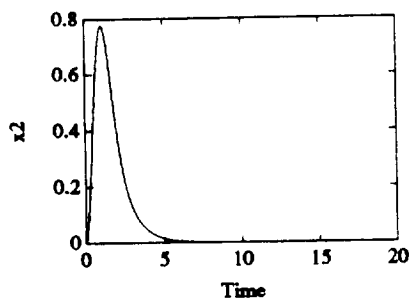
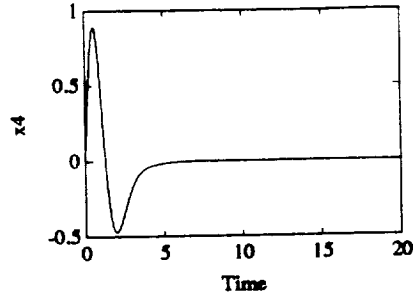
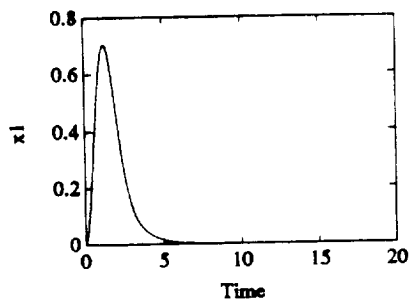


PERFORMANCE COMPARISONS: RLQR (LEFT) VS MISMATCHED LQR (RIGHT)



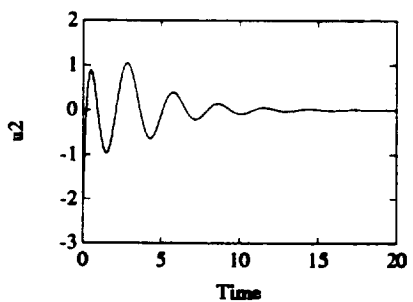
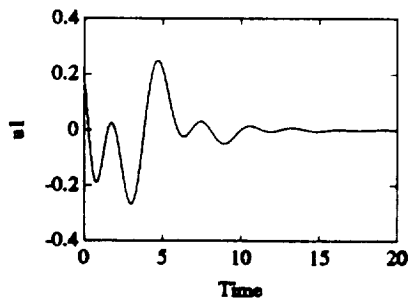
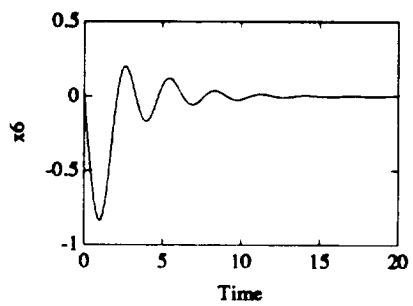
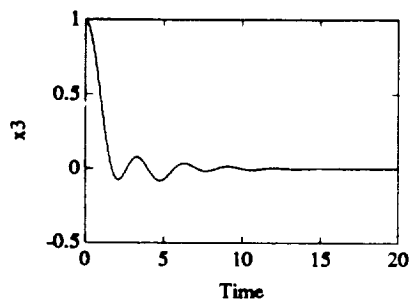
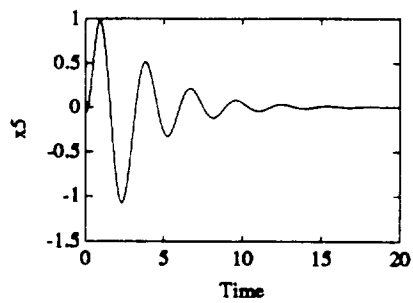
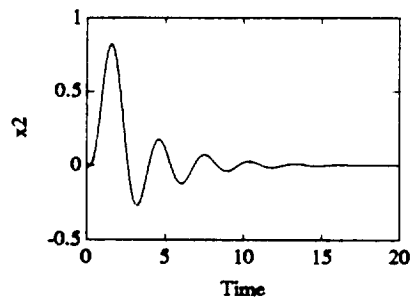
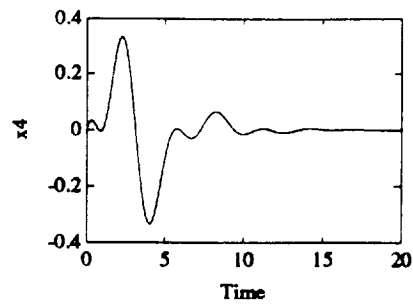
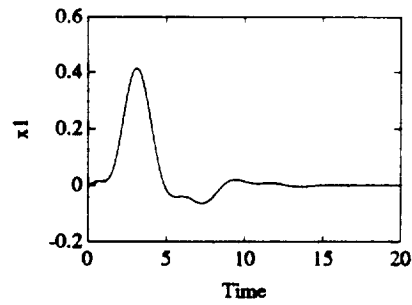
RLQR TRANSIENTS: 2-SPRING SYSTEM

$$K_1 = .5, K_2 = 1.25$$



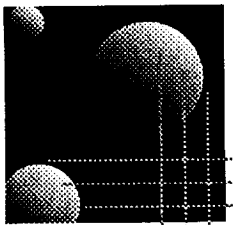
MISMATCHED LQR TRANSIENTS: 2-SPRING SYSTEM

$$K_1 = .5, K_2 = 1.25$$



CONCLUSIONS

- RLQR design is a full state method
- Guarantees stability as well as some robustness
- Interesting energy interpretations
- Understanding underlying fundamentals will help us when we extend to output feedback



*MIT
Space
Engineering
Research
Center*

Cost Averaging Techniques for Robust Control of Flexible Structural Systems

**Nesbitt W. Hagood
Edward F. Crawley**

**Third Annual SERC Symposium
July 1, 1991**

N 93 - 28175

58 63
160330
P. 111

Outline

- Introduction
- Modeling of Parameterized Systems
- Average Cost Analysis
- Reduction of Parameterized Systems
- Static and Dynamic Controller Synthesis
- Examples

Problem Statement

- The problem is to design a controller that provides stability robustness over a set of plants described by real parameter uncertainty.
- This type of uncertainty is common in structural plants.
 - Uncertain stiffness
 - Uncertain damping
 - Uncertain modal parameters
- Stability examined in the context of the performance-robustness trade.

Background in Robust Control Synthesis

Bounding Methods

- Develop robustness analysis test
 - Lyapunov, Kharitonov, Small Gain, μ
- Incorporate analysis test into performance metric
 - modify Lyapunov equation or develop stability index
- Find controller which minimizes modified performance metric subject to constraints.

Sensitivity Methods

- Sensitize the cost to the uncertainties, then minimize.
- Multiplicative White Noise (MEOP): Hyland, Bernstein
- Cost Sensitivity Minimization: Skelton
- Multi-Model Techniques: Bryson, Li

Approach of This Work

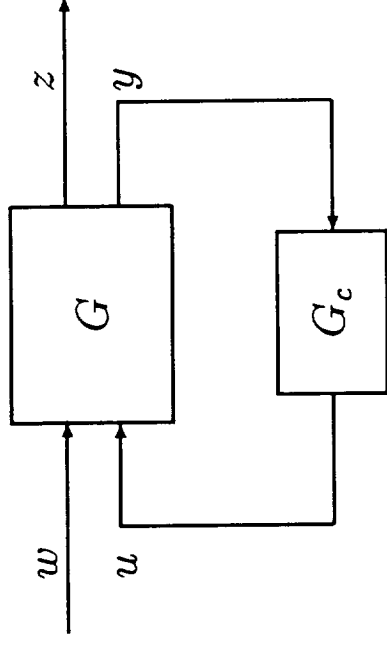
- Examine cost averaged over a continuously parameterized set of plants.
- Derive analysis tools to determine approximations and bounds to the average cost.
- Apply these analysis tools to the problem of determining critical components and uncertainties.
- Apply these analysis tools to the problem of nonconservative robust controller design.

Modeling Notation

- A system $G(s)$ can be represented in state space notation as:

$$\begin{bmatrix} \dot{x} \\ z \\ y \end{bmatrix} = \begin{bmatrix} A & B_1 & B_2 \\ C_1 & 0 & D_{12} \\ C_2 & D_{21} & 0 \end{bmatrix} \begin{bmatrix} x \\ w \\ u \end{bmatrix}$$

- The controlled system can be represented schematically:



Sets of Systems

- The set, Ω , of parameters is defined on the compact interval

$$\Omega = \left\{ \alpha : \alpha \in \mathbb{R}^r, -\delta_i^L \leq \alpha_i \leq \delta_i^U \quad i = 1, \dots, r \right\}$$

- The set \mathcal{G} of systems is parameterized as follows

$$\mathcal{G} = \{G(\alpha) \mid \alpha \in \Omega\}$$

— for structured parameter dependence

$$G(\alpha) = \begin{bmatrix} \frac{A_0 + \sum_{i=1}^r \alpha_i A_i}{C_1} & \frac{B_1}{0} & \frac{B_{2_0} + \sum_{i=1}^r \alpha_i B_{2_i}}{D_{12}} \\ C_{2_0} + \sum_{i=1}^r \alpha_i C_{2_i} & D_{21} & 0 \end{bmatrix}$$

The Average Cost

- The exact average cost is defined as the closed-loop \mathcal{H}_2 -norm (quadratic cost) averaged over the model set.

$$J = \int_{\Omega} \|G_{zw}(\alpha)\|_2^2 d\mu(\alpha)$$

- Finite average cost implies:
 - The closed-loop systems are stable $\forall \alpha \in \Omega$ except possibly at isolated points.
 - No closed-loop system can have eigenvalues with positive real parts.
- Controllers based on minimization of the average cost will guarantee stability without necessarily guaranteeing performance.

Average Cost Calculation

- The average cost is calculated

$$J = \text{tr} \left\{ \langle \tilde{Q}(\alpha) \rangle \tilde{C}^T \tilde{C} \right\}$$

- For each $\alpha \in \Omega$, $\tilde{Q}(\alpha)$ is given by

$$0 = \tilde{A}(\alpha)\tilde{Q}(\alpha) + \tilde{Q}(\alpha)\tilde{A}^T(\alpha) + \tilde{B}\tilde{B}^T$$

- The problem is how to compute the average solution to a parameterized Lyapunov equation.
 - Monte-Carlo
 - Direct Integration
 - Stochastic Operator Methods

Operator Decomposition

- Can utilize techniques from the field of wave propagation in random media and turbulence modeling.
- The parameterized Lyapunov equation can be decomposed into a nominal part and a parameter dependent part.

$$\tilde{A}(\alpha)\tilde{Q} + \tilde{Q}\tilde{A}^T(\alpha) + \tilde{B}\tilde{B}^T = 0$$

is equivalent to

$$\mathbf{L}_0[\tilde{Q}] + \mathbf{L}_1(\alpha)[\tilde{Q}] + \tilde{B}\tilde{B}^T = 0$$

$$\begin{aligned}\mathbf{L}_0[\tilde{Q}] &= \tilde{A}_0\tilde{Q} + \tilde{Q}\tilde{A}_0^T \\ \mathbf{L}_1(\alpha)[\tilde{Q}] &= \tilde{A}_1(\alpha)\tilde{Q} + \tilde{Q}\tilde{A}_1^T(\alpha)\end{aligned}$$

- Two methods of computing the average: Perturbation Expansion and Dyson Equation.

Perturbation Expansion Approximation

- Perturbation expansion series can be approximated by retaining only the first two terms.
- The perturbation expansion approximate cost is given by

$$\tilde{Q}^P = \tilde{Q}^0 + \mathbf{A}(\mathbf{L}_0^{-1} \mathbf{L}_1(\alpha))^2 \tilde{Q}^0$$

$$J^P = \text{tr} \left\{ \tilde{Q}^P \tilde{C}^T \tilde{C} \right\}$$

where \tilde{Q}^B is the solution of

$$0 = \tilde{A}_0 \tilde{Q}^P + \tilde{Q}^P \tilde{A}_0^T + \tilde{B} \tilde{B}^T + \sum_{i=1}^r \sigma_i \left(\tilde{A}_i \tilde{Q}^i + \tilde{Q}^i \tilde{A}_i^T \right)$$

$$0 = \tilde{A}_0 \tilde{Q}^i + \tilde{Q}^i \tilde{A}_0^T + \sigma_i \left(\tilde{A}_i \tilde{Q}^0 + \tilde{Q}^0 \tilde{A}_i^T \right) \quad i = 1, \dots, r$$

- The equations for the perturbation expansion are related to those used in Skelton's cost sensitivity controller design method.
- The two sets of Lyapunov equations are coupled hierarchically and easily solved using standard techniques.

Bourret Approximation

- The Dyson Equation can be approximated by retaining only the first term of \mathbf{M} .

$$\tilde{Q}^B = \tilde{Q}^0 + \mathbf{A}(\mathbf{L}_0^{-1} \mathbf{L}_1(\alpha))^2 \tilde{Q}^B$$

- The Bourret approximate cost is given by

$$J^B = \text{tr} \left\{ \tilde{Q}^B \tilde{C}^T \tilde{C} \right\}$$

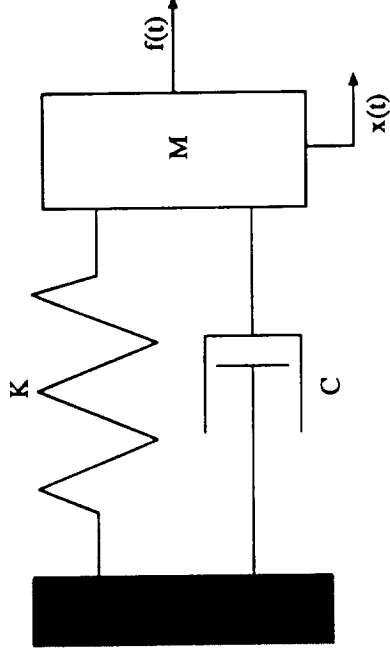
where \tilde{Q}^B is the solution of

$$\begin{aligned} 0 &= \tilde{A}_0 \tilde{Q}^B + \tilde{Q}^B \tilde{A}_0^T + \tilde{B} \tilde{B}^T + \sum_{i=1}^r \sigma_i \left(\tilde{A}_i \tilde{Q}^i + \tilde{Q}^i \tilde{A}_i^T \right) \\ 0 &= \tilde{A}_0 \tilde{Q}^i + \tilde{Q}^i \tilde{A}_0^T + \sigma_i \left(\tilde{A}_i \tilde{Q}^B + \tilde{Q}^B \tilde{A}_i^T \right) \quad i = 1, \dots, r \end{aligned}$$

- The Bourret equation represents an infinite series expansion for the approximate average solution.
- The cross-coupling complicates the solution procedure.
- Positive definite solution the Bourret equation guarantees stability over a set smaller than the design set.

Second Order System Example

- Consider the simple spring-mass-damper represented.

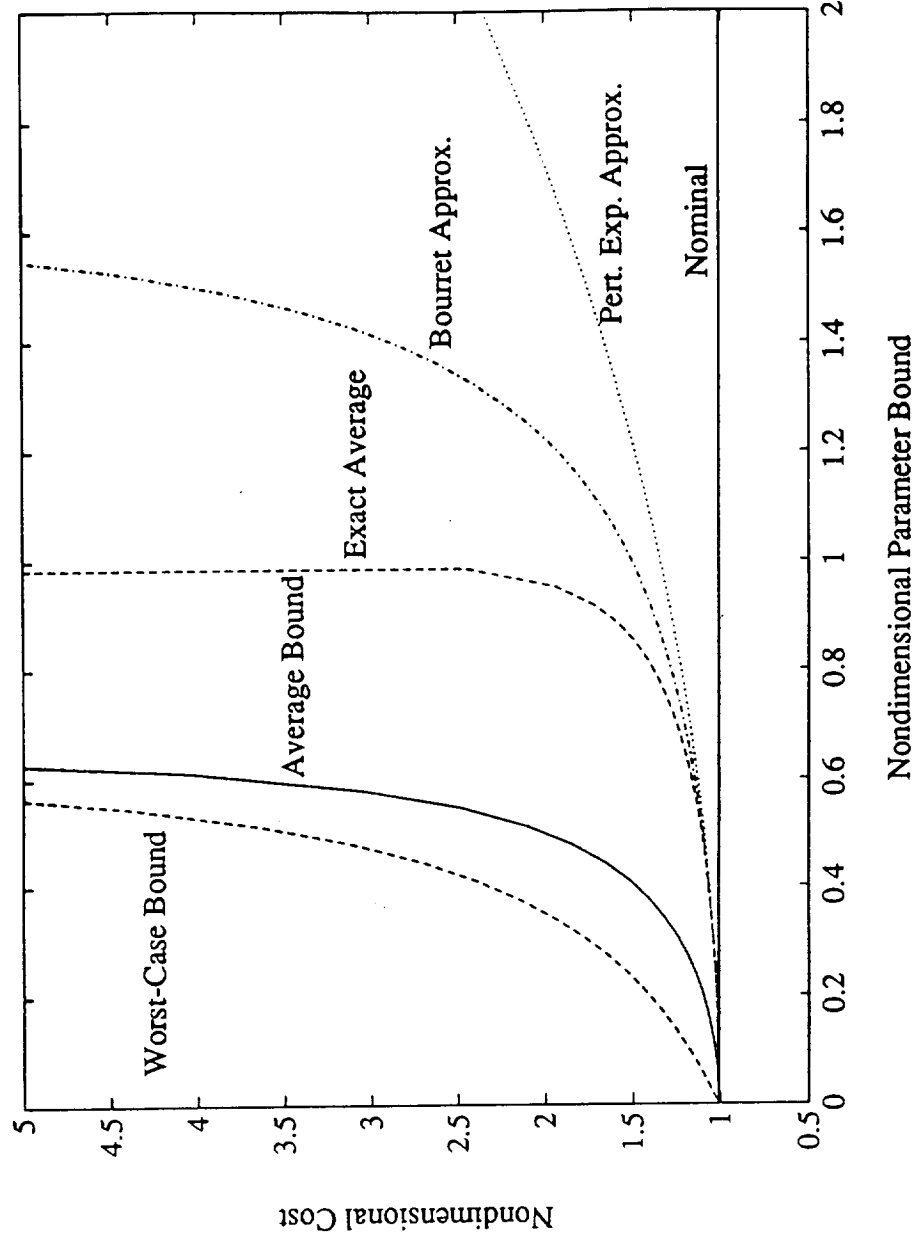


- The system has dynamics
$$\ddot{x}(t) + 2\zeta\omega\dot{x}(t) + \omega^2x(t) = bf(t)$$
- Let the natural frequency and damping ratios of the system be uniformly distributed uncertain parameters of the form

$$\begin{aligned}\omega^2 &= \omega_0^2 + \tilde{\omega}^2 & -\delta_{\omega^2} \leq \tilde{\omega}^2 \leq \delta_{\omega^2} \\ \zeta &= \zeta_0 + \tilde{\zeta} & -\delta_{\zeta} \leq \tilde{\zeta} \leq \delta_{\zeta}\end{aligned}$$

Cost vs. Model Uncertainty

- The cost as a function of the uncertain damping bound.



Robust Control Synthesis

- Fixed-form controllers

$$G_c = \left[\begin{array}{c|c} 0 & 0 \\ \hline 0 & D_c \end{array} \right] \text{ or } \left[\begin{array}{c|c} A_c & B_c \\ \hline C_c & 0 \end{array} \right]$$

- Controller Parameter Optimization Design Procedure

Step 1: Define cost based on exact average, bounding or approximating cost.

Step 2: Append the appropriate equation to the cost using a matrix of Lagrange multipliers.

Step 3: Determine the necessary conditions for optimality using matrix calculus.

Step 4: Minimize the cost numerically using necessary condition for gradient information.

Step 5: Evaluate the resulting controllers for stability and performance robustness.

Necessary Conditions

- For exact average cost minimization with static output feedback.

$$D_c = -R^{-1}B_2^T \langle \tilde{P}(\alpha) \tilde{Q}(\alpha) \rangle \langle \tilde{Q}(\alpha) \rangle^{-1}$$

where

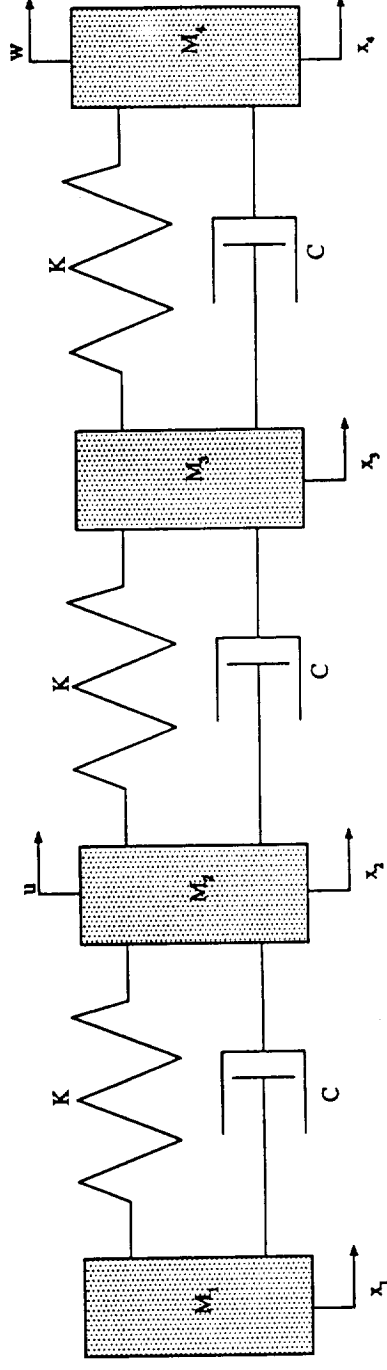
$$0 = \tilde{A}(\alpha)\tilde{Q}(\alpha) + \tilde{Q}(\alpha)\tilde{A}^T(\alpha) + \tilde{B}\tilde{B}^T$$

$$0 = \tilde{A}^T(\alpha)\tilde{P}(\alpha) + \tilde{P}(\alpha)\tilde{A}(\alpha) + \tilde{C}^T\tilde{C}$$

- The necessary conditions have a form very similar to the necessary conditions derived for the static output feedback problem.
- Uncertainty couples the two parameterized Lyapunov equations.
- The same form is present with the approximations and bounds but with parameter independent equations.
- For dynamic output feedback the necessary condition comprise
 - three gain equations obtained by taking derivatives with respect to A_c, B_c , and C_c
 - two Lyapunov-based equations

Example 2: The Cannon-Rosenthal Problem

- Consider the four mass/spring/damper system with uncertain body one mass.

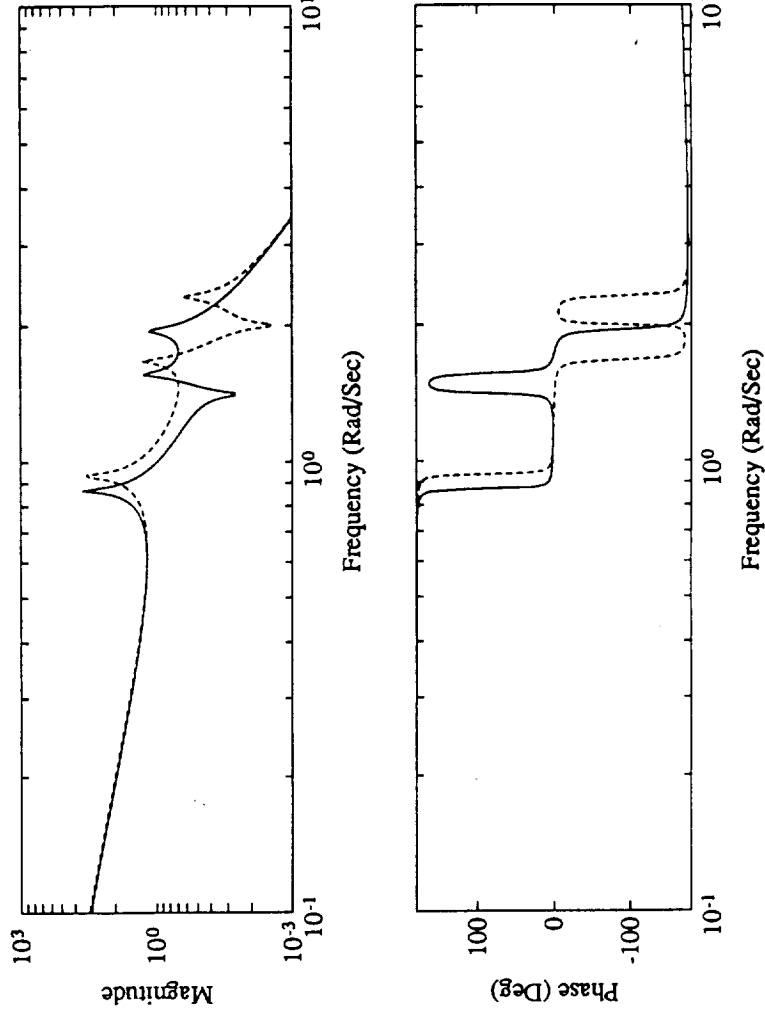


- The uncertain mass is represented

$$1/m_1 = 1/m_{1_0} + \tilde{m} \quad m_0 = 0.5 \quad |\tilde{m}| \leq \delta_m$$
- Spring and mass uncertainty treated by numerous researchers.

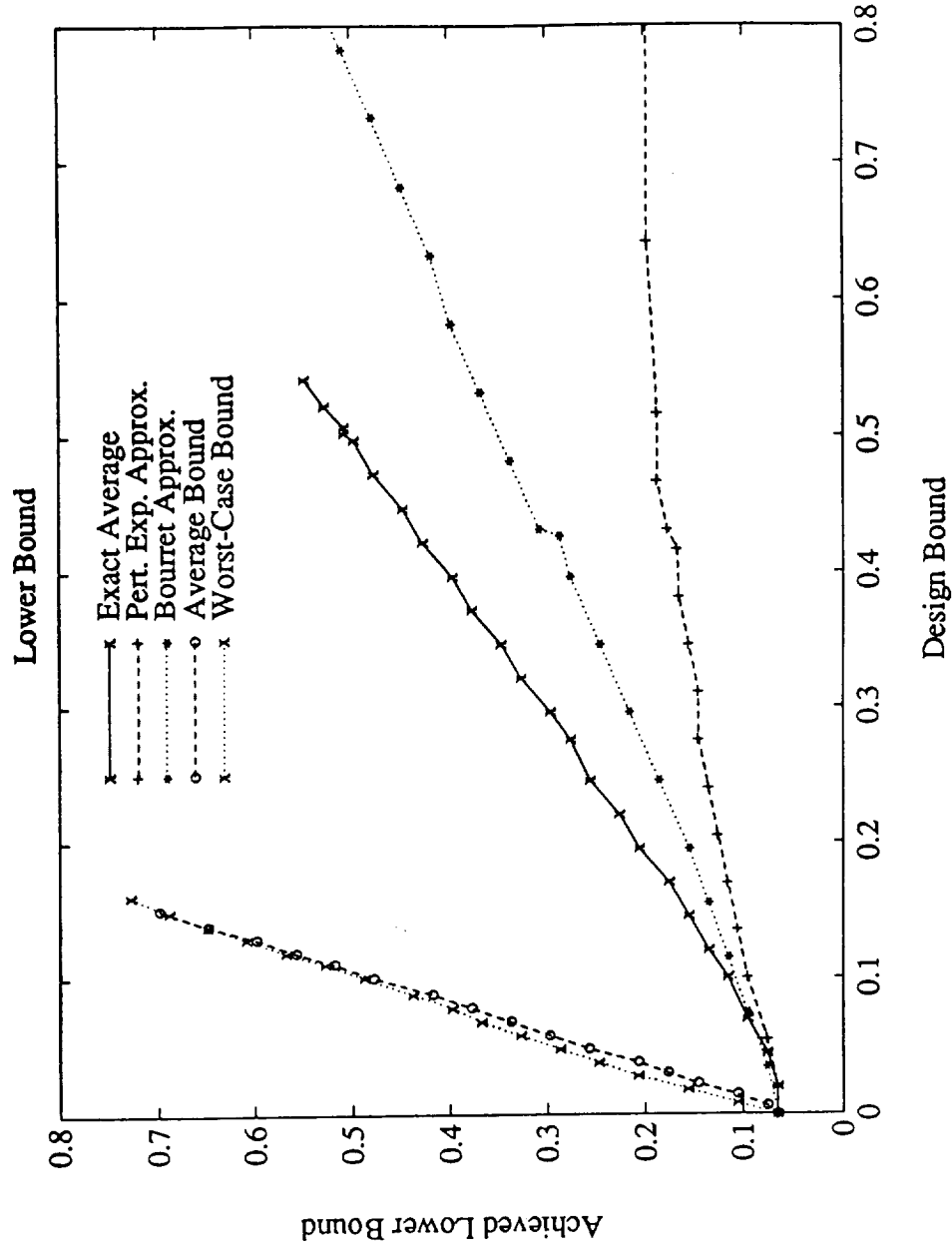
Pole-Zero Flip

- The problem was chosen because the plant zero and second mode change relative positions as the parameter is increased to $\tilde{m} = 0.6$
- The open loop u - y transfer functions for the Cannon-Rosenthal problem for $m_1 = 0.5$ (solid) and $m_1 = 0.25$ (dashed)



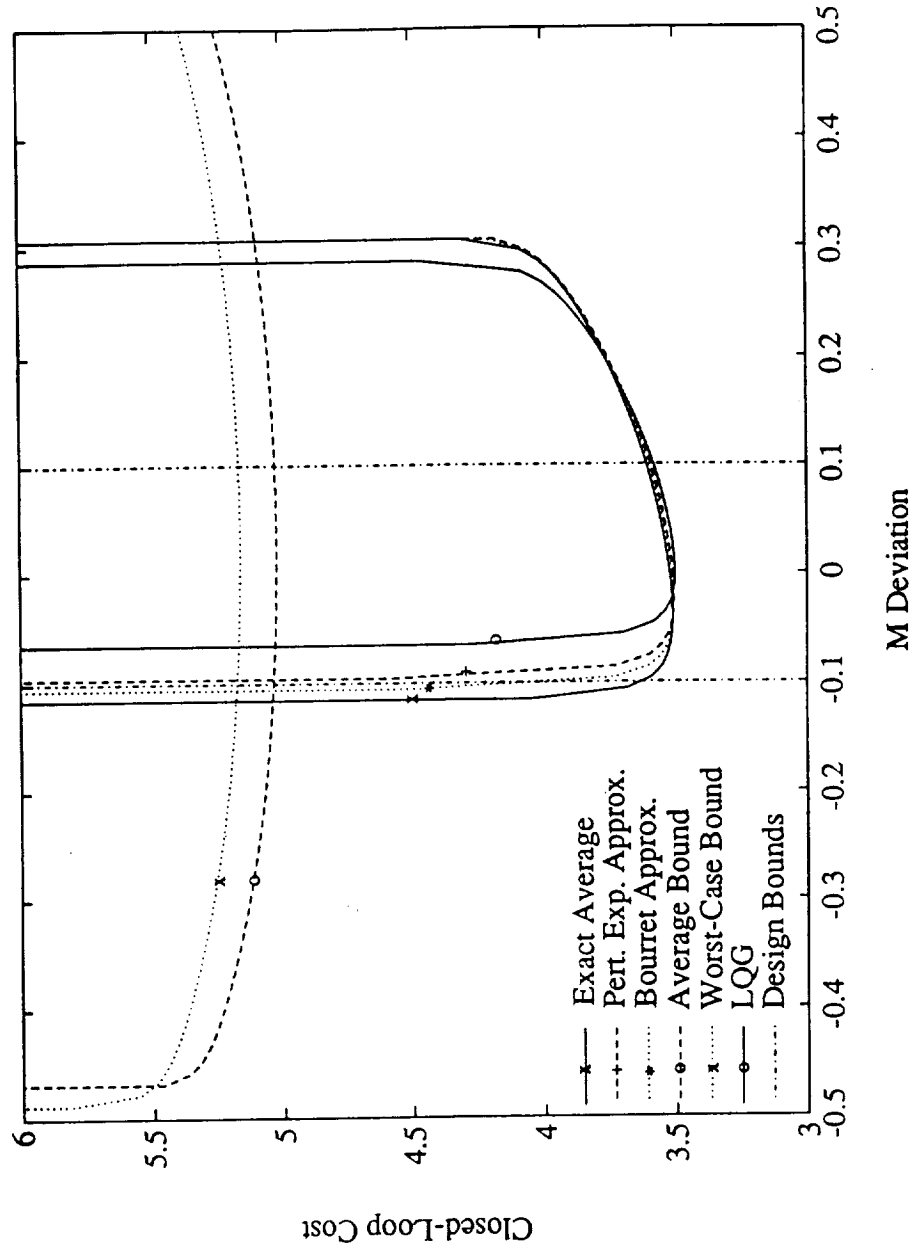
Achieved vs. Designed-for Robustness

- Achieved closed loop stability bounds as a function of the design bound, δ_m .



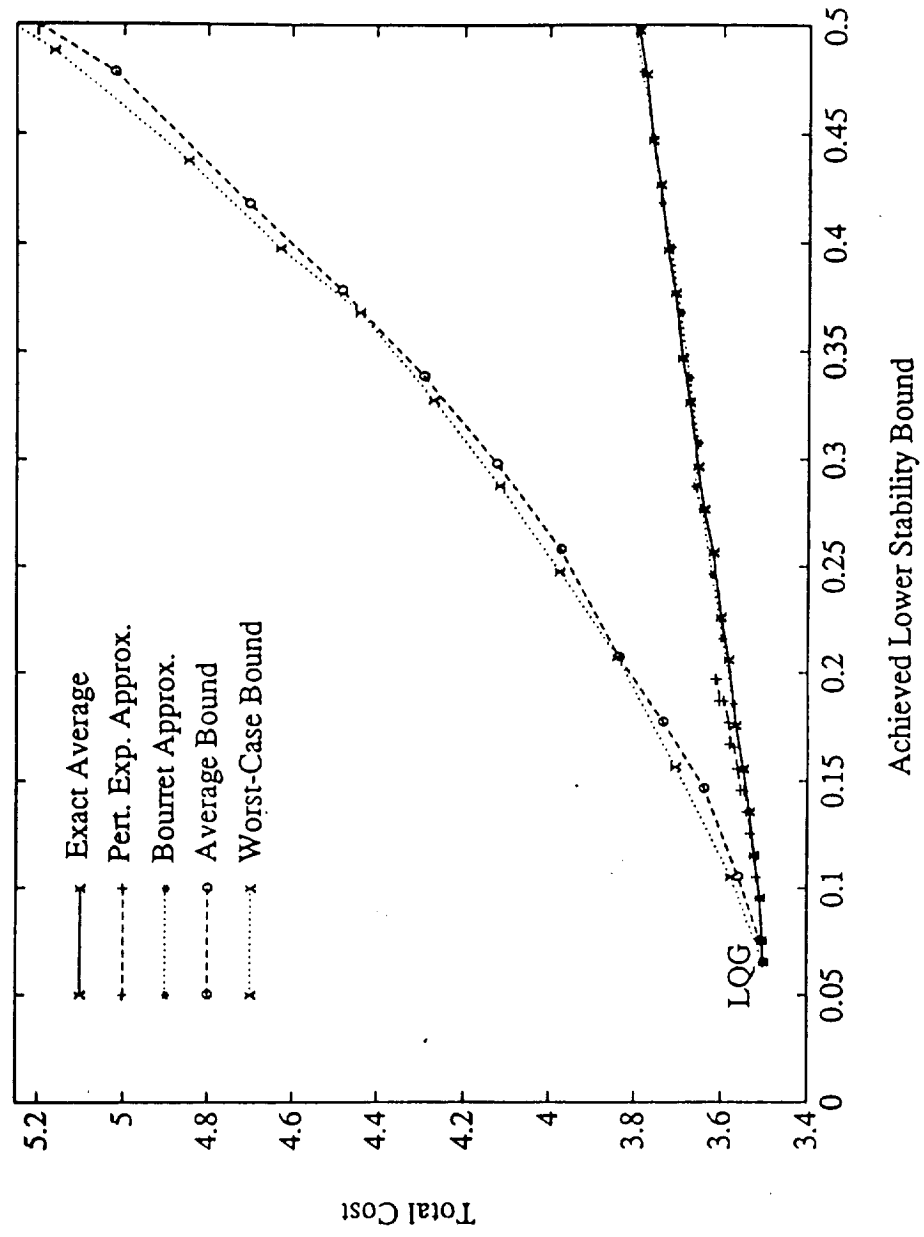
Cost vs. Parameter

- System closed-loop \mathcal{H}_2 -norm as a function of \tilde{m} , the deviation about $1/m_1$, for controllers designed Using $\delta_m = 0.1$.



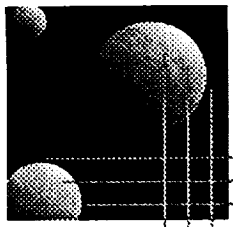
Efficiency Plot

- Nominal cost as a function of the achieved stability bound.



Conclusions

- Have investigated a new class of controllers based on minimizing quantities related to the cost averaged over a parameterized set of plants.
- While possessing useful properties, the average cost based controllers were difficult to compute.
- The perturbation based controllers were easy to compute but performed well only at low uncertainty levels.
- The average bound designs were essentially equivalent to the worst case bound designs.
- The worst case bound performed as predicted but gave low efficiency due to conservatism.
- The Bourret approximation based designs were overall best in computability and efficiency.



MIT
Space
Engineering
Research
Center

INTELLIGENT STRUCTURES TECHNOLOGY

Edward F. Crawley

Controlled Structures Technology
MIT Space Engineering Research Center
3rd Annual Symposium

July 1, 1991

939
100331
7-26
N 9 3 - 2 8 1 7 6

Overview

- Embedding electronic components for control of intelligent structures.
- Single-chip microcomputer control experiment
- Structural shape determination
- Distributed sensor systems for structural control

Motivation

- Precision control of flexible structures is more readily achieved with large numbers of sensors and actuators
- Signal quality can be improved by distribution of analog processing circuitry along with transducers
- Connectivity (number of lines) can be greatly reduced by distribution of A/D, D/A conversion with digital bus interface circuitry
- Control loop speed can be substantially elevated by distribution of digital processors in a hierarchic controller

Missing element in fully integrated intelligent structures concept:
embedded electronics

Objectives

Establish the feasibility of physically embedding electronic components for the control of intelligent structures.

Demonstrate structural control using processor with minimal number of chips

Embedding Electronics: Approach

- Select a suitable candidate chip for embedding
- Develop embedding technique
- Test mechanical static and fatigue properties
- Test temperature-humidity-bias reliability

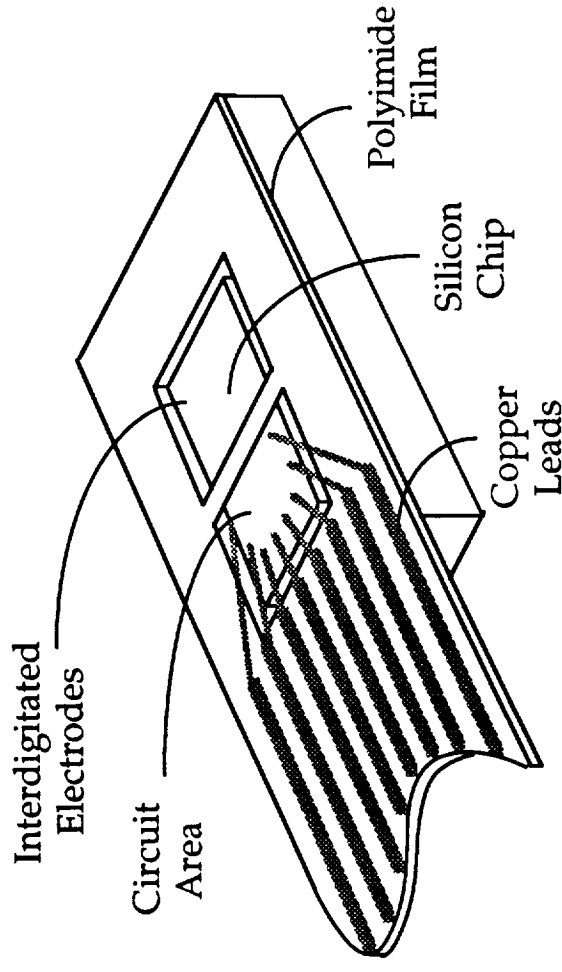
Electrical and Mechanical Compatibility

Issues:

- Manufacturing - autoclave pressures and temperatures
- Operational mechanical stress – brittle Si, delicate SiO₂ and metal structures
- Electrical insulation from graphite fibers
- Ionic contamination – device lifetime is typically limited by corrosion
- Minimal disruption of structural plies

Integrated Circuit Chip Packaged for Embedding

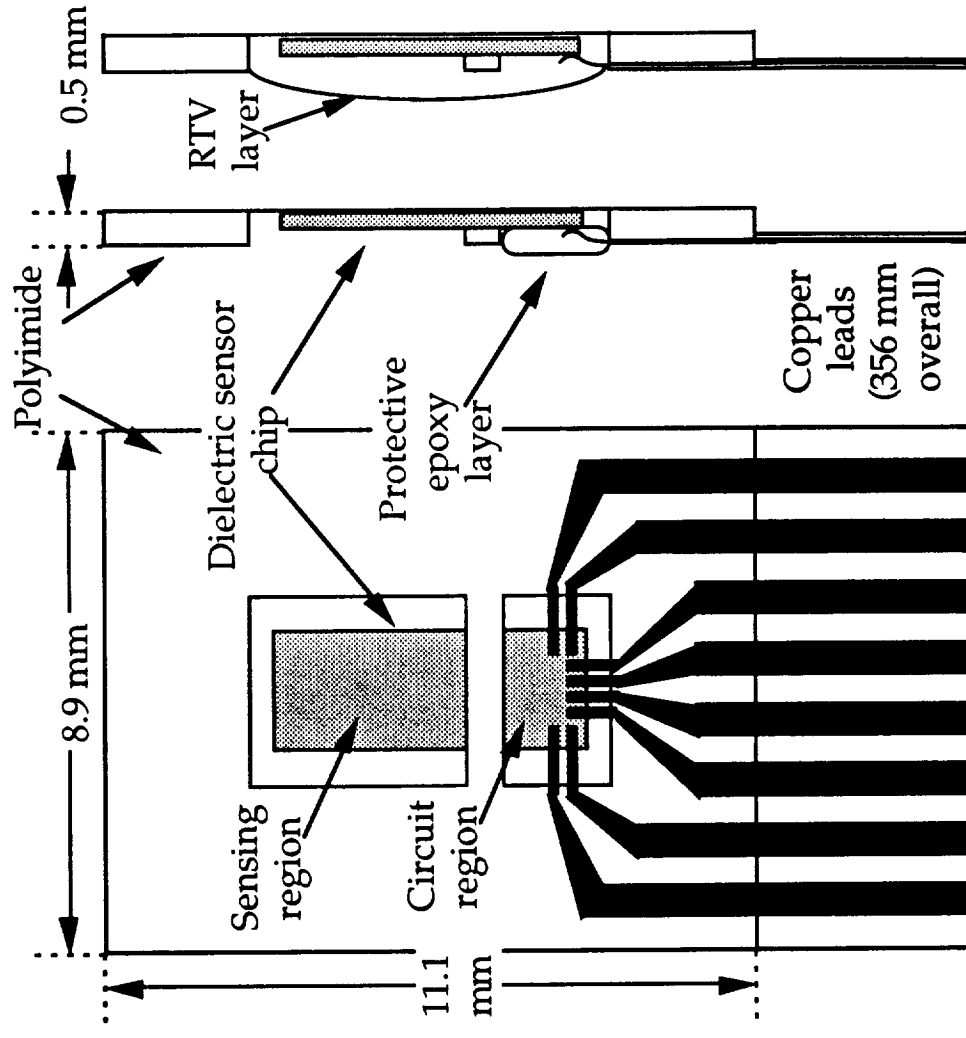
Dielectric integrated circuit sensor (Micromet Instruments, Inc.)



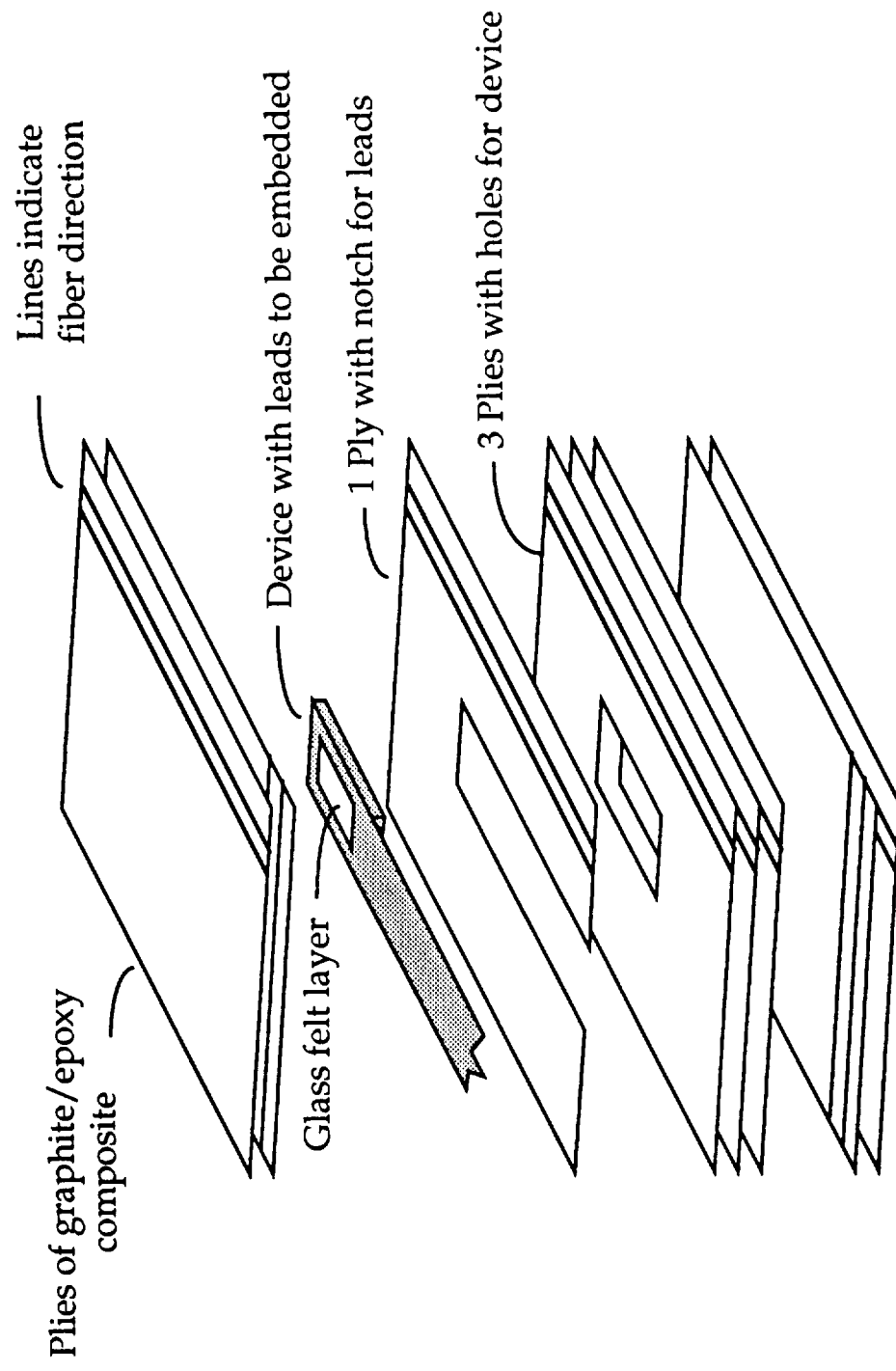
Circuit area consists of two metal-oxide-semiconductor field effect transistors and one diode

Packaging is similar to Tape Automated Bonding (TAB)

Integrated Circuit Chip Packaged for Embedding

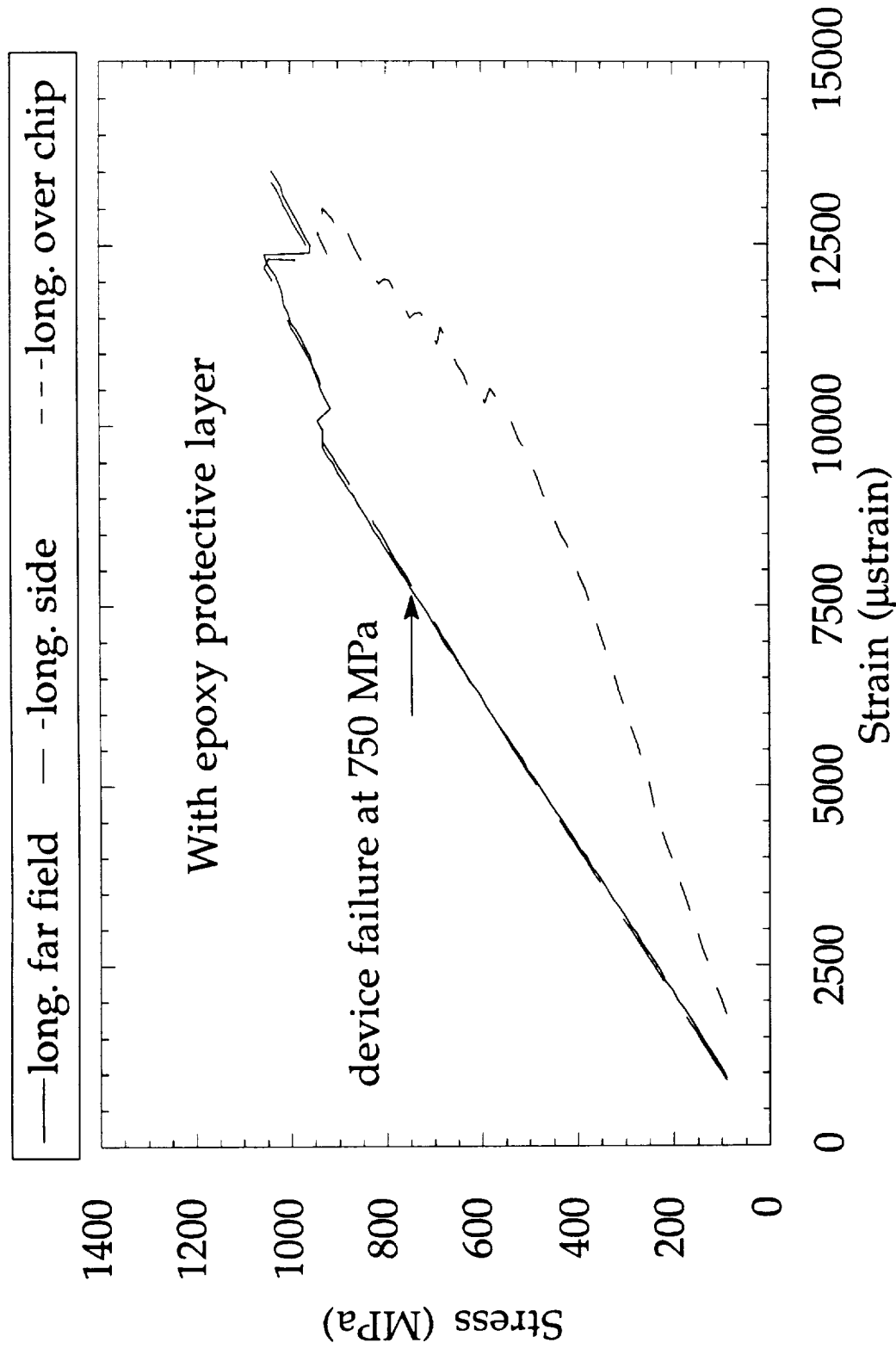


Embedding Devices within Composite Structures

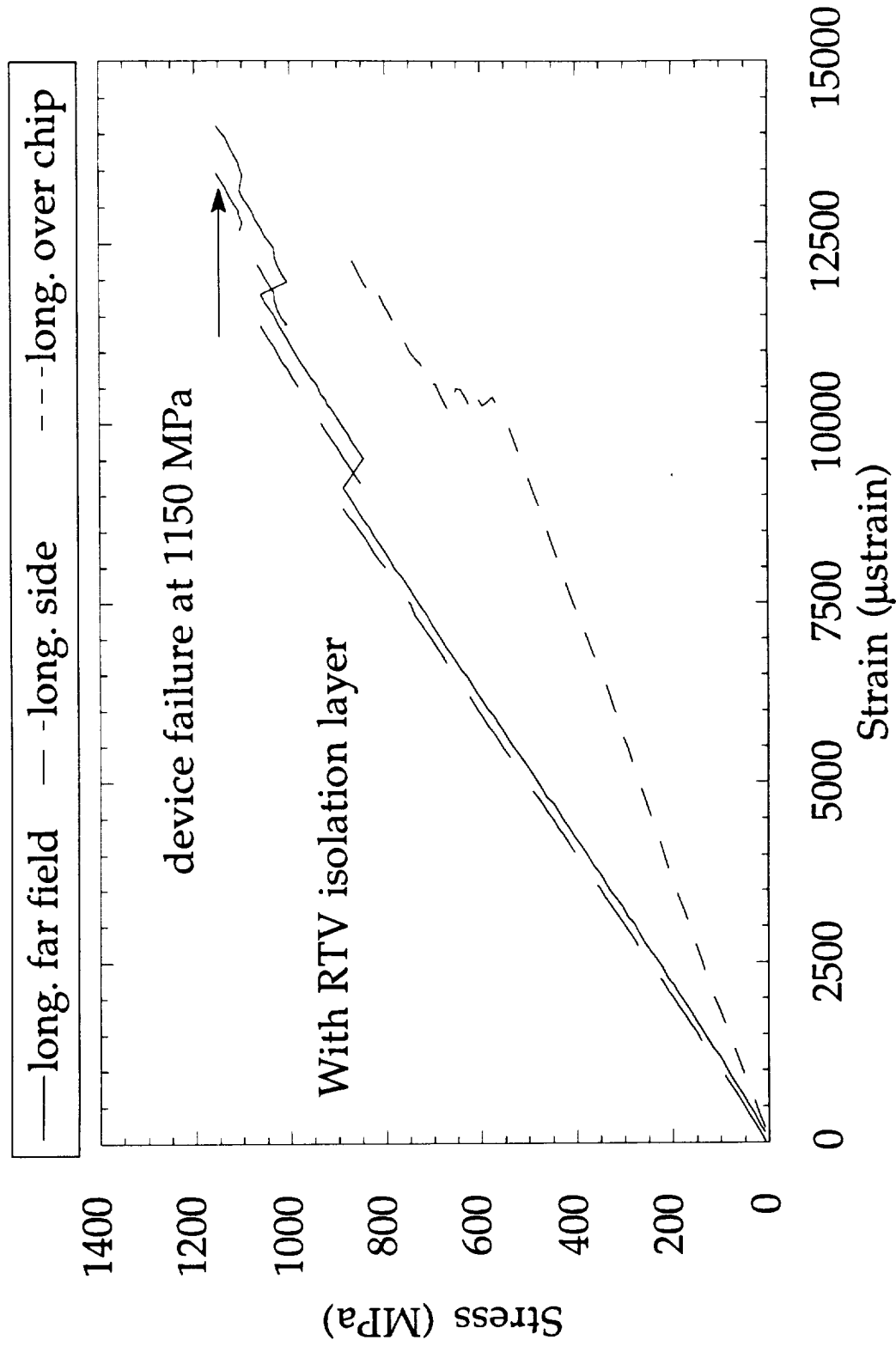


Layup is $[0/90/0_2]_s$

Test of Embedded Circuit in G/E Coupon



Test of Embedded Circuit in G/E Coupon



Temperature/Humidity/Bias Test

- Test conditions:

3 chips embedded in 60 mm x 75 mm laminates subjected to 80°C and 80% R. H. for 125 hours

Transistor drain-source currents while under constant bias continuously monitored; characteristic curves recorded at log time intervals

Two conventional MOSFETs included as experimental controls

- Results:

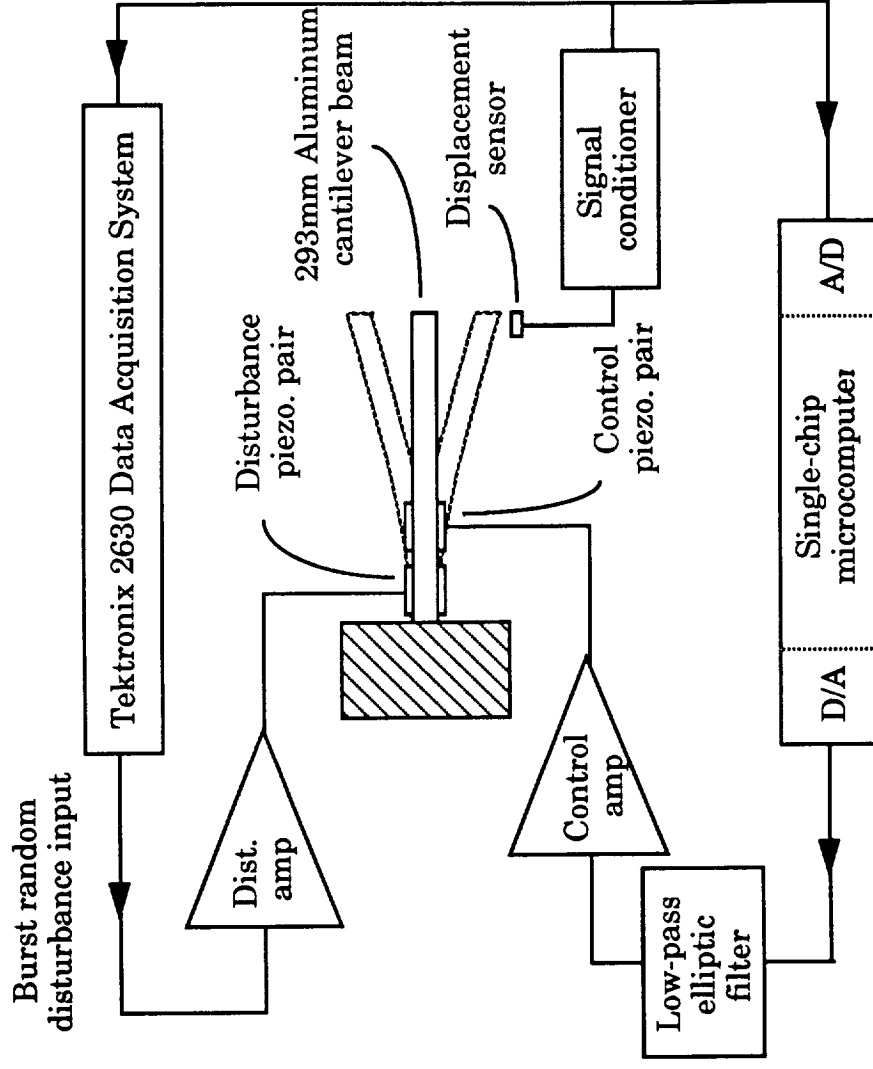
One sensor showed intermittent anomalies (hysteresis, elevated current) as early as 14 hours - possible leakage currents through epoxy

One sensor showed progressive drop in current during final 4 hours - consistent with lead corrosion

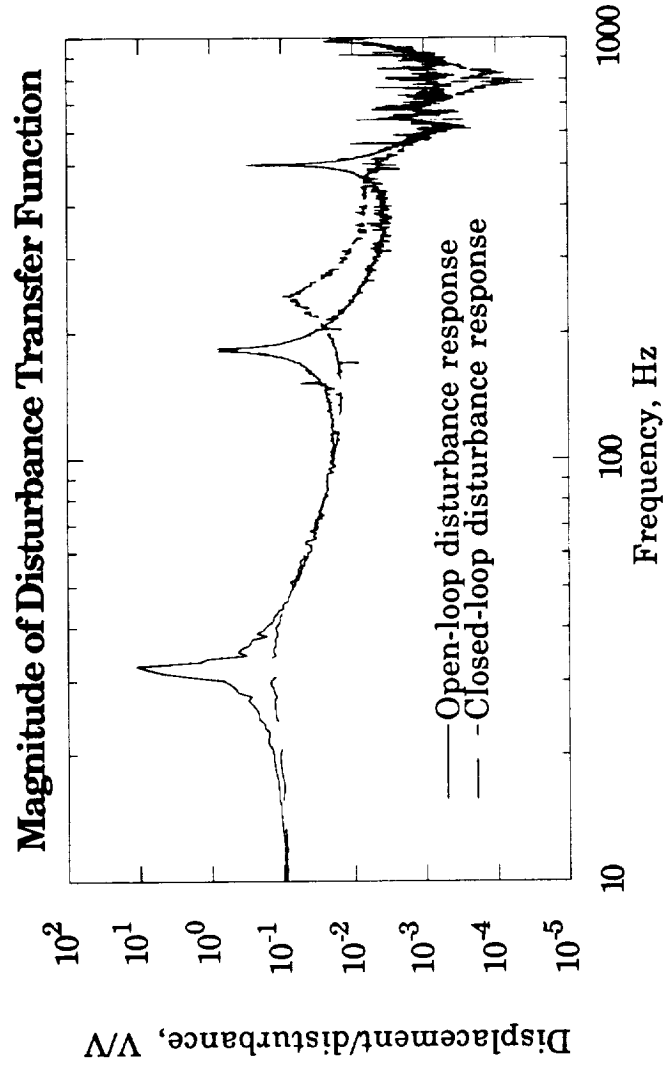
One sensor showed no anomalies

Conventional controls showed no anomalies

Single-chip Microcomputer Control Experiment



Performance Achieved



Increased damping:	1st mode	0.36% OL	31% CL
	2nd mode	0.15% OL	4% CL
	3rd mode	0.20% OL	11% CL

Major Results

- Embedding electronics is feasible
 - Compliant isolation layer allows device function to laminate failure
 - Chemical isolation is inferior to commercial devices, requires further work
 - All failures were at or near lead-chip bond
- Embedding local processors are plausible
 - Distribution of processing can be justified, depending on problem size
 - Nearly all of the required functions included on currently available monolithic devices

Structural Shape Determination Objectives

Objective is to determine “optimal” type and number of sensors to allow accurate reconstruction of structural shape from discrete curvature measurements.

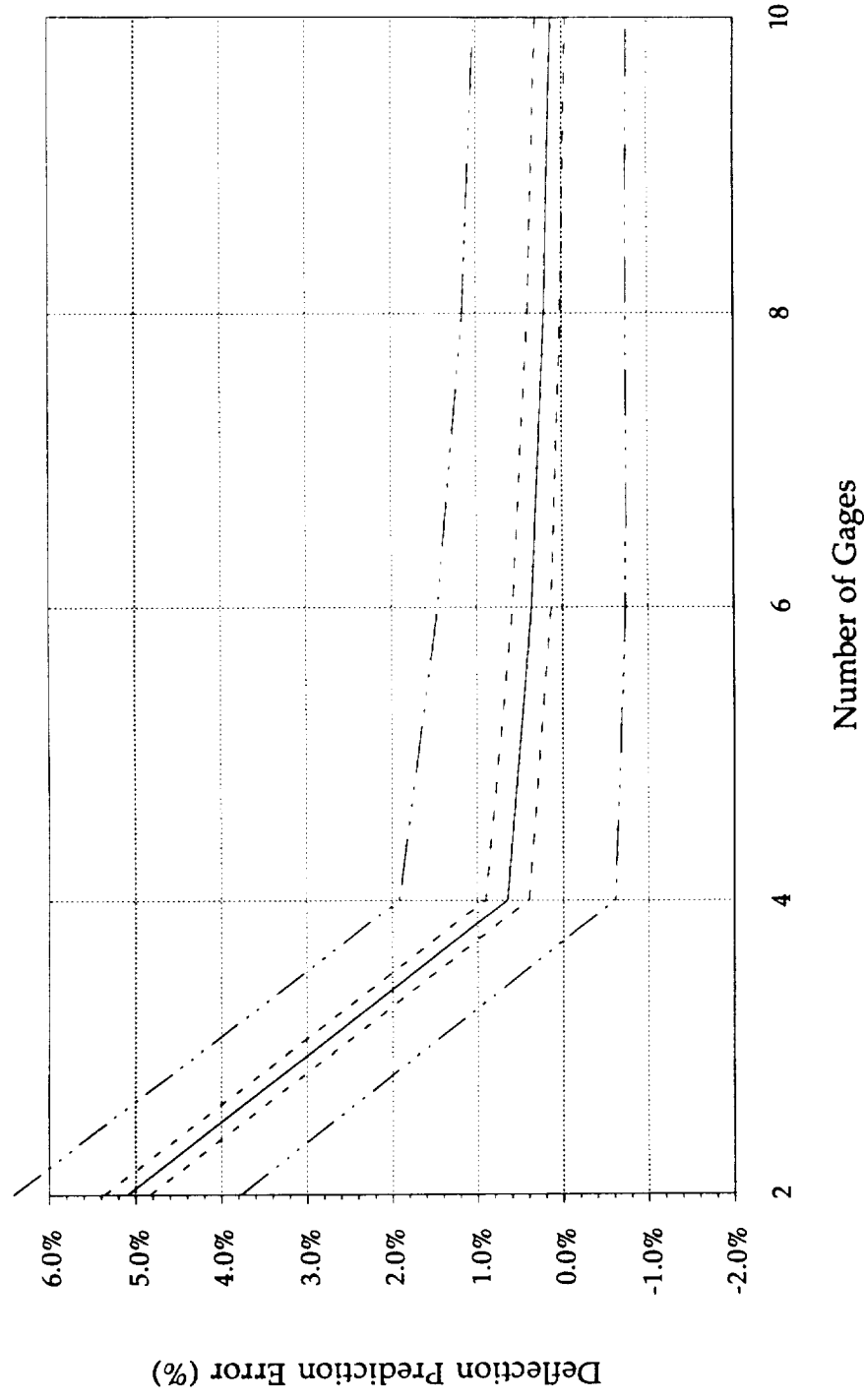
Issues considered include:

- Accuracy of predicted slope and displacement for various integration rules as a function of the number of gages.
- Static and dynamic mode shape determination with strain averaging sensors.
- Frequency characteristics of a single sensor.
- Frequency characteristics of integrated shape measurement.

Approach to Integration Rule Study

- Consider a cantilevered beam subjected to a representative set of simple static loadings.
- Distribute a set of strain gages along the length of the beam/
- Integrate the curvature using a variety of integration rules to obtain an estimate of the shape of the beam.
- Vary gage factor and gage placement to obtain error bounds for experimental uncertainties.
- Compare performance of short and long gages to determine whether a “point” or an averaged strain measurement yields better performance.

Deflection Prediction Error vs Number of Gages



Spline integration rule and long gages

- Solid line: No gage factor or placement error.
- Dashed line: 1% gage factor error and placement error of 0.2% of the beam length.
- Dot-dashed line: 5% gage factor error and placement error of 1% of the beam length.

Functional Requirements for Distributed Sensor Systems

- The sensors should be able to sense static modes and resolve them in detail.
- The integral of the static shape, and therefore output of each sensor should roll off quickly in frequency and not have negatives.
- The sensors must have good observability of the dynamic modes targeted for control in the bandwidth.
- The observability of dynamic modes must roll off quickly beyond the control bandwidth.
- The sensors should be easily implementable and must be finite in length.
- If possible, the sensors should not contain negative regions.

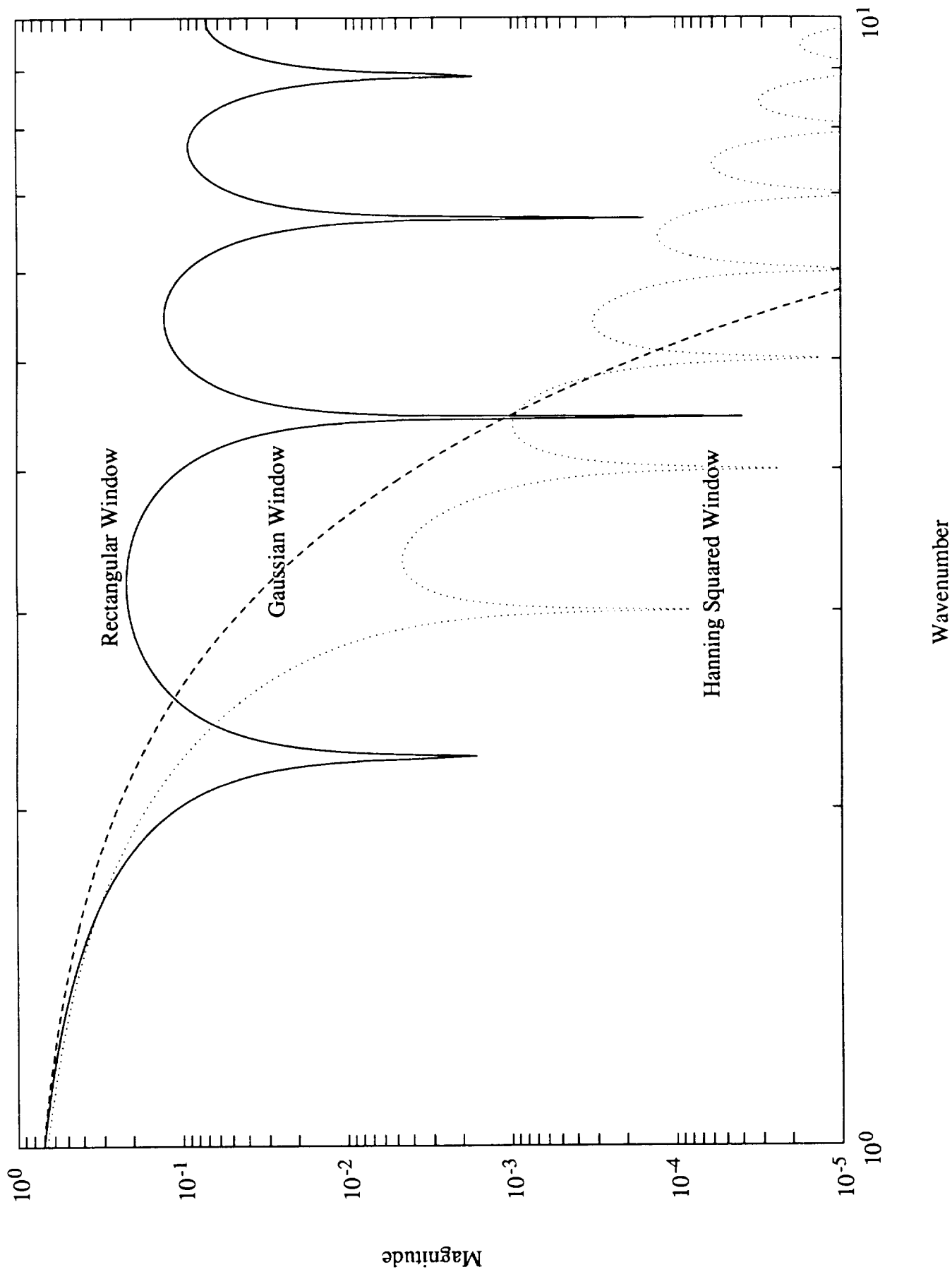
Approach

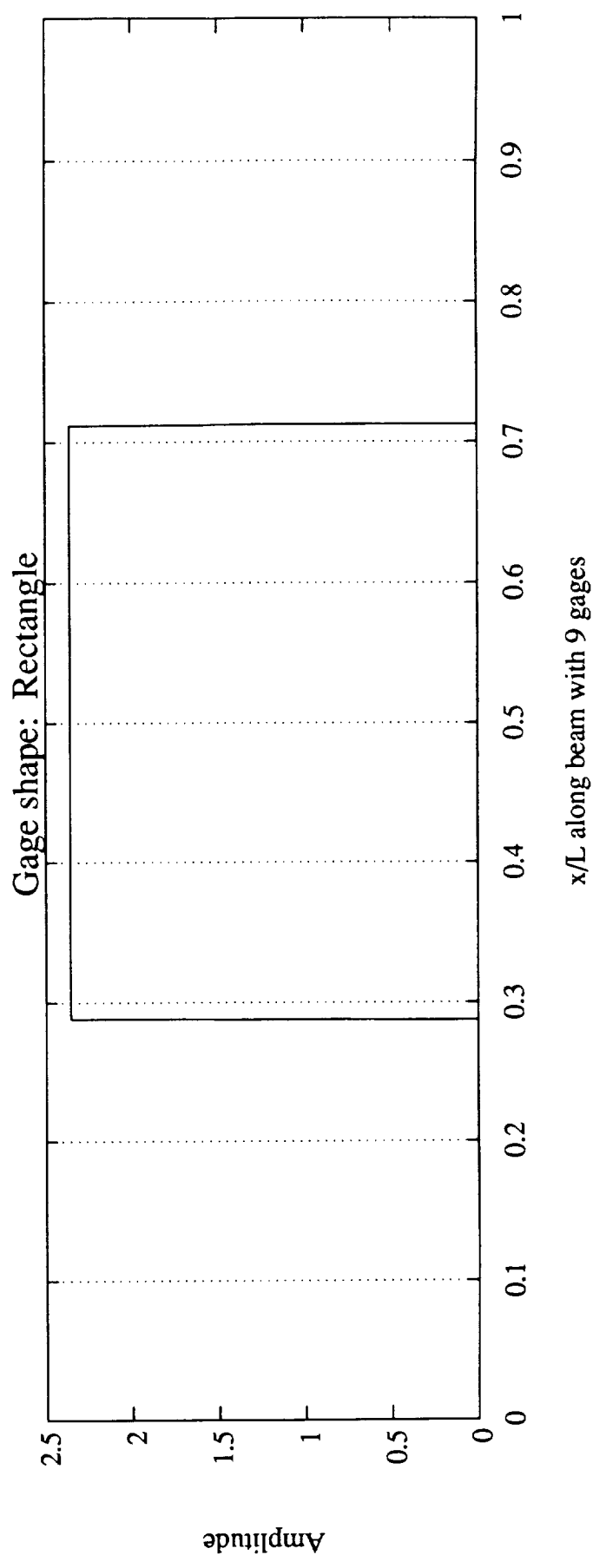
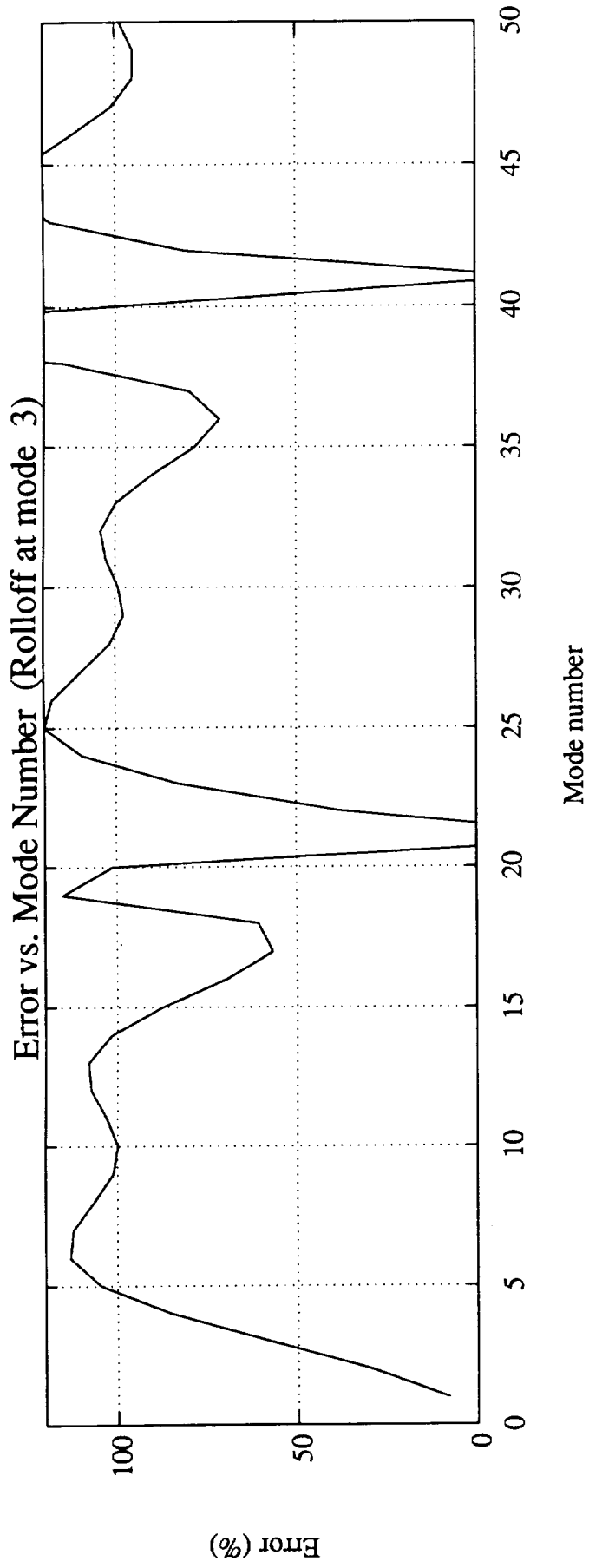
- Consider a pinned-pinned beam with 9 gages distributed along its length.
- Vary the length and spatial weighting of the gages.
- Integrate the sensor measurements to obtain an estimate of the shape of the beam.
- Increase the frequency of the dynamic mode of the beam, and examine the behavior of the tip deflection estimate.
- Verify that observability rolls quickly and monotonically approaches zero.
- Optimize the roll off characteristics by varying spatial weighting of the sensors.

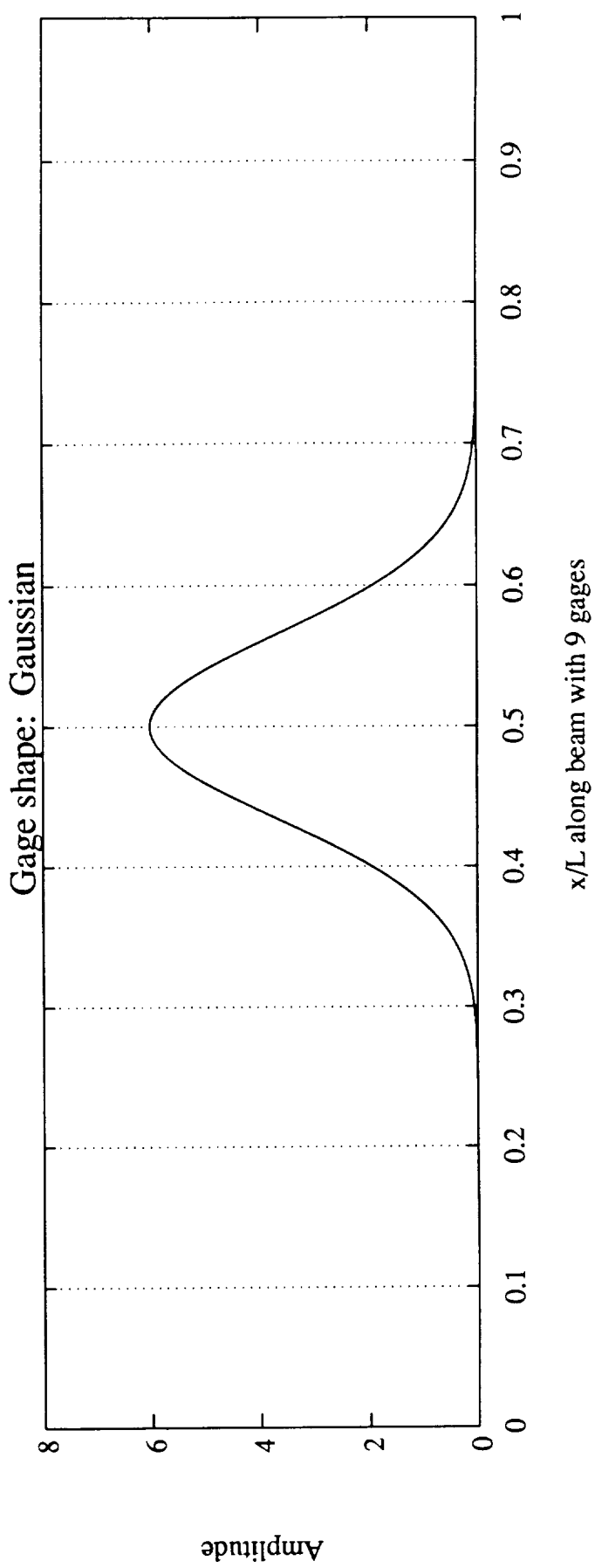
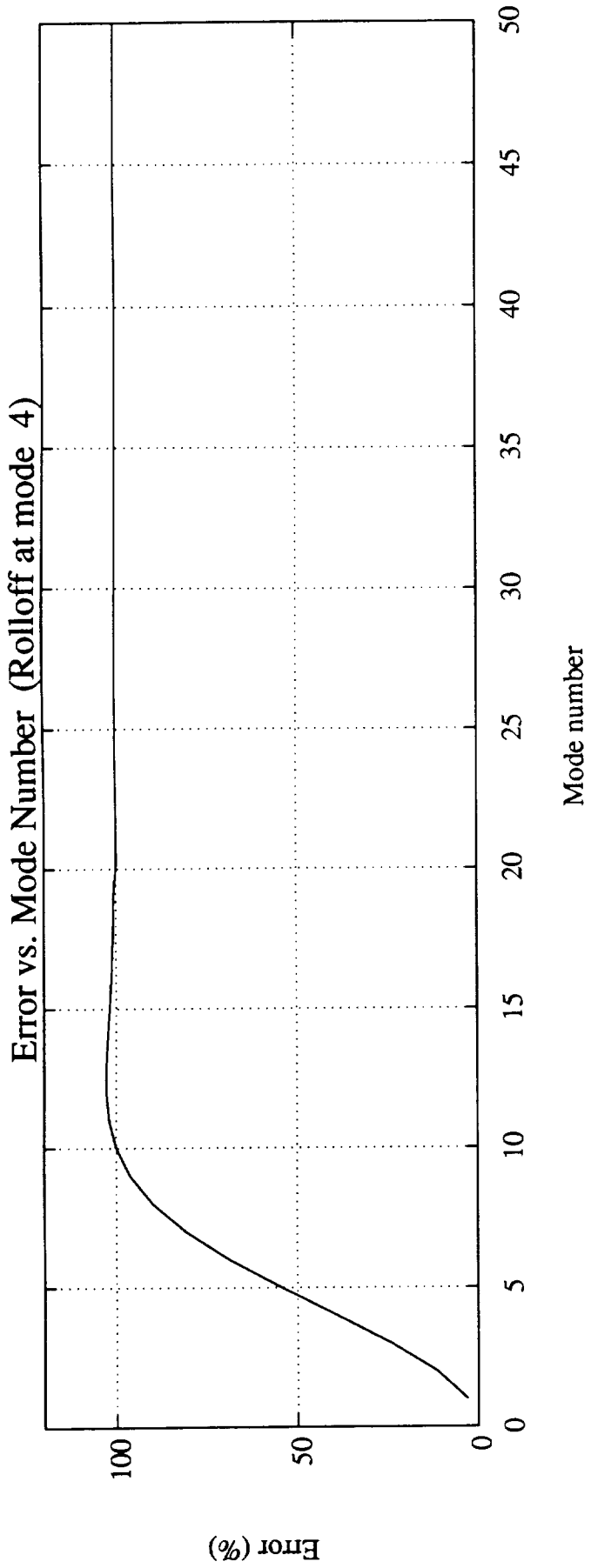
Examples of Single Sensor Characteristics

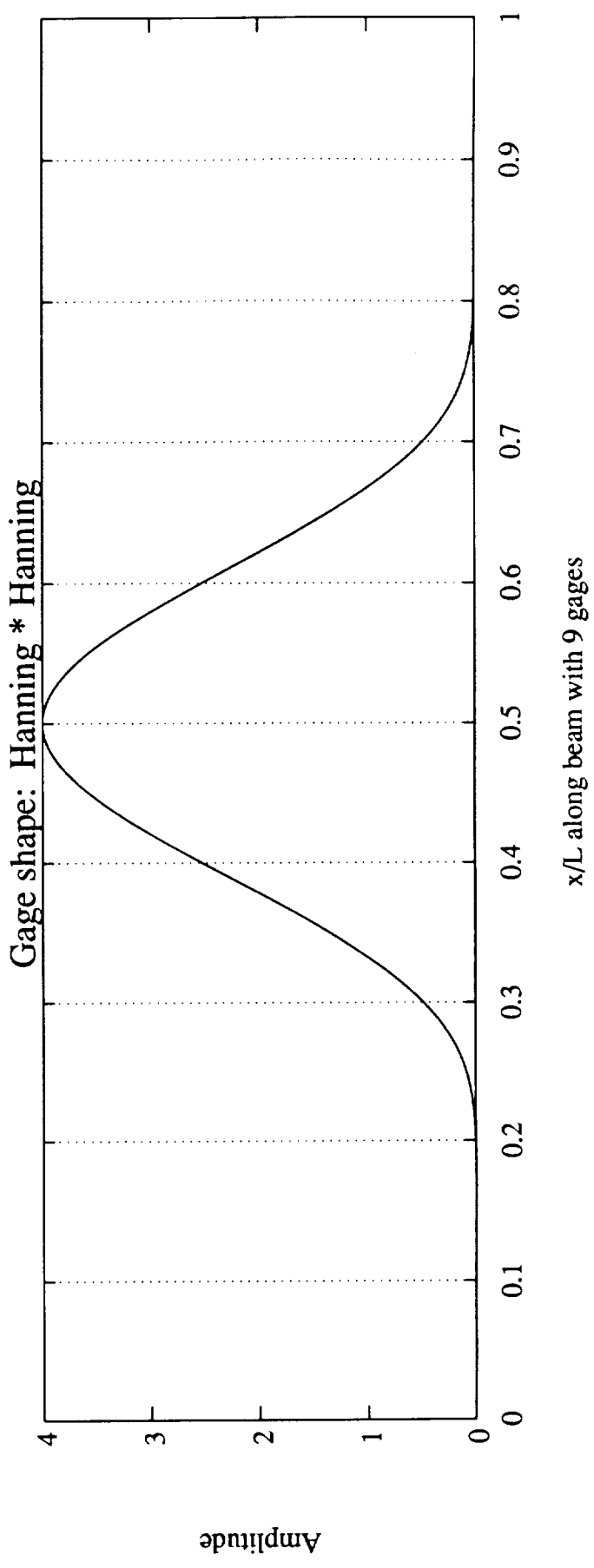
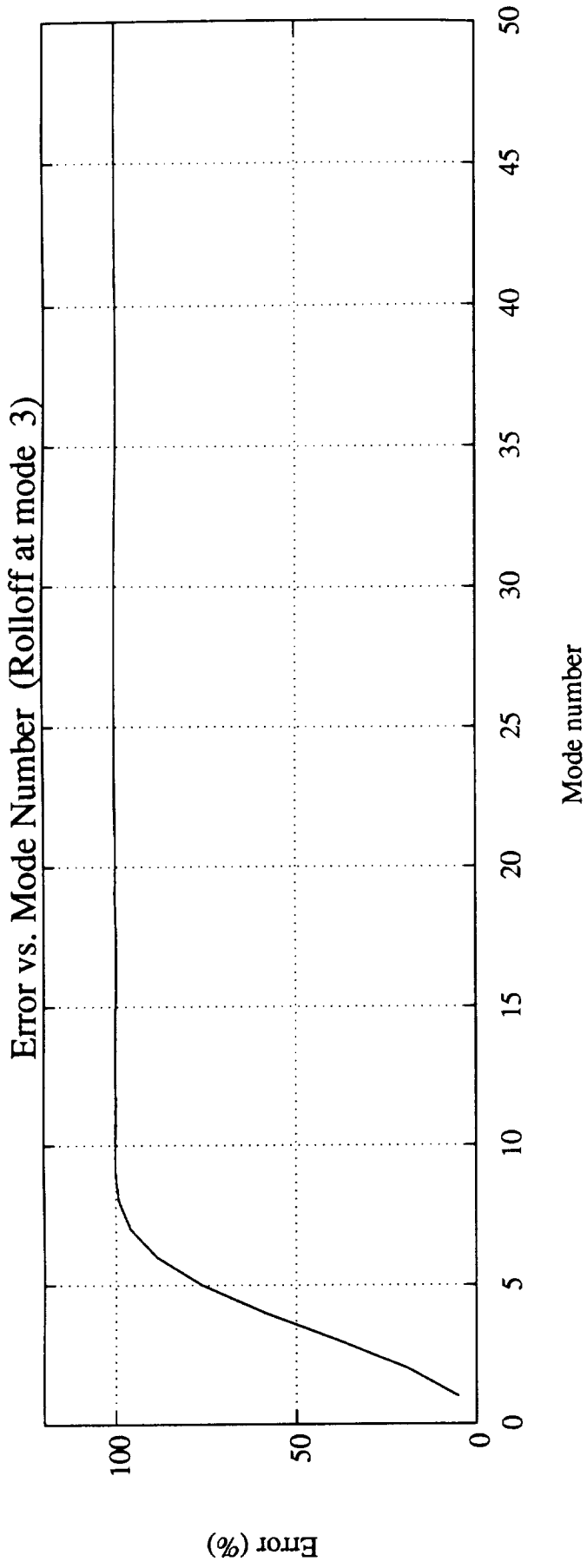
Shape	Advantages	Disadvantages
Sinc	Gives perfect rolloff with no phase lag.	Is of infinite extent in x. Has negative regions in x. Hard to manufacture and distribute.
Rectangle	Very simple shape. Can be distributed easily. Has no negative regions in x.	Only -20 db/decade rolloff. Has large negative regions in k.
Gauss	Has no negative regions in x or k. Has good rolloff (-300 db in 1st decade). Can be distributed.	Is of infinite extent in x.
Hanning ²	Has no negative regions in x. Has good rolloff (-100 db/decade) Can be distributed.	Has small negative regions in k.

Fourier Transforms of Rectangular, Gaussian and Hanning Squared Windows









Conclusions

- Numerical integration schemes have been found that yield accurate shape prediction with a minimum of sensors.
- Spatial weightings for distributed sensors have been identified that yield quick rolloff in:
 - Individual outputs of each sensor
 - Integrated output of all the sensors (tip displacement)
- The functional requirements can nearly be met by simple sensor shapes that are relatively easy to implement.
- Meaningful experiments must be carried out in order to verify theoretical predictions and determine sensitivity of performance to errors incurred during physical implementation of a distributed sensor system.

